The University Of Sheffield.

NATIONAL NUCLEAR LABORATORY

PROCESS DEVELOPMENT FOR THE MANUFACTURE OF PLUTONIUM CONTAINING WASTES AND RESIDUES

JONATHAN SQUIRE

A THESIS SUBMITTED TO THE DEPARTMENT OF MATERIALS SCIENCE AND ENGINEERING AT THE UNIVERSITY OF SHEFFIELD FOR THE DEGREE OF DOCTOR OF ENGINEERING (ENGD)

JANUARY 2013

ABSTRACT

This thesis explores the process development and scale-up challenges for the immobilisation of plutonium containing wastes and residues. The first section details the difficulties encountered with utilising an attrition mill operated in the dry mode to prepare zirconolite samples for consolidation by hot isostatic processing. The failure to remove the milling additives from the milled powders led to porous and heterogeneous products with no correlation between the candidate wasteform properties and milling conditions.

Similar attrition milling conditions were examined with a zirconia candidate wasteform. Pellets, prepared by cold isostatic and cold uniaxial pressing, showed a clear correlation between the increased milling aggressiveness and the density and microstructure of the products. Cold isostatic pressing produced pellets with the highest density.

The effect of precursor particle size, by utilising manufacturer size defined precursors, showed that homogenous and dense zirconolite products could be manufactured by HIP. The experiment confirmed that the failure to remove the lubricant from the HIP cans led to low quality products.

Further work examined the effect that different precursor treatments had on the ability of zirconolite precursors to be planetary milled. The powders were pressed into pellets and sintered in either air or nitrogen. The air sintered pellets were all highly porous but homogenous whilst the nitrogen sintered pellets were heterogeneous. The difference in sintering behaviour was determined to be the result of a eutectic point between the iron and titanium oxides.

Brief studies examined how the density and homogeneity of zirconolite samples improve with increased milling durations. Another experiment attempted to

demonstrate a fine precursor digestion method that did not work. Modified attrition mill internals are also considered.

Finally, the impact of this work on the design of a candidate bulk plutonium immobilisation plant is discussed as well as the on going experimentation with uranium active samples.

Table of Contents

List of Acronyms

Acronym		Description
ACOP	Activity Containment Over Pack	A device in which a HIP can is placed to minimise the spread of activity in case of a malfunction during the HIP cycle
ADU	Ammonium Diuranate	Chemical compound used in the manufacture of uranyl species
AGR	Advanced Gas cooled Reactor	The UK second generation nuclear power reactor
ANSTO	Australian Nuclear Science and Technology Organisation	Australian nuclear research company
AUC	Ammonium Uranyl Carbonate	Chemical compound used in the manufacture of uranyl species
BE	British Energy	Historical UK reactor operator
BNFL	British Nuclear Fuels Limited	Historical UK nuclear fuel cycle company
CEA	Commissariat à l'énergie atomique et aux energies alternatives	French national nuclear research organisation
CIP	Cold Isostatic Pressing	A ceramic forming technique that applies pressure uniformly around a body without additional temperature
CUP	Cold Uniaxial Pressing	A ceramic forming technique that applies force uniaxially to form, usually, a pellet without the addition of temperature
DOE	Department of Energy	US Governmental body
EdF	Electricity de France	Nuclear reactor operator (now owner of BE)
EDS	Electron Dispersive Spectroscopy	A technique for determining the composition of substances by analysing their characteristic X-Rays
FWHM	Full Width at Half Maximum	A method to describe the sharpness of a peak
GDF	Geological Disposal Facility	An underground final storage location for nuclear waste
HEPA	High Efficiency Particulate Air	A type of filter for removing solids form a gas stream

HIP	Hot Isostatic Press(ing)	A consolidation technique that utilises the simultaneous application of heat and pressure
HLW	High Level Waste	Nuclear waste that is highly radioactive and generates a significant amount of heat
IDR	Integrated Dry Route	Chemical process to manufacture UO_2 for fuels
ILW	Intermediate Level Waste	Nuclear waste that is highly radioactive but does not generate significant amounts of heat
LLNL	Lawrence Livermore National Laboratory	American nuclear research organisation
LLW	Low Level Waste	Nuclear waste that is slightly radioactive. Disposed of at LLWR
LLWR	Low Level Waste Repository	The disposal facility for the UK LLW
LWR	Light Water Reactor	A generic term for any nuclear reactor that uses ordinary water.
Magnox	Magnesium Non-oxidising	The name for the UK first generation nuclear fuel cladding, and associated nuclear power plants
MELOX		French MOX manufacturing plant
MOD	Ministry of Defence	UK military organisation
MOX	Metal Oxide	A type of nuclear reactor fuel typically comprising of a mixture of $UO_2/ThO_2/PuO_2$
MWe	Megawatt Electrical	The net power output exported to the grid from a reactor
NDA	Nuclear Decommissioning Agency	The governmental body responsible for the UK nuclear legacy
NIMBY	Not In My Backyard	An attitude to restrict development near one's house
NNL	National Nuclear Laboratory	The UK National Nuclear Laboratory is the UK leading nuclear research organisation (and location of this work)
OK	Odourless Kerosene	Organic fraction used in the PUREX process
PCM	Plutonium Contaminated Material	Waste products that contain trace amounts of plutonium
PUREX	Plutonium Uranium Extraction	A reprocessing technique

PVC	Polyvinyl Chloride	Polymer material used to over pack plutonium product cans
PWR	Pressurised Water Reactor	A type of nuclear reactor in common use around the world (one in the UK at Sizewell B)
RBMK	Reaktor Bolshoy Moshchnosti Kanalniy	Russian nuclear power reactor. It utilises a waster coolant in graphite channels.
RTG	Radioisotope Thermoelectric Generator	An item that generates electricity by harnessing radioactive decay
SEM	Scanning Electron Microscopy	A technique for the direct imaging of microscopic structures using electrons
SF	Spontaneous Fission	A form of radioactive decay in which the atom undergoes fission without the need for neutrons
SGHW	Steam Generating Heavy Water Reactor	Prototype nuclear power reactor
SMP	Sellafield MOX Plant	A former MOX fabrication facility on the Sellafield site
SPRS	Sellafield Products and Residues Store	A plutonium storage facility on the Sellafield site
Synroc	Synthetic Rock	A polyphase ceramic designed to immobilise HLW
TBP	Tri Butyl Phosphate	Complexing agent for use in the PUREX process
TD	Theoretical Density	The calculated maximum density a ceramic can be. Useful for normalising the measured densities of samples
ThORP	Thermal Oxide Reprocessing Plant	Oxide fuel reprocessing plant on the Sellafield site
VLLW	Very Low Level Waste	The lowest classification of nuclear waste
VVER	Vodo-Vodyanoi Energetichesky Reaktor	Russian nuclear power reactor, equivalent to a PWR
WAGR	Windscale Advanced Gas cooled Reactor	The prototype AGR reactor built at the Windscale (now a part of the Sellafield) site
XRD	X-Ray Diffraction	Analytical technique used to measure the spacing between atoms in a crystalline structure and thus help identify phases present
XRF	X-Ray Fluorescence	Analytical technique for determine the composition of a sample

List of Phases Discussed

Number	Phase	Prototype
1	Zirconolite	$CaZrTi_2O_7$
2	Perovskite	$CaTiO_3$
3	Ceria	CeO_2
4	Zirconia	ZrO_2
5	Titania	TiO_2
6	Perovskite (substituted)	$CaTiO_3$
7	Ilmenite	$FeTiO_3$
8	Titanium metal relic	
9	Reaction phase 1	
10	Reaction phase 2	
11	Alumina tray	
12	Al, Fe rich phase	
13	Ti, Al, Fe rich phase	
14	Alumina	Al_2O_3

1: Background to the UK Nuclear Fuel Cycle and Plutonium Disposition Methods

1 Abstract

This chapter firstly details the history of the UK nuclear power industry from the initial military programme to the present status of the sector. There is a description of the UK nuclear fuel cycle showing the sources of plutonium as well the history of plutonium and its isotopes of note. A detailed discussion on the credible options for the disposition of the UK civilian stockpile concludes that whilst the UK government may currently favour re-using the material as a MOX (Mixed Oxide) fuel in thermal reactors, there will always be a proportion of the stockpile that will require immobilisation.

One option for the immobilisation of plutonium is by utilising ceramic wasteforms. The background and intentions of the original Synroc waste disposal strategy are introduced before focusing the dialogue on the use of single host phase ceramics tailored to the immobilisation of plutonium. Methods for the manufacture of these ceramics are introduced. These are broadly material processing techniques such as attrition and planetary milling, as well as consolidation techniques.

Lastly, the use of cerium as a plutonium surrogate in non active development work is justified. The source of a 'realistic' ceria material is compared with direct images of freshly manufactured PuO_2 and shown to be a limiting case in regard to particle shape and size.

2 The UK Nuclear Power Industry

2.1 History of Nuclear Power In The UK

The UK civil nuclear programme grew out of the military requirement for an independent nuclear deterrent. At the end of The Second World War, the desire to create nuclear weapons had brought a realisation that the same technology could be used for a more peaceful purpose, the metaphorical turning swords into ploughshares (all history from (Ham and Hall 2006))

The initial reactor piles built at the Windscale works were designed for the production of plutonium with no intention of heat recovery for electricity generation. Remarkably, the piles were built in just three years from 1947 to 1950 an achievement overseen by Christopher Hinton. The reactors consisted of a large block of graphite into which horizontal channels for fuel and cooling were placed. The fuel was pure uranium metal encased in an aluminium cladding while temperature control was via air-cooling. A concrete biological shield surrounded the entire core (UKAEA 1989). It was soon realised that the 'waste' heat could be harnessed to produce steam, which could go on to be used in turbines and produce electricity.

Power generation necessitated a change in reactor design and three major modifications were required. The cooling gas had to be pressurised; a low-pressure gas does not have sufficient heat removal properties to produce steam. The increased pressure allows for a greater thermal efficiency so that conventional steam turbines could be used. Pressurisation was to be realised by surrounding the reactor core in a steel pressure vessel. The second modification was the move away from air as the cooling medium. At sufficiently high pressures, nitrogen would act as a neutron absorber and this would limit the effectiveness of the reactor. Carbon dioxide was chosen as it has low neutron absorption and good thermal properties. Finally, the increased operating temperature required a change in cladding to a magnesium alloy. The use of this alloy led to the generic name of Magnox (MAGnesium-Non-Oxidisable) for

these first generation nuclear power plants. The Magnox cladding had the advantage of a low neutron cross section, which was important for the neutron economy. In the development of Magnox, there was no spare civilian capacity for uranium enrichment, thus the reactors had to use natural uranium (Carruthers 1965).

The first Magnox reactor was to be built near Windscale, at Calder Hall. Construction started in 1953 and the reactor was opened in 1956 (The Engineer Magazine 1956), a mere 14 years since Enrico Fermi, in Chicago, demonstrated the first sustained nuclear reaction (World Nuclear Association 2010). The opening was a source of national pride. The Suez crisis was limiting the amount of oil reaching the UK and nuclear power offered an alternative. Calder Hall, rated at 50 MWe (Megawatt electrical), was the first nuclear power station to generate electrical power on an industrial scale (although, the Soviet reactor at Obninsk had a 5 MW output connected to the public supply in 1954, the 'industrial scale' qualifier, implying a commercially usable reactor, differentiates between the two. USA stakes a claim to the first entirely civil nuclear power plant with the Shippingport reactor, first operational in 1957 (World Nuclear Association 2010).).

In February 1955, the government published a white paper indicating its desire to pursue a nuclear option (The Minister of Fuel and Power (Mr Geoffrey Lloyd) 1955). The document stated that the initial generation of reactors would be based on the Magnox design but future generations would seek improvements to the gas-cooled design and further generations should attempt to exploit a liquid coolant. It also outlined the limited amounts of known uranium sources at the time and that fast breeder reactor technology should be investigated.

The technological process required to separate plutonium for weapons was the same technology used as a base for future fuel reprocessing. The economical justification for Magnox stations included a 'plutonium credit' that assigned a

value to the plutonium produced. While this credit was never paid to the plant operators, it showed a commitment that plutonium should not be considered as a waste.

At the time, no single British company had the necessary skills and expertise to build a reactor. A number of consortia were created and allowed to compete to build each new station. This parallel construction has led to problems in terms of decommissioning; almost every reactor is unique. Yet, the constant improvement did have some benefits, for example in the pressure vessel welding. At Calder Hall, the thickest weld was two inches, while at Dungeness A, a thickness of four inches was achievable. In doing so, the operating pressure was substantially increased from 6.9 to 19.35 bar with power outputs increasing from 50 to 219 MWe (Ham and Hall 2006). A further white paper in April 1957 (The Paymaster-General (Mr Reginald Maudling) 1957) suggested an increase in nuclear power generation to between 5,000 and 6,000 MW by 1965.

In October 1957, a routine operation in Windscale Pile 1 caused a major incident. A fire developed and an amount of radioactive material was released to the environment. This caused the shut down of the two piles and a full investigation was launched. One of the major outcomes of the investigations was the founding of the NII (Nuclear Installations Inspectorate) in July 1959. This technically competent group is seen as a foundation for a safe nuclear industry. The nuclear plant build programme continued without pause and the Magnox fleet was constructed in a series of tranches as summarised in Table 1. The capacity desired in the 1957 report was reached by 1971, six years after the original 1965 target. The reasons cited were a difficulty in rolling out the technology and the rapid decrease in oil price. The increase in power rating for the Wylfa station was a result of the decision to use pre-stressed concrete containment rather than steel, an idea taken from the French nuclear industry. This technology was fully utilised in the next generation of reactor, the AGR.

The AGR (Advanced Gas-cooled Reactor) was the next logical step from the Magnox design. The desire for an increased operating temperature to match standard steam turbines necessitated the change from uranium metal fuel to the ceramic uranium dioxide. In addition, for the first time, there was now spare civil enrichment capacity to produce enriched uranium, which would allow an increased power density in the reactor cores. A prototype station was built at Windscale, the WAGR (Windscale Advanced Gas-cooled Reactor). The prototype performed excellently and the design was selected to provide a further 8,000 MW of power in total. The first AGR programme was plagued by difficulties with Dungeness B taking 20 years from construction until generating electricity reliably. None of the other stations suffered such serve delays.

Tranche	Station	Contract Year	Commissioning Year	Closure Year	Output (MW)
1	*2 intended* Berkeley Bradwell	1957 1956 1956	1960/61 1961 1962	 1989 2002	 270 300
2	*2 intended* Hunterston A Hinkley A	1958/1959 1956 1957	1963 1964 1965	 1989 2000	 320 500
3	*4 intended* Trawsfynydd Dungeness A Sizewell A Oldbury Wylfa	1960 1960 1960 1961 1962 1964	1963/64 1965 1966 1966 1967 1971	 1991 2006 2006 2012 >2012	 500 550 580 600 1180
3a	*4 intended*	1961/62	1965		
Total Capacity					4800

Table 1: Proposed and actual Magnox fleet power stations

The following years were marked by political turmoil. The over arching decision to "buy-British" was detrimental to the advance of nuclear technology in general. The American PWR (Pressurised Water Reactor) design that had been rolled-out in France was a source of contention with politicians favouring the SGHW (Steam Generating Heavy Water, prototype at Winfrith) while more technical minded professionals favoured the PWR. Two more AGRs were seen

as a politically easy option and the decision about the PWR was to be delayed. Eventually, after the longest running UK public enquiry, the first PWR in the UK was built as Sizewell B. The second build programme is summarised as Table 2.

Build Programme	Station	Contract Year	Commissioning Year	Expected Closure	Output (MW)
First	Dungeness B	1965	1983-85	2018	1200
	Hinkley Point B	1966	1976	2023	1250
	Hunterson B	1967	1976	2023	1250
	Hartlepool	1967	1983-84	2019	1250
	Heysham	1970	1983-84	2019	1250
Second	Heysham II	1980	1988-89	2023	1240
	Torness	1980	1988-90	2023	1240
	Sizewell B (PWR)	1983	1994-95	2035	1180

Table 2: AGR and PWR Plant builds

While this history represents all of the commercial stations ever built in the UK, it does not include the history of the companies that own and operate the stations nor does it include the various prototype reactors. The main stories are; the rise, fall, and rise again of BE (British Energy); the privatisation of the generating boards; the formation of Magnox PLC; the creation and then break up of BNFL (British Nuclear Fuels Limited); and the formation of the NDA (Nuclear Decommissioning Authority). The NDA has overall responsibility for the legacy sites that were deemed not commercially viable for BE to own and operate (namely Sellafield, the Magnox fleet, Low Level Waste Repository near Drigg, and others). They also have the responsibility for the waste produced by this large variety of power stations.

The current UK picture is that all of the AGR are still in use as well as the PWR at Sizewell. The only operating Magnox reactor is at Wylfa. The current capacity is ~11 GWe and accounts for about 19% of UK power generation (World Nuclear Association 2012).

2.2 The UK Nuclear Fuel Cycle

The uranium fuel cycle can be operated in two ways; the differences lie after the power station. A **once through cycle** involves the mining, enrichment and production of fuel to be irradiated in a reactor. The spent fuel is allowed to cool for a period before being disposed of intact. In a **closed cycle,** a true cycle, the initial fuel is manufactured as in a once through cycle but after burning in a reactor, it is reprocessed and the fission products are treated as waste. The large amounts of reusable material, between 96 and 99% by weight (depending on the fuel/reactor combination) (Wilson 1996), can be manufactured into new fuels. The new fuel could be burnt in a further reactor and reprocessed again. In theory, the cycle continues until all the fissile material has been consumed. The UK operates a partial closed fuel cycle in that the spent nuclear fuel is reprocessed once and the separated fissile materials are stored for future use rather than re-used (much of the following section is based on lecture notes from (Robertson 2010) which were based on (Wilson 1996)).

The UK has complete closed fuel cycle facilities after the initial ore exploitation. Uranium is enriched at Capenhurst, fuel manufactured at Springfields, the fuel is consumed in reactors across the country and finally it is reprocessed at Sellafield. The decision to operate a closed fuel cycle is a historical one based on the weapons programme and the subtleties of the original Magnox power plants (the Magnox cladding corrodes extensively in wet storage) (World Nuclear Association 2012).

The closed fuel cycle is summarised as follows.

Uranium is found naturally as an ore and must be **mined and milled** to produce a useful product. Uranium ores may be up to 20 wt% uranium but currently viable ore deposits are greater than 0.1 wt% uranium (World Nuclear Association 2012). Over twenty countries operate uranium mines although 58% of the world's supply comes from just ten mines in six countries (Australia, Kazakhstan, Russia, Canada, Niger and South Africa). The uranium is extracted

from the ground by open cast, underground or in-situ leaching. Which method is used is dependant on the properties of the ore body.

The uranium bearing materials must be separated from the waste rock. It is possible that other minerals can be co-extracted. Milling is a combined physical and chemical process in which the product is concentrated uranium oxide, also known as yellowcake[1]. Often the mill is co-located with the mine in order to minimise the transportation of unwanted excess material.

The concentrated uranium must be **purified and converted** into a form suitable for enrichment (UF_6). Conversion takes place at Springfields. The uranium concentrate may still contain small impurities that will adversely affect the performance of the fuel and must be purified. These two processes are typically combined but may be carried out in a different order. For example, purification may be carried out first, as in the wet process, or it may be carried out after conversion, as in the dry process.

In the dry process, the yellowcake is reduced to UO_2 and some impurities. This mixture is then hydro-fluorinated and many of the impurities are collected as volatile fluorides. The uranium is converted to UF_4, which is then further fluorinated to the final UF_6 product required. This gas is then chilled to form a liquid (at above atmospheric pressure) and the final impurities are removed by distillation. The advantage of the dry process is that it has fewer stages and therefore fewer mechanical parts could go wrong but in practice, it is less robust and reliable than the wet process.

The wet process removes the impurities in the first stage by solvent/solvent extraction. The yellowcake is dissolved in nitric acid. This is then filtered and cooled to remove the insoluble material. TBP (Tri-n-butyl phosphate) is added in an organic solvent. TBP selectively forms organic soluble uranyl complexes. The organic solvent is then separated from the aqueous layer, which includes

[1] U_3O_8, so called because of its yellow colour.

all the impurities. The organic phase is then calcined to dryness and the uranium is reduced to UO_2. This is hydro-fluorinated and fluorinated to UF_6, which is cooled and stored as the product.

For the AGR and PWR reactors, natural uranium is not sufficiently rich in fissile material to be used as a fuel and it must undergo **enrichment (**natural uranium is 0.72% ^{235}U whereas PWR and AGR fuel requires the ^{235}U to be between 3-5%)**.** In the UK, Urenco at Capenhurst undertakes enrichment. Enrichment is a process that separates the uranium isotopes by their mass differences. No chemical reactions take place and this separation is an entirely physical process. The UF_6 is a gas at relatively low temperatures and pressures[2] and this allows gas separation technologies to be used

Gas centrifuges are the principle technology in use by Urenco and rely on the mass difference between molecules. A rapidly rotating cylinder containing the gas produces an outward force equivalent to a 100,000 times the acceleration due to gravity. This forces the slightly heavier $^{238}UF_6$ towards the outer of the cylinder and the lighter $^{235}UF_6$ concentrates in the inner. Approximately 20 stages are required for 3% enrichment but the low capacity means that up to 10,000 are needed in an operational plant. Centrifuge technology consumes 5% of the power required by the older diffusion plants, has lower hold up times (~days as apposed to years for diffusion) and has a good modularity which is important for expansion potential. Centrifuge technology has been very difficult to develop. The technical challenges of having such fast rotating equipment are the main barrier to entry.

The enriched uranium hexafluoride must be **de-converted** to produce uranium in a suitable form for **fuel manufacture**. Westinghouse at Springfields manufactures all UK fuel types. Magnox fuel is metallic uranium produced from UF_4 (obtained part way through the conversion process) in a redox

[2] UF_6 sublimes at 56.5 °C at atmospheric pressure.

reaction with magnesium metal. The resultant uranium metal is poured and moulded. The fuel rod is placed in the eponymous Magnox cladding and sealed to form the fuel element.

AGR and PWR fuels are uranium dioxide fuel pellets. UO_2 can be de-converted from UF_6 by two main methods: wet chemical routes including ammonium diuranate (ADU) route and the ammonium uranyl carbonate (AUC) route and the integrated dry route (IDR).

All three routes use the basic process of precipitation into an intermediate, solid-liquid separation, and calcination and reduction.

The ADU route takes the UF_6 feed and reacts it with aqueous ammonia hydroxide. This precipitates the ADU, which is separated, washed, and calcined and reduced to give the desired uranium oxide. Advantages include the controlled precipitation reactions to provide the optimal particle size distributions and that the effluents streams can be recycled to improve efficiency. Care must be taken to avoid criticality in the aqueous streams.

The AUC route takes a very similar path to that of ADU except that the AUC can be precipitated in the first stage upon the addition of UF_6 to ammonium hydroxide and uranyl carbonate. The main advantage is that the product is a free flowing powder of uniform size eliminating the need for further processing.

Finally, IDR, now commonly used in the UK, uses the counter-current flow of hydrogen gas against the UF_6 and steam. At the end of the reactor, free flowing UO_2 granules are produced without the need for an aqueous environment and removing the need for batch-wise processing.

The UO_2 must be manufactured in fuel pellets before further use. The powders are mixed with suitable additives to provide the necessary properties; porosity controllers, burnable neutron poisons and pressing lubricants. This mixture is pressed and sintered to form dense pellets. These pellets are assembled into fuel rods, which are further combined into fuel assemblies.

The fuel is loaded into a reactor. Here it is "**burned" (i.e. irradiated)** to produce thermal energy, which is harnessed to produce electricity. Power generation within the UK was discussed earlier. After irradiation the spent fuel is highly radioactive and still generates a significant amount of heat. From this point, the fuel must be handled with radioactive shielding to protect the operators.

A standard nuclear reactor uses fission to release energy. Nuclear fission is the splitting of an atom by the impact of a neutron. In splitting apart, the atom splits into two or more parts, releases energy (typically as kinetic energy of the new atoms) and more neutrons. This energy is transferred to the coolant, typically water but can be CO_2 in the case of AGR and Magnox. This heat energy is used to produce steam, which powers a turbine and in turn generates electricity.

The atoms produced are termed the fission products. These typically unstable radionuclides decay and continue to produce radiation and heat energy. They may also act as poisons that absorb the neutrons required for fission of the fuel. These poisons are the reason why all of the fissile material in the reactor fuel cannot be completely consumed. Additionally, some of the neutrons may be absorbed by part of the fuel, which does not undergo fission, and produce heavier new synthetic elements. These elements are the trans-uranics and include plutonium.

The uranium fuel contains two main isotopes, ^{235}U that is fissile, and ^{238}U, which is fertile. ^{235}U will undergo nuclear fission with thermal neutrons while ^{238}U will absorb a neutron and after successive decays will become a new fissile element, plutonium.

The scheme below is given as an example of plutonium production from uranium *via* a neptunium intermediate.

$$^{238}_{92}\mathrm{U} + ^{1}_{0}\mathrm{n} \rightarrow ^{239}_{92}\mathrm{U} \xrightarrow[23.5\ \mathrm{min}]{\beta^-} ^{239}_{93}\mathrm{Np} \xrightarrow[2.36\ \mathrm{days}]{\beta^-} ^{239}_{94}\mathrm{Pu}$$

The text on the arrows gives the type of decay and half-life. The ^{239}Pu may also absorb further neutrons and increase in mass up to ^{243}Pu. ^{238}Pu is an important isotope but is produced in useful quantities by a different route.

Spent LWR (Light Water Reactor) fuel contains approximately 96% uranium, 1% plutonium and 3% fission products. The UK historically operated a complete policy of **reprocessing** this spent fuel to extract the 97% of still useful materials. The initial decision to reprocess is a remnant from the weapons programme, which was compounded by the need to reprocess Magnox spent fuel. Reprocessing is undertaken on the Sellafield site.

Two reprocessing plants exist at Sellafield: B205 for Magnox metallic fuels and ThORP (Thermal Oxide Reprocessing Plant) for oxide fuels from most other reactor types. Both plants utilise the PUREX process. PUREX (Plutonium, Uranium Extraction) is a solvent/solvent extraction technique that uses TBP as the complexing agent in OK (Odourless Kerosene) as the non-aqueous solvent (World Nuclear Association 2012). The spent fuel rods are sheared into small sections, which have the fuel dissolved out of them by nitric acid. This is exposed to the TBP/OK mix. The uranium and plutonium are selectively complexed to form non-aqueous soluble complexes. These complexes are retained in the OK, which is washed with further nitric acid to remove any actinides that may have remained in the product stream. This is repeated a number of times. The uranium and plutonium selectivity against fission products is high leaving only trace amounts of fission products in the uranium/plutonium stream.

The uranium/plutonium stream is passed through a similar solvent/solvent extraction process as for the actinide stripping, to separate the two. Finally, the materials are calcined to produce oxide powders that are suitable for long-term

storage. The fission products stream is sent for further processing and is eventually immobilised in a vitrified product[3].

Reprocessing does not produce radioactive wastes but it does separate them into distinct categories. The UK uses four classifications of waste[4].

VLLW (Very Low Level Waste) is waste that can be safely disposed of with ordinary refuse. Each 0.1m^3 must have an activity less than 400 kBq of beta/gamma activity or single items with less than 40 kBq.

LLW (Low Level Waste) is waste that is not suitable for disposal with ordinary waste but must not contain more that 4 GBq/tonne of alpha activity or 12 GBq/tonne of beta/gamma. These wastes are typically sent to the Low Level Waste Repository near Drigg in Cumbria.

ILW (Intermediate Level Waste) is waste with a greater radioactivity than LLW but is not significantly heat generating. It is typically fuel cladding and reactor components. Predominantly it is encapsulated in cement and will be disposed of in the GDF (Geological Disposal Facility).

HLW (High Level Waste) is waste that is more radioactive than LLW and generate significant amounts of heat that must be accounted for when designing any storage or disposal facilities. The waste is typically fission products, which are separated through reprocessing and vitrified.

Further details about the UK waste inventory can be found in The Radioactive Waste Inventory (NDA 2010).

After reprocessing, the useable fissile material can be recycled into new fuel. The uranium may be re-enriched and the plutonium may be down blended with uranium to produce **MOX fuels**. MOX fuel is a blend of uranium oxide and plutonium oxide that is a suitable fuel to be used in thermal reactors.

---

[3] Vitrification is the process of turning a material into a glass.

[4] A waste is any material that has no further useful purpose.

Technical subtleties, such as power fluctuations across the core, prevent an unmodified reactor, or one that was not designed for, being 100% MOX loaded.

3 Plutonium as a Material

Plutonium has one of the most interesting histories of any chemical element. After neptunium, it was the second synthetic element to be created. The interest in plutonium has been fed from its dual use; the unprecedented power for weapons and domestic power production. Indeed, within five years of its discovery, its main use was in weapons.

From a technological perspective, it is one of the most complex elements. The metal exhibits six different allotropes and with small changes in the environmental conditions, its density can change by up to 25%. Every isotope of plutonium is radioactive. Some of these isotopes are useful while others make handling of the material radioactively difficult. In terms of reactor physics, the odd numbered isotopes (^{239,241}Pu) are fissile whereas the even numbers (^{238,240,242}Pu) are fertile.

3.1 History

When the first of the trans-uranic elements, neptunium, was produced there was a quick realisation that its β-decay should lead to element 94. Although, by this technique, the quantity isolated precluded any detailed analysis. The first measurable amounts were produced by Seaborg, McMillan, Kennedy and Wahl in 1940 (Seaborg, McMillan et al. 1946). They bombarded uranium with deuterons[5].

$$^{238}_{92}\mathrm{U} + ^{2}_{1}\mathrm{H} \rightarrow ^{238}_{93}\mathrm{Np} + 2\,^{1}_{0}\mathrm{n}$$

$$^{238}_{93}\mathrm{Np} \xrightarrow[2.1\ \mathrm{d}]{\beta^-} ^{238}_{94}\mathrm{Pu}$$

[5] Deuterium or heavy hydrogen is an isotope of hydrogen with one proton, one neutron and one electron; ^{2}H.

The short half-life of ^{238}Pu was amenable to tracer studies and allowed enough chemical information to develop suitable separation techniques for other isotopes. In 1941, ^{239}Pu was created and the importance of this isotope was confirmed when Kennedy, Seaborg, Segré and Wahl established its fissile nature (Kennedy, Seaborg et al. 1946). In March 1942, the new element was christened plutonium in keeping with the sequence of the previous elements and the planets at that time[6]. ^{239}Pu was created using the same method as for ^{238}Pu but with a cyclotron providing neutrons (as apposed to deuteron ions). In August 1942, Cunningham and Werner (Cunningham and Werner 1949) had produced the first visible quantity of a man-made element.

3.2 Nuclear Properties

Twenty different isotopes of plutonium have been synthesised ranging from mass numbers 228 to 247. Table 3 summarises the key isotopes, their half-lives and the main method of production. The main isotopes are produced in thermal nuclear reactors and the plutonium is chemically separated during spent fuel reprocessing.

There are lighter isotopes but these are created through heavy ion bombardment or through a low probability series of neutron captures. Heavier isotopes are created through more neutron captures of lighter plutonium. The short half-life of ^{243}Pu greatly decreases the probability of further unlikely neutron captures.

The design of a reactor greatly influences the isotopic mix of the plutonium produced. The first iteration of the Magnox reactors was for the dual purpose of producing weapons grade plutonium and energy. Magnox spent fuel has the highest isotopic proportion of ^{239}Pu after reprocessing.

[6] Uranus → Neptune → Pluto: Uranium → Neptunium → Plutonium

Mass Number	Half-Life	Mode of Decay	Main Radiations (MeV)	Method of Production
238	87.7 yr 4.77 x 10^{10} yr	α SF 1.85 x 10^{-7}%	α 5.499 (70.9%) 5.456 (29.0%)	^{242}Cm daughter ^{238}Np daughter
239	2.411 x 10^{4} yr 8 x 10^{15} yr	α SF 3.0 x 10^{-10}%	α 5.157 (70.77%) 5.144 (17.11%) 5.106 (11.94%) γ 0.129	^{239}Np daughter
240	6.561 x 10^{3} yr 1.15 x 10^{11} yr	α SF 5.75 x 10^{-6}%	α 5.168 (72.8%) 5.124 (27.1%)	multiple n capture
241	14.35 yr	β^->99.99% α 2.45 x 10^{-3}% SF 2.4 x 10^{-14}%	α 4.896 (83.2%) 4.853 (12.2%) β^- 0.021 γ 0.149	multiple n capture
242	3.75 x 10^{5} yr 6.77 x 10^{10} yr	α SF 5.54 x 10^{-4}%	α 4.902 (76.49%) 4.856 (23.48%)	multiple n capture
243	4.956 h	β^-	β^- 0.582 (59%) γ 0.084 (23%)	multiple n capture
244	8.08 x 10^{7} yr 6.6 x 10^{10} yr	α 99.88% SF 0.1214%	α 4.589 (81%) 4.546 (19%)	multiple n capture

Table 3: Selected plutonium isotopes from (Clark, Hecker et al. 2008). SF is Spontaneous Fission.

3.3 Isotopes of Note

3.3.1 ^{238}Pu

^{238}Pu is of note due to its use as a radioisotope power system. In such a system, the heat generated by the radioactive decay of the material is converted into an electrical potential. It is obtained, in useful quantities, by the neutron bombardment of ^{237}Np (Tetzlaff 1962) or by the alpha decay of ^{242}Cm. Its large power density of 6.8-7.3 W cm^{-3} (specific power 0.57 W g^{-1}) allows this material to be used as a heat and power source in spacecraft. ^{238}Pu is enriched to 83.5% and converted to PuO_2. Oxygen is also enriched in the ^{16}O isotope (i.e. reduction

of $^{17,18}O$) and this helps reduce the neutron emission to 6000 neutrons $s^{-1}g^{-1}$, which aids in handling. These RTG (Radioisotope Thermoelectric Generators) have been used by the US in space exploration since 1961. Indeed, the five Apollo missions that landed on the moon used RTG.

^{238}Pu has also been used as power sources in pacemakers. The first of such was implanted in 1970 but advances in electronics have rendered them obsolete. Some of the pacemakers had functioned for over 30 years (Parsonnet, Berstein et al. 1990).

^{238}Pu can also be used for accelerated aging studies of candidate wasteforms. Its much shorter half-life (87.7 years) allows samples containing predominately ^{238}Pu to experience a similar number of radioactive decays in ~45 years that a sample containing ^{239}Pu would in ~12000 years. Potentially allowing one sample to be continuously followed throughout the research career of an individual (or at least a single company).

3.3.2 ^{239}Pu

^{239}Pu is the most important isotope of plutonium. Its half-life is of sufficient length to allow chemical studies to be performed and most scientific analysis is carried out on this isotope. Although its half-life may be long, it is still sufficiently short to cause handling issues. ^{239}Pu has a large cross-section of fission by thermal neutrons and is accordingly the isotope that is of most importance as nuclear fuel for power generation and for weapons. This ease of fission can cause difficulties in handling; less than 500g can become critical in a nitrate solution.

^{239}Pu is formed by a single ^{238}U neutron capture, as discussed earlier. In a thermal power reactor, approximately a third of the energy produced is by the fission of ^{239}Pu. Indeed, over half of the plutonium created is burnt in the reactor before the fuel is removed.

3.3.3 ^{240}Pu

^{240}Pu is a neutron emitter and has a higher specific heat production than ^{239}Pu. These characteristics make it a difficult contaminant in weapons: weapons grade plutonium is defined by having less than 8% ^{240}Pu. It is formed by successive neutron captures from a long burn up in a reactor.

3.3.4 ^{241}Pu

^{241}Pu is another fissile isotope and can be used as well as ^{239}Pu in fuel. Its decay to ^{241}Am with a half-life of 14 years means that stored plutonium becomes less fissile with time. The threat of the in-growth of ^{241}Am encourages any separated plutonium to be used quickly and suggests that the longer any plutonium is stored, the less useable it may become. Examination of the half lives suggests that an extended storage period will allow all the ^{241}Pu to decay to ^{241}Am which can be easily separated from the remaining ^{239}Pu, thus allowing power reactor plutonium to become closer to weapons grade.

3.4 Chemistry

The chemistry of plutonium has been analysed in detail elsewhere and is beyond the scope of this piece of work. For further information, the reader is directed to The Chemistry of the Actinide and Transactinide Elements (Clark, Hecker et al. 2008).

4 Plutonium Options

4.1 Introduction

The NDA has sole responsibility of discharging the policy of the UK Government for the UK civil stockpile of plutonium (NDA 2011). As such, it is their decision as to how to implement policy on this zero-value asset. A zero-value asset is an asset that has no value on the balance sheet. Accordingly, it

will not depreciate over time[7]. This classification allows the NDA to judge all of the available disposition options without having already defined the fate of the material.

The scope of the strategy comprises all the plutonium currently stockpiled on the Sellafield site. This includes foreign material and material owned by EdF (Élecitcitè de France, formerly BE). The foreign material is included, as any strategy implemented is required to deal with the material on a continuing basis. Thus, interim storage of foreign materials needs to be accounted for. It is recognised that this strategy could change if;

- EdF decide not to reprocess their fuel, favouring a different route
- MOD owned material was added into the scope
- An alternative strategy was adopted for foreign material

The UK has the largest stockpile of civil separated plutonium in the world (NDA 2010). Of the ~290 tonnes worldwide separated civilian plutonium, the UK holds approximately 100 tonnes. In recent years, there have been international moves to reduce the plutonium stockpiles to limit the threat of terrorist activities and to aid world politics. The New START (Strategic Arms

[7] A zero value asset arises in two situations. A normal situation would be that an asset has depreciated linearly over its life until it is now worthless. If the company was required to liquidate its assets then zero value could be realised. The other situation is almost unique to the nuclear industry. As soon as an asset (such as machinery or equipment) or material is irradiated, even though it still has an intrinsic value, it will incur a cost to realise that value. In this case, the equipment has a value but it may cost the same amount to decommission in order to realise that value, thus summing to zero net charge.
The subtlety is that plutonium is essentially free to the NDA and they can do with it as they wish but no other organisation in the UK is suitable to deal with the material, so they will always be liable.

Reduction Treaty) came into force on the 8th April 2010 and with it a renewed vigour to reduce weapons (BBC 2010). Obviously, a reduction in warheads will lead to an increase in separated plutonium.

Although the UK is not a signatory to New START, any technology developed to serve the UK needs, may be applicable to other nations. It should be noted that each country will have different grades of separated plutonium and a strategy for one country may not be directly applicable to another but the fundamentals of any immobilisation technology will be transferable.

Figure 1 shows the world's separated plutonium as stored by country. There are four large contributors, other than the UK, and a number of smaller stocks.

France has a large home grown nuclear industry with ~75% of their electricity coming from nuclear power (World Nuclear Association 2012). The industry is well harmonised with fuel reprocessing at the La Hague site since 1976 and MOX manufacture at the MELOX plant in Marcoule, which is irradiated in French reactors with approximately 17% of all electricity coming from recycled nuclear fuel. This consumption of plutonium has led to a civil stockpile of ~50 tonnes. The French CEA (Commissariat à l'énergie atomique et aux energies alternatives, Atomic Energy and Alternative Energies Commission) has been pursuing a research and development programme into Generation IV reactors as a plutonium disposal option.

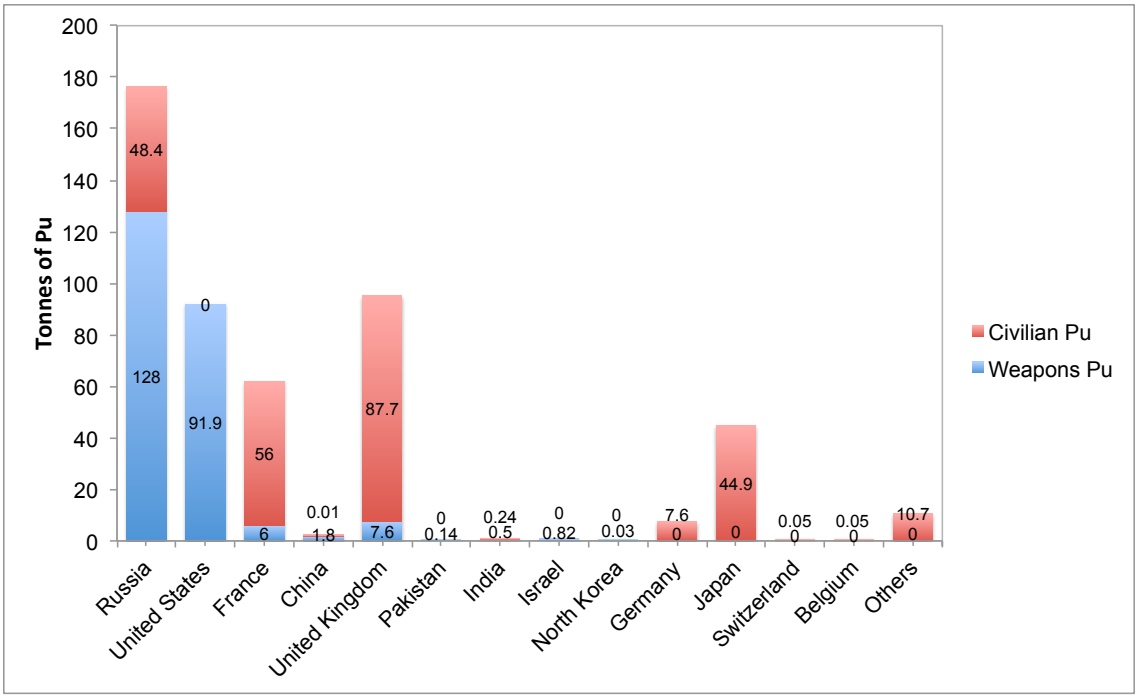

Figure 1: World Plutonium Stockpiles as of January 2012. Russian data is highly variable and best estimates are given. Some civilian stockpiles are likely to have increased through further separation and others decreased through consumption in reactors. This figure is drawn from data in The Global Fissile Material Report (International Panel on Fissile Materials 2011)

The **United States** has not utilised a programme of reprocessing civil fuel since 1977 citing concerns over non-proliferation (World Nuclear Association 2012). Even so, there is a declared stockpile of 61.5 tonnes of ex-military plutonium. Of this, the government has agreed to dispose of 34 tonnes by 2014. As part of the US-Russia Plutonium Management and Disposition Agreement, the intention is to incorporate it into MOX fuel (World Nuclear Association 2012). Construction of a MOX facility has begun at DOE Savannah River. This plant is designed to process the 34 tonnes of weapons-grade[8] plutonium into ~1,700 fuel assemblies.

[8] Weapons grade plutonium has a much higher fissile isotope concentration than reactor grade. It is defined as having less than 8% ^{240}Pu with the remainder being ^{239}Pu. It is produced by low fuel burn up in specifically designed reactors. It is unfeasible to produce weapons grade plutonium from normal reactor burnt fuel. For International Atomic Energy Agency, IAEA, safeguards all plutonium is defined as 'direct-use'. While they accept that the material can only explode

There is an option for the disposition of more plutonium should the government see fit. In parallel, Duke Energy has used four MOX test fuel assemblies at its Catawba 1 site. Two further sites have started MOX loading trials with the intention of 20-40% core loading starting in 2010, however, as of 2012, this does not appear to have happened.

Russia's policy is to close the fuel cycle as far as possible (World Nuclear Association 2012). The intention is to recycle the uranium as well as re-use the plutonium[9]; this has not been the case in practice, however. At present, spent fuel from the later generation of VVER (Vodo-Vodyanoi Energetichesky Reactor, the Russian equivalent to the PWR) and the RBMK (Reaktor Bolshoy Moschnosti Kanalniy) fleet is not reprocessed. The older generation of VVER fuel is reprocessed along with naval reactor fuel. A MOX facility for ex-weapons plutonium is under construction at Seversk with the same design being used for the US plant. The aim is to demonstrate parity with the US weapons disposal programme. Unfortunately, MOX experience in VVER is limited and the Russian programme appears to have stalled. The main limits are funding and preference for a fast reactor programme.

Japan currently imports ~80% of its energy requirements (World Nuclear Association 2012). The Fukushima accident in March 2011 has placed the energy policy of the country into turmoil. Previously, the intention was to increase the proportion of energy to come from nuclear to 40% by 2017, this is now under review. Historically, Japan attempted to recover all the energy possible from the uranium fuel; reprocessing at Sellafield and La Hague in France has done this. Japanese Nuclear Fuels Limited has constructed a new

---

under extremely technically demanding conditions, they believe all plutonium should be monitored.

[9] Russian opinion has always been that plutonium is a resource and is not to be discarded.

reprocessing facility at Rokkasho-mura (scheduled to open in October 2013). Nevertheless, ~26 tonnes of Japanese owned separated plutonium is stored in France and the UK. In April 2005, the J-MOX plant's construction was approved (expected to open in March 2016). Located adjacent to the Rokkasho-mura facility it has a capacity of 130 tonnes per year MOX fuel. A MOX burning strategy has had governmental support since 1994 even though it was not until late 2009 that a Japanese reactor was licensed to burn MOX.

4.2 The Current UK Strategy and Why The Need For Change

The current UK long term strategy for plutonium management is poorly defined. Plutonium is safely and securely stored on the Sellafield and Dounreay sites. The classification of plutonium as a zero-value asset and the lack of a government decision have not allowed the site licensees to plan their future activities.

The material is stored at two separate locations: Sellafield (as PuO_2 powder) and Dounreay (as a component of fast reactor fuel) (NDA 2011). The current plan of on site storage extends to the site closure dates but then assumes that the plutonium will remain *in situ*. There is no allowance for support and infrastructure to be kept in place after that. New stores, such as SPRS (Sellafield Product and Residues Store) have a design life of 100 years that requires refurbishment at 50 years: sufficient for site end dates but not for indefinite storage. Furthermore, the regulator does not consider plutonium oxide powder as a suitable passive form for long-term storage (NDA 2010).

As the operating budget of the site licensee, Sellafield Ltd, is limited, the company needs to prioritise its funds as to the management of materials. Without this clarification, decommissioning plans cannot be completed. There is also a need to include a cost of dealing with this material. Whichever disposition strategy is adopted a cost will be incurred. The lack of a pressing decision will also lead to the loss of skills and infrastructure to support any final

decision. Indeed, if the planned GDF is designed without plutonium in mind, there may need to be a second facility built.

The continuing storage of plutonium will require new facilities to be built or old ones upgraded. In doing so there may need to be a re-packaging of materials and this will increase costs. It may be less expensive to dispose of the material rather than continued storage. In addition, plutonium ages and with extended storage the ingrowth of americium reduces the fissile content of the material. This will make the fabrication of MOX much more difficult as the americium is a strong gamma emitter that increases the worker uptake dose. It is clear that there needs to be a defined plan for the future of the plutonium stockpile. What is not clear is what that plan will be.

4.3 Credible Options

In order to discuss the credible options available, a 'credible option' must be defined. The NDA uses:

"those options which could potentially be accomplished, safely, while complying with the law, and using technology which is either available or capable of being developed within the foreseeable future, and which allow decisions to be made on a timescale that is commensurate with any strategic imperatives"

For plutonium, the timescale has been set at 25 years (NDA 2010). This period was chosen as the longest foreseeable timescale for which a detailed technological future could be planned. This timescale immediately removes the possibility of certain advanced "Gen IV" reactors, such as fast reactors or high temperature reactors, which are currently estimated to have an operational lead-time of 40-60 years (the reader is directed to (OECD Nuclear Energy Agency 2010) for further details on Gen IV reactors).

Thus, the generic options for plutonium are:

- Store for a limited time
- Disposal as waste

- Recycle in a thermal reactor and ultimate disposal as spent fuel
- Some combination of the above

As noted before, there is a need to produce a strategy for the future management of plutonium but all of the above options include some period of interim storage. It is the view of the NDA that from a decision being made, there will be a lead-time of 30-50 years.

All of the options are judged against a number of criteria.

Reversibility is the ability to re-asses any option against future technologies. Any decision taken now will not be future proof.

Public Acceptability attempts to judge how well the public will tolerate or accept the option. A high level of acceptability is associated with reduced fear.

Policy Implications are how the chosen option will fit in with other government policies.

Risks are the outside factors that could affect the option. Examples are interdependent facilities not being constructed or a suitable market not being found.

Opportunities are the cost and safety improvements that could be achieved if the option is implemented.

None of these criteria is weighted but help provide a framework for each option to be measured against. Importantly, the base case for plutonium is the on going storage on the Sellafield site. What follows is a discussion on the general aspects of each generic option.

4.3.1 Continued Storage

This is defined as the contingency option. This option delays the need for a decision to be made. It is not sustainable nor is it prudent in the long-term. In order to assign a cost to this option, storage is assumed to last until 2120

(Sellafield site closure), by which time some other strategy will have been implemented.

Storage is inherently reversible, as no real decision has been made as to the end state of the material. As noted before, plutonium will age and this may preclude some of the recycle options. The lack of an end state is difficult for the public to accept, as shown by the pressure applied from a number of bodies, such as the regulator (however, their concern is related to the impact of safety on public perception). In defining disposal as an end state after continued storage then this option does have a conclusion. Conversely, some stakeholders will prefer a protracted decision period to allow new technologies to be developed and perfected.

The main risk is in the changing date of the Sellafield site closure. If the date was significantly brought forward then the time available for a final decision would be decreased. In addition, research may show that the material may become less stable with time. Indeed, the first separated plutonium was stored in PVC bags and due to radiolysis effects the polymer bags have broken down and led to the plutonium becoming contaminated with chlorine (Scales, Maddrell et al. 2007). Again, the ageing process will increase the gamma radiation emitted due to the in growth daughter products, which will require increased operator shielding.

4.3.2 Disposal

Disposal is "*the emplacement of waste in a specialised land disposal facility, without intent to retrieve it at a later time – retrieval may be possible but, if intended the appropriate term for this is storage.*" (DECC 2010). It is important to note that other wastes will be disposed of. These wastes will contain small amounts of plutonium in spent fuel or as PCM (plutonium-contaminated materials). Thus, there will have been experience in disposing of nuclear wastes. Disposal is considered the default option.

Furthermore, disposal can be broken down into two types: isolation and immobilisation. Isolation implies that the wasteform has no effect upon waste retention and that the repository design will account for all material losses. Whereas immobilisation states that, the wasteform will resist ground water infiltration and the repository design is secondary.

The four main processing routes are: encapsulation[10] in cement; immobilisation in glass; or immobilisation in a ceramic; or immobilisation in disposal MOX (these options are discussed in more detail in the next section).

The main advantage, yet potential disadvantage, of disposal is the lack of reversibility. It is by definition a permanent solution. If reversibility is desired from a policy perspective, then storage should be re-considered. For members of the public who view plutonium as an asset, disposal is not readily acceptable. Yet, stakeholders who believe the material should never have been separated typically view it as the 'least bad' option. A NIMBY[11] mentality can also form when siting the final depository.

Disposal assumes that the government has decided that plutonium will play no part in the energy future of the UK whether as part of security of supply or as an energy source. It also assumes that no foreign country, subject to legislation, has determined a need for the material. The design of the GDF will need to consider the suitability of any plutonium wasteform.

---

[10] The difference between immobilisation and encapsulation in a wasteform is subtle. Immobilising a material chemically bonds it to the wasteform. Encapsulation is the material becoming surrounded by the wasteform, rather than bonded to it.

[11] Not in my backyard – a mentality in which members of the public broadly agree to an idea yet disagree to it being located near their homes.

The reputation of plutonium may cause potential host communities to reject the location of the GDF. The fear that this fissile material may be more dangerous than other wastes is a concern that would have to be allayed. The siting and construction of a second GDF solely for plutonium would be very resource intensive. The advantages of taking an early decision to dispose of the material would be reduced storage and security costs and this would have to be offset against the need to store the immobilised waste before the repository has been commissioned. There will be a compromise between the decreased packing density of the wasteform (lower criticality concerns) and the increased volume.

4.3.3 Recycle

The recycle option is considered a route to final disposal whilst utilising some of the energy contained within the plutonium. The intention would be to manufacture new fuel[12], which would be consumed and not reprocessed. This would produce spent fuel that could be disposed of in the GDF. The isotopic concentration of the plutonium will have changed. To separate the plutonium again, the fuel would have to be reprocessed in a similar manner to the original spent fuel. The so-called "spent fuel standard"[13] (Office of International Affairs 2000) is a point of contention. There is no consensus that it is strictly necessary for ultimate disposal. As of December 2011, the preferred choice of the UK Government is to recycle plutonium as MOX for thermal reactors (DECC 2011). This decision is due to the evidence that recycling the fuel in a thermal reactor is the only proven method for sufficiently modifying the fissile vector of the plutonium so that it is no longer attractive for proliferation. The decision to re-use as MOX fuel may be revised subject to economic constraints.

---

[12] Current thinking is that the fuel would be MOX and loaded into conventional rectors rather than fast reactors.

[13] The spent fuel standard states that the waste should be as proliferation resistant as spent fuel.

The recycle option assumes that there is a market for the new fuel and that the Government is willing to sell this asset. There are a number of points in which the material can enter the supply chain:

- Sell or lease the plutonium to another country with the sole intention of creating new fuel
- Contract a 3rd party to fabricate MOX, either in the UK or abroad, and sell the fuel
- Directly fund the MOX fabrication and sell the fuel
- Fabricate MOX, utilise it in UK commercial reactors and take a share of the resulting electricity sales
- Fabricate MOX, utilise it in state owned reactors and sell the resulting electricity

Currently, MOX fuel can be used in Canadian and some European reactors. No UK reactor is licensed to use MOX but the potential nuclear new build will provide a larger market for MOX.

The recycle option is intended to be irreversible. The plutonium is consumed in the reactor and no amount of separation can recover the original material. However, the spent fuel still contains an amount of fissile material that could be extracted. If this were deemed necessary then it would require a large facility such as ThORP.

The level of public acceptability is the opposite to that of disposal. Those who view plutonium as an asset would view a recycle option positively as it will allow the energy contained within the material to be recovered. Although, some would prefer to see the plutonium more effectively used in fast reactor systems. Those who would have preferred plutonium never to have been separated may see recycling the material as an afterwards justification for the historical decision to reprocess.

A recycle option is a risky choice. There needs to be a defined market for the material and judging this market value will be difficult. New build has the possibility to increase the demand for MOX in the UK market and thus increase the cost of the material. It is likely that the most a utility will be willing to pay for MOX is equivalent to the cost of UO_2 fuel or potentially much less. The extra complexities of handling the un-irradiated fuel (e.g. extra security costs associated with handling plutonium containing materials, shielding for the fresh MOX fuel) may mean that the utilities ask for extra compensation and this will reduce the overall revenue the NDA can claim.

Assuming the technical feasibility, a proper assessment of the recycle option can only be taken if the Government makes further decisions as to what part plutonium plays in the UK energy strategy and the value it places on carbon off-setting.

4.3.4 Combinations

The final choice will undoubtedly be a combination of the other options. Continued interim storage will be used to give more time for technology to be developed. It is difficult to believe that disposal will not be required to dispose of some of the plutonium. The preference of the Government is towards re-use as MOX in thermal reactors, however this may change depending on the economic climate.

4.4 Conclusion

Clearly, many competing factors must be accounted for in deciding the future of the UK plutonium stockpile. The final decision will be a combination of the political will, technical feasibility and the economics. As stated, the preference is for re-use, however, there will always be a proportion of the plutonium that will not be suitable for re-use and must be immobilised.

5 Analysis of Options

The NDA have analysed the credible options in further detail allowing them to consider the financial implications, time scales and the technical readiness of each option (NDA 2010).

5.1 Definitions

The general options are split into:

Store until 2120 and dispose assumes the plutonium is stored on the Sellafield site under existing conditions, with the necessary maintenance, until 2100. Afterwards, the material is encapsulated or immobilised over a period of 20 years and transferred to the GDF. No allowance is made for the material stored at Dounreay.

Dispose of as a glass uses similar technology to the current operational vitrification plant. The immobilisation of 10 wt% plutonium is assumed and the process is to be completed by 2050. The wasteform is then stored until 2075 when it is placed in the GDF over a 20-year period.

Disposal as disposal MOX (use SMP) assumes that SMP[14] will become available to produce a disposal specification MOX fuel pellet that would not be suitable as a fuel and is correspondingly less expensive to manufacture[15]. The fuel pellets are then placed in an existing style of waste can. The plant will operate from 2025 to 2050 and disposal will begin in 2075 when a HLW GDF is available.

[14] SMP (Sellafield MOX Plant) was a MOX fabrication facility that was shut down in August 2011 as a direct result of the reduced markets for MOX fuel from Japanese reactor operators after the Fukushima incident.

[15] Disposal specification may be a differing level of fissile material or physical properties, such as size tolerances.

Disposal as disposal MOX (new plant) as the above option but the manufactured fuel pellets are placed into fuel assemblies and disposed of in the same manner as spent fuel. The timescale is the same.

Dispose of as a ceramic uses a ceramic wasteform to immobilise the plutonium. In the NDA strategy, the ceramic is not defined but it is to be processed by HIP (Hot Isostatic Pressing). The facility is assumed to operate from 2025 to 2050; the wasteform is then transferred to the GDF from 2075 onwards.

Disposal in cement assumes that the plutonium can be encapsulated in a cement matrix. Cement is extensively used to encapsulate a wide range of ILW including some PCM. Incorporation rate has a significant effect upon the cost. The facility is assumed to operate for 20 years from 2025 to 2045. If the material has a low waste loading then transfer to the disposal facility is assumed to occur from 2045 onwards. If the waste loading is high, then the material will have to be disposed of in a HLW GDF available from 2075 onwards.

Recycle as MOX assumes that the customer is Canadian or European. The fuel will be fabricated in the UK and then transported to the utility. The fuel is to be manufactured between 2025 and 2055.

Selling the plutonium powder to a third party for fuel is assumed to begin in 2013 and take 30 years to complete.

5.2 Technical Readiness

The technical readiness has been judged of each option (NDA 2010). Figure 2 shows the technical readiness of the eight options against their estimated lead-time.

A readiness of level 1 indicates that the technology has been researched at a basic level with the fundamental principles being observed. Levels 2 to 3 indicate that there has been some research to prove the feasibility whilst levels 4 to 5 are technological development and demonstration. This is characterised by component or bench validation in a relevant (active) environment. Levels 6 to 7

show that the system has been developed as a whole and prototypes have been demonstrated and then operated in the relevant environment. Level 8 indicates a full system has been constructed, tested and qualified through demonstration and finally, Level 9 represents a technology that has been implemented and proven through successful operation. The levels are not meant to be taken as exact figures but rather to illustrate where each technology is considered to be and their lead-time from when they mature (original definitions and development found at (Defence Acquisition University 2006)).

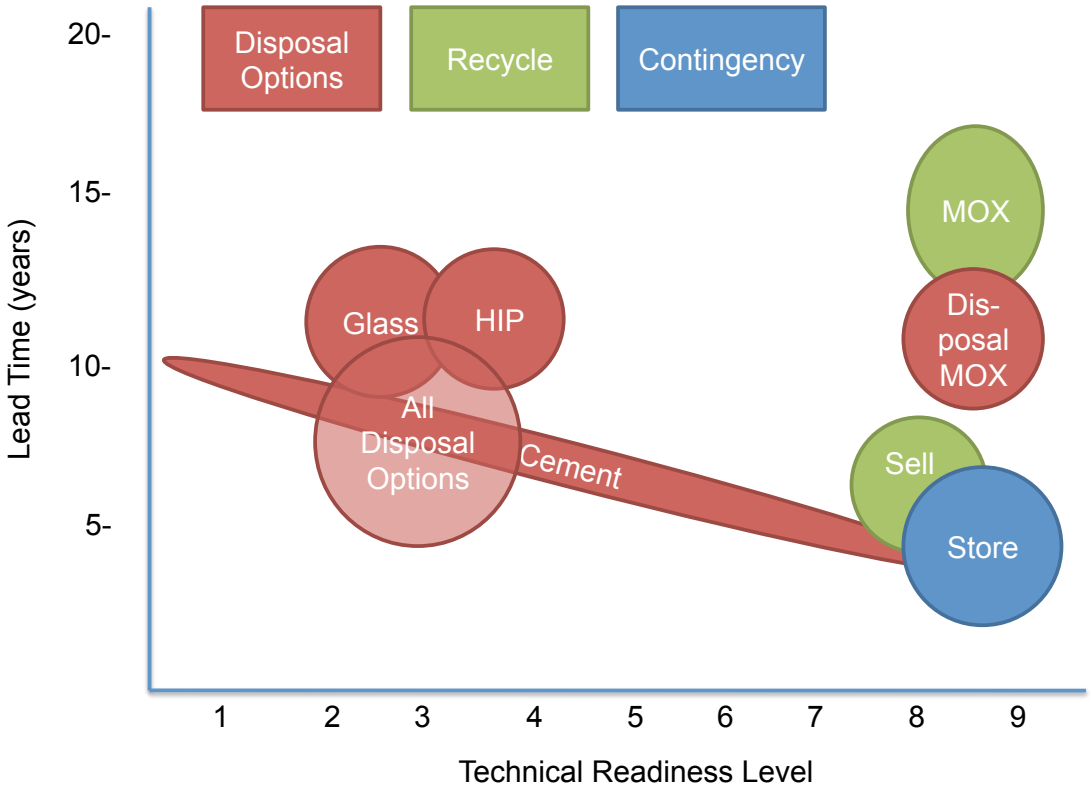

Figure 2: Technical readiness against lead-time, once the technology is mature, for the various plutonium options under discussion (NDA 2010). See text for an explanation of scoring system.

As expected, the technical readiness of storage, MOX manufacture and selling are high. Each of these options has a directly comparable operating facility within the UK. Selling is slightly less ready as there is no direct experience in doing so. HIP immobilisation and glass encapsulation have been demonstrated with inactive simulants but there is no experience of a full-scale active

demonstration plant[16] (Brummond, Armantrout et al. 1998). Cement readiness depends on the incorporation rate assumed. There is some experience with PCM but there is little experience with just plutonium encapsulation. The main issue appears to be difficulties in ensuring criticality control with a fissile material in a highly protonated medium. There is experience with building and operating active facilities but again, no experience with plutonium. It is possible that for higher waste incorporation rates, large modifications would be required for any existing wasteform design.

Lead-times associated with MOX indicate that this option may require policy change as well as constructing the facility. The slightly elliptical bubble indicates this uncertainty. The key point to draw from Figure 2 is that for the disposal option, a component of every plan, without further research, is not sufficiently mature for implementation.

5.3 Economic Analysis

At this stage in the development of the disposition options, it is very difficult to give exact costs. Each of the options will have a large uncertainty in its implementation. Accordingly, the NDA figures given should not be used for detailed analysis, but rather to be indicative.

In general, the disposal options have less uncertainty than recycling. In the disposal options, only the waste treatment plant and GDF have to be built, whereas recycling has an extra uncertainty with market development required to discover what reactor operators are willing to pay for MOX fuel. Correspondingly, MOX recycle is the most uncertain option whilst storage is the least.

[16] LLNL (Lawrence Livermore National Laboratory) in the USA got as far as designing a full-scale non-active plant and demonstrating each component in isolation. ANSTO (Australian Nuclear Science and Technology Organisation) have demonstrated the process on a small scale with active samples.

Estimates for each option on a 'per tonne plutonium dealt with' basis are shown in Figure 3. The costs include any revenue derived from the option (e.g. selling MOX fuel). Continued storage is the least expensive option and cement is the most. Encapsulation in cement is the most expensive as incorporation rates into the cement matrix are poor requiring a large number of waste packages. The sale of conditioned material requires what market there is for MOX fuel to be determined, however, the majority of costs are associated with transportation and initial treatment of the PuO_2 so that it is a suitable quality for fuel manufacture.

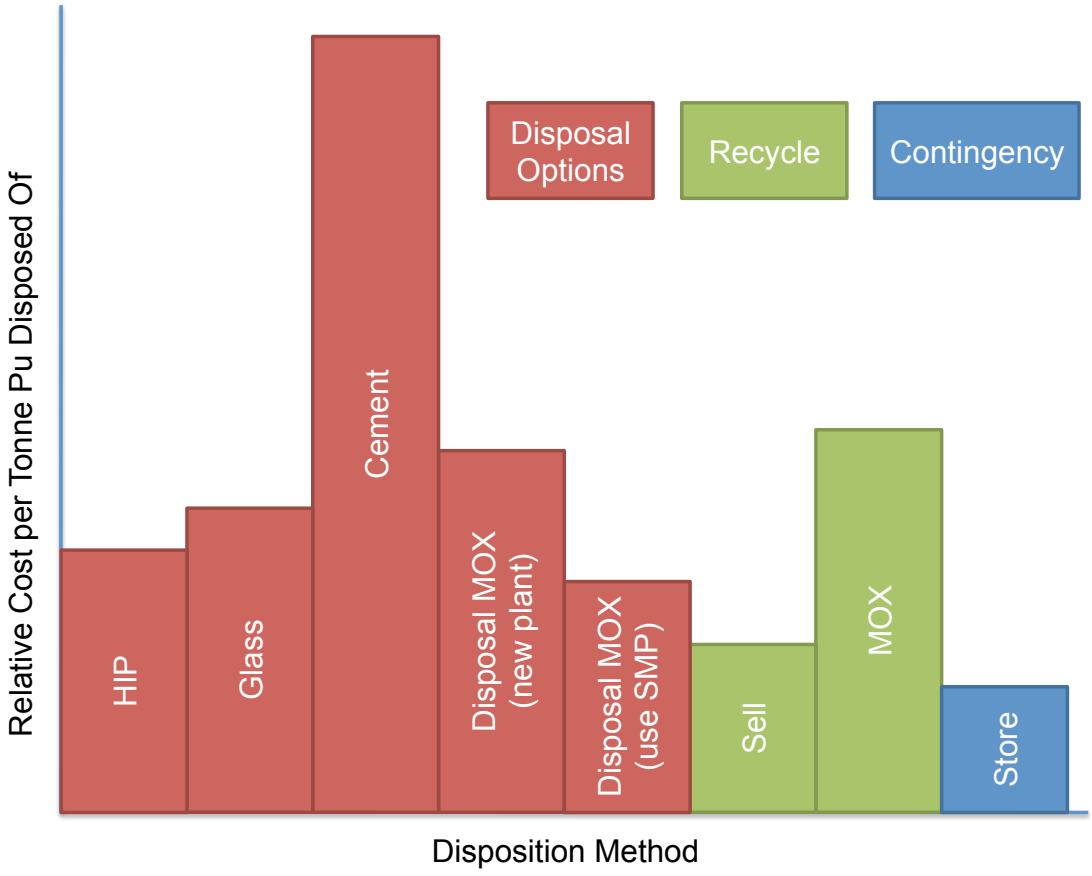

Figure 3: Comparative costs for 'each tonne of plutonium dealt with' for each option. Disposal MOX now includes 'new plant' and 'use SMP'. The lower cost represents not having to build a new facility (NDA 2010).

Each cost estimate consists of:

- New stores
- Capital cost of a new plant, including decommissioning
- New store for the immobilised waste prior to internment in the GDF and decommissioning of these stores
- Cost of transport
- Disposal costs

On a purely economic basis, selling the material is preferred and the least expensive disposal option is 'disposal MOX using SMP'. The closure of SMP has changed the possibility of utilising it for a disposal mission. It is unknown whether the likelihood has increased (the NDA may decide to make full use of the asset) or decreased (the plant suffered from technical difficulties and it is likely these would continue with the new mission). If a new plant is to be built, the ceramic disposal route becomes the most cost effective disposal option.

5.4 Socio-economic Implications

In siting nuclear facilities, there is always an impact on the local community. Accordingly, some indication of the employment potential of each option is important. Figure 4 gives the number of years of employment, which is created per option in the Sellafield Travel to Work Area. As with the other figures in this section, the numbers are purely indicative.

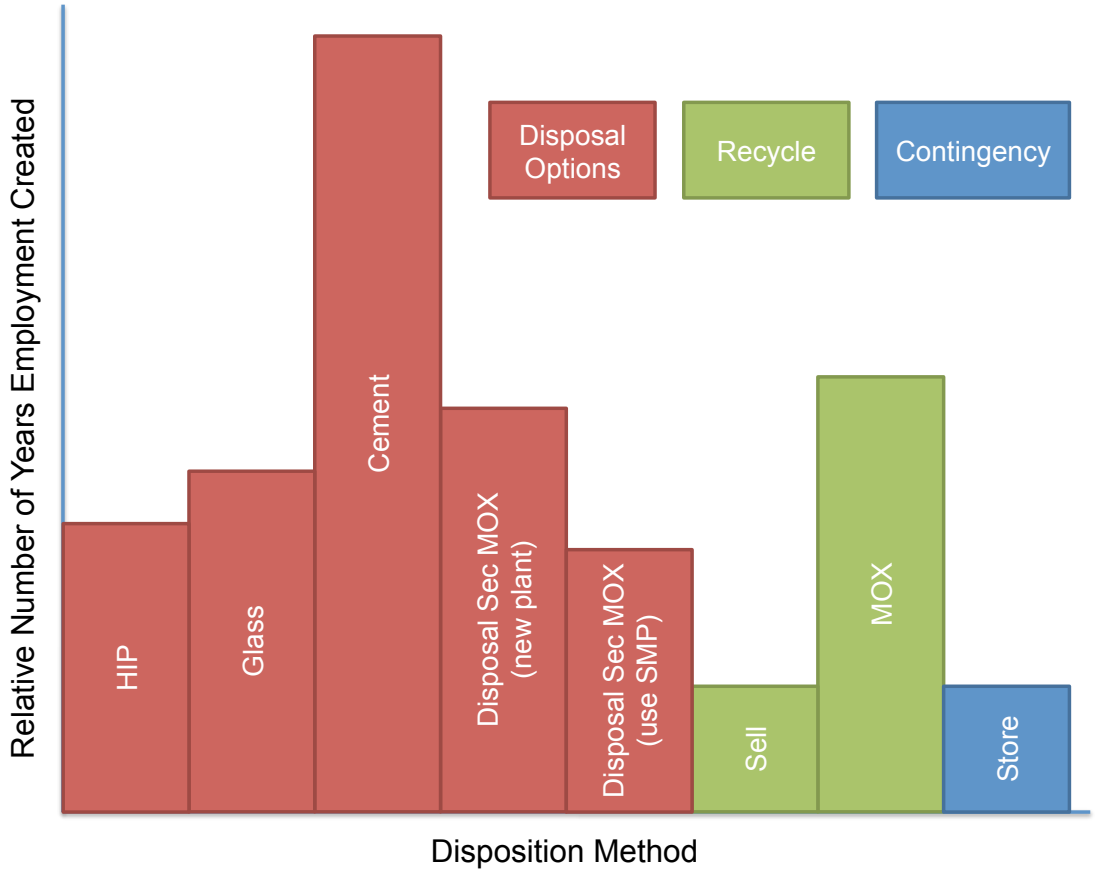

Figure 4: Job impact of the implementation of plutonium option (NDA 2010). The number of jobs is closely related to the overall cost leading to similarities with Figure 3.

As the number of jobs is closely linked to the cost, Figure 4 bares a close resemblance to Figure 3. The store and sell options only include the employment required to monitor and maintain the material, rather than including the final disposal costs as the others do (i.e. estimated costs for transport and packaging for disposal in the GDF).

5.5 Conclusions

The plutonium options have been discussed in further detail. The technical readiness metric shows that all of the disposal options require more research and require active demonstration. The socio-economic implications have shown that selling the material may be the least expensive yet it provides the fewest jobs. The most attractive disposal option is the manufacture of low spec MOX using the existing SMP. However, if SMP does not become available, a likely scenario, ceramics produced by HIP becomes the best disposal option.

6 Ceramics for Disposal

The search for alternative methods to glass for HLW disposal since the 1970s (McCarthy 1977) led to the development of Synroc in 1978 (Ringwood, Kesson et al. 1988). Synroc, or Synthetic Rock, is a particular combination of natural minerals designed to fully incorporate HLW. It is an advanced polyphase ceramic, with, for example, Synroc-C (designed for immobilising LWR wastes) comprising a blend of hollandite, zirconolite and perovskite. Each phase has been chosen to incorporate certain components of the waste stream. For example, zirconolite and perovskite are targeted towards the actinides.

Initial development focused on immobilising HLW from LWR but by 1980, those nations reprocessing their fuel had decided to adopt borosilicate glass technology, as it was the most technically mature. Because of this decision, ceramic disposal technology was forced to specialise into differing wastes, with a particular focus on niche wastes that cannot be easily incorporated into glasses. From this specialisation came more of a focus upon single-phase ceramics and the use of HIP for consolidation. In addition, numerous complementary mineralogical studies have been performed (Lumpkin 2006) that have added credence to long-term performance work.

A key aspect of a ceramic wasteform is to be better than its borosilicate glass competitor. This can be achieved by having a greater waste loading or a superior chemical durability. The best of the tailored ceramics have superior leach rates to glasses. Dissolution rates are a key indicator of ceramic performance as they represent the rate in which the radioactive components may be leached from the wasteforms. Lower dissolution rates represent longer-term stability in the repository environment. One point of concern is the tendency of a ceramic wasteform to undergo amorphisation due to alpha decay. This can lead to swelling and increased cracking and with them a reduced chemical durability (Weber, Ewing et al. 1998).

6.1 POLYPHASE WASTEFORMS

As mentioned, the initial wasteforms were polyphase ceramics containing a blend of synthetic minerals to incorporate various components of the waste. The logical step was to specialise these general wasteforms for specific actinide wastes (Stefanovsky, Yudintsev et al. 2004). Table 4 gives a summary of the wasteforms and their intended uses, also included are the single-phase wasteforms. Lumpkin et al. (Lumpkin, Smith et al. 1995) have performed studies into the partitioning of waste species in polyphase ceramics and conclude that zirconolite has a greater affinity for smaller lanthanide ions and tetravalent actinides while large lanthanide ions and trivalent actinides preferentially partition into the perovskite. The main outcome of this work was to direct future study on more tailored ceramics.

Dissolution rates typically approach 0.001 g m^{-2} d^{-1} after 90 days in periodically replaced aqueous fluids at 70-100 °C. Leachable elements such as aluminium, calcium, caesium and barium, exhibit a non-linear decrease in rate while rare earth elements exhibit rates an order of magnitude lower. Titanium and zirconium rates are lower still with Ringwood (Ringwood, Kesson et al. 1988) suggesting that the dissolution rates of the actinides are about two orders of magnitude lower than the other most soluble elements. In short term leaching tests, less than 60 days, values of 10^{-4} g m^{-2} d^{-1} were recorded.

Mitamura et al. (Mitamura, Matsumoto et al. 1992, Mitamura, Matsumoto et al. 1994) completed some measurements of accelerated radiation damage due to alpha decay with ^{244}Cm doped Synroc samples. Up to the maximum dose of 1.3 x 10^{15} α/mg, the sodium-free samples showed a consistent decrease in density with increasing dose. While a sodium-rich specimen showed a large change in density with dose due to cracking of the samples, as apposed to swelling. In further dissolution tests, the release rates of calcium and strontium increased with dose. Importantly for single-phase ceramics, the major source of the leached elements appears to be the perovskite phase. It would seem that the

zirconolite phase, while more likely to be damaged by radioactive decay, would retain a higher leach resistance.

Wasteform	Main Phases	Application / Waste Loading
Synroc-C	zirconolite, perovskite, hollandite, rutile	HLW from reprocessing / Up to 20wt%
Synroc-D	zirconolite, perovskite, spinel, nepheline	US defence Wastes / 60-70 wt%
Synroc-F	Pyrochlore, perovskite, uraninite	Conversion of spent fuel / ~50 wt%
Tailored Ceramics	Magnetoplumbite, zirconolite, spinel, uraninite, nepheline	US defence wastes / 60 wt% or higher
Pyrochlore	pyrochlore, zirconolite-4M, brannerite, rutile	Separated actinides or Pu / up to ~30 wt%
Zirconolite	zirconolite, rutile	Separated actinides / Up to ~25 wt%
Monazite	monazite	Actinide-lanthanide wastes / Up to ~25 wt%
Zircon	zircon	Pu-rich wastes from weapons
Glass-ceramics	titanate, zirconolite, pyrochlore, perovskite, nepheline, sodalite, alumino-silicate glass	Canadian wastes (low actinide content), complex legacy wastes, intermediate level wastes
Others	britholite, kosnarite, murataite, crichtonite	Proposed for actinides and lanthanides

Table 4: Summary of wasteforms for HLW and other specialist functions. Adapted from (Lumpkin 2006)

6.2 Single-Phase Wasteforms

Single host phase wasteforms are typically designed and chosen to immobilise reasonably pure waste streams, they represent the necessity to compete in different markets from borosilicate glasses. Termed single-phase, they may contain a number of closely related phases. It may be more appropriate to term these formulations as single host-phases, for example pyrochlore targeted wasteform may contain perovskite and brannerite (however, this is likely due to the mixed valency of the substituted wastes stabilising the different phases). In addition, an excess of TiO_2 may be included to buffer against deleterious secondary phases in titanates. Any ceramic produced to immobilise a pure

plutonium stream will be single host phase as the input stream is well characterised eliminating the need for extensive chemical flexibility.

6.2.1 PYROCHLORE

Pyrochlore is based on the fluorite structure and is represented by the general formula $A_2B_2X_6Y$. A is an 8 coordinated cation site while B is 6 coordinated. Typically, A= sodium, calcium, yttrium, lanthanides and actinides and B= titanium, zirconium, niobium, hafnium, tantalum, tin and tungsten. X and Y are 4-coordinated anion sites, usually oxygen or fluorine. While nature has produced minerals with many different ions, prototype wasteforms can be based on $CaUTi_2O_7$. In this formulation, the other actinides substitute for uranium and the neutrons absorbers hafnium and gadolinium are substituted for titanium and, calcium and uranium, respectively.

Investigations into dissolution rates initially focused on the single-phase pyrochlore $Gd_2Ti_2O_7$ doped with ^{244}Cm (Weber, Wald et al. 1986). The tests were limited to annealed, fully crystalline samples and fully amorphous sample in 90 °C pure water for 14 days. Mass losses of 0.02% for the crystalline and 0.05% for the amorphised samples were recorded. The dissolution rate of the ^{244}Cm was increased by a factor of 17, which was attributed to amorphisation. However, the experimental procedure utilised static leachate in Teflon (PTFE) containers. Both of which will have undergone radiolysis to produce aqueous protons and F^- ions, respectively. It is likely that these will have increased the overall leach rates.

Other results for pyrochlore doped with cerium or plutonium-uranium have given release rates of 0.0013 to 0.0002 g m^{-2} d^{-1} for solutions of 85-90 °C buffered to pH 2 (Strachan, Scheele et al. 2005, Icenhower, Strachan et al. 2006). Importantly, this work showed that the dissolution rates of the crystalline and X-ray amorphous samples are the same, within experimental error.

Lumpkin and Ewing (Lumpkin and Ewing 1988) showed that natural pyrochlores are subject to amorphisation at a dose of ~10^{16} α mg^{-1}, which is 2-3 times the dose required for $CaPuTi_2O_7$ amorphisation. The report suggests that this result points to long-term annealing by atomic diffusion yet care should be taken to note that the dose received by these natural materials is spread over a vast time scale and it is not directly representative of wasteforms. These mineral studies have also given examples of radiation-damaged pyrochlores that have existed for 40 million years without significant loss of uranium or thorium.

6.2.2 Cubic Zirconia

Cubic zirconia is essentially a fluorite-defect fluorite structure based on the general formula $Zr_{1-x}M_xO_{2-y}$, where M is calcium, lanthanides or actinides. In order to stabilise ZrO_2 in the cubic phase, dopants are added. For highly abrasive tasks, fully yttrium stabilised tetragonal zirconia is used. Cubic zirconia has excellent resistance to amorphisation and its solubility in water is very low. Some work has focused on the use of cubic zirconia as inert matrix fuel that is irradiated and then buried as is (Degueldre and Paratte 1999, Ledergerber, Degueldre et al. 2001). The concept is that this eliminates the need for further waste processing steps yet still provides a suitable wasteform. In practice, the inert matrix must be flexible enough to retain all fission products and to do so within a reactor operating temperature. It is likely that this is impossible. The main draw back with using cubic zirconia as a wasteform is in the difficulty of processing requiring high, ~1600-1700 °C, sintering temperatures and possibly precluding the use of HIP.

6.2.3 Zirconolite

Zirconolite is another derivative of the fluorite structure and can be considered as a less symmetric version of pyrochlore. Figure 5 shows the crystal structure of zirconolite-2M. Note the large calcium cations (potential substitutions sites) and the TiO_6 octahedra (light red). Prototypical composition is $CaZrTi_2O_7$ for the 2M polytype; increasing amounts of lanthanide and actinide substitution

can produce other polytypes such as 3T, 3O, and 4M. Actinides and lanthanides can be substituted onto both the calcium and zirconium sites with suitable charge balancing on the titanium site. For example, Ce^{4+} can be substituted onto the Ca^{2+} by charge balancing with Al^{3+} on the Ti^{4+} site to give, $Ca_{1-x}Ce_xZrTi_{2-2x}Al_{2x}O_7$. Natural zirconolites exhibit many different combinations of substitutions showing an excellent chemical flexibility. Its amorphisation dose is nearly identical to the pyrochlore (Clinard, Rohr et al. 1984). Resistance to aqueous dissolution is excellent even with amorphised samples retaining uranium, thorium and their daughter products. Zirconolite also exhibits exceptional corrosion resistance up to 250 °C in various acidic and basic solutions, important for proliferation resistance. Ion irradiation studies (Wang, Lumpkin et al. 2000) have shown there is a significant relationship between radiation tolerance and cation mass with heavier cations giving greater resistance.

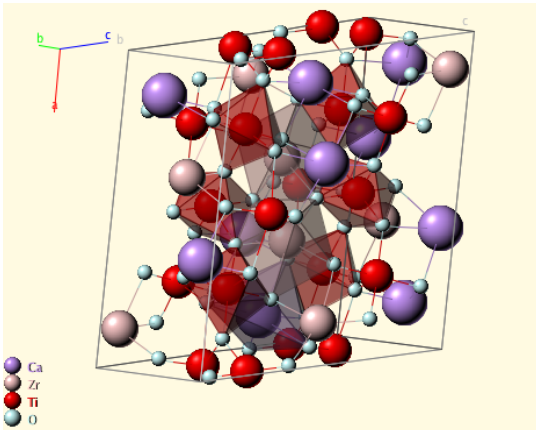

Figure 5: Crystal structure of Zirconolite-2M from (Webmineral 2012) based on original data from (Rossell 1980). Large purple ions are calcium, pink are zirconium, red are titanium and light green for oxygen.

6.2.4 Perovskite

Perovskite has the general structure ABX_3 with a corner sharing octahedral framework of B-site cations and large A-site cations. A cations include sodium, calcium, strontium, lanthanides and minor actinides while the B-site is typically occupied by titanium or aluminium; $CaTiO_3$ is the prototype formulation. Ion irradiation and natural analogue studies have shown the critical amorphisation

dose to be 2-2.5 times higher than pyrochlore and zirconolite (Smith, Zaluzec et al. 1997). However, dissolution studies have shown it to be the least durable phase in polyphase wasteforms. Perovskite reacts quickly with aqueous fluids to form an amorphous Ti-O-H film at temperatures below 100 °C. Thermodynamic calculations have shown perovskite to be unstable with respect to titanite ($CaTiSiO_5$) in SiO_2 aqueous solutions. Therefore, it can be said that perovskite is not the best host for actinides in wasteforms if they are destined for a geological repository.

6.2.5 Others

Brannerite, ideally UTi_2O_6 is a minor, but actinide rich, phase in some of the pyrochlore-based formulations. Brannerite may account for up to 20% of the uranium and 15% of the plutonium containing phases in these wasteforms (Thomas and Zhang 2003). Natural and synthetic brannerites can incorporate substantial amounts of calcium, rare earth elements, thorium and others.

Zircon is commonly found in a number of geological environments. Nominally $ZrSiO_4$, it often has a hafnium impurity substituted on the zirconium site. The mineral is highly durable in most environments and can survive weathering to be recycled in the earth's crust (Holland and Gottfried 1955). However, it has a low capacity for actinide wastes and, whilst plutonium baring wasteforms have been manufactured on the lab scale (2 mm crystals after 72 hours of heat treatment (Burakov, Hanchar et al. 2002)), it will be difficult to develop to full process scale implementation.

Monazite has a similar general structure to xenotime (YPO_4) with the general formula ABO_4 except that the crystal consists of alternating BO_4 tetrahedra and AO_9 polyhedra (Clavier, Podor et al. 2011). It has good durability, however it is difficult to manufacture.

Other minerals, as well as those discussed, are summarised in Table 5.

Ceramic	Aqueous Durability	Chemical Flexibility	Waste Loading	Radiation Tolerance	Volume Swelling	Natural Analogues?
Perovskite $(Ca,Sr)TiO_3$	Low	Medium	Low	Medium	High	Yes
Pyrochlore $Gd_2(Ti,Hf)_2O_7$	High	High	High	Low-High	Medium	Yes
Zirconolite $CaZrTi_2O_7$	High	High	Medium	Low-Medium	Medium	Yes
Zircon $ZrSiO_4$	High	Medium	Low(?)	Low	High	Yes
Monazite $LnPO_4$	High	Medium	High	High	Low	Yes
Zirconates $Gd_2(Zr,Hf)_2O_7$	High	Medium	Medium	High	Low	No
Zirconia $(Zr,Ln,Act)_xO_{2-x}$	High	Medium	Medium	High	Low	No
Brannerite UTi_2O_6	Medium	Medium	High	Low	?	Yes
Crichtonite $Ca(Ti,Fe,Cr,Mg)_{21}O_{38}$	?	High	Medium	Low (?)	?	Yes
Murataite $Zr(Ca,Mn)_2(Fe,Al)_4Ti_3O_{16}$	High	High	Medium	Medium	?	Rare
Garnet $Ca_3Zr_2(Al,Si,Fe)_3O_{12}$	?	High	Medium	Low	?	Yes
Titanite $CaTiSiO_5$	Medium	Medium	Low	Low	Medium	Yes
Minerals of the apatite group (eg britholite)	Medium	Medium	Low	Low	Medium	Yes
Kosnarite $NaZr_2(PO_4)_3$	Medium	Medium	Medium	Low	?	Yes

Table 5: Summary of selected ceramics. A high performing wasteform will have high aqueous durability, chemical flexibility, waste loading, and radiation tolerance. It should have low volume swelling and have natural analogues. From (Lumpkin 2006).

7 Ceramic Processing

This section outlines the fundamental processes required for the manufacture of ceramics. Each of the stages may be modified or achieved in a slightly different way, but the basics are outlined as Figure 6.

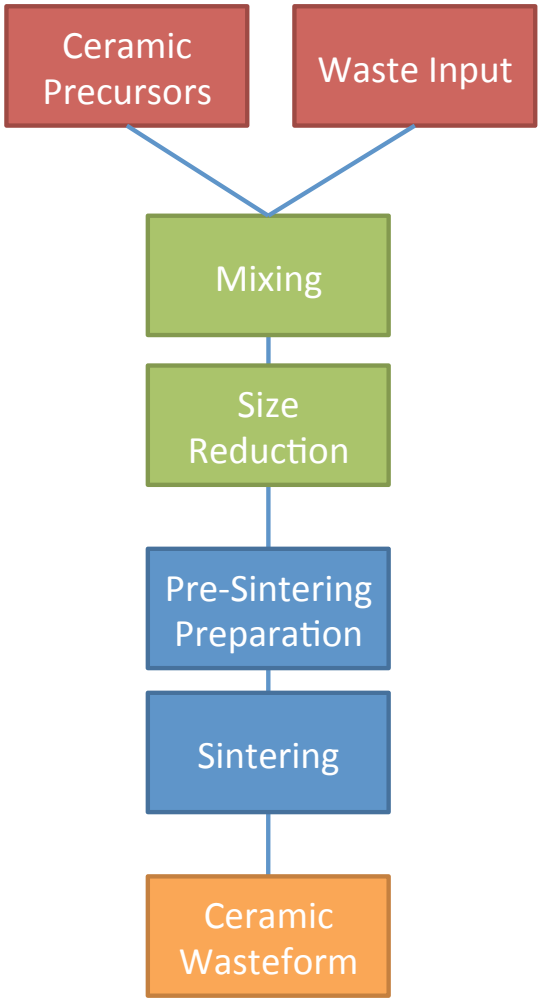

Figure 6: Process outline for the formation of a ceramic. The coloured sections, while they may be physically different, may rely upon each other or be interchangeable. See text for a more detailed explanation

Figure 6 shows the basic process required to produce a ceramic wasteform. While each of the stages may be independent, typically they are all interrelated. For example, if a zirconia waste form is required, then HIP may not be used as a useful consolidation technique and thus it requires a different pre-sintering preparation to a ceramic that was to be manufactured by HIP. It may also mean that the size reduction and mixing of the precursors may need to be more

vigorous or more thorough. In addition, the size reduction and mixing processes may be swapped in order or even carried out at the same time.

7.1 Inputs

The waste input will be the key factor in deciding the final ceramic wasteform. As previously discussed, the wasteform may be one of many single phases or a multiphase product. Great care must be taken in choosing a suitable ceramic. The inputs are typically the metal oxides in the required stoichiometry, termed the precursors, scaled up to the required batch size. The 'recipe' can be calculated by comparison of the number of moles of each species required and the target ceramic. In many feeds, an excess of one or more of the precursors will be included to ensure the desired host-phase is favoured and any deleterious secondary phases are minimised.

7.2 Mixing

This may be achieved by mixing the materials by hand (e.g. in a bowl), the use of a Turbula mixer, paddle blender or another device. If this stage is carried out before the size reduction then it typically does not have to be exact. The purpose is to ensure that none of the components are localised in any one position. This stage also provides an opportunity to introduce any additives that may improve powder handling characteristics, such as adding a lubricant, or improve the final ceramic for example adding a porosity controller in fuel manufacture.

7.2.1 Turbula

An image of a Turbula mixer extensively used in this work is shown in Figure 7. Typically, the precursor components required for the specific wasteform targeted are added individually to a 2 litre mixing vessel. This vessel is secured to the Turbula mixer and operated for 10-15 min. The mixing action is gyrational in nature.

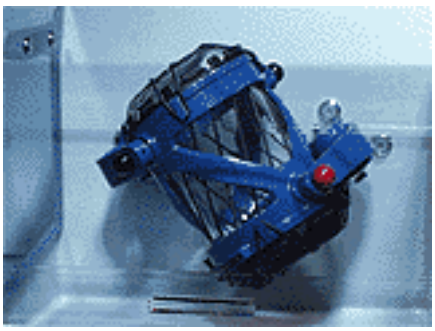

Figure 7: Turbula mixer, image from Glenmills.com (Glenmills.com 2011)

7.3 Size Reduction

Depending on the input streams, a series of size reductions may be required. The aim is to create a waste and precursor mix that can be sintered by the desired technique. A primary size reduction stage may need to be reduced from ~1-5 mm to < 1 mm. Examples of this stage may be disc mills or jaw crushers. Attrition mills and planetary mills may accomplish further size reduction.

7.3.1 Attrition Mills

Attrition mills can produce extensive size reduction and homogenisation in dry powders and is one of the key foci in this work (Austin and Bagga 1981). The attrition mill consists of a stationary outer metal container, ~2/3 of which is filled with milling media (typically stainless steel ball bearings) (Shi, Morrison et al. 2009). An agitator shaft is inserted into this milling media that consists of a central steel core off which horizontal steel bars are attached (see Figure 8). When the machine is operational, the horizontal bars move and agitate the milling media into a quasi-fluidic state. The material to be milled is added to this moving media through an inlet port in the lid of the mill pot. The main size reduction mechanism is through torsional interactions between two balls and the powders. Shearing forces also introduce a significant amount of the total milling energy. Impact between two balls and the powder does occur but it is not the main mechanism for size reduction (Williams 1997, Tomas 2007). Attrition mills have advantages for operation in the nuclear industry as they can be operated without a carrier fluid, in the batch mode, and can input a high level of energy into the milling process. They can also be remotely charged and

discharged by only moving certain valves (i.e. without dismantling or handling the mill pot). Attrition mills are one of the key plant items in SMP (BNFL and Edwards 2002).

Rydin et al have reported a study in to the dynamics of an attrition mill (Rydin, Maurice et al. 1992). Utilising a transparent outer mill pot direct imaging of the milling media was possible. They found that the media behaved comparably to a fluid in that upon increased agitator speed the media would travel further up the sides of the mill pot. They also note that the powders to be milled typically travel to the base of the mill by gravity. This may be a concern for powder agglomeration.

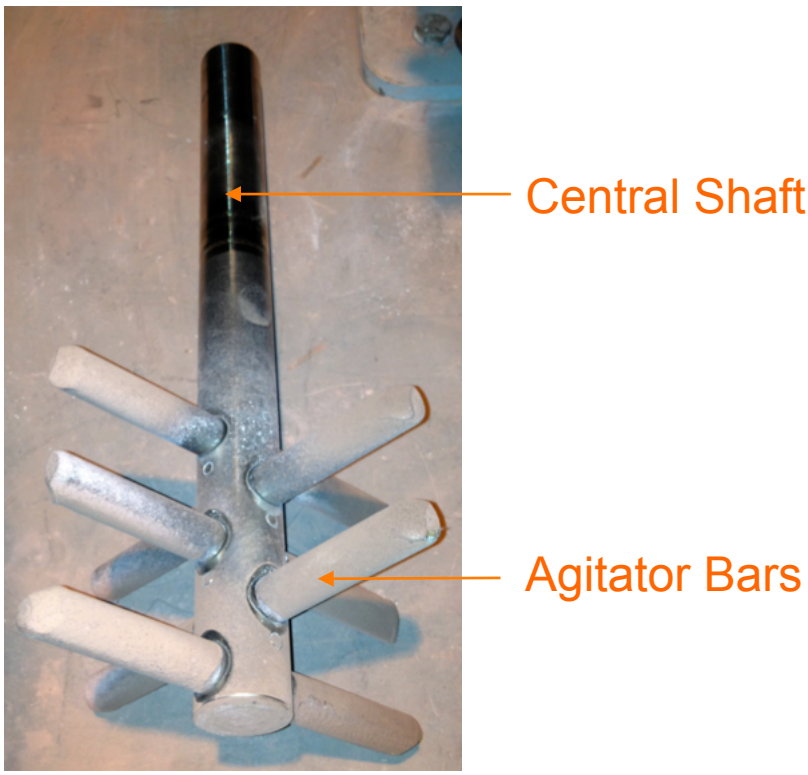

Figure 8: Agitator from attrition mill

7.3.2 Planetary Mills

Planetary mills have a similar mode of operation to attrition mills in that they utilise the interactions between milling media to size reduce material. The significant difference between planetary and an attrition mill is that with planetary mills the entire mill pot rotates. As the pot rotates upon its own axis, the whole pot assembly rotates around another point. This contra rotation

increases the energy imparted into the powders. The disadvantage of this system is that in order to recover the milled powders, the entire contents of the mill pot must be emptied out. This would decrease the throughput of any full scale implementation.

7.4 Pre-Consolidation Preparation

This stage is entirely dependent on the consolidation technique employed. For example, if the powders were to be cold pressed, it would be in this stage. If the ceramic were to be produced by HIP then this stage would be the can loading and additive removal. Other techniques take the loose powders and press them in to pellets or other preformed shapes. CUP, Cold Uniaxial Pressing, involves applying pressure through the longitudinal axis of the powders at ambient temperature to produce a green pellet. This pellet is then transferred to a sintering furnace. CIP, Cold Isostatic Pressing, applies a pressure to the green pellet using a working fluid, typically a liquid, at ambient temperature isostatically. The green pellet must be sealed against the working fluid; a deformable plastic bag normally achieves this. The pellet is then removed to a furnace for sintering.

7.5 Consolidation

The type of consolidation employed is dependent on the ceramic chosen. Consolidation[17] is the heating of powders to below their melting point until those particles consolidate to form a solid object. It is characterised by the application of heat typically for a period of hours. Pressure may, or may not be applied with heat, or it may be applied in the pre-sintering preparation to form green pellets[18].

---

[17] Sintering is the application of heat without the addition of pressure and is considered a subset of consolidation.

[18] Green pellets are powders that have been compressed into a solid form but have not reactively combined to form the final product.

The focus of this work is consolidation by HIP. HIP has many advantages over other sintering techniques for processing high-level wastes, notably there are no radioactive volatile emissions in the high temperature consolidation step, as the HIP cans are sealed, there are less secondary wastes and there are many processing conditions available for consolidation (Li, Zhang et al. 2006). One draw back is the sample container material limits the temperature of operation. For this reason highly refractory ceramics (e.g. zirconia) may be restricted in use as the workable limit of stainless steel is ~1350 °C compared to the zirconia sintering temperature of ~1700 °C. A HIP typically consists of a pressure vessel capable of withstanding at least 100 MPa, a method of heating and gas compressors (Atkinson and Davies 2000, Bocanegra-Bernal 2004). A HIP operation involves using argon as an inert gas to apply an isostatic pressure to the work piece while resistance heating increases the temperature. Pressure and temperature are independent but it is usual for them to be increased simultaneously to the target consolidation conditions.

A further technique, initially favoured until the development of HIP, by ANSTO (Ringwood, Kesson et al. 1979) is Hot Uniaxial Pressing. HUP applies a pressure to powders through the centre of the sample, whilst holding the powders at sintering temperature.

7.6 Other Techniques

The basic stages outlined above are typical of a dry powder-processing route. It is also possible to use wet chemistry processes such as using hydroxide and alkoxide precursors, nitrates or by sol-gel methods (Donald, Metcalfe et al. 1997). Whilst these methods produce very fine and intimately mixed precursor blends, they do utilise carrier fluids that lead to secondary effluents and many pose a criticality concern. The application of the alkoxide/nitrate route is detailed later in this work.

7.7 Cerium

As plutonium is a radioactive material the extra cost and difficulty of using it means that an inactive surrogate is required for preliminary research. In this work, cerium was selected. Whilst no element can exactly substitute for another, cerium has a similar ionic radii to plutonium (Shannon and Prewitt 1969) and is comparable for ceramic substitutions (Bingham, Hand et al. 2008). However it does differ in its redox potential and is more prone to autoreduction than PuO_2. Cerium is a common surrogate and, for example, Begg and Vance (Begg and Vance 1997) have published results on the behaviour of cerium in zirconolite.

7.7.1 Comparison of 'Realistic' Ceria and Plutonium Oxide

The manufacturing technique for the plutonium surrogate will have an important impact on the particle shape, size and distribution. For some aspects of experimental work that do not require specified particle shapes, such as initial milling experiments, an 'off the shelf' standard ceria source may be preferred in terms of cost. However, for more detailed work a more realistic simulant would be required.

An ideal simulant would be manufactured in the same process as the material it is representing. In this work, the 'realistic' simulant was manufactured at the University of Leeds Particle Size Laboratory and was produced for another aspect of wasteform development at NNL. There are two main sources of PuO_2 that may need to be immobilised: Magnox and ThORP. The primary difference is whether the material is batch (ThORP) or continuously precipitated (Magnox). The Leeds process aimed to directly simulate the manufacture of ThORP derived PuO_2. The outline of the process is the batch precipitation of $Ce(C_2O_4)_2$ from the $Ce(NO_3)_3$ solution by the addition of oxalic acid. The precipitate is separated, dried and calcined in air to form CeO_2. Stennett *et al.* (Stennett, Corkhill et al. 2013) have recently discussed the $Ce(C_2O_4)_2$ decomposition process with reference to the manufacture of simulated UO_2 fuel. They conclude that CeO_2 derived from the oxalate is comparable, with regard to

microstructure, to UO_2 pellets produced from ThORP derived material. This gives confidence that the CeO_2 will be representative of the PuO_2, also derived from a similar process to ThORP, required for this work.

The Magnox plutonium source is initially mixed valence $Pu^{(III/IV)}$ from reprocessing, which is conditioned with H_2O_2 to Pu^{IV} as $Pu(NO_3)_4$ solution. This is fed to a stirred precipitator into which $H_2C_2O_{4\,(aq)}$ (oxalic acid) is fed. The precipitate, $Pu(C_2O_4)\cdot 6H_2O$ (plutonium oxalate) overflows as a slurry to be collected. This slurry is vacuum dried before being calcined to form PuO_2. One interesting aspect in the manufacture of PuO_2 is that the original design was for the plutonium to go on to be manufactured into MOX fuel. Thus, the shape and condition of the PuO_2 was always targeted to be in a form easily made into fuel (e.g. free flowing, consistent particle size, high specific surface area) and not for long term storage. Figure 9 shows the forms of the PuO_2 before and after calcination. The left hand image shows a very fibrous material that would not be suitable for further processing. The thread like nature would have a low packing density (as the fibres interact with other particles), they would easily break during handling leading to increased airborne fines and they would flow poorly (due to particle interlocking). The right hand image shows the particles after further heat treatment (calcination) and the change in the particle shape is clear. These shaped particles are more likely to flow freely.

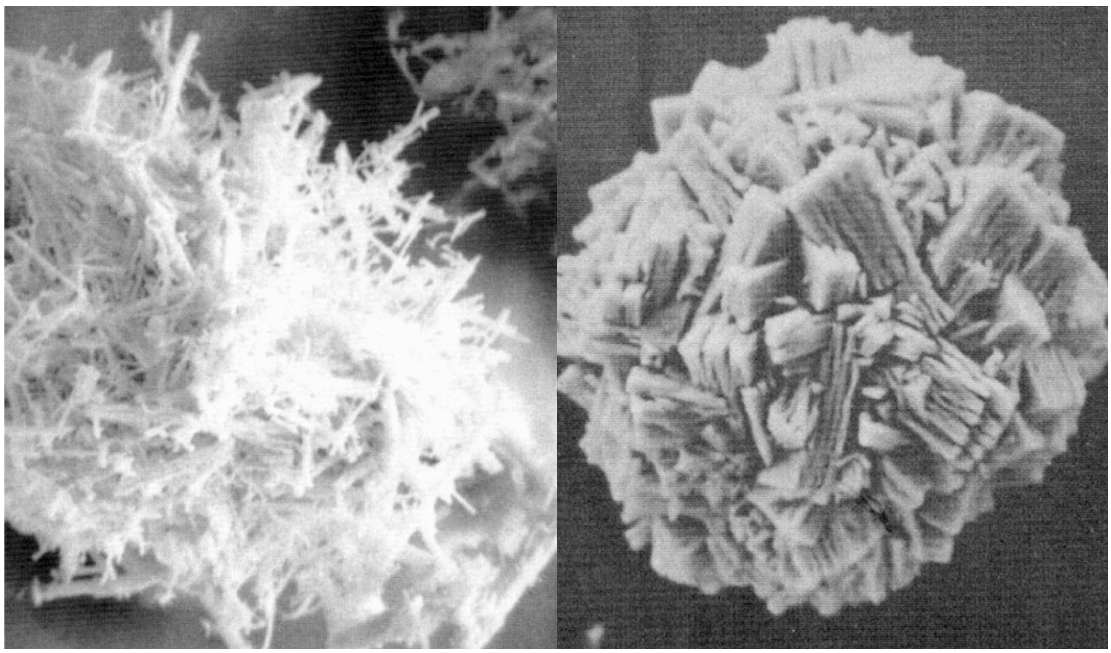

Figure 9: Magnox derived PuO_2. Left, after precipitation and oxalate decomposition for 2 hours at 350 °C. Right, after calcination at 600 °C for 5 hours. No scale was present on the original images but in references with other images, it is thought both particles are of the order 20-35 μm (Sellafield Ltd. 2007)

As mentioned, the two different manufacturing techniques for the plutonium oxalate precipitate can led to differences in the structure of the PuO_2 powders. Figure 10 shows example particles from the Magnox derived material. The top left image shows material similar in nature to the calcined material in Figure 9. That is, the fibrous nature has coarsened into a series of particles attached to a central core. Observation of this particle would suggest that as it appears compacted in nature it would be resistant to low energy size reduction. The particle in the top right image, however, appears to be a series of lightly agglomerated primary particles. This agglomerate would be relatively easy to break apart through milling. The overview image shows the majority of particles to be the first agglomerate type (coarsened fibres) and are approximately 20-40 μm in size.

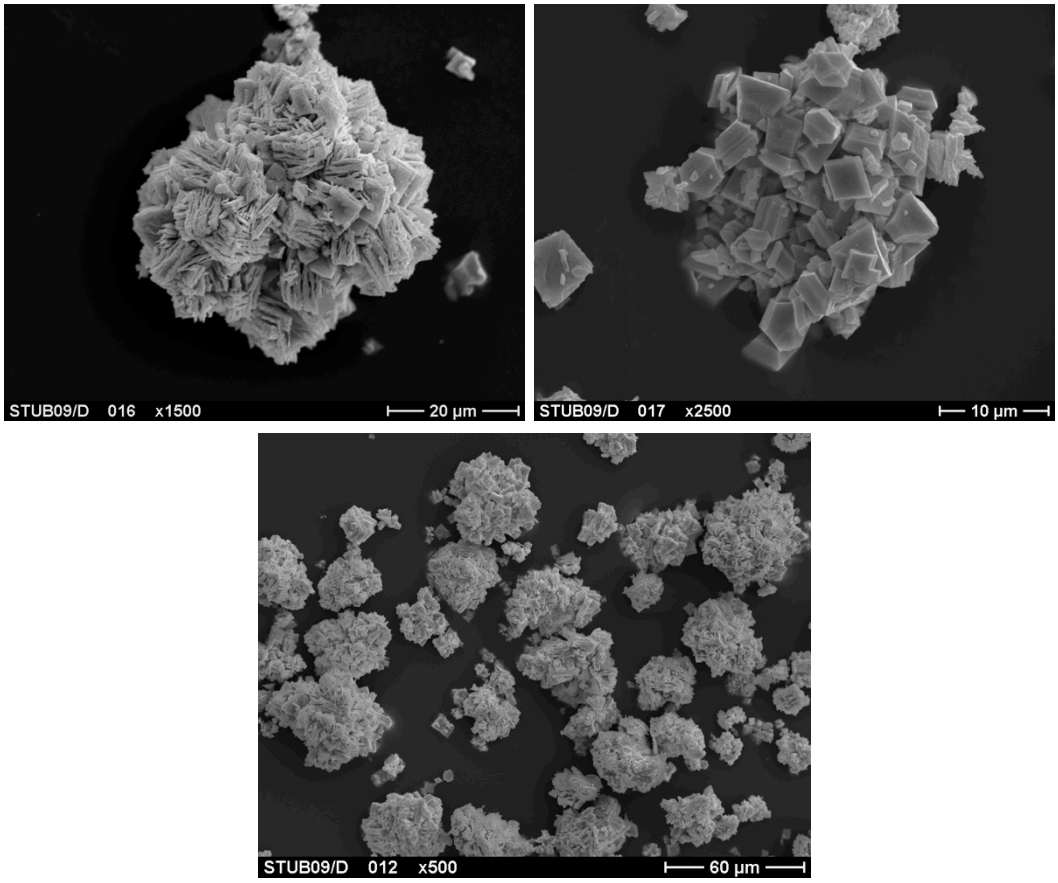

Figure 10: Magnox PF&S derived PuO_2. Images on left x1500 magnification and shows a typical agglomerate of ~25 µm and to the right, are primary particles closer to 5 µm. The image on the right, shows a less tightly bound agglomerate of primary particles at 2500x magnification. The bottom image is a low, 500x, magnification overview image (Rhodes 2011).

An example of the ThORP derived PuO_2 is shown as Figure 11. The agglomerates are similar in size to the Magnox material at ~20-35 µm. The top right image shows an example of the coarse primary particles in the ThORP material. Comparing to the Magnox material, this particle is larger than the Magnox primary particles yet it is atypical in the samples. The agglomerate produced from the fibrous material appears to be closer packed than the Magnox material. This ThORP material may be more difficult to size reduce than the Magnox PuO_2.

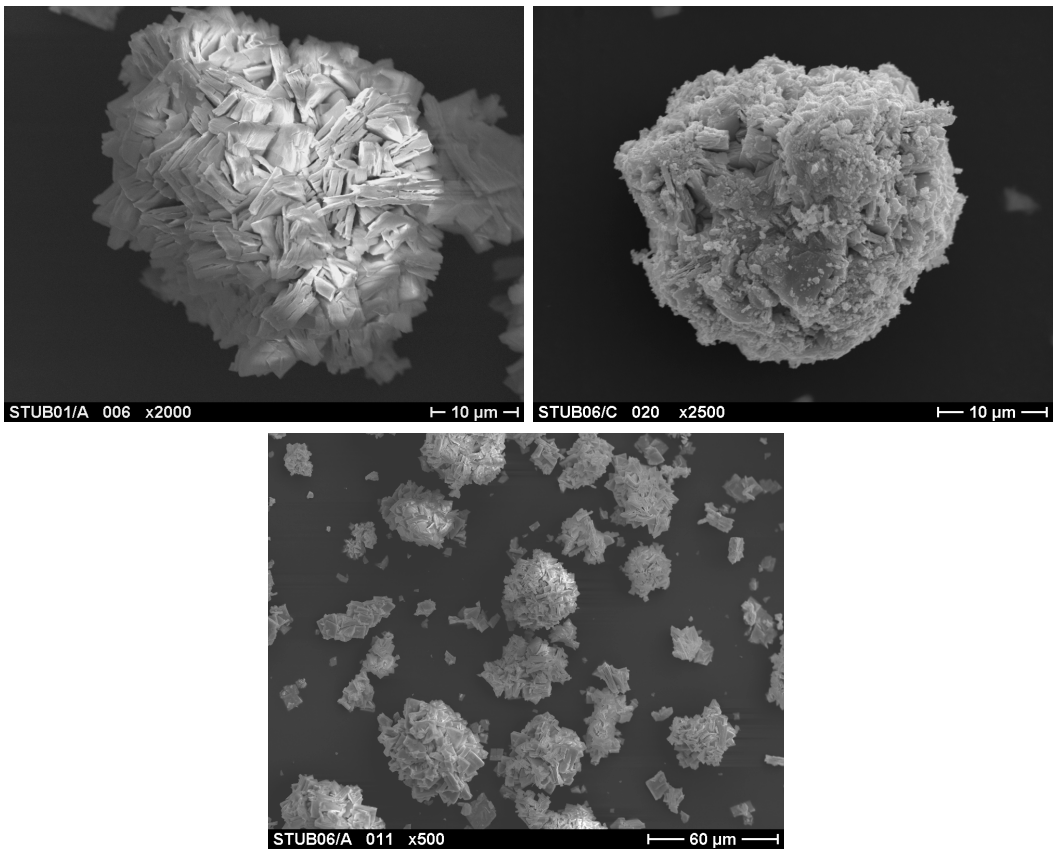

Figure 11: THORP derived PuO_2. Top left image shows a typical agglomeration of ~25 µm at 2000x magnification. Top right, gives an example of a primary particle, these are atypical. Bottom image is 500x overview (Rhodes 2011).

To date, no systematic particle size distribution analysis has been undertaken on any of the PuO_2 material. Manual counting of the grains in the above images (and others in their series) has been undertaken and the average particle size is given as ~28 µm. For further detail we can examine the customer specification which states >98% of the material, measured by mass, to pass a 100 µm sieve and >95% to pass 45 µm. Typical results are 100% passes 100 µm and ~99% passes 45 µm (there is no publicly available reference for these figures yet they are referred to in internal NNL and Sellafield Ltd documents). With no well defined specification for the material any further processing must be suitably flexible to account for these product variations.

Figure 12 shows examples of the Leeds University manufactured 'realistic' ceria simulant. It is typically particles of approximately 5-10 µm with the occasional larger (200-300 µm) piece. These large particles appear to be more than just loosely agglomerated primary particles, as in the PuO_2. It is likely these large

particles have formed during the surface area adjusting heat treatment step after the oxalate decomposition. This structure may be responsible for some intra granular residual porosity in the samples manufactured from these materials. This may be eliminated by more vigorous milling or through the application of pressure (i.e. HIP). One difficulty with relying on consolidation mechanisms to remove the agglomerates is that the addition of heat and pressure may only serve to strengthen the particle rather than causing it to break down thus only leaving diffusion mechanisms to incorporate the material. Care must be taken to eliminate these by either clearly specifying the input feed or by ensuring, the milling is sufficient to break them down. The other two images show similar secondary agglomerate sizes to the PuO_2 feeds yet they do not have the same fibrous nature.

In comparison to the two PuO_2 sources, this CeO_2 is different. The secondary structures are larger and less fibrous. It is likely that this simulant represents an upper limit in terms of particle size, as the particles are coarser than the PuO_2 feeds. Differences in the strength of the PuO_2 and CeO_2 crystals are unknown but they will exhibit different milling properties.

Finally, the SEM images were taken on freshly manufactured PuO_2 and the material liable for immobilisation may be up to 40 years old. There has been no work on the characterisation of the material after such a long period of storage and it is unknown what state the material will be in. Radioactive decay of the material may have weakened the structures leading to easier size reduction and milling or it may have further coarsened the agglomerates. Thus the conclusion is that the 'realistic' ceria source represents the best surrogate accessible for this work yet it still may not be wholly representative. Thus, a level of flexibility will always be required in the design of a process.

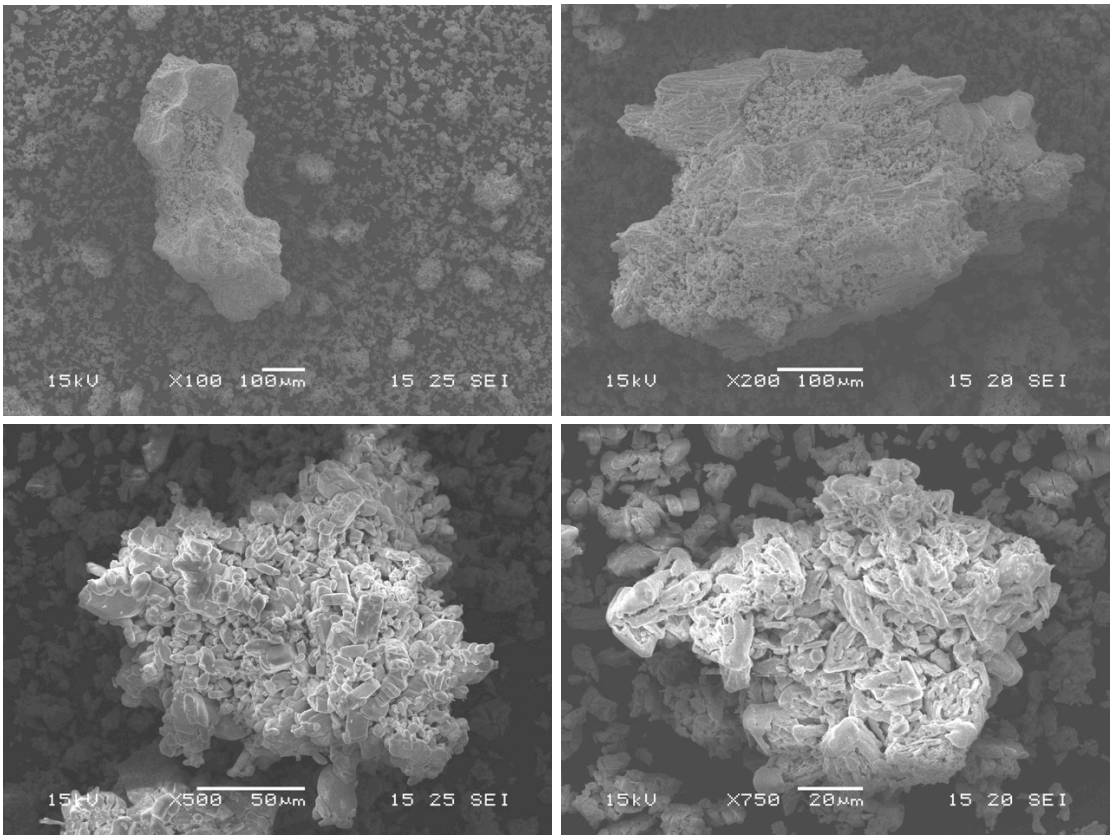

Figure 12: Example SEM images of the 'realistic' ceria simulant. All images taken at a working distance of 15 mm and a spot size of 20 or 25 in the secondary electron imaging mode.

8 Analytical Techniques

8.1 SEM

Investigation of the microstructure and composition of the samples can be undertaken by the use of a SEM (Scanning Electron Microscope). SEM utilises a tightly focused electron beam to scan across the surface of the sample being investigated(Goodhew, Humphreys et al. 2000). Certain electrons in the atoms in the sample are excited and attracted to the sensor. These secondary electrons are detected and used to form an image. This information is useful for topographical studies. Elastic scattering of electrons can also be detected, which are referred to as backscattered electrons. The energy of these electrons is strongly associated with the average atomic mass of the part of the sample they rebounded from. In backscattered images, the colour of the phase is indicative of its average atomic mass in comparison to the rest of the sample. A further detector may be used to detect the characteristic X-rays being emitted from an

excited atom in a technique known as EDS (Energy Dispersive X-ray Spectroscopy). As each element has a unique electron structure, the x-ray photons emitted from an excited atom will have a series of characteristic energies than can be identified against a list of known standards to determine which element is present.

In this work, the SEM utilised was a JEOL JSM-5600. Typically the images presented are in the backscattered mode with 15 kV accelerating voltage, spot size of 35 and a working distance of 15 mm (or otherwise noted). Two images were acquired of the same area: one at 200x magnification and one at 1500x. Energy Dispersive X-ray (Princeton Gamma Technologies with a PRISM Si(Li) digital detector), coupled to the SEM, was used for elemental mapping.

8.2 XRD

XRD (X-Ray Diffraction) is a technique that exposes samples to X-rays of a known wavelength. The X-rays diffract through the spaces between the atoms in the lattice structure of the sample to give a characteristic interference pattern, which can be assigned to a crystalline material. A large database of all known and published patterns is consulted to identify unknown phases.

The XRD utilised in this work is an Inel Equinox1000 with Co Kα radiation and a resolution of 0.1°. Due to significant Ti fluorescence in many of the samples, it was necessary to smooth the data with a 5-point moving average. XRD patterns are reported with Miller indices for the most abundant phase in the sample. The secondary phase signals are only marked if they are within 10% of relative intensity of the primary phase. This was to aid clarity in the presentation of figures.

8.3 Density

Sections of each sample were removed from the main body for density measurements *via* the Archimedes (or immersion method). The samples were weighed in air before being weighed whilst submerged in water. The difference

between the two masses, multiplied by the density of water, is the volume of the sample. From these measurements the density can be calculated.

Masses were measured to four decimal places on a four figure balance. The calculated error is ± 0.003% or ±0.00015 g (based on the accuracy of the balance and a typical density of 5.00 g cm^{-3}). A second method to estimate the errors is by using the NNL internal quality procedures (Brown 2012). This method took 25 separate density measurements of the same sample of Al (density of 2.702 g cm^{-3}). There was a mean result of 2.6868 g cm^{-3} with a standard deviation of ±0.0010 g cm^{-3} (±0.03%). This gives accuracy for the method as -0.0152 g cm^{-3} and a precision of 0.0010 g cm^{-3}. All densities are quoted to two decimal places as this is considered the most useful level of detail. There is also confidence in this level of precision. The density results are therefore quoted below the level of accuracy to which they were recorded to and any differences in the results are hence considered significant. Shaw (Shaw 1998) showed that the critical density between interconnected and closed porosity is 92% of TD (Theoretical Density) in plutonium containing ceramics. Accordingly, 92% TD has been set as the target density for all wasteforms manufactured in this work.

2: Influence of Lubricants and Attrition Milling Parameters on The Quality of Zirconolite Ceramics, Consolidated by HIP

1 Abstract

The effect of attrition milling on the processing of precursor oxides was investigated, with regard to the fabrication of titanate ceramics for the immobilisation of plutonium and actinides, consolidated by hot isostatic pressing. Difficulties encountered during the lubricant removal step masked any correlation between the milling conditions and the final product. This work trialled four lubricants, zinc stearate, Ceridust™, polyethylene glycol and oleic acid, which were added to the precursor blends to ensure the powders remained free flowing whilst dry milling in an attrition mill. All except Ceridust™ allowed the milled powders to consistently be freely discharged. The powders were divided into two batches and each batch was consolidated by either a high temperature HIP cycle (1320 °C) or a low temperature HIP cycle (1000 °C). Examination of the high temperature HIP cycle products showed that each sample was highly porous and all were far below the target of 92% of theoretical density. XRD and SEM analysis showed the production of a multiphase ceramic (zirconolite, perovskite, ilmenite) rather than the single target phase zirconolite. The low temperature HIP cycle products showed a notable decrease in the fraction of free ceria inclusions with increased milling. A

correlation between ease of powder discharge and milling quality was not found. Suggested modifications to the HIP processing line, including the addition of a sintered metal filter into the HIP can evacuation tube, the use of fumed metal oxides and the introduction of electrical conductivity in the precursors, are discussed.

2 Introduction

The focus of this section of work was on the applicability of attrition milling to the manufacture of zirconolite candidate wasteforms consolidate by HIP. Zirconolite, ideally $CaZrTi_2O_7$, is a monoclinic derivative of the cubic pyrochlore structure. Actinides and lanthanides can be substituted onto both the calcium and zirconium sites with suitable charge balancing on the titanium site. For example, Pu^{4+} / Ce^{4+} can be substituted onto the Ca^{2+} site by balancing the charge with Fe^{3+} on the Ti^{4+} site to give: $Ca_{1-x}(Pu,Ce)_xZrTi_{2-2x}Fe_{2x}O_7$; the plutonium solid solution of this type was recently documented by Gilbert *et al* (Gilbert, Selfslag et al. 2010). Natural zirconolites show many different combinations of element substitutions, demonstrating excellent chemical flexibility, and resistance to aqueous dissolution is very high (Hart, Vance et al. 1998). Zirconolite also exhibits exceptional corrosion resistance up to 250 °C in various acidic and basic solutions, which is important for demonstrating resistance to proliferation (Lumpkin 2006). Operating regimes for consolidation of zirconolite ceramics by HIP typically involve temperatures in the region of 1300 °C (generally limited by the HIP can material) and an applied pressure of 100 MPa Ar (Zhang, Stewart et al. 2009).

The correct preparation of the precursor feeds is critical for the manufacture of high quality ceramics. This section of work is an experimental introduction to the attrition mill described in Chapter 1. In order to satisfy the general design principle of minimising secondary effluents, the mill is operated in the dry mode, that is, without carrier fluid. Ensuring the powders remain free flowing

during milling is a key issue in this operating mode. If the powders are allowed to settle on the base of the mill they will compact into an immovable agglomerated "foot" that prevents mill discharge. Lubricants, typically hydrocarbon waxes, must be added to minimise such an occurrence.

Previously, it was noted that tip speed and duration of milling are two of the key parameters in preparing precursor batches. Accordingly, this work examines their effect on product quality, with regard to density, phase development and microstructure. This is achieved, primarily, by utilising a low temperature HIP cycle that will trap (or freeze) the as-milled microstructure in a form that is suitable for microstructure analysis (i.e. monolithic and robust). Further samples were consolidated by a high temperature HIP cycle with the intention of developing the zirconolite target phase fully.

The focus of this work is the application of an attrition mill to the manufacture of candidate zirconolite plutonium wasteforms consolidated by HIP with primary focus on the ability of different lubricants to ensure powders are kept free flowing throughout milling. There is a secondary focus on the effect of milling conditions on the microstructure of partially phase developed ceramics.

3 Material and Methods

Zirconolite was chosen as the target ceramic wasteform for this work. The substitution of cerium was selected to be 0.25 formula units of cerium, supplied as Ce^{4+} (CeO_2), on the calcium-site, with co-substitution of $Fe^{2/3+}$ (supplied as Fe_3O_4) for charge balancing *via* substitution on the titanium site. Ce^{4+} is used as a Pu^{4+} surrogate due to their similar ionic radii, 1.11 and 1.10 Å respectively in 8-fold co-ordination (Shannon and Prewitt 1969, Bingham, Hand et al. 2008). The mixed valency of iron was also expected to aid SEM imaging by producing an electrically conductive sample. Thus, the target stoichiometry was $Ca_{0.75}Ce_{0.25}ZrTi_{1.625}Fe_{0.375}O_7$ (Fe^{2+}: $2Fe^{3+}$).

The raw powders were either as purchased metal oxides (iron, cerium, titanium) all supplied by Alfa Aesar or from a premixed batch, which was being used for another aspect of wasteform development. The batch was, by mass fraction, 21.3 % CaO, 8.7 % ZrO_2 and 70.0 % TiO_2. This material had been calcined at 1200 °C for 10 hours in order to stabilise the CaO as perovskite, $CaTiO_3$. The production of a non-active precursor in a non-active environment is representative of the intended full-scale process. An additional 1 wt% of ZrO_2 and TiO_2 was included to buffer against the potential formation of deleterious secondary phases.

The four lubricants selected for this work were chosen on previous experience. Jenni (Jenni, Stennett et al. 2008) reported success with polyethylene glycol, zinc stearate, Ceridust and oleic acid in the free milling of powders. Polyethylene glycol, $H[OCH_2CH_2]_{\sim 6000}OH$ (molecular weight is approximately 6000), is a common mould release agent; zinc stearate, $[CH_3(CH_2)_{16}COO]_2Zn$, is used to improve powder flow properties and was used for mill lubrication in SMP (BNFL and Edwards 2002); Ceridust™ 3620 (a polyethylene wax, $H[CH_2CH_2]_nH$) is a commercial powder flow agent and; oleic acid, $CH_3(CH_2)_7CH=CH(CH_2)_7COOH$, is a common excipient and lubricant in the pharmaceutical industry. The precursor batches were mixed in a Turbula mixer with either 1.5 or 1.0 wt% of lubricant.

The attrition mill was operated in dry mode. Before milling, the mill was heated to ~65 °C as this had been shown in previous experimental work to reduce the likelihood of foot formation. The mill was filled with 16.00 kg of 3/8" Stainless Steel ball bearings (based on the recommendation of the manufacturer). Batches of 800 g (approximately 1 litre) of the metal oxide precursors were added to the mill whilst operating at a tip speed of 1.73 ms^{-1} (200 RPM). The mill was quickly brought to the desired speed of 2.16, 3.24 or 4.32 ms^{-1} (250, 375 or 500 RPM) and run for either 30 or 60 minutes. The mill was discharged whilst operating at the same speed as when charging.

Due to budgetary constraints (cost of HIP cans), the powders milled at 3.24 m s^{-1} for 30 min were not included from the zinc stearate, polyethylene glycol and oleic acid sample sets. The other milling parameters (2.16 or 4.32 ms^{-1} for 30 or 60 minutes) represent limits of milling and offer more information in the now limited sample set. In addition, a full set of milling parameters was investigated with the 'realistic' ceria simulant. Furthermore, a can of non-milled material (Turbula mixed only) with no lubricant was included in both HIP cycles as a control.

Each of the chosen batches of milled powders was packed into two stainless steel HIP cans 60 mm tall by 35 mm outside diameter. Each can was filled with loose material, which was compacted uniaxially by approximately 30 MPa of pressure. The cans were then filled with loose powders again and the process repeated until they were full, typically containing 160-170g of compressed powders. Lids, with 3 mm inside diameter evacuation tubes, were autogenously welded to the cans. The sealed cans were attached to a vacuum line and heated to 600 °C for four hours with the intention of fully removing the lubricant. The bake out temperature was higher than the highest boiling point (260-450 °C) of the lubricants. After bake out, the can stems were crimped, cut and welded closed without releasing the vacuum or reducing the temperature.

The batches of milled material were divided into two sets of HIP cans. One set of cans was consolidated by HIP at 1320 °C and the other at 1000 °C. Both HIP cycles had a two hour dwell at temperature and 100 MPa of pressure applied during the dwell, supplied by argon. The intention of this low temperature HIP cycle was not to form the zirconolite phase but to trap (or 'freeze') the as-milled microstructure of the powders in a form suitable for analysis (i.e. monolithic and sufficiently robust for ceramographic analysis). Heating rates in the HIP were typically ~8 °C min^{-1} below 1100 °C and <5 °C min^{-1} otherwise. Pressure was increased steadily with temperature and was kept constant throughout the hold.

A core of the consolidated material was removed from the cans for examination. A section was hot mounted with conductive resin and ground with successively finer grit papers (300, 500, 800) before being polished with 5 and 1 μm diamond suspensions to obtain an optical finish. SEM images were obtained whilst operating in the back-scattered electron composition mode with 15 kV accelerating voltage, spot size of 35 and a working distance of 15 mm. Two images were acquired of the same area: one at 200x magnification and one at 1500x. Energy Dispersive X-ray spectroscopy coupled to the SEM, was used for elemental mapping. Another aliquot was ground into a fine powder and X-ray diffraction data were obtained. Due to significant Ti fluorescence, it was necessary to smooth the data with a 5-point moving average. Sample densities were measured using the Archimedes method with water as the immersion fluid.

4 Results

4.1 Lubricant Performance

Lubricant performance during milling was judged on the ability of the additive to prevent the powder forming a foot during the milling operation. For the current purpose, a foot was considered to be two or more layers of milling balls tightly packed with powder. To remove a compaction, the mill must be fully disassembled and the powders discharged by hand. Only the addition of Ceridust™ lubricant failed to consistently prevent the compaction of powders in the mill. A crude measurement of discharge rate was used to rank the other three lubricants; the discharges were timed until approximately 99%, by mass of the milled powders had been collected in a receiving jar. Oleic acid typically allowed the milled powders to be discharged within 2 minutes, while polyethylene glycol and zinc stearate took between 4 and 10 minutes to achieve discharge, respectively.

4.2 Lubricant Removal

Complete removal of the lubricant during the bake out step would result in a theoretical weight loss of ~1.5%. However, the actual weight loss was determined to be between 1.0 – 11.3 % over the range of samples investigated, with no obvious correlation between the type of lubricant and weight loss achieved, see Table 6. There was an observation that after removal of the sealed HIP can from the vacuum system, there was often an oily liquid dripping from the evacuation tube. This was assumed to be a form of the lubricant and implies the lubricant is condensing in the evacuation system rather than being removed.

Tip Speed ($m\ s^{-1}$)	Duration (minutes)	Lubricant	Lubricant Addition (wt%)	Mass Loss (wt%)
2.16	30	zinc stearate	1.5	1.7
2.16	60	zinc stearate	1.5	1.5
4.32	30	zinc stearate	1.5	1.5
2.16	30	Ceridust	1.5	1.5
2.16	60	Ceridust	1.5	1.7
4.32	30	Ceridust	1.5	1.6
2.16	30	polyethylene glycol	1.5	3.8
2.16	60	polyethylene glycol	1.5	11.2
4.32	30	polyethylene glycol	1.5	1.4
2.16	30	oleic acid	1.0	1.3
2.16	60	oleic acid	1.0	1.1
4.32	30	oleic acid	1.0	1.0

Table 6: Comparison of expected mass loss after lubricant removal step and actual weight loss for all packed high temperature HIP cycle cans

It was concluded that weight loss during bake out was dominated by removal of powder material from the HIP can (into the vacuum system) and the loss of entrained water. Post HIP, the cans with the largest recorded mass loss showed gross deformities at the top of the can indicating the removal of material. The removal of any material is not acceptable in an active operating environment and highlights the need for careful consideration of the bake out vacuum system and connecting filter design. This work was undertaken at the beginning of exploration of HIP can styles and was the first to utilise an in-house can design (as apposed to an external prescribed design). Subsequent

HIP can designs will include a sintered metal filter at the base of the evacuation tube. This filter will retain all solid material yet allow gases to pass through.

4.3 Observations On Sample Preparation

To measure the density of the samples, a core of material was taken from the consolidated product. During this process, the cut surfaces of the sample produced a sound that was indicative of the release of gas. Many small bubbles forming on the surface of the sample were also observed, accompanied by a smell similar to burnt oil. Even a few minutes after cutting, this sound continued implying the release of pressurised gas from the ceramic matrix. It was therefore concluded that the lubricant had not been removed fully during the bake out step. It may be that the lubricants had undergone pyrolysis during the bake-out step, leaving behind highly reductive C that had scavenged oxygen from the metal oxides to form CO/CO_2 or it may be that the lubricant had depolymerised or vaporised and the resulting gas became entrained in the ceramic product. This gas was only released when a suitable pathway for discharge became available. Attempts to quantify the mass of entrained lubricant, by heating the ceramic product at 2 °C min^{-1} to 1100 °C with an 8 hour dwell, resulted in the ceramic bodies exploding. The explosion indicates an increase in internal pressure within the ceramic and clearly shows that some remnant of the lubricant remains within the product.

4.4 Product Densities

4.4.1 Low Temperature HIP Cycle

The measured densities of the samples consolidated during the low temperature HIP cycle are given as Table 7. The samples are ordered by increasing density. Theoretical density has been calculated by assuming zero phase development and that all precursor components remain in their initial form (i.e. as ZrO_2, TiO_2 etc.) and is given as 4.80 g cm^{-3}. There does not appear to be any strong correlation between the milling parameters and the density of the products. While three of the four samples manufactured from powders milled

at 2.16 m s^{-1} for 60 min have the lowest densities (3.80, 3.82, 3.87 g cm^{-3}), the fourth sample (polyethylene glycol) has the seventh highest density. It is likely that this grouping is a coincidence. Examination of other milling conditions shows that the samples made from powders milled at 4.32 m s^{-1} for 30 min, nominally the most aggressive milling condition, are spread over the observed density range (4.06, 4.06, 4.23, 4.25 g cm^{-3}) with no obvious grouping or correlation. Notably, the densest product is the sample that was made from non-milled powders. These raw precursors did not have any lubricant added and were only lightly mixed (Turbula mixed).

Tip Speed (m s^{-1})	Duration (min)	Lubricant	Density (g cm^{-3})	% TD
2.16	60	zinc stearate	3.80	79.2
2.16	60	Ceridust	3.82	79.6
2.16	60	oleic acid	3.87	80.6
2.16	30	Ceridust	4.05	84.4
4.32	30	zinc stearate	4.06	84.6
4.32	30	polyethylene glycol	4.06	84.6
2.16	30	polyethylene glycol	4.09	85.2
2.16	60	polyethylene glycol	4.21	87.7
3.24	30	oleic acid	4.22	87.9
4.32	30	oleic acid	4.23	88.1
4.32	30	Ceridust	4.25	88.5
2.16	30	oleic acid	4.25	88.5
2.16	30	zinc stearate	4.36	90.8
0	0	none	4.43	92.3

Table 7: Density of samples, ordered by increasing density. Samples consolidate by the low temperature HIP cycle. Theoretical density calculated as 4.80 g cm^{-3}.

4.4.2 High Temperature HIP Cycle

The measured densities of the ceramic products manufactured by the high temperature HIP cycle are reported in Table 8 (in order of increasing density). The samples have a range of densities between 79.5 % and 89.2 % of theoretical density. The theoretical density was calculated as 4.78 g cm^{-3}, based on the published unit cell volume of the zirconolite structure and nominal composition. Shaw (Shaw 1998) determined the critical porosity, the point between closed (i.e. isolated) and open (i.e. interconnected) porosity, to be 92% in plutonium

ceramic wasteforms and this was set as the target product density. Elimination of open porosity is desirable to minimise product surface area available for dissolution in the disposal environment. None of the milled samples prepared in this study were found to exhibit ceramic density above this 92% threshold and there did not appear to be any clear correlation between the speed and duration of milling, choice of lubricant and the final density. Again, the densest sample was manufactured from non-milled powders.

Tip Speed ($m\ s^{-1}$)	Duration (min)	Lubricant	Density ($g\ cm^{-3}$)	% TD
2.16	30	Ceridust	3.80	79.5
2.16	60	polyethylene glycol	3.90	81.5
4.32	30	oleic acid	3.98	83.2
2.16	30	polyethylene glycol	4.06	84.9
2.16	60	oleic acid	4.06	84.9
2.16	30	zinc stearate	4.07	85.2
4.32	30	Ceridust	4.10	85.8
2.16	60	Ceridust	4.16	87.0
4.32	30	polyethylene glycol	4.16	87.1
2.16	60	zinc stearate	4.18	87.5
3.24	30	oleic acid	4.18	87.5
2.16	30	oleic acid	4.26	89.1
4.32	30	zinc stearate	4.26	89.2
0	0	none	4.72	98.8

Table 8: Density of samples ordered by increasing theoretical density. Samples consolidated by the high temperature HIP cycle. Theoretical density calculated as 4.78 g cm^{-3}.

If the density variations were a result of the milling parameters only, the expectation would be that the two sample sets show the same trends. That is, for example, the densest sample in each set should be from the same milled powders (excluding the non-milled control). This has not been observed. Thus, the conclusion is that the sample variations are a result of a post milling action.

4.5 XRD AND SEM

More useful information can be displayed through the comparison of XRD and SEM results than either technique on their own. Accordingly, the XRD patterns and corresponding SEM images are presented together in this section. The

samples are categorised by the different HIP cycles before being broken down in to each lubricant. For reference and comparison, the two consolidated samples manufactured from non-milled powders are also given.

4.5.1 Non-Milled Samples

Figure 13 gives two XRD patterns for the samples manufactured from the non-milled powders. These samples are included as a reference and a control. The low temperature sample shows a highly multiphase product with a series of strong reflections attributable to perovskite and free ZrO_2. There are also a number of reflections in the XRD pattern of the low temperature sample as a result of free TiO_2, marked '5'. Remembering the low temperature HIP cycle was not intended to form the single host phase but rather trap the milling microstructure, such a polyphase sample is not surprising. The lack of clear reflections directly attributable to any FeO_x is interesting. It is likely that the iron has partitioned in to the zirconolite, perovskite or ilmenite phases. The high temperature HIP cycle has produced a different XRD pattern implying a different level of phase development has occurred. In the XRD pattern, the majority of the reflections are associated with zirconolite (marked as 1) as well as significant signals for CeO_2 and ZrO_2 (marked 3 and 4). This shows that the coarsest particle sized precursors (i.e. non-milled) can go on to form the zirconolite host phase, as long as they undergo the high temperature HIP cycle.

Comparing the low temperature HIP cycle XRD data with the corresponding SEM, Figure 14, the multiphase nature of the sample is clarified. In the 200x magnification image, left, there are large inclusions (~100 μm) of perovskite. There is a greater fraction of perovskite inclusions than zirconolite bulk phase and this is shown in the XRD pattern. These perovskite inclusions are a remnant of the precursor manufacturing process. There are also numerous inclusions, 10-20 μm, of unreacted CeO_2 (shown as bright white areas). Considering these powders have not been milled, this largely heterogeneous nature is expected.

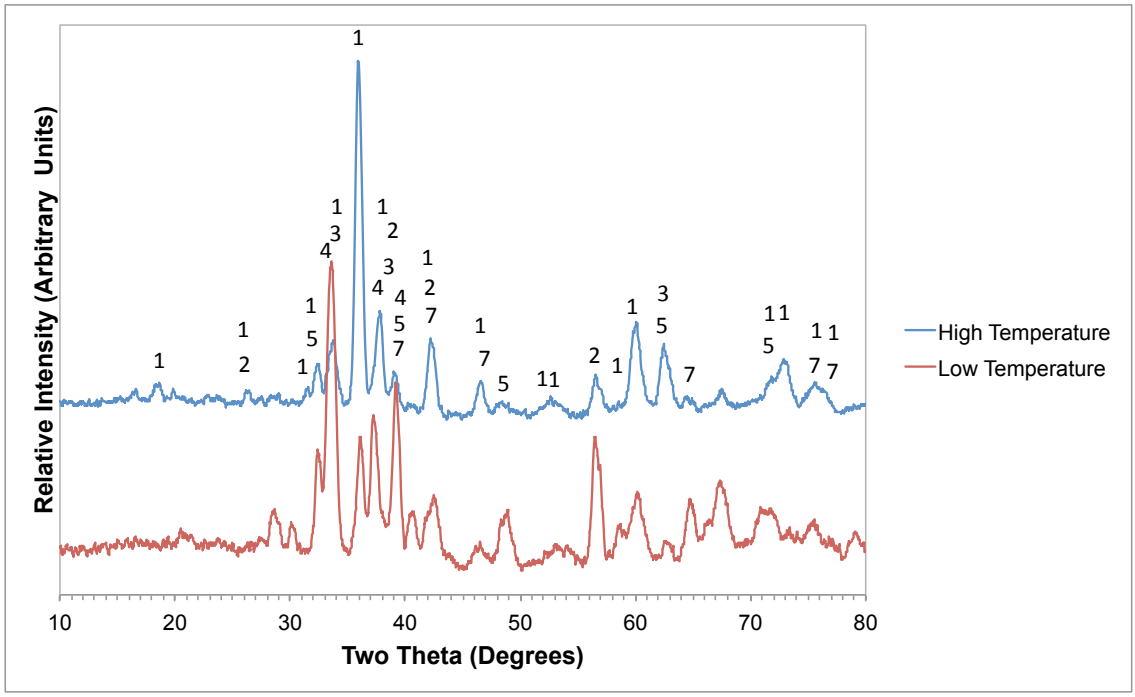

Figure 13: Comparison of two samples consolidated from non-milled powders at low (1000 °C) and high (1320 °C) HIP cycles. Major reflections labelled as; 1: zirconolite; 2: perovskite; 3: ceria; 4: zirconia; 5: titania; 7: ilmenite

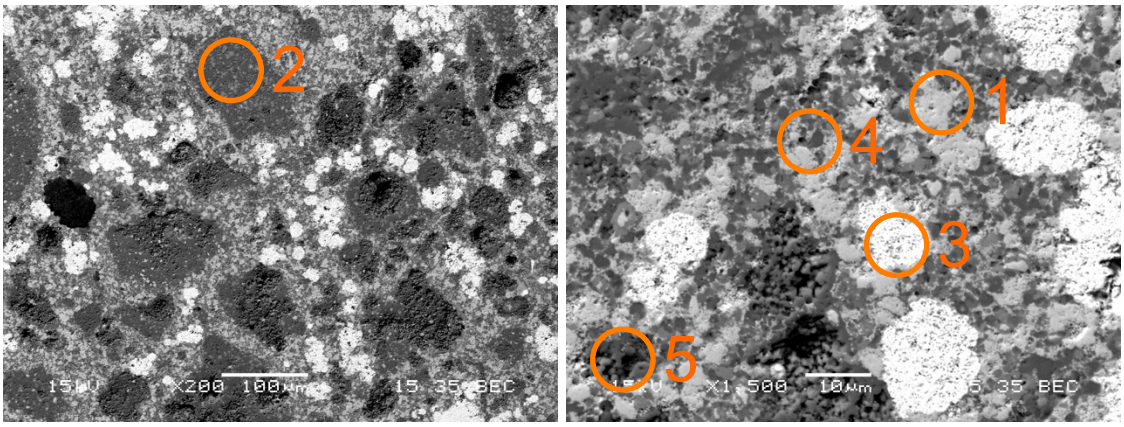

Figure 14: SEM of low temperature HIP cycle consolidated non-milled material. Left image 200x magnification, right image, 1500x magnification. Phases labelled as; 1: zirconolite; 2: perovskite; 3: ceria; 4: zirconia; 5: titania

Figure 15 shows the SEM images of the high temperature HIP cycle consolidated material. The XRD pattern implied a significantly less heterogeneous sample than the low temperate HIP cycle with zirconolite phase development and less perovskite; this is reflected in the SEM images. There are still remnants of the perovskite inclusions shown in Figure 14, however, there is far greater extent of zirconolite host phase present. Notably, the number and size of free ceria inclusions has not significantly changed, judged by comparison of the two pairs of SEM images. The low temperature sample does

not appear to have a significant level of porosity. The high density of this sample (compared to other low temperature samples) would confirm this observation.

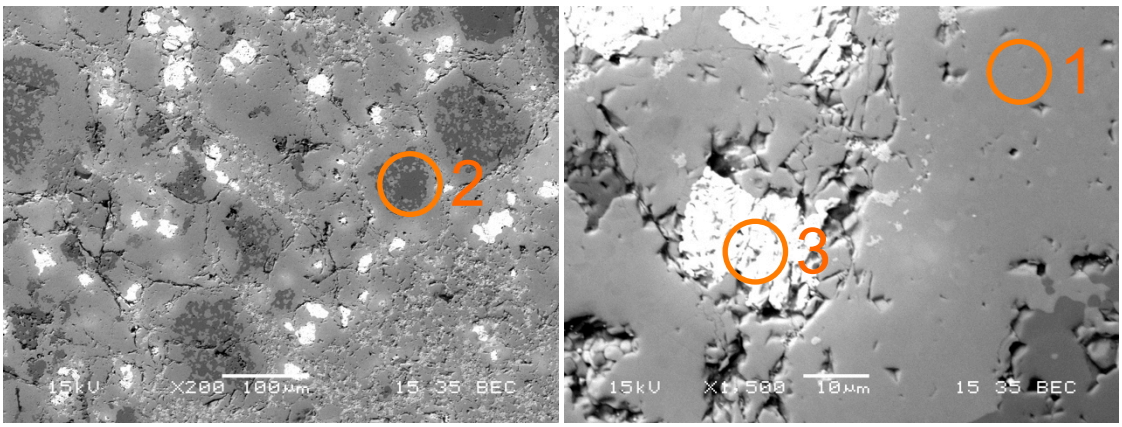

Figure 15: SEM of high temperature HIP cycle consolidated non-milled material. Left image 200x magnification, right image, 1500x magnification. Phases labelled as; 1: zirconolite; 2: perovskite; 3: ceria

4.5.2 Low Temperature HIP Cycle

The following samples were consolidated during the low temperature HIP cycle (1000 °C). The intention of these samples was not to form the zirconolite host phase, but to 'freeze' the milled powders into a form suitable for analysis. The size and distribution of the ceria inclusions should give some indication of the extent of milling.

4.5.2.1 Zinc Stearate

Figure 16 shows the XRD pattern for samples manufactured from powders milled with zinc stearate as the lubricant and consolidated by the low temperature HIP cycle. All three of the samples show very similar patterns indicating a similar phase development between each sample. All of the milling runs freely discharged and it seems logical to assume that all of the powders were milled (rather than remaining on the base of the mill). The XRD patterns show the development of the zirconolite phase, marked with the Miller indices of the significant responses, as well as a significant proportion of perovskite. Interestingly, the number of phases developed, shown by the XRD patterns, appears to be consistent throughout all of the zinc stearate samples.

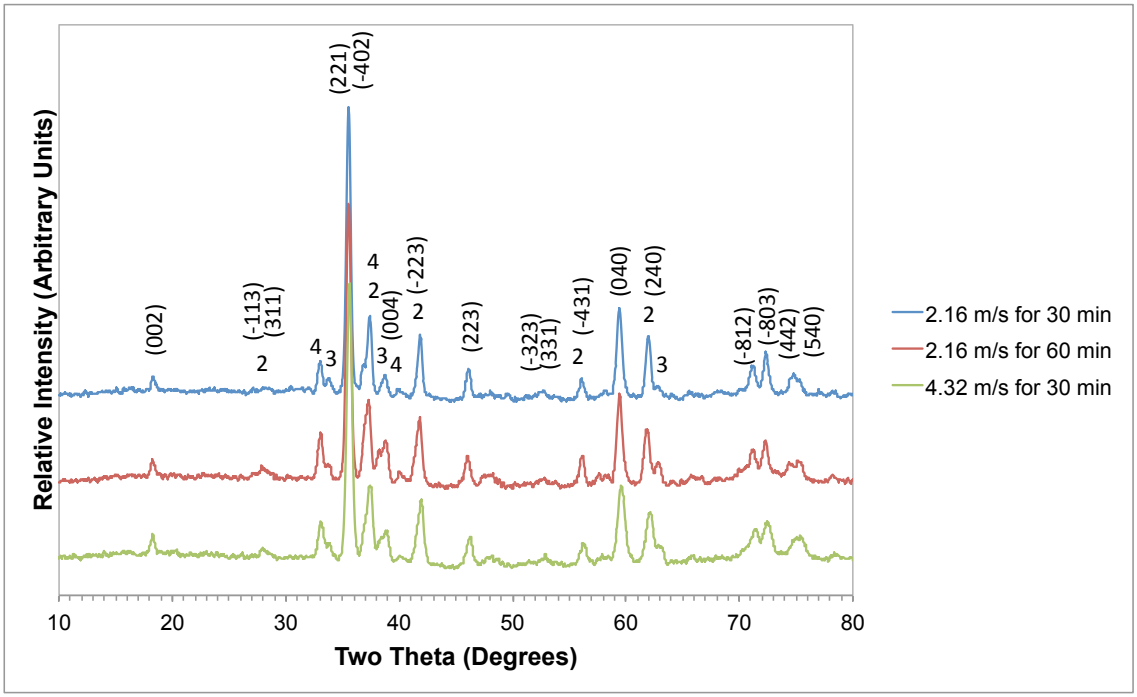

Figure 16: XRD traces of samples milled with zinc stearate and consolidated by HIP at 1000 °C. Main phase zirconolite marked with the Miller indices. Major reflections labelled as; 2: perovskite; 3: ceria; 4: zirconia

Figure 17 shows SEM images of the three samples consolidated from material milled with zinc stearate. All three samples are broadly similar and this confirms the XRD data. The ZrO_2 has tended to form the zirconolite phase, which appears as a continuous component (light grey). Interspersed in the sample are more perovskite particles (dark grey) and titania (black). The least aggressively milled powder sample has significantly fewer ceria inclusions than the non-milled sample presented earlier, indicating that milling at 2.16 m s^{-1} for 30 min is not below the lower limit of milling; that is, the powders are being size reduced. The middle image gives the sample made from powders milled at 2.16 m s^{-1} for 60 min. Slightly fewer ceria inclusions are noticeable in the 200x magnification image but, as noted in the 1500x magnification image, there are still ceria inclusions of approximately 20 μm. There are no obvious large perovskite particles, as observed in the non-milled sample. These appear to have been broken into ~10 μm particles. The increased milling duration does seem to improve the product quality in terms of reducing the number of large unreacted components. Examining the 4.32 m s^{-1} for 30 min sample there are, again, fewer obvious ceria inclusions than the other milling conditions. This

indicates an increased milling speed is required to impart more energy into the milling process rather than solely increasing the number of mill revolutions.

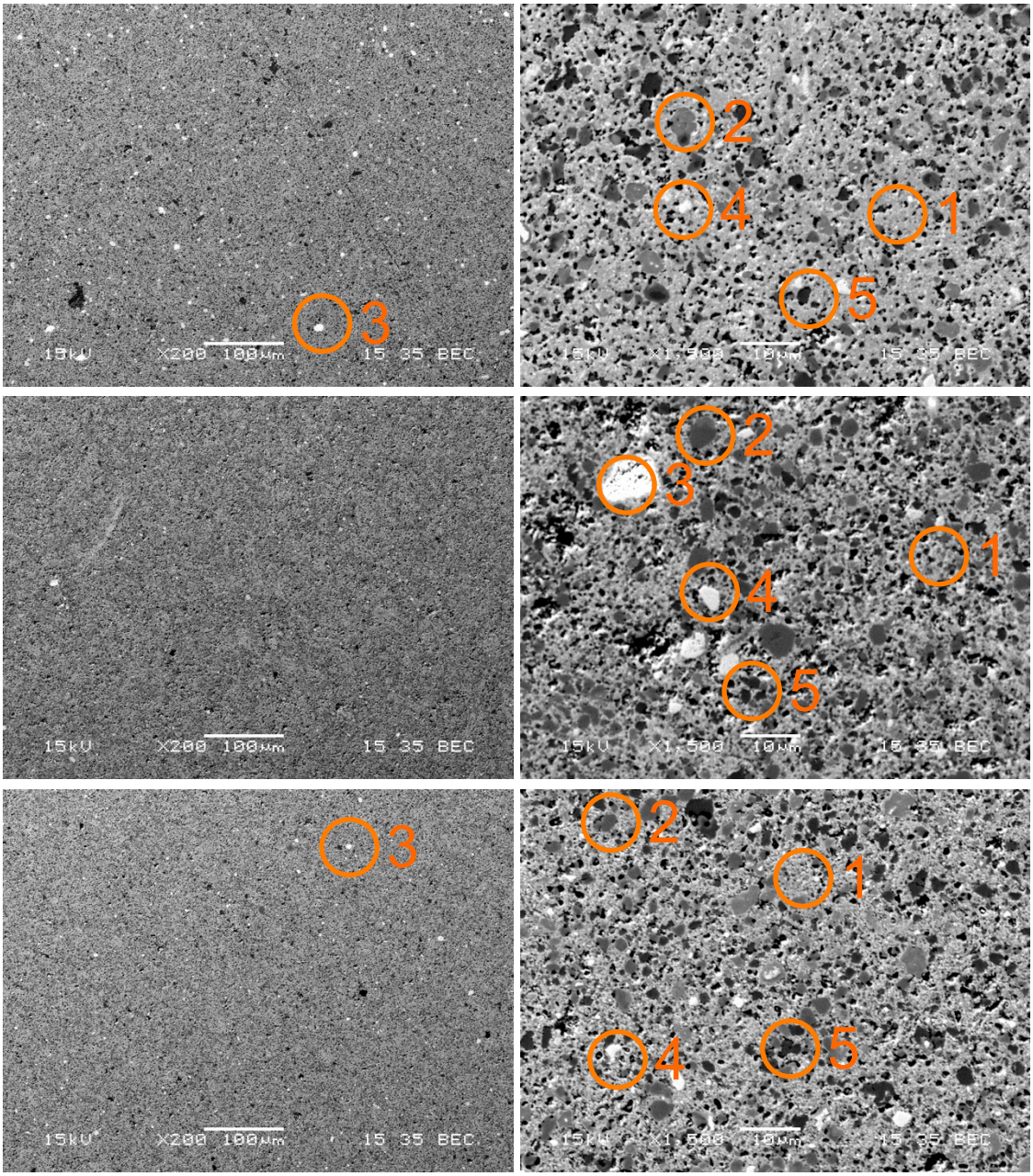

Figure 17: SEM of samples consolidated by the low temperature HIP cycle from powders milled with zinc stearate. From top, 2.16 m s^{-1} for 30 min, 2.16 m s^{-1} for 60 min, 4.32 m s^{-1} for 30 min. Left image 200x magnification, right image, 1500x magnification. Phases labelled as; 1: zirconolite; 2: perovskite; 3: ceria; 4: zirconia; 5: titania

4.5.2.2 Ceridust

Figure 18 gives the XRD patterns for the samples consolidated during the cold HIP cycle from powders milled with Ceridust. The three patterns are clearly

different from each other, in contrast to those milled with zinc stearate, Figure 16. Ceridust failed to prevent foot formation consistently and the two batches of powders milled at 2.16 m s^{-1} (both 30 min and 60 min) failed to freely discharge.

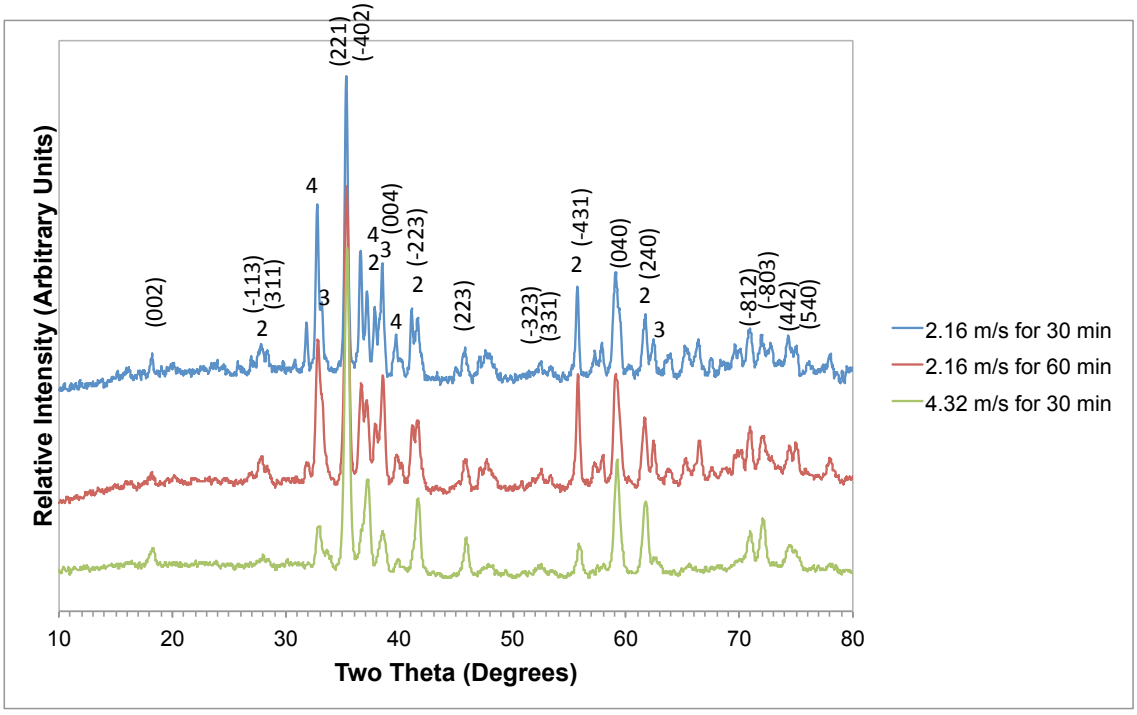

Figure 18: XRD patterns of samples milled with Ceridust and consolidated by HIP at 1000 °C. Main phase zirconolite marked with the Miller indices. Major reflections labelled as; 2: perovskite; 3: ceria; 4: zirconia

This failure to successfully mill and discharge the powders is revealed in the variation of the phase development, as shown by the XRD patterns. In SEM images, Figure 19, the same change in sample quality can be seen. The two samples manufactured from powders milled at 2.16 m s^{-1} show a large number of free ceria inclusions (white), which are not present in the 4.32 m s^{-1} for 30 min sample. This would imply that the powders have not been milled to the same extent. The initial belief was that if the powders were going to agglomerate and form a foot during milling, it would be as soon as the powders were added to the mill. Comparing Figure 19 with the non-milled samples, Figure 14, there are far fewer large perovskite particles (dark grey), indicating that some size reduction has occurred. The conclusion is that if the powders fail to discharge fully from the mill, they may still have undergone some milling before agglomerating at the base of the mill. The SEM image of the sample milled at

4.32 m s^{-1} for 30 min is equivalent to the corresponding 4.32 m s^{-1} for 30 min sample in Figure 17. Both show a clear reduction in the number of free ceria inclusions and an increase in the overall homogeneity. That is, a reduction in large particles and improved mixing of all the phases.

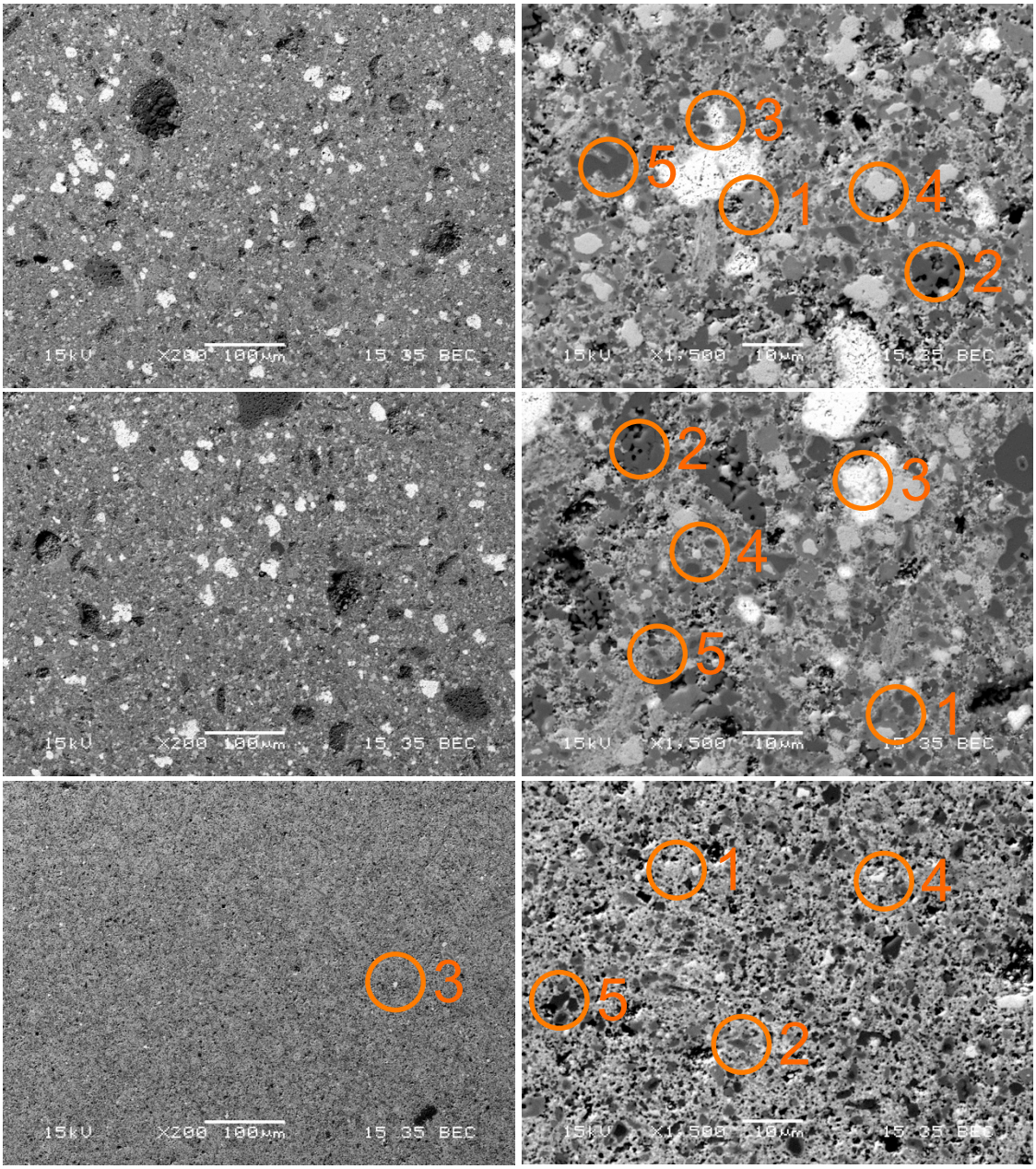

Figure 19: SEM of samples consolidated by the low temperature HIP cycle from powders milled with Ceridust. From top, 2.16 m s^{-1} for 30 min, 2.16 m s^{-1} for 60 min, 4.32 m s^{-1} for 30 min. Left image 200x magnification, right image, 1500x magnification. Phases labelled as; 1: zirconolite; 2: perovskite; 3: ceria; 4: zirconia; 5: titania

4.5.2.3 Polyethylene Glycol

The XRD patterns for samples consolidated by the low temperature HIP cycle from powders milled with polyethylene glycol are given as Figure 20. Similar to the case of the Ceridust samples, Figure 18, the XRD patterns do show a correlation with milling conditions. Again, there appears to be an improvement in the samples as the milling becomes more aggressive, from 2.16 m s^{-1} for 30 min to 4.32 m s^{-1} for 30 min. The intensity of the reflections associated with perovskite, ceria and zirconia decrease, as the samples become progressively more milled. All of the polyethylene glycol samples freely discharged and it was expected that Figure 20 would be similar to the zinc stearate samples, that is, with minimum variation in the XRD patterns and thus, the phase development of the samples.

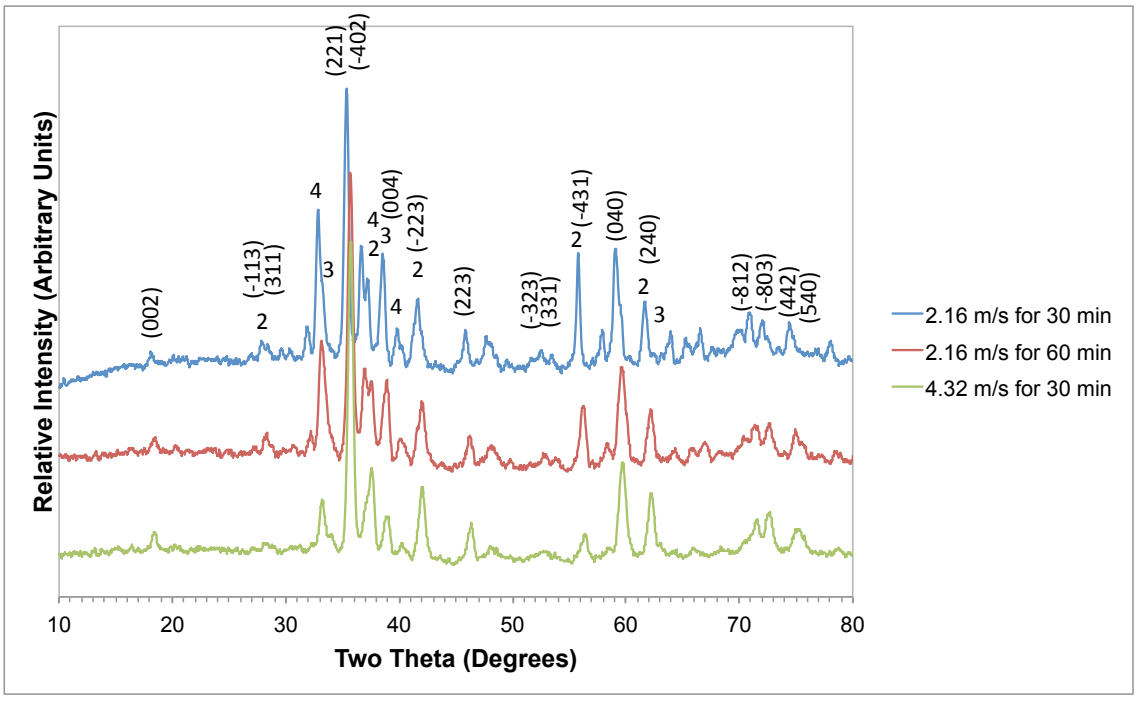

Figure 20: XRD patterns of samples milled with polyethylene glycol and consolidated by HIP at 1000 °C. Main phase zirconolite marked with the Miller indices. Major reflections labelled as; 2: perovskite; 3: ceria; 4: zirconia

Examining the SEM images, Figure 21, there is the same progression in samples shown in the XRD patterns. The most aggressively milled sample (4.32 m s^{-1}) has the most uniform grain distribution and the smallest number of obvious ceria inclusions. In comparison to Figure 19, there are fewer large perovskite

particles in the samples made from powders milled at 2.16 m s^{-1} indicating the powders used to make the samples in Figure 21 have been size reduced to a greater extent. However, there are still a large number of ceria inclusions.

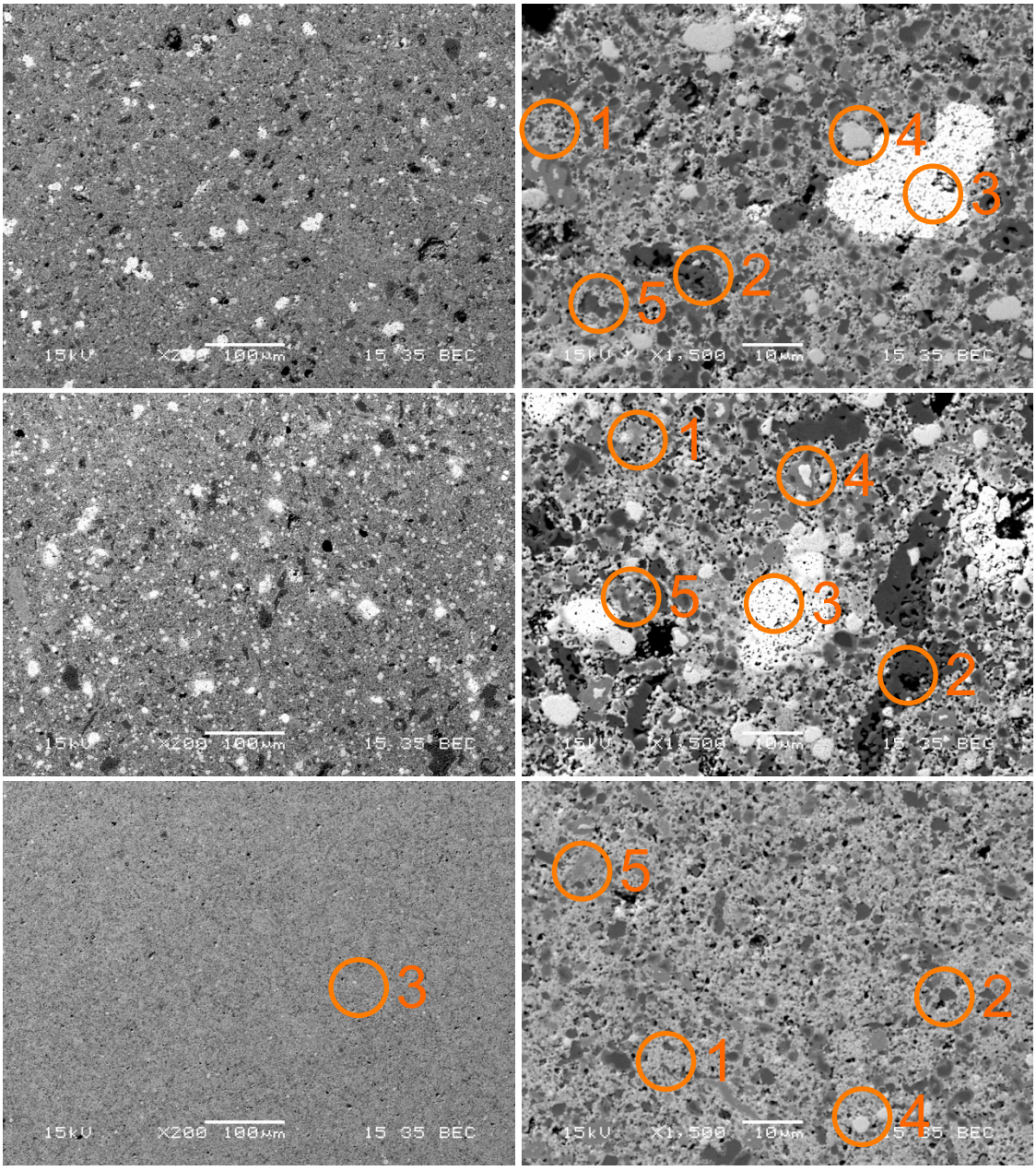

Figure 21: SEM of samples consolidated by the low temperature HIP cycle from powders milled with polyethylene glycol. From top, 2.16 m s^{-1} for 30 min, 2.16 m s^{-1} for 60 min, 4.32 m s^{-1} for 30 min. Left image 200x magnification, right image, 1500x magnification. Phases labelled as; 1: zirconolite; 2: perovskite; 3: ceria; 4: zirconia; 5: titania

Figure 22 shows a ~1500 µm of non-milled material inclusion from the sample consolidated from powders milled at 4.32 m s^{-1} for 30 min. This material is believed to be typically a result of powders gathering in the mill discharge

valve, this material generally only accounts for 2-3 g or 0.2-0.4 wt% of total powders. As it is such a small percentage of the overall material, it is likely that small inclusions can be tolerated in the final wasteform. However, if possible, in the active implementation, the valve should be designed so that there is no dead space for non-milled material to accumulate.

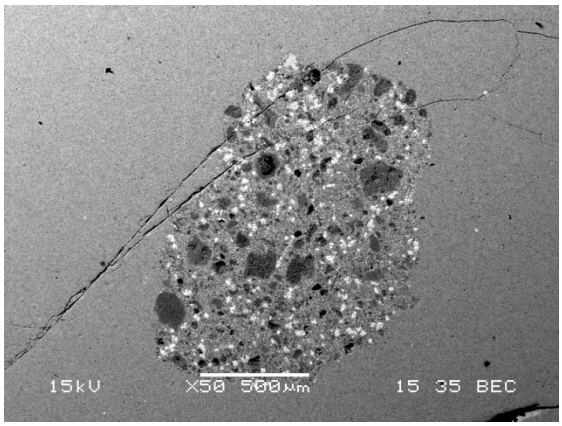

Figure 22: SEM image showing detail of a non-milled inclusion in the sample manufactured from powders milled at 4.32 m s^{-1} for 30 min. This image was taken at 50x magnification.

4.5.2.4 Oleic Acid

The XRD patterns for the samples consolidated by the low temperature HIP cycle from powders milled with oleic acid are given as Figure 23. All four of the patterns are broadly similar to each other indicating the development of the zirconolite main phase and a perovskite minor phase. The four batches of powder freely discharged from the mill and can be considered to have undergone some size reduction and homogenisation, leading to consistent phase development throughout the sample set. As a complete set of results, the samples milled with oleic acid show the same correlations with milling and phase development as those milled with zinc stearate.

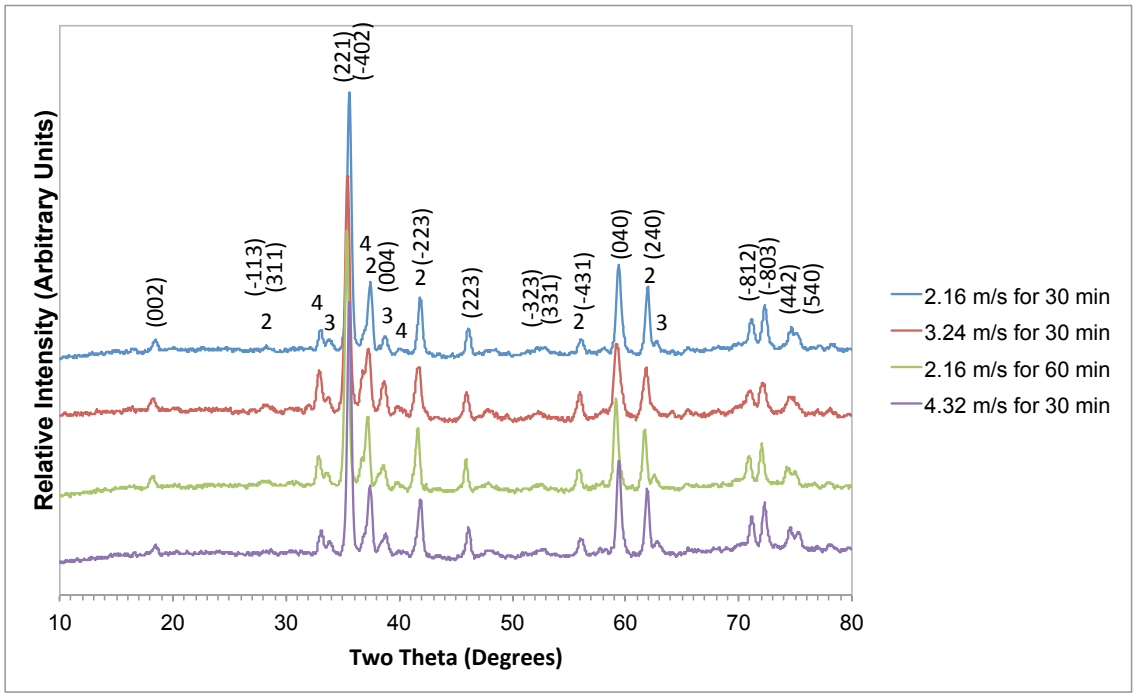

Figure 23: XRD patterns of samples milled with oleic acid and consolidated by HIP at 1000 °C. Main phase zirconolite marked with the Miller indices. Major reflections labelled as; 2: perovskite; 3: ceria; 4: zirconia

Examination of the SEM images, Figure 24, shows the same phases identified in all the images. There is a decrease in the size and number of free ceria inclusions as the milling becomes more aggressive (from 2.16 m s^{-1} for 30 min to 4.32 m s^{-1} for 30 min). The large holes in the third image (2.16 m s^{-1} for 60 min) are a result of sample preparation and are not genuine pores. However, the pores in other samples in Figure 24 are considered real.

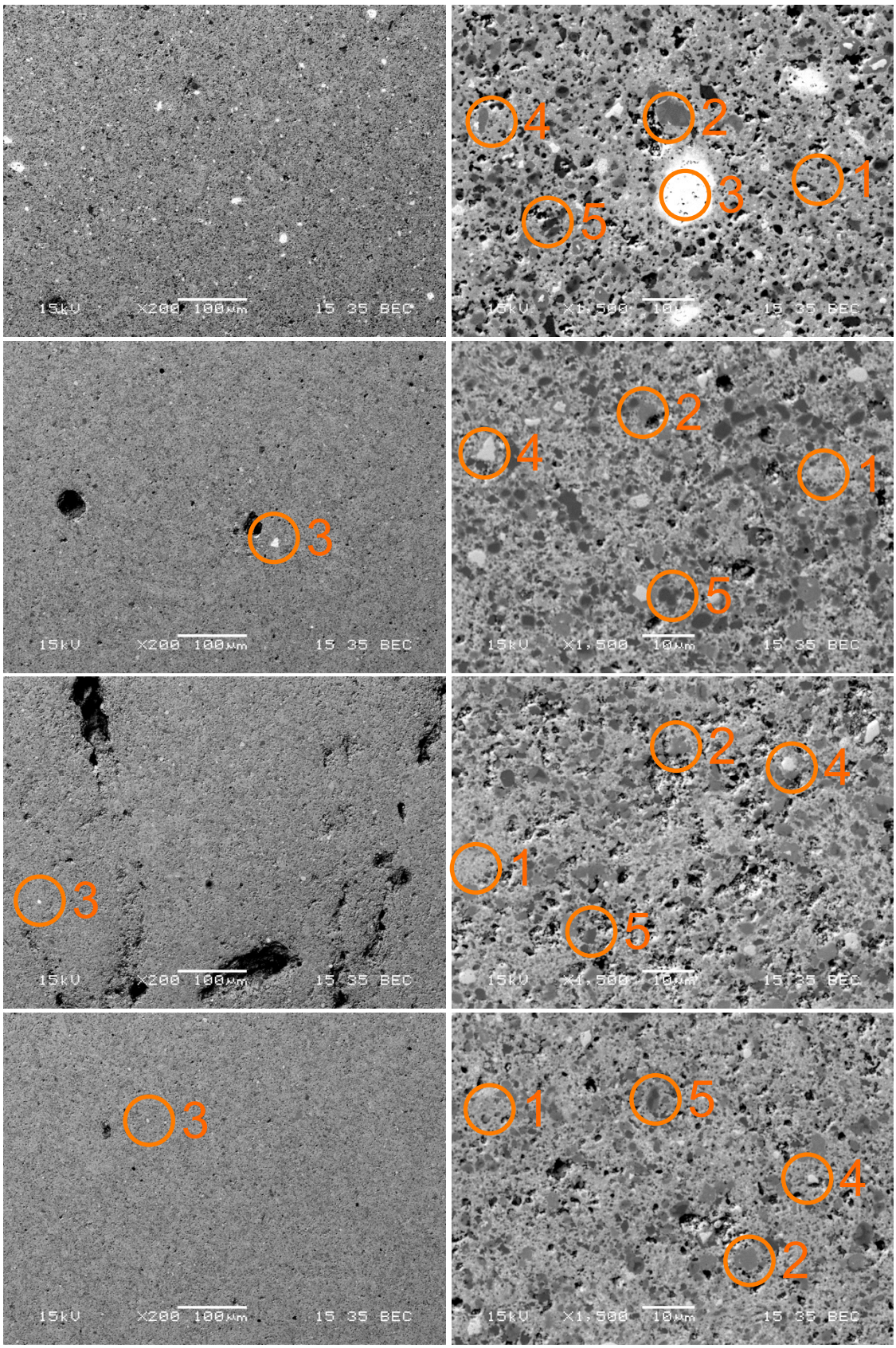

Figure 24: SEM of samples consolidated by the low temperature HIP cycle from powders milled with oleic acid at, from top, 2.16 m s^{-1} for 30 min, 3.24 m s^{-1} for 30 min, 2.16 m s^{-1} for 60 min, 4.32 m s^{-1} for 30 min. Left image 200x magnification, right image, 1500x magnification. Phases labelled as; 1: zirconolite; 2: perovskite; 3: ceria; 4: zirconia; 5: titania. Large black areas on the 3.24 m s^{-1} for 30 min sample are damage induced during sample preparation.

4.5.2.5 Discussion

The purpose of the low temperature HIP cycle (1000°C) was to trap the post milling microstructure in a form suitable for analysis. Each of the samples was analysed by XRD and SEM with a good correlation between the phases identified by XRD and those observed by SEM. The more visibly homogenous samples (typically 4.32 m s^{-1} for 30 min in all lubricants) showed a more intense signal in the XRD patterns corresponding to zirconolite and a reduced signal for perovskite, ceria and zirconia. The phase development, as shown in the XRD patterns, of all of the milled and consolidated by low temperature HIP cycle samples were comparable to the non-milled high temperature consolidated sample. This is as opposed to these samples being comparable to the non-milled low temperature consolidated sample as expected. This is due to the large perovskite grains that remained in the low temperature non-milled sample dominating the XRD results. This coarse phase is not present in the milled samples and is predominately consumed in the formation of the zirconolite main phase. The extra thermal energy imparted during the high temperature HIP cycle allowed the non-milled sample to develop the zirconolite phase from the coarser starting material. It would follow that any size reduction of the powders will encourage the formation of zirconolite at both the high and low HIP cycle temperatures.

The samples milled with zinc stearate and oleic acid showed a reduction in the size and number of ceria inclusions implying that the milling set-up used could reduce the size of the powders. Interestingly, the high level of ceria digestion (incorporation into other phases) shown was not expected at this consolidation temperature. It was thought that the majority of ceria would not be fully incorporated into any of the phases, rather, having a small transitional boundary between the ceria inclusion and the bulk phase. The likely explanation is that the attrition mill reduced the particle size of the material and more intimately mixed the precursors than expected. The more intimate mixing results in small diffusional lengths for materials to travel to form the phases.

All of the samples milled with Ceridust, even the powders that formed a foot and failed to discharge from the mill, still appear to have undergone some size reduction and homogenisation. This is shown by the SEM images indicating fewer large perovskite grains and the XRD patterns being closer to the high temperature non-milled sample. It was thought that material forming a foot would travel directly to the base of the mill and not undergo any milling. The inference is that as the powders move from the feed port at the top of the mill to the base, where they form a foot, they still undergo some interaction with the milling media. This has the interesting implication that the size reduction task of the mill may be completed far earlier than thought and residence times could be minimised whilst still having the same size reduction effect. Care must be taken to ensure complete mixing still occurs. A further interpretation of the Ceridust results may be that as the powders are reduced in size, the overall surface area of the powders increases, thus increasing the likelihood of attractive powder-powder interactions. If the lubricant cannot act to interrupt these attractive forces, as intended, a foot may form when the powders have reached a certain size. This would explain the observation in the SEM images that the powders have undergone some size reduction and milling, yet they still failed to freely discharge from the mill.

A further impact of this work is from the results of the samples milled with polyethylene glycol. All of the powders milled with this lubricant freely discharged and by extension, did not form a foot. The assumption was that if the powders did not form a foot then they have been well milled. The XRD and SEM results suggest that the samples made from powders milled with polyethylene glycol are more similar to those milled with Ceridust: a lubricant that did not prevent foot formation consistently. Thus, whether powders freely discharge or not is not necessarily a good indicator of milling performance.

4.5.3 High Temperature HIP Cycle

The intention of the high temperature HIP cycle was to fully phase develop the zirconolite target product. As discussed in the density results section, there is no correlation between the milling conditions and the product density. The following XRD patterns and SEM images are to determine what relationship microstructure and phase development has with each lubricant and milling conditions.

EDS was undertaken on the samples. Detailed analysis of each phase in the sample manufactured from powders milled at 4.32 m s^{-1} for 30 min with oleic acid as the lubricant is given as Figure 25. These phases are found in all of the high temperature HIP cycle samples and this figure can be used as a key for the full results set.

Figure 25 shows a host matrix of zirconolite ($(Ca,Ce)Zr(Ti,Fe)_2O_7$, labelled 1) interspersed with dark coloured grains with lower average atomic numbers. Within many of these grains, a darker core is apparent. Analysis of the core region revealed a composition consistent with perovskite (nominally $CaTiO_3$) phase (2) with the outer shell to be another form of perovskite (6) substituted with cerium, calcium, iron, and titanium (i.e. $(Ca,Ce)(Ti,Fe)O_3$). There are also a number of iron rich grains, thought to be ilmenite (prototypically $FeTiO_3$), (7). These observations are consistent with XRD data.

All samples have a large number of pores and this is reflected in the low percentage theoretical densities recorded, Table 8. The size and distribution of grains and pores appears to be constant throughout the samples.

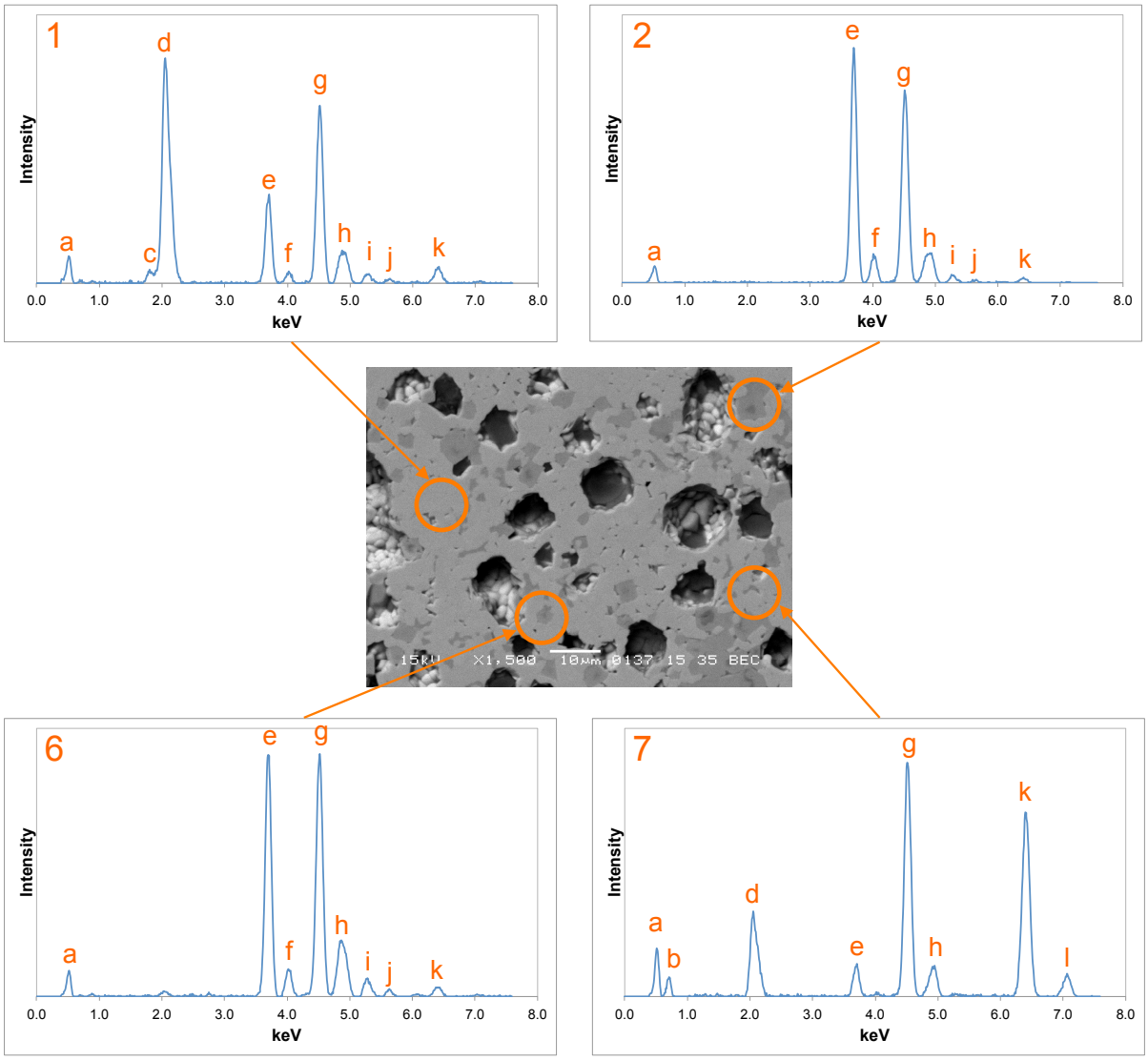

Figure 25: EDS traces for the four phases: 1: zirconolite; 2: perovskite; 6: substituted perovskite; 7: ilmenite. Peaks labelled as per Table 9.

Signal	Energy (keV)	Assignment
a	0.5	O(Kα)
b	0.7	Fe(Lα)
c	1.8	Zr(Lα)
d	2.1	Zr(Lα)
e	3.7	Ca(Kα)
f	4.0	Ca(Kβ)
g	4.5	Ti(Kα)
h	4.7-4.9	Ce(Lα)/Ti(Kβ)
i	5.4	Ce(Lβ)
j	6.1	Ce(Lγ)
k	6.4	Fe(Kα)
l	7.1	Fe(Kβ)

Table 9: EDS peak assignments for Figure 25

An example grain map from the polyethylene glycol sample is shown in Figure 26. Titanium has a homogeneous distribution throughout the product. Zirconium is equally distributed throughout the bulk with no zirconium observed within the perovskite grains. Calcium also tends to be well distributed in the primary zirconolite phase but with localised concentrations in the perovskite phases. Iron tends to localise in the ilmenite phase, however some still partitions in the zirconolite phase as the designated charge compensator. Cerium does not exhibit any localised concentrations and this is considered a positive observation, since agglomerations of plutonium within the wasteform would be undesirable.

The grain map and the SEM both show that the product is not homogenous with a large number of perovskite grains interspersed in the zirconolite matrix. Perovskite has been shown to be thermodynamically unstable in the repository environment (Lumpkin 2006). The EDS analysis shows a proportion of the cerium has partitioned into these grains and this could be a concern for the wasteform performance.

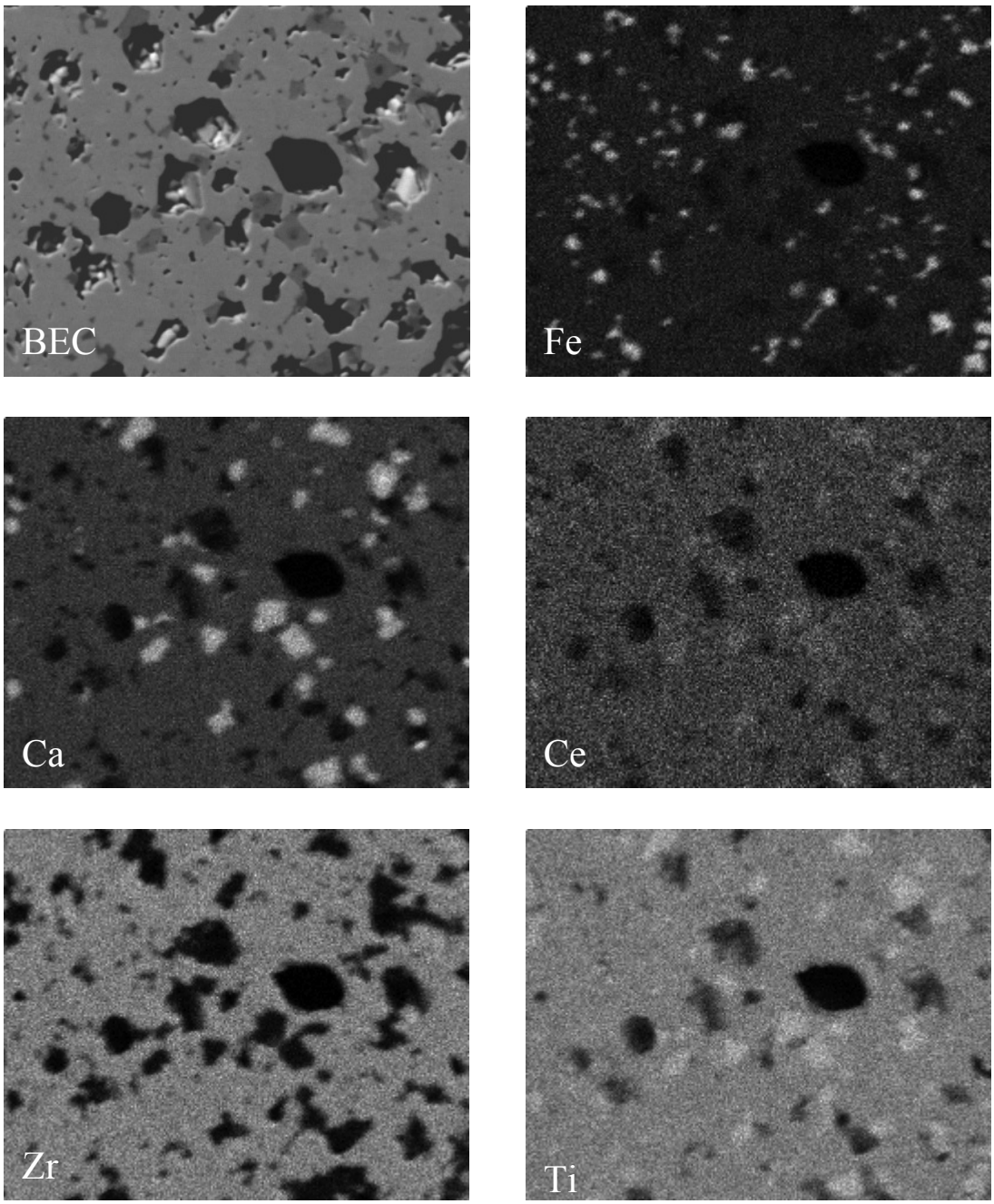

Figure 26: Elemental maps of consolidated powders milled at 4.32 ms^{-1} for 30 minutes with polyethylene glycol. Brighter pixels indicate more of each element at that particular location. Each image is labelled with its respective element and the backscattered image labelled as 'BEC'.

4.5.3.1 Zinc Stearate

The XRD patterns for samples manufactured from powders milled with zinc stearate are given as Figure 27. Regardless of the milling conditions (2.16 m s^{-1} for 30, 60 min and 4.32 m s^{-1} for 30), the XRD patterns show the same phase development, namely zirconolite, perovskite and ilmenite. Referring to the low temperature HIP cycle samples made from the same powders, Figure 16, these samples also show little variation in the phase development with the varying milling conditions. This result suggests that regardless of the milling conditions, the consolidation process will tend to produce final products that have the same phase development.

SEM images of the samples are shown in Figure 28. The same phases identified earlier are clearly visible and there is little variation in microstructure between the milling conditions. What is important to note are the large number of pores. One of the reasons HIP was chosen was that it is known to minimise or eliminate internal porosity. The source of this porosity is the failure to remove the lubricant completely from the HIP can before consolidation. If any of the lubricant remains, under the high temperatures (1320 ºC) used during this HIP cycle, it will either decompose into gaseous products or pyrolyse into C, which will go on to react to form CO/CO_2. These gases will then resist the consolidation processes and form the pores observed in the final products. This is unacceptable for a plutonium waste immobilisation process. The perovskite cores identified are likely a remnant of the large perovskite grains identified in the cold HIP cycle samples.

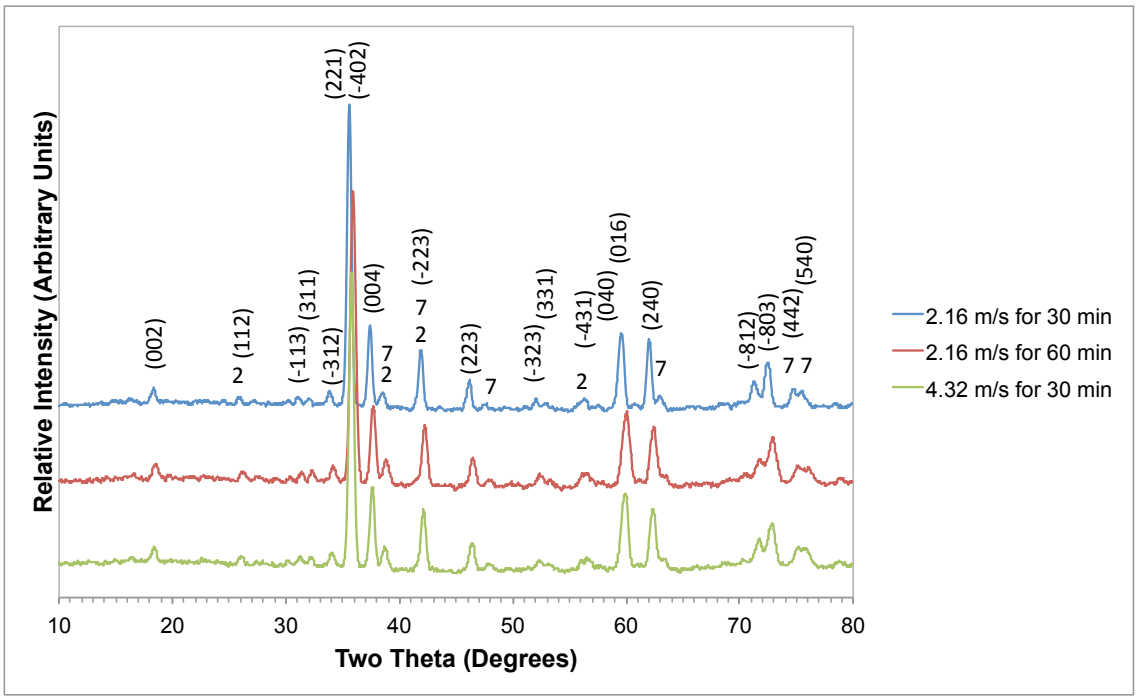

Figure 27: XRD patterns of samples manufactured from powders milled with zinc stearate and consolidated by high temperature HIP cycle. Main phase zirconolite marked with the Miller indices. Major reflections labelled as; 2: perovskite; 7: ilmenite

If coarse particles of these perovskite grains have remained, the attrition milling conditions have not been aggressive enough to fully size reduce the material. Noticeably, as the milling conditions become more aggressive, the size of these perovskite remnants does not substantially change. It follows that the large perovskite grains are easily reduced in size, however, as milling continues, the now smaller grains will be more difficult to size reduce further. It is these smaller, difficult to mill, remnants that are visible in the SEM images of Figure 28.

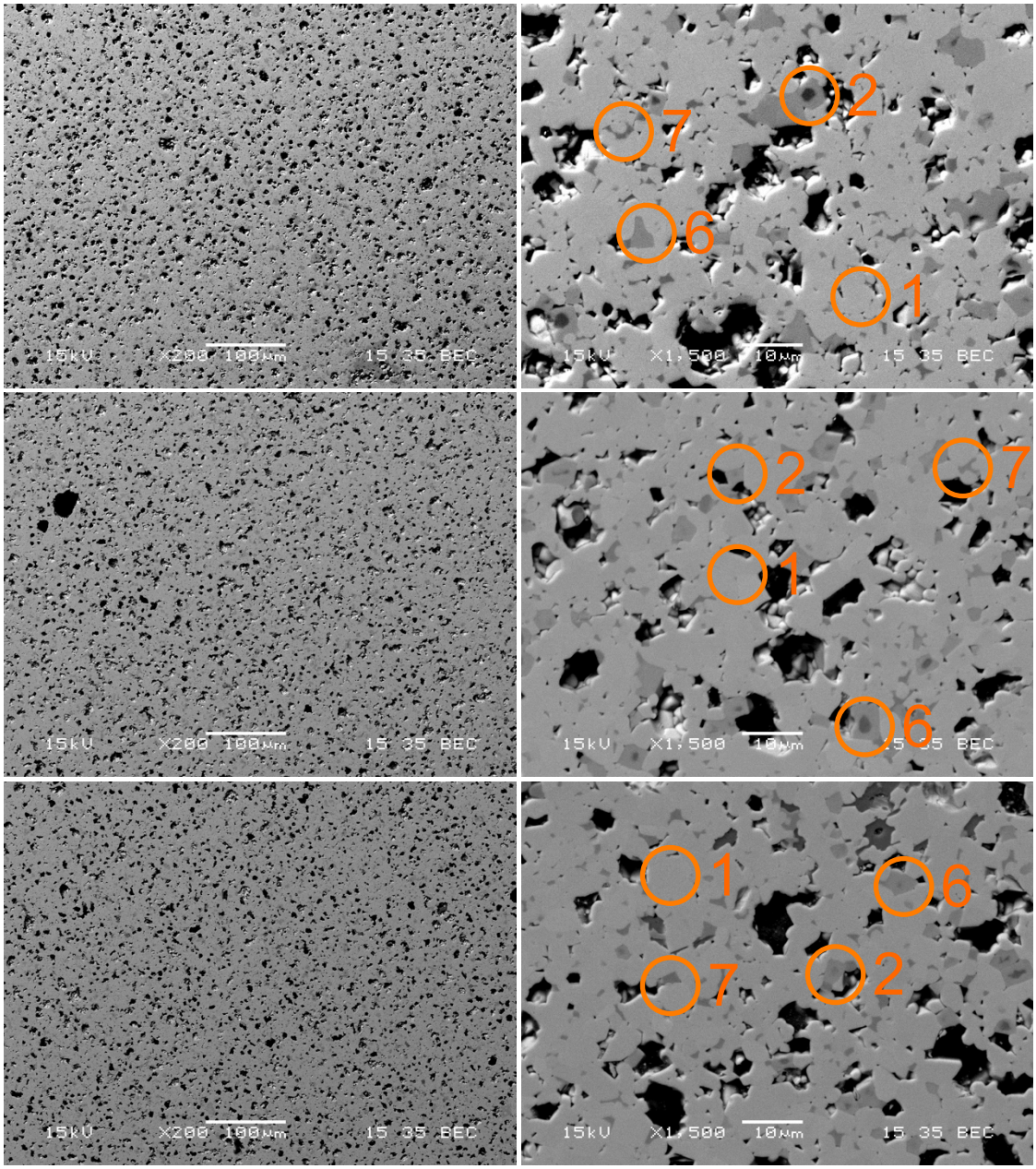

Figure 28: SEM of samples consolidated by the high temperature HIP cycle from powders milled with zinc stearate. From top, 2.16 m s^{-1} for 30 min, 2.16 m s^{-1} for 60 min, 4.32 m s^{-1} for 30 min. Left image 200x magnification, right image, 1500x magnification. Phases labelled as; 1: zirconolite; 2: perovskite; 6: perovskite; 7: ilmenite

4.5.3.2 Ceridust

Figure 29 shows the XRD patterns for samples manufactured from powders milled with Ceridust. The two samples milled at 2.16 m s^{-1} (30 and 60 min) exhibit very similar XRD patterns demonstrating the same phase development. However, the sample manufactured from powders milled at 4.32 m s^{-1} for 30 min shows a small additional reflection at $2\theta \approx 41°$, although this could not be

assigned unambiguously to a particular phase. This reflection is not observed in the XRD patters of the other samples milled with Ceridust. The low temperature HIP cycle samples show considerable variability between samples, but this is not evident in the samples produced by the high temperature cycle. It may be that the extra energy imparted during the high temperature run is sufficient to drive diffusion to overcome the coarseness of the precursors. The SEM images, Figure 30, show a similar phase assemblage and level of porosity to the other lubricants and the phases are the same as discussed earlier. Again, the samples are very porous, which is reflected in the low sample densities.

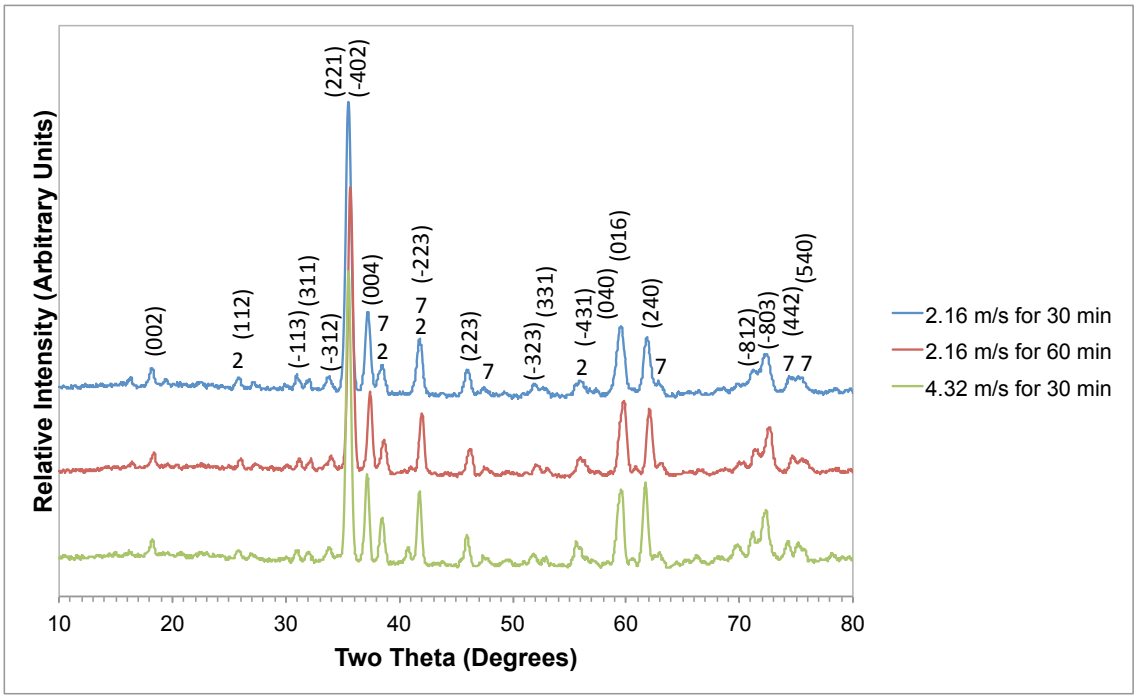

Figure 29: XRD patterns of samples manufactured from powders milled with Ceridust and consolidated by HIP at 1320 °C. Main phase zirconolite marked with the Miller indices. Major reflections labelled as; 2: perovskite; 7: ilmenite

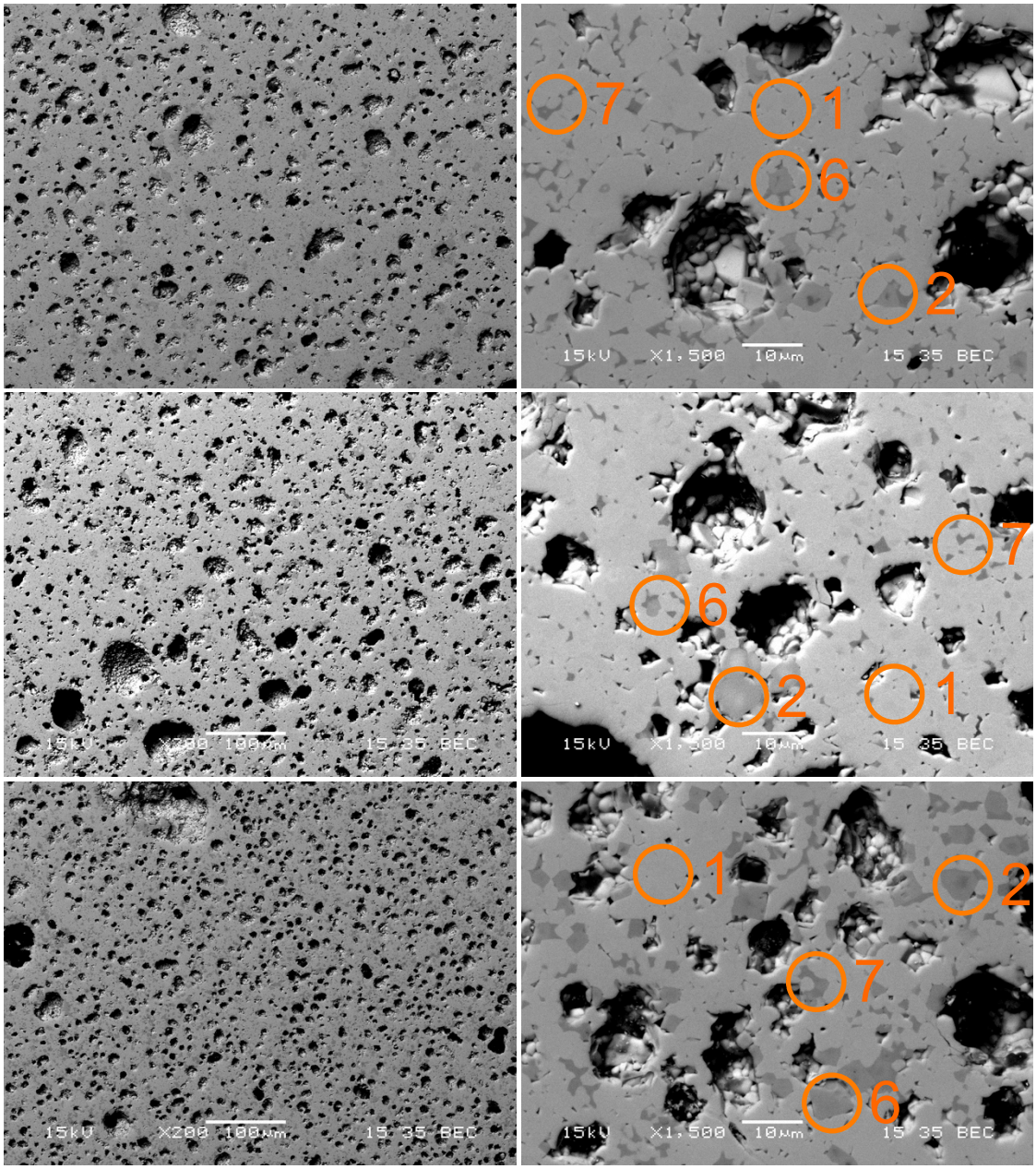

Figure 30: SEM of samples consolidated by the high temperature HIP cycle from powders milled with Ceridust. From top, 2.16 m s^{-1} for 30 min, 2.16 m s^{-1} for 60 min, 4.32 m s^{-1} for 30 min. Left image 200x magnification, right image, 1500x magnification. Phases labelled as; 1: zirconolite; 2: perovskite; 6: perovskite; 7: ilmenite

4.5.3.3 Polyethylene Glycol

The XRD patterns for the samples manufactured from powders milled with polyethylene glycol are given as Figure 31. Again, regardless of the different milling parameters, each sample has the same phase development, shown in the XRD patterns. SEM images of the samples are given as Figure 32.

The two samples milled at 2.16 m s^{-1} (30 and 60 min) are very porous, which is a reflection of the low densities recorded 84.9 and 81.5%, respectively. The 2.16 m s^{-1} for 60 min and 4.32 m s^{-1} for 30 min samples shows the same zirconolite and perovskite phase development as discussed previously. The SEM images of the sample manufactured from powders milled at 2.16 m s^{-1} for 30 min does not appear to show this standard phase development. However, this is likely to be due to the areas selected for presentation rather than an absence of the perovskite phases. The XRD patterns do show the same phase development throughout all of the samples manufactured from powders milled with polyethylene glycol.

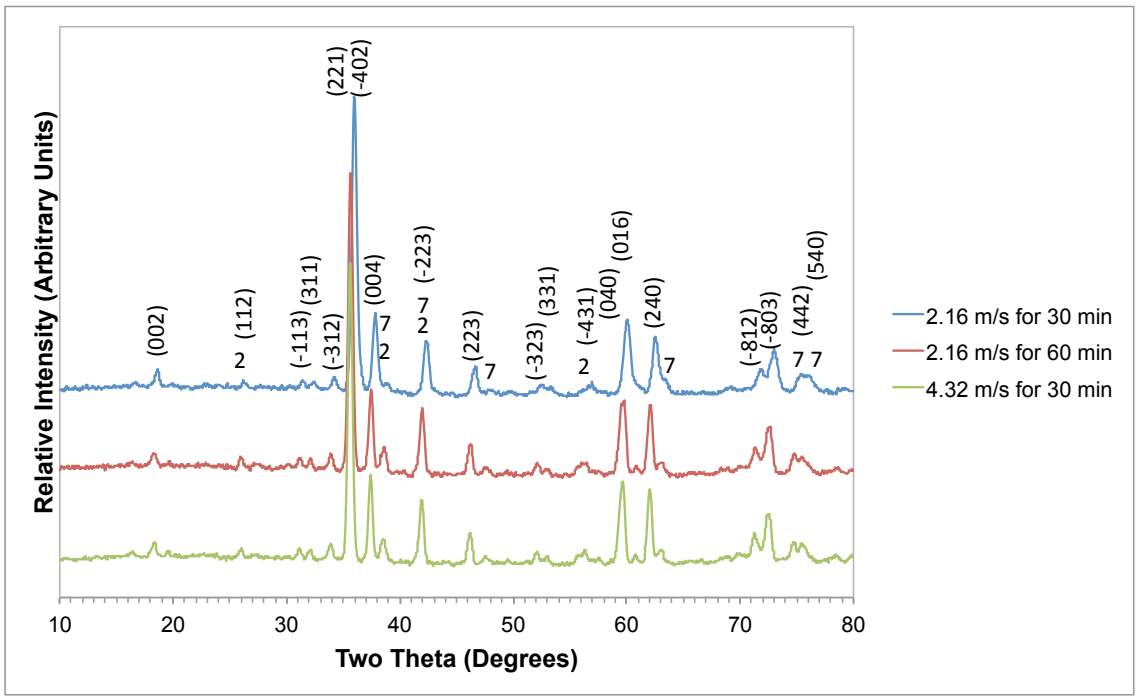

Figure 31: XRD patterns of samples manufactured from powders milled with polyethylene glycol and consolidated by HIP at 1320 °C. Main phase zirconolite marked with the Miller indices. Major reflections labelled as; 2: perovskite; 7: ilmenite

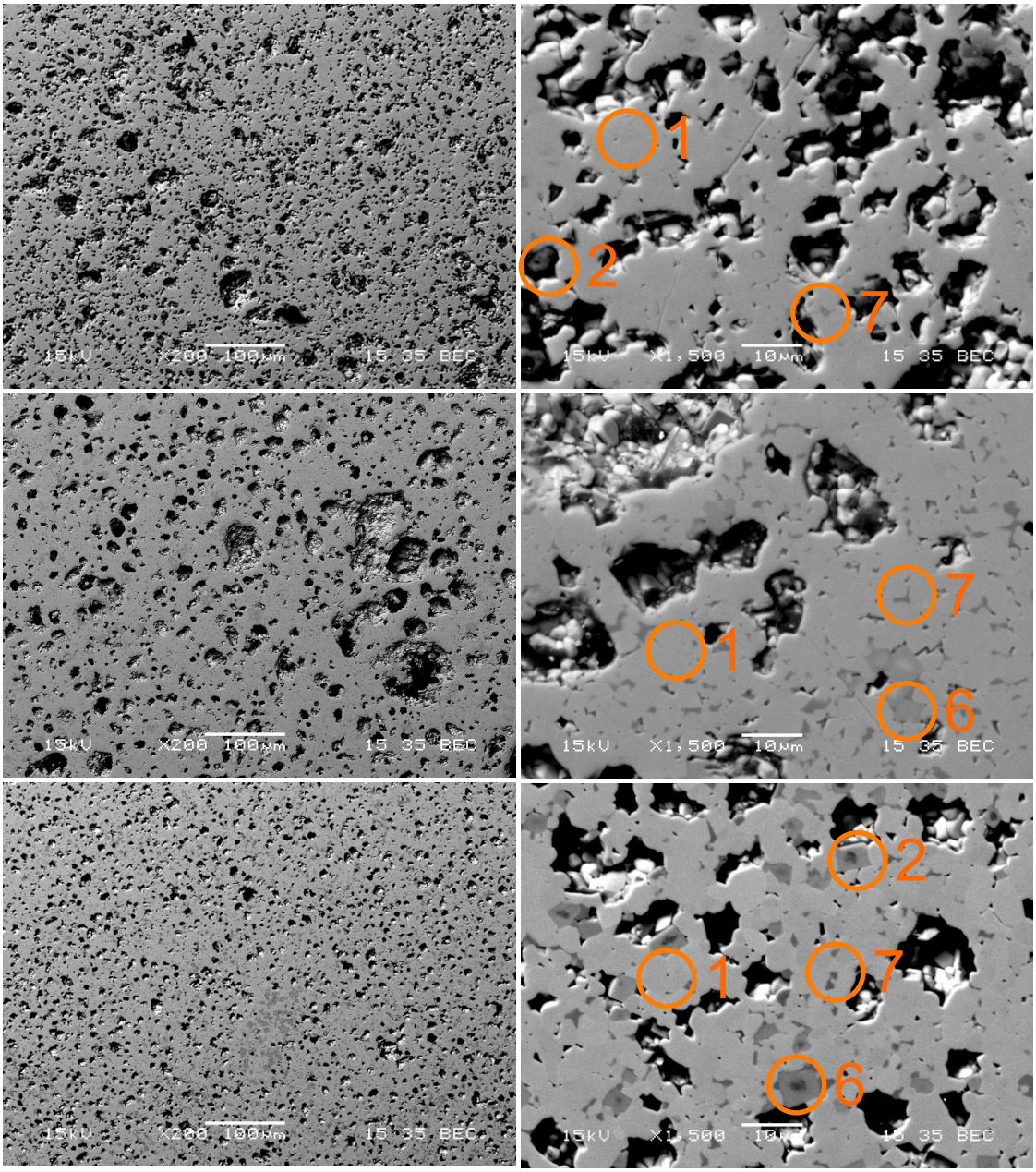

Figure 32: SEM of samples consolidated by the high temperature HIP cycle from powders milled with polyethylene glycol. From top, 2.16 m s^{-1} for 30 min, 2.16 m s^{-1} for 60 min, 4.32 m s^{-1} for 30 min. Left image 200x magnification, right image, 1500x magnification. Phases labelled as; 1: zirconolite; 2: perovskite; 6: perovskite; 7: ilmenite

4.5.3.4 Oleic Acid

Figure 33 gives the XRD patterns for samples manufactured from powders milled with oleic acid. Again, each of the milling conditions has produced the similar XRD pattern indicating the same zirconolite and perovskite phase development. The most aggressively milled sample (4.32 m s^{-1} for 30 min) does show sharper (smaller full width at half maximum height (FWHM)) peaks in

the 2θ≈ 72-75° range. These have been identified as perovskite. The reduced FWHM reflects the greater energy imparted through milling. This extra energy improves homogenisation and size reduction of the powders leading to reduced local compositional variations in the final product. These smaller variations lead to smaller variations in d-spacing and, hence, narrower peaks.

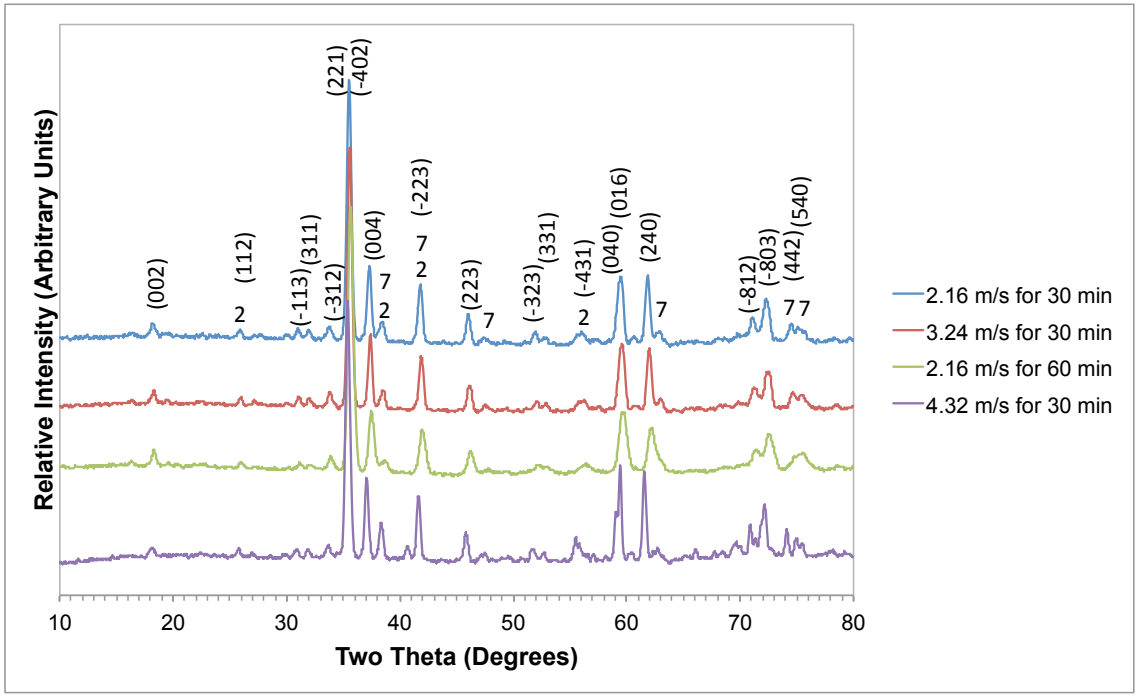

Figure 33: XRD patterns of samples manufactured from powders milled with oleic acid and consolidated by HIP at 1320 °C. Main phase zirconolite marked with the Miller indices. Major reflections labelled as; 2: perovskite; 7: ilmenite

The SEM images, Figure 34, do show a larger number of lower average atomic mass phases (e.g. perovskite) present in the sample manufactured from powders milled at 4.32 m s^{-1} for 30 min than in samples made from powders milled at 2.16 m s^{-1} for 30 min.

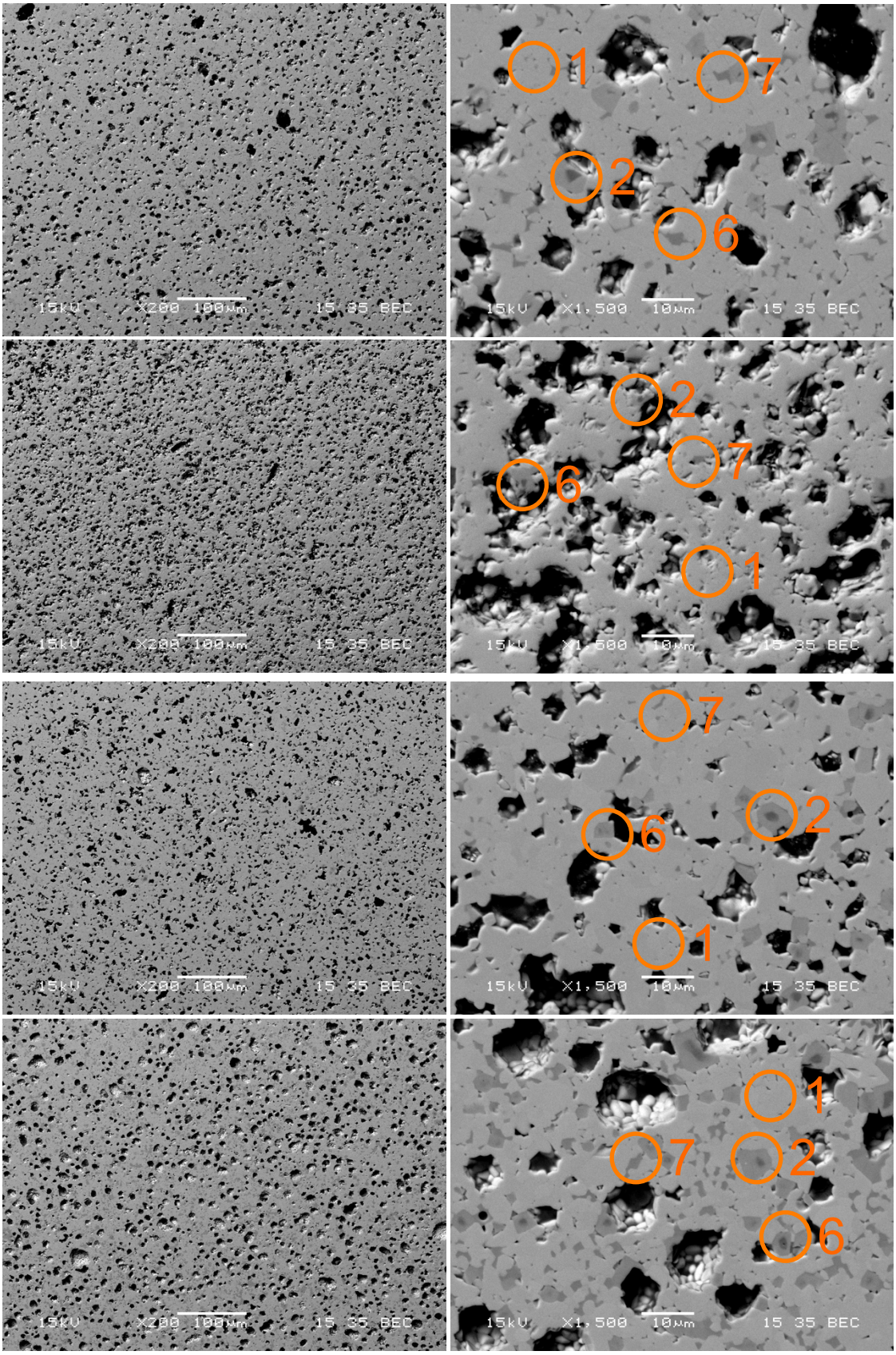

Figure 34: SEM of samples consolidated by the high temperature HIP cycle from powders milled with oleic acid. From top, 2.16 m s^{-1} for 30 min, 3.24 m s^{-1} for 30 min, 2.16 m s^{-1} for 60 min, 4.32 m s^{-1} for 30 min. Left image 200x magnification, right image, 1500x magnification. Phases labelled as; 1: zirconolite; 2: perovskite; 6: perovskite; 7: ilmenite

4.5.3.5 Discussion

The overall impression of the samples consolidated by the hot HIP cycle is one of broad uniformity. Whilst the low temperature HIP cycles showed some variation with milling parameters (e.g. amount of free ceria, size and number of grains), there do not appear to be large differences between the samples and milling conditions. This positive result implies that as long as a certain level of milling has been achieved, the high temperatures used for consolidation will allow coarse material to form the zirconolite phases. However, the poor quality of the products makes definitive conclusions difficult to state.

It has been shown that zirconolite can be manufactured from attrition milled metal oxide powders. None of the samples showed any indication of a separated ceria phase, implying full digestion of the simulant, and this is a positive indication that the digestion of the PuO_2 feed will be achievable (noting PuO_2 is less reactive than the ceria simulant). The HIP method was selected for consolidation, as it is known to minimise internal porosity in ceramics. However, the samples were clearly very porous. The conclusion is that the failure to remove the lubricant completely has interfered with product consolidation. In addition, it does appear that the selection of lubricant does influence product phase development; whether this is due to lubricant performance during milling, removal or consolidation is unknown. If the lubricant fails to keep the powders free flowing then it may be that the powders are less milled, in regard to both size reduction and homogenisation, than expected. This would introduce different phases by leaving remnants of the coarse precursors in the final product. It is also possible that the decomposition products of the lubricant could interact with the local oxidation states of the precursors and this could interfere with phase development. It is known that reducing conditions (provided in this case by the pyrolysed lubricant) favour the formation of perovskite. The behaviour of the lubricant under HIP pressures and temperatures is unknown and some further work may help. However, the main result is not in the ability of the lubricants to prevent foot

formations but in the observation that the lubricant is difficult to remove from the packed HIP cans.

5 'Realistic' Ceria

In the previous work, oleic acid was judged to be the best performing lubricant, based on powder discharge from the mill and ease of use. As such, it was selected for the 'realistic' ceria work. The same milling parameters (2.16, 3.24, 4.32 m s^{-1} for 30 or 60 min) as previously were repeated but with the 'realistic' ceria source. The samples underwent the same low (1000 °C) and high (1320 °C) temperature HIP cycles.

5.1 Density

The measured densities of samples manufactured using the 'realistic' ceria surrogate, as well as the standard source for comparison, are given as Table 10. The samples are grouped by HIP cycle temperature and then ordered by increasing density. The lack of a correlation between milling parameters and the product density has already been discussed. There is also no correlation with utilising the 'realistic' ceria source.

Tip Speed (m s^{-1})	Duration (min)	Ceria Source	HIP Cycle	Density (g cm^{-3})	% TD
2.16	60	Standard	Low	3.87	81.0
4.32	30	Realistic	Low	4.08	85.4
3.24	30	Realistic	Low	4.12	86.2
2.16	60	Realistic	Low	4.14	86.5
2.16	30	Realistic	Low	4.14	86.7
3.24	30	Standard	Low	4.22	88.4
4.32	30	Standard	Low	4.23	88.5
2.16	30	Standard	Low	4.25	89.0
2.16	60	Realistic	High	3.93	82.1
4.32	30	Standard	High	3.98	83.2
2.16	30	Realistic	High	3.99	83.4
3.24	30	Realistic	High	4.00	83.8
2.16	60	Standard	High	4.06	84.9
4.32	30	Realistic	High	4.17	87.3
3.24	30	Standard	High	4.18	87.5
2.16	30	Standard	High	4.26	89.1

Table 10: Density of samples manufactured with from powders milled with oleic acid. Grouped by HIP cycle and ordered by increasing density.

5.2 XRD AND SEM

The intention of manufacturing products with the 'realistic' ceria was to study how the different particle sizes and surface behaviours affect the incorporation of the ceria into the zirconolite structure. If the ceria is not incorporated, XRD analysis should show reflections attributed to free ceria and SEM images should, likewise, demonstrate the presence of distinct bright white grains of ceria.

5.2.1 LOW TEMPERATURE HIP CYCLE

Figure 35 shows the XRD patterns for samples manufactured from powders containing the 'realistic' ceria and milled with oleic acid. The 2.16 m s^{-1}, 3.24 m s^{-1} for 30 min and the 2.16 m s^{-1} for 60 min samples have similar patterns to each other. The patterns are also similar to the samples manufactured using the standard ceria, Figure 23. The sample consolidated from powders milled at 4.32 m s^{-1} for 30 min is different. There is a double peak at $2\theta \approx 34°$ that is not present in the other samples in Figure 35. These peaks have not been uniquely identified.

The SEM images of each of the four samples are given as Figure 36. All four images show the same continuous phase of zirconolite interspersed with darker grains. These darker grains are either titanium based (e.g. TiO_2) or perovskite. Notably, there are very few obvious ceria inclusions. Compared with the standard ceria simulant, Figure 24, there is a decrease in the number of free CeO_2 inclusions in the 'realistic' ceria samples. This implies the realistic ceria is either: more easily milled thus leaving fewer large particles post milling; more easily digested by the ceramic matrix or; a combination of the two. Full incorporation of the plutonium simulant, even utilising the low temperature HIP cycle, is encouraging in that this wasteform would be suitable, on a waste incorporation basis, for implementation with PuO_2.

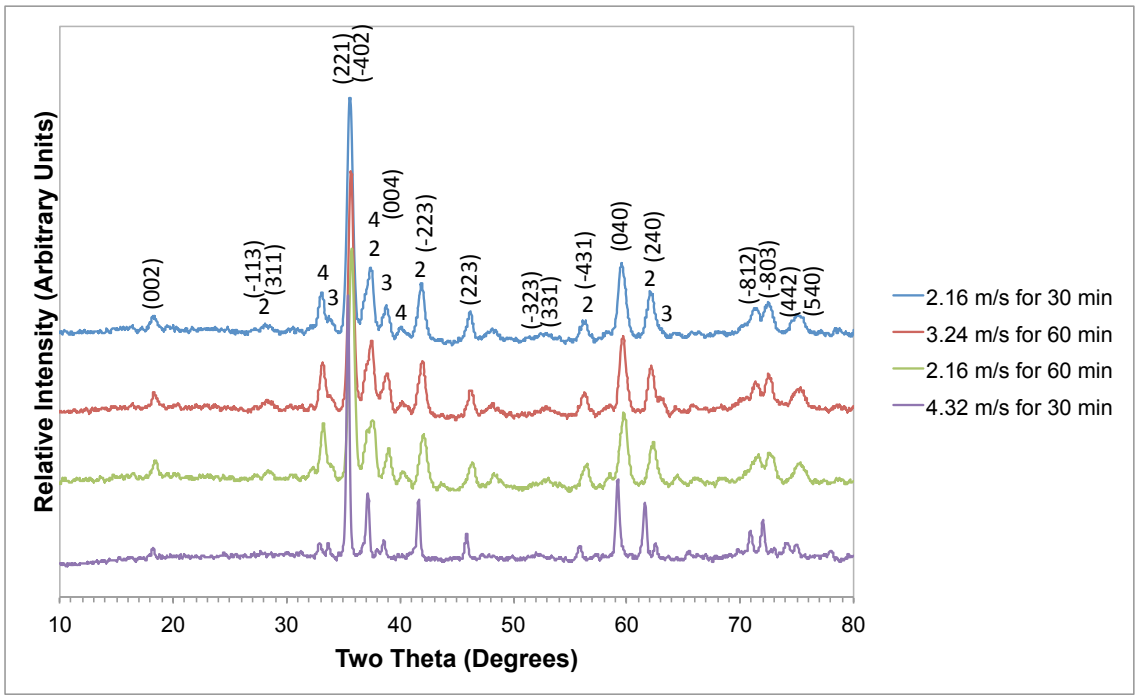

Figure 35: XRD patterns of samples manufactured from powders milled with oleic acid, containing 'realistic CeO_2' and consolidated by HIP at 1000 °C. Main phase zirconolite marked with the Miller indices. Major reflections labelled as; 2: perovskite; 3: perovskite; 4: zirconia

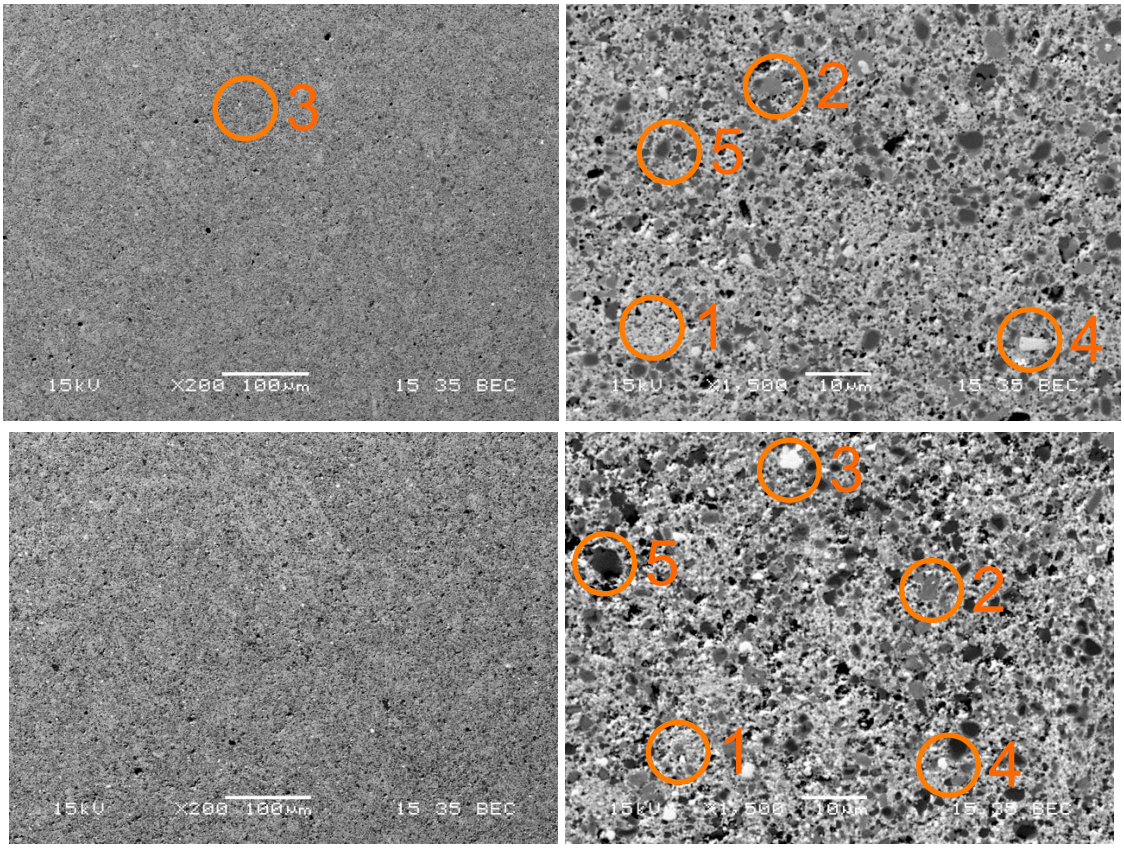

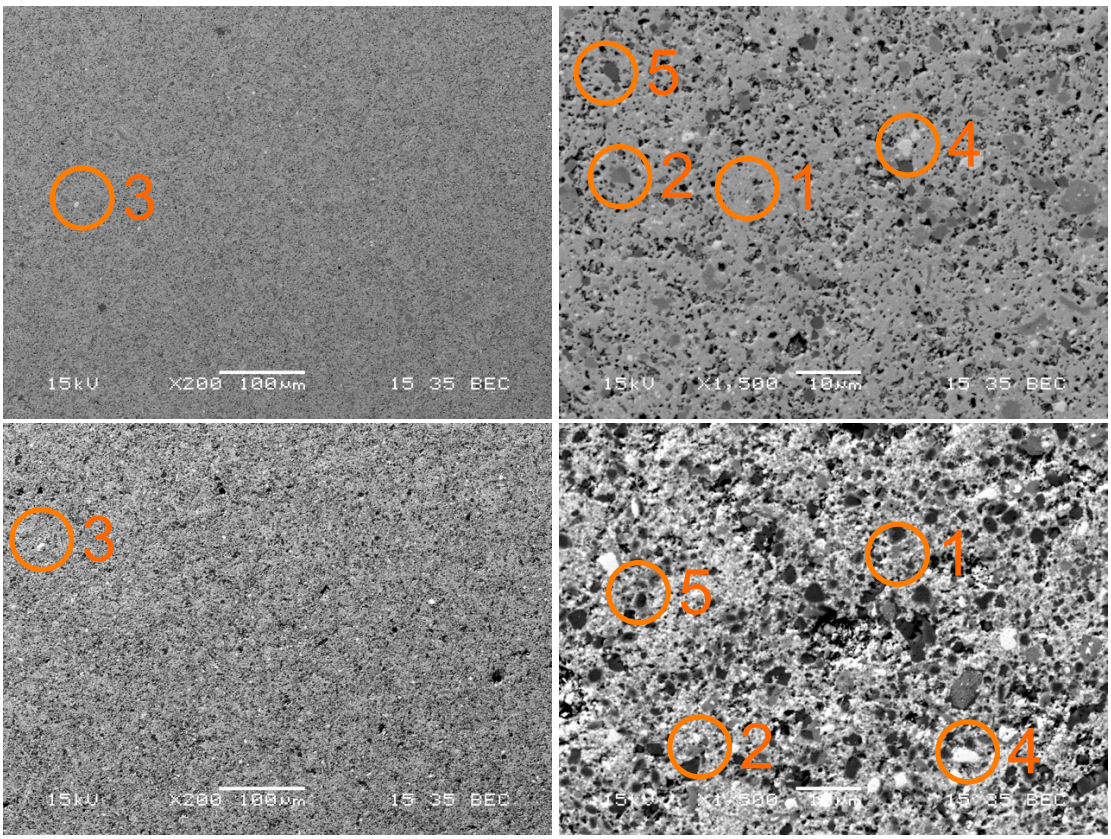

Figure 36: SEM of samples consolidated by the low temperature HIP cycle from powders milled with oleic acid and. From top, 2.16 m s^{-1} for 30 min, 3.24 m s^{-1} for 30 min, 2.16 m s^{-1} for 60 min, 4.32 m s^{-1} for 30 min. Left image 200x magnification, right image, 1500x magnification. Phases labelled as; 1: zirconolite; 2: perovskite; 3: ceria; 4: zirconia; 5: titania.

5.2.2 High Temperature HIP Cycle

Figure 37 shows the XRD patterns for samples consolidated by the high temperature HIP cycle from powders containing the 'realistic' ceria and milled with oleic acid. Each of the different milling conditions has produced powders that, when consolidated, have the same phase development. The patterns are comparable to the samples made with the standard ceria, Figure 33. Further consideration of Figure 37 shows that as the milling speed and duration increases (from 2.16 m s^{-1} for 30 min to 4.32 m s^{-1} for 30 min) the FWHM of the reflections in the XRD patterns decreases. Reducing the broadening of XRD reflections is usually indicative of a more homogenous sample with less localised concentration variations throughout the sample. The SEM images, Figure 38, do not show an increase in homogenisation with increased milling. All four images show the standard phase development for this system

(zirconolite host phase, perovskite cores and ilmenite dispersed throughout) with no obvious variability in the distribution of phases between the samples manufactured from powders milled at 2.16 m s^{-1} or 4.32 m s^{-1} for 30 min. A reduction in the phase composition variability is most likely a result of improved homogenisation of the powders during milling. This could be a result of improved size reduction, that is, smaller particles becoming more intimately mixed with other components of the precursor blend with increased milling aggressiveness (i.e. from 2.16 m s^{-1} to 4.32 m s^{-1} for 30 min). None of the SEM images shows any free ceria, which a positive result as it implies the full and complete digestion of PuO_2 if this manufacturing method was implemented. However, the samples are unacceptably porous.

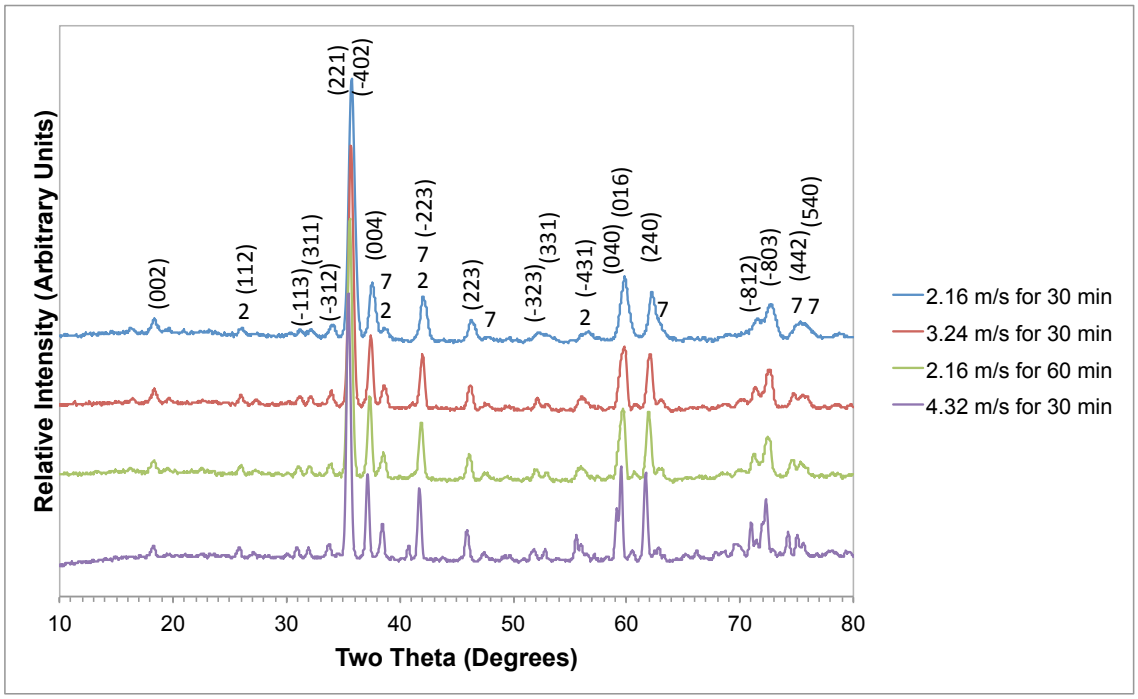

Figure 37: XRD patterns of samples manufactured from powders milled with oleic acid, containing 'realistic CeO_2' and consolidated by high temperature HIP at 1320 °. Main phase zirconolite marked with the Miller indices. Major reflections labelled as; 2: perovskite; 7: ilmenite

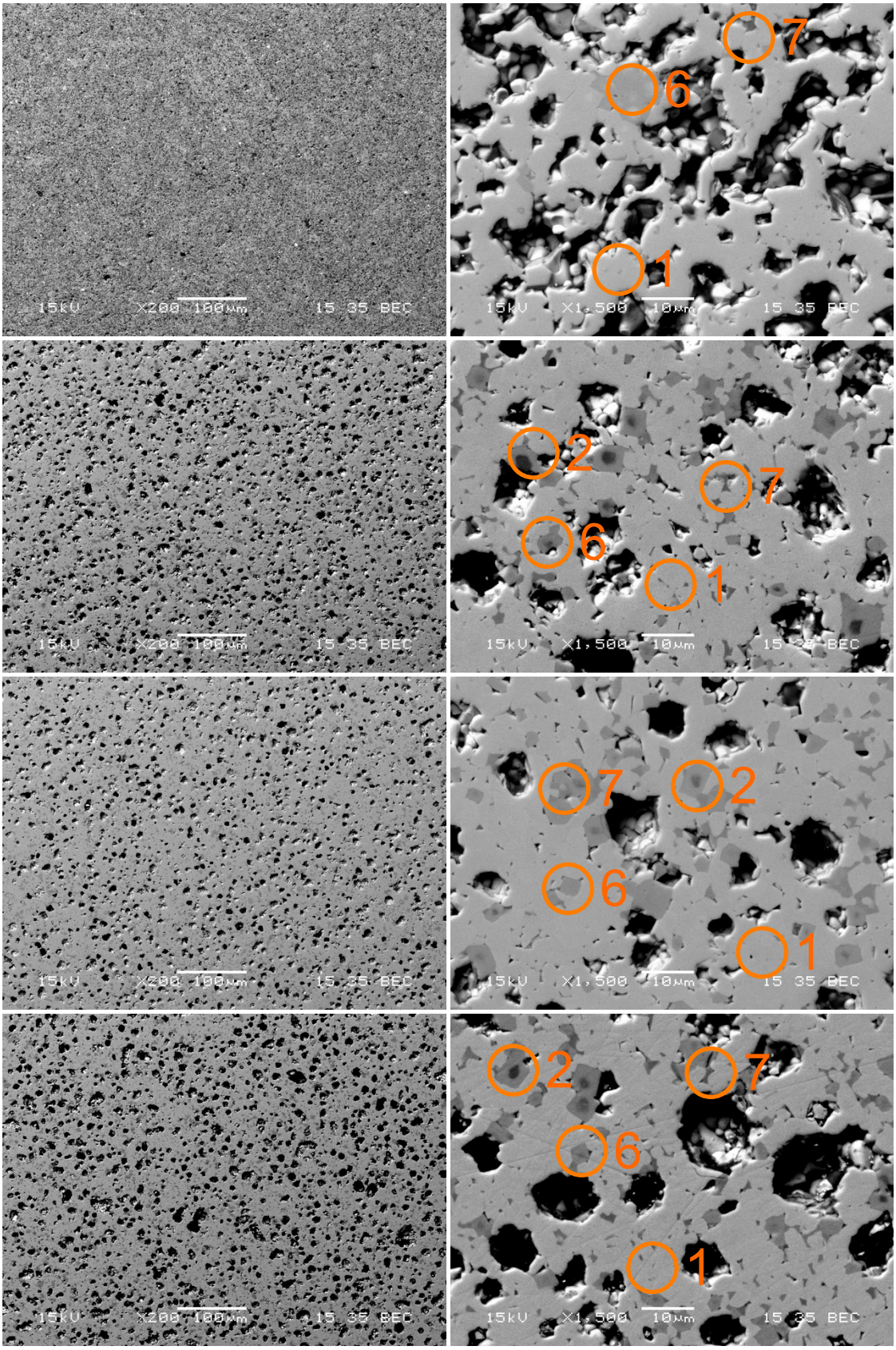

Figure 38: SEM of samples consolidated by the high temperature HIP cycle from powders containing the 'realistic' CeO_2 and milled with oleic acid. From top, 2.16 m s^{-1} for 30 min, 3.24 m s^{-1} for 30 min, 2.16 m s^{-1} for 60 min, 4.32 m s^{-1} for 30 min. Left image 200x magnification, right image, 1500x magnification. Phases labelled as; 1: zirconolite; 2: perovskite; 6: perovskite; 7: ilmenite

6 Discussion

The main observation throughout this work was the lack of correlation between milling conditions and final product density. The intention of the work, particularly the high temperature HIP cycle products, was to investigate the effect of both milling speed and duration on product quality. As no correlation was shown, it is difficult to draw extensive conclusions about milling performances. However, there are a number of other observations that can be discussed.

Examination of the low temperature HIP cycle samples showed that there was no correlation between the ease of powder discharge from the mill and the extent of milling shown, as shown in the microstructure of the consolidated samples. Any lubricant chosen for utilisation must be capable of allowing the mill to discharge, however it was thought that if the powders formed a foot, this was at the beginning of the milling operation. That is, after the addition of the batch of precursors to the mill they travelled directly to the base of the mill and did not undergo any milling. Observation of the perovskite grains in the SEM images of samples that were manufactured from powders that agglomerated in the mill, e.g. Figure 19, and comparison to the non-milled samples show that some size reduction must have occurred; in contradiction to the original assumption. An explanation may be that the powders are milled to some extent as they pass through the mill from the charging port at the top of the mill to the base. Only as they reach the bottom, they are compacted in to a foot by the motion of the milling media above and do not undergo any further size reduction. This would account for the partial size reduction observed of the components in the samples manufactured from powders that did not fully discharge (e.g. Ceridust, 2.16 m s^{-1} for 30 min). The implication is that for coarse size reduction (e.g. from 50-100 μm to 20-50 μm) one pass through the attrition mill by leaving the discharge valve open, may be sufficient. This may be useful for conditioning of feeds that are coarser than expected.

A more concerning observation is of the samples milled with polyethylene glycol. All of these samples were consolidated from powders that freely discharged from the mill yet the microstructures in the samples milled at 2.16 m s^{-1} (both 30 and 60 min), Figure 21, shows perovskite grains as coarse as those in the samples that failed to discharge when milled with Ceridust. The intention was to use the free discharge of material as an operational control: if the material discharged, then the milling operation was sufficient. These results suggest that this would not be a useful operating parameter and underlines the need for extensive process development and research.

Throughout all of the low temperature samples, there were consistently low levels of free ceria observed. Whilst it is known that PuO_2 is more refractory and therefore more difficult to incorporate than ceria, the high level of ceria incorporation is an encouraging result. The high level of incorporation is likely to be due to a result of the suitability, in terms of chemical flexibility, of the zirconolite host phase for actinide immobilisation. It should also be noted that the high temperature HIP cycle did produce the zirconolite host phase as expected.

Only three of the selected lubricants succeeded in consistently keeping the powders free flowing during milling. In examining the chemical structure of the lubricants, it is noted that Ceridust is the only material that does not contain a functional group. The lack of molecular polarity, and in turn water insolubility, may be the origin of the poor performance of this lubricant. As the material lacks the functionality to be soluble within the surface moisture layer on the powder particles, there is potentially no mechanism to coat the particles and act as a lubricant. An adsorbed surface layer of water may also be the cause of powder agglomeration. It is widely recognised that damp powders and humid environments are detrimental to free powder flow. Lubricants are used widely with little appreciation of the fundamentals of their performances and this lack

of predictability serves to emphasize the need for detailed quantitative understanding of additives in milling systems.

Interestingly, the samples consolidated by the high temperature HIP cycle did not show the same level of variability in their microstructures as their low temperature counterparts. This shows that the consolidation temperature of the HIP cycle is sufficient to overcome poor milling performance, both in terms of mixing and size reduction. The development of the zirconolite host phase in the high temperature non-milled sample is indicative of this. The argument follows that striving for the perfect milling conditions may be counterproductive, knowing that a suitable HIP cycle can be used to overcome non ideal powder preparation. It is known, however, that suitable sized and mixed precursors can utilise lower consolidation temperatures. There is clearly a balance between the level of milling and the consolidation temperature; this could be investigated further through a series of experiments linking milled powders particle size and the HIP temperature required before there are no signs of unincorporated material in the final product.

It is clear that poor performance during lubricant bake out complicates the fabrication of dense zirconolite ceramics by HIP. As described above, the mass loss observed during bake out must be derived from a combination of sources: lubricant removal, lubricant decomposition and partial removal, powder removal, and moisture losses. The removal of any powder is clearly unacceptable in a radioactive processing environment. It may be possible to prevent powders from being removed by the addition of a sintered metal filter at the base of the evacuation tube. This filter could allow the vaporised lubricant to leave the HIP can without any further powder disturbances. Whilst the HIP can containing the material was heated to 600 °C, far above the boiling points of the lubricants, the additives were not completely removed. It is thought that the extensive packing of the material into the HIP can, in order to improve the green packing density and thus the final wasteform density, may

have produced an environment not conducive to lubricant removal. Observations on heating the product showed there was a destruction of the monolith through the expansion of internally entrained gas. This behaviour does not give confidence that the wasteforms still containing the lubricant after consolidation could perform acceptably in accident scenarios.

Changes in the onset of bake out temperature of similar lubricants between pressed pellets and loose powders have been shown by Chandler *et al*(Chandler, Cozzi et al. 1999). Thermal analysis showed an increase in the temperature required to fully remove polyethylene glycol (molecular weight 8000) from loose powders and pucks (large pellets) of a candidate wasteform material when compared to pure polyethylene glycol. They showed that the decomposition region shifted upwards by approximately 75 ºC. While they did not offer an explanation for this change, it is thought that some combination of reduced heat transfer in the material, leading to lower internal temperatures, and increased diffusional pathway length for the gases through the material, may have increased the overall decomposition temperatures. Repeating these experiments with slower ramp rates, ensuring thermal equilibrium in the powders and pucks is reached at every stage, may prove illuminating.

Based on the present study, removing the lubricant from milled powders whilst in the HIP can would appear to be a flawed approach. Increasing the temperature and duration of the removal step may give improved results, however, the current bake out temperature is far above the stated lubricant boiling points, even allowing for the potential boiling point elevation as reported by Chandler (Chandler, Cozzi et al. 1999). Increasing the duration of the bake out process is also unlikely to improve the removal step, as the amount of additive to be removed is small. It may be possible to remove the lubricants from the milled powders before they are packed into the HIP can. However, working with loose powders in an active environment is often impractical due to the increased dusting leading to equipment contamination and thus worker

dose uptake. Packing material directly into a HIP can from a mill is very attractive in its simplicity. Thus, any additive must be easily removed or eliminated.

Further work detailed in this thesis will investigate the use of electrically conductive precursors (typically by reducing Ti^{4+} to Ti^{3+} and in doing so forming a semi-conducting Magnéli phase, e.g. Ti_5O_9). It is thought that minimisation of tribo-electric charging helps to mitigate powder agglomerations. Through careful modification of the charge compensation species added to the precursor blend, the reduced titanium species would be accommodated in the final wasteform, eliminating the difficult lubricant removal step. An alternative approach is the use of fumed metal oxides. These materials are amorphous oxides agglomerated into secondary structures to give an extremely low powder density with a very large surface area. They are widely recognised as useful flow promoters with dry powders (Harnby 2000). One further option is a modification of the mill internals. The addition of a method to sweep constantly the base of the mill may prevent an agglomeration of powders ever occurring. This could be by the addition of a trapezoidal bar to the agitator shaft. The bar would sit horizontally at the base of the mill and rotate with the agitator shaft. This bar is shaped so that with each rotation the bottom layers of milling media, and powders, are lifted into the mill promoting powder circulation and helping to minimise powder compactions. The attrition mills within SMP already utilise a form of this bottom rotor (BNFL and Edwards 2002). In reality, it is likely that some combination of introduced conductivity, modified lubricant and a modified mill may be required to provide a suitable plutonium wasteform manufacturing line.

7 CONCLUSIONS

Zirconolite, target formulation $Ca_{0.75}Ce_{0.25}ZrTi_{1.625}Fe_{0.375}O_7$, has been manufactured utilising an attrition mill operating in the dry mode and a high temperature (1320 °C) HIP for consolidation.

There was no correlation between milling conditions and the final product properties (microstructure, density and porosity), this has been traced to a failure in the ability to remove lubricant from the packed HIP can before consolidation.

Of the four lubricants, zinc stearate, polyethylene glycol and oleic acid are suitable for use in an attrition mill, operated without carrier fluid, with the metal oxides precursor components as they kept the powders free flowing during milling. Ceridust has, however, been shown not to be suitable. Also of note is the failure of polyethylene glycol, whilst allowing the powders to freely discharge, to allow the precursor powders to be milled to the same extent as with zinc stearate and oleic acid. Based on this work, the recommendation is to use zinc stearate as the lubricant of choice for implementation. This is because of the ease of handling a solid powder as apposed to a liquid (oleic acid).

The results do not conclusively show how aggressive the milling must be to produce ceramics densities above 92% of theoretical. The failure to remove the lubricant added to aid milling has undermined any attempts to assess wasteform performance.

3: Manufacture of Zirconia Candidate Wasteforms by Cold Isostatic Pressing and Cold Uniaxial Pressing

1 Abstract

The effect of attrition milling on the processing of precursor oxides was investigated with reference to the fabrication of a candidate wasteform based on zirconia for the immobilisation of plutonium. The work was intended to compliment that in Chapter 2 and sought to establish that a relationship between milling parameters and product quality did exist but only after complete removal of the lubricant from milled powders. Two sets of pellets were manufactured from the milled powders, one set was cold uniaxially pressed and the other was cold isostatically pressed. Both sets of pellets were sintered in air. All of the samples manufactured from powders milled at 4.32 m s^{-1} for 30 min achieved the target of >92% of theoretical density. SEM analysis of the products showed them to be homogenous with regards to microstructure and phase development. The analysis also showed an increase in average grain size with increased milling speed and durations. There was also a corresponding decrease in the number of pores. Samples prepared with the 'realistic' ceria were less dense than their standard ceria counterparts were. This was determined to be a result of the 'realistic' ceria manufacturing process.

2 Introduction

The results from Chapter 2 were inconclusive regarding definitive correlation between milling parameters and product quality. The interpretation was that the failure to remove the lubricant completely had masked a possible correlation between milling and product quality. To establish further evidence in support of this hypothesis, a second set of experiments, utilising the same attrition mill and milling parameters but using metal oxides suitable for the manufacture of a wasteform based on zirconia was completed.

A candidate wasteform based on cubic zirconia was selected as it has been shown to have excellent resistance to amorphisation and its solubility in water is very low (Degueldre and Paratte 1999, Ledergerber, Degueldre et al. 2001). Cubic zirconia adopts a defect fluorite structure based on the general formula $Zr_{1-x}M_xO_{2-x}$, where M is calcium, yttrium, lanthanides or actinides (Proffen, Neder et al. 1993, Bechepeche, Treu et al. 1999). The cubic structure must be stabilised first by the addition of calcium or yttrium. Further substitution of metal ions can then occur. Yttrium is used when the material is required for highly abrasive tasks (Bechepeche, Treu et al. 1999). In this role it is stabilised in the tetragonal structure and is known as fully yttrium stabilised zirconia (YSZ). It is commonly used in, for example, low contamination milling.

Zirconia has also seen some favour as an inert matrix nuclear fuel, IMF (Ledergerber, Degueldre et al. 2001, Degueldre 2007, Holliday, Hartmann et al. 2010). The design concept for IMF states that the fuel form should be flexible enough to retain all fission products during and after irradiation in a reactor. This fuel is disposed of in the same form as it is discharged from the reactor, eliminating the need for further processing. The wasteform must withstand the extreme operating conditions present in a nuclear reactor and maintain the physical properties required to form a suitable disposal product. While this challenge may be insurmountable, it does highlight that cubic zirconia can be considered a suitable host phase for nuclear waste disposal.

The main draw back to the use of zirconia ceramics for nuclear applications is the requirement of high consolidation (1600-1700 °C) temperatures to fully sinter zirconia from oxide precursors, potentially precluding the use of HIP without utilising expensive HIP can materials (e.g. tantalum or molybdenum). The current HIP cans are manufactured from stainless steel, which has a maximum working temperature of ~1350 °C. Maddrell (Maddrell 1996) has shown that zirconia based wasteforms can be consolidated by HIP but only if the precursors are alkoxide derived and nitrate solutions of the plutonium simulant are used. This processing route produces precursor materials that are intimately mixed on the atomic scale as well as having a very fine particle size and corresponding large surface area; both characteristics are useful for promoting diffusion amongst precursors and product development during sintering. As the plutonium stockpile is a dry oxide powder it is impractical to design a process that requires the re-dissolution of plutonium, as this will produce secondary effluents, which are to be minimised. There has been some work on the use of HIP for the secondary processing of zirconia products (Kim, Uchida et al. 1990, Khor and Gu 1998) but this has been primarily to reduce the porosity of previously sintered ceramic monoliths without a HIP can. This technique would be not allowable in a nuclear waste immobilisation plant as the design intentions are to minimise the number of processing steps. There is the added benefit that the HIP can acts as a barrier to contain the loose powders during processing.

The inapplicability of HIP as the consolidation technique lead to two other processing methods being studied: cold isostatic pressing (CIP) and cold uniaxial pressing (CUP). Both methods utilise the application of pressure to the precursor powders in order to form a green pellet. These green pellets are sintered in a separate step (as apposed to HIP where pressure and temperature are applied simultaneously). CUP is widely used in the manufacture of tablets in the pharmaceutical industry (Schaber, Gerogiorgis et al. 2011, Šibanc, Kitak et

al. 2013) and in the manufacture of UO_2 and MOX nuclear fuels (Williams 1997). CUP is undertaken in a pellet press. This device consists of a smooth cylindrical hole in the centre of a large metallic block, Figure 39. Two machined cylinders are placed into the hole with a measured mass of powders in between. Pressure is applied uniaxially through the cylinders externally by a separate press. Pressure is typically held for short period and care is taken to release the pressure gradually. A sudden release can cause cracking in the now formed green body. The green pellet is transferred to a separate furnace for sintering.

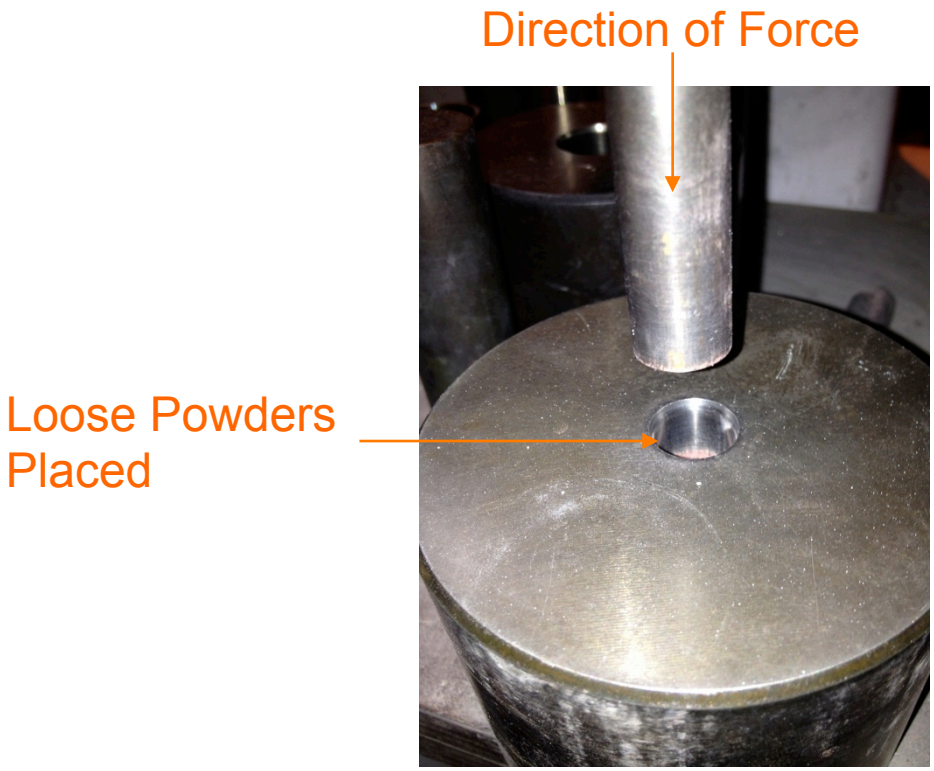

Figure 39: Pellet press

Work completed by Congdon, as part of the US plutonium immobilisation programme, showed difficulty in manufacturing candidate wasteforms pucks without gross deformities (Congdon 2001). The pucks, approximately 80 mm in diameter, would crack or split utilising standard flat faced dies. A modified die, that was machined to allow trapped gases to escape, was suggested and this did minimise the number of cracked pucks produced. In this work, the smaller size of pellets manufactured means that trapped gases will not be an issue.

CIP requires the input of free flowing powders to a flexible shaped container and uses a working fluid to apply pressure uniformly. In a lab scale process, a green pellet is typically formed by CUP before being placed into the flexible mould (in this work, a latex glove was used). In a full scale production line, however, loose powders may be added directly to the flexible mould before isostatic pressure is applied (Kim, Lee et al. 2001). The mould is unique for the shape of the product desired. In CUP, wall friction between the inside of the pellet press and the powders can lead to pressure gradients and a resulting variation in density throughout the pellet. The elimination of wall interactions in CIP minimises density changes in the pressed body and, at the cost of extra complexity, should give a denser product (Kingrey, Bowen et al. 1976).

For comparison with the work discussed in Chapter 2, the green pellets produced by the two methods were sintered in an unconstrained manner. That is, the green pellets were not contained within a sealed unit (i.e. a HIP can). This has the advantage that any entrained gas or decomposition product is easily released from the pellet during the initial temperature increases before sintering. This should give further evidence to support the conclusion in Chapter 2 that failure to completely remove the lubricant from the samples had masked any relationship between milling conditions and the final product.

A similar array of milling conditions to Chapter 2 was utilised with the notable omission of Ceridust. Ceridust failed to consistently prevent foot formation in the mill and thus has been eliminated from subsequent work.

3 Materials and Methods

The target formulation for the zirconia product was $(Zr_{0.85}Ca_{0.15}O_{1.85})_{0.9375}(CeO_2)_{0.0625}$. Calcium is used as the cubic structure stabilising ion and cerium as the plutonium surrogate. The formula units of cerium substitution were chosen to be equivalent to the formula units used in Chapter 2 (0.25 in the zirconolite formulation). Zirconium was provided by ZrO_2,

calcium by $CaCO_3$ and cerium by CeO_2. $CaCO_3$ was chosen as the precursor for CaO as it is stable in air, giving a known quantity of CaO for a given mass, and it is known to decompose below the chosen sintering temperature (decomposition at 850-900 °C). Batches of 1200 g of stoichiometric quantities of the three materials, with 1.5 wt% of the selected lubricant (zinc stearate, polyethylene glycol, oleic acid), were Turbula mixed for ~15 min. The 1200 g batch size (compared with 1000 g in the Chapter 2 work) was to account for the decrease in the powder density of zirconia precursors compared to the zirconolite precursors. For comparable mill performance, the same volume of material must be used regardless of the powders composition as the mill is sized to accept a given volume rather than mass.

The same mill and internal mill geometry were as used as in Chapter 2, again operating in the dry mode. The powder batches were charged into the attrition mill whilst it was operating at 1.73 m s^{-1} (200 RPM). The mill was quickly brought to the desired speed of 2.16, 3.24 or 4.32 ms^{-1} (250, 375 or 500 RPM) and run for either 30 or 60 minutes. A further repeat of the milling parameters was completed with 'realistic' ceria as the feed simulant, which was milled with oleic acid. The powders were discharged from the mill at the same operating speed as they were charged (1.73 m s^{-1}).

Particle size analysis was undertaken on the milled powders using a Malvern Masterziser 2000. Less than 0.2 g of material was ground into a paste, using a pestle and mortar, with the minimum methanol required. Whilst acknowledging that this technique will remove the majority of secondary agglomerates it was impossible to achieve repeatable results by the direct addition of powder to the instrument alone. There was also a certain amount of agglomeration during the measurement process and this is discussed with the results presented later. Methanol was chosen as the carrier fluid due to its availability.

One aliquot of 20 g and another of 10 g were taken from each large batch of milled powder. The 20 g aliquot was CUP into a 30 mm diameter pellet at 4 tonnes (56 MPa) whilst the other was pressed into a 15 mm diameter pellet at 1 tonne (56 MPa) (the size difference was to aid sample identification). The smaller pellets were CIP at 200 MPa (30 kPSI) with water as the working fluid. The two sets of pellets were sintered at 1700 °C with a 2 hour dwell and the furnace was left open to air. The ramp rate was 5 °C min^{-1} with reductions to 2 °C min^{-1} at 200-300 °C and 800-900 °C for lubricant burn out and $CaCO_3$ decomposition, respectively.

The density of the sintered pellets was measured by the Archimedes method with water as the immersion fluid. For the purpose of microstructure characterisation, the pellets were cold mounted in an epoxy resin before being ground and polished by successively finer stages (500, 800, 1200 grit grinding papers, 6 µm and 2 µm diamond polish). The CUP samples were released from the mounts before thermally etching at 1500 °C (~90% of absolute sintering temperature) for 2 hours with the intention of developing the contrast between the grain boundaries and grains. The CIP samples were damaged irreparably whilst removing from the mounts and were not thermally etched. The small differences in the densities between the CIP and CUP samples showed there would be little value in manufacturing further CIP samples for SEM imaging. The CUP samples were analysed by SEM after being carbon coated.

4 Results and Discussion

4.1 Lubricant Performance

The three lubricants performed similarly to the zirconolite work in Chapter 2 with regard to the ability of the lubricant to allow powder discharge after milling. The milled material would discharge rapidly immediately after the discharge valve was opened and slow as it neared completion. The amount of material that had been released was manually judged on the visible flow rate of

the discharging material. That is, when the flow had almost stopped, the discharge was considered complete. When approximately 95-100%, by volume, had been collected, the collection jar was removed and weighed. Typically, at the point of weighing, 99-100%, by mass, of material had been collected. This gave good confidence that the visual method used to judge the level of discharge completion gave useful results.

Oleic acid, again, provided the fastest discharge conditions with powders typically taking 2 minutes to fully discharge. Powders milled with polyethylene glycol were discharged in 2-3 minutes, whilst those milled with zinc stearate were discharged in 4 minutes. Discharge time is not strictly the best indication of powder flow in the mill, as the quickest discharge does not necessarily mean the best milling conditions. It is, however, a good indicator of the material behaviour in the mill. For example, if a foot forms and the mill does not discharge, then it is fair to assume that the powders have not been milled as expected. It is also an important operating parameter. If the powders fail to discharge fully, it is irrelevant how well the powders have been milled.

4.2 Particle Size Analysis

Figure 40 shows the particle size distribution of the powders milled with zinc stearate. The graph does not show a clear change between the milling conditions in the most common sized particle, with all samples being around 1.9 – 2.5 μm range. However, more detailed examination of the d_{10} values (10% of all particles are smaller than this size), Table 11, does show a decrease in the size of the primary particles as the aggressiveness of the milling increases. This is also reflected in the generally decreasing trend of the d_{50} (50% of all particles are smaller). The d_{90} (90% of all particles are smaller) values do not show this same trend. The particles larger than 10 μm shown in Figure 40 are likely to be a result of agglomeration during analysis and are not a consequence of milling. In preparation of the paste, any weak agglomerates will have been destroyed yet it is possible they reform in the fluid in the instrument. In addition,

methanol did not wet the surface of the powders as well as expected. Thus, any real agglomerates from milling may have been retained in this wet particle size analysis. Direct SEM imaging, Figure 48 and Figure 49, explores the extent of secondary agglomerates in the milled powders.

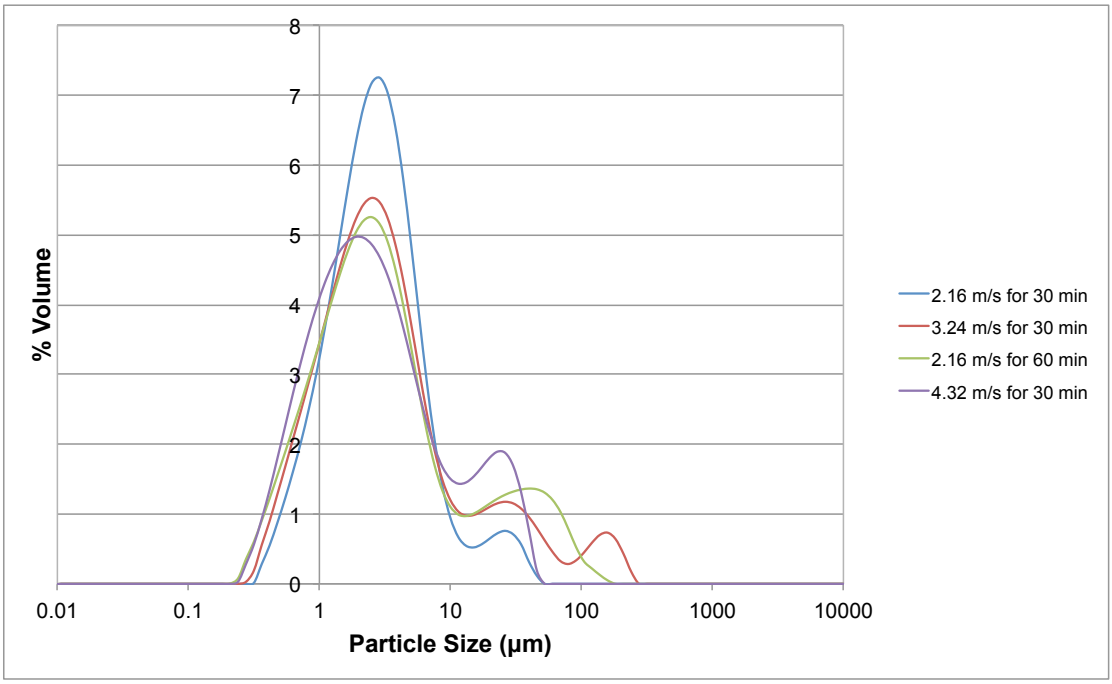

Figure 40: Particle Size Distribution of powders milled with zinc stearate.

Speed ($m\ s^{-1}$)	Duration (min)	d_{10} (µm)	d_{50} (µm)	d_{90} (µm)
2.16	30	0.87	2.46	6.82
3.24	30	0.73	2.50	19.82
2.16	60	0.66	2.38	22.78
4.32	30	0.63	2.24	16.74

Table 11: $d_{10,50,90}$ values for powders milled with zinc stearate.

Figure 41 shows the particle size distribution of the powders milled with polyethylene glycol. Again, superficially, there is little difference in the size of the most common particle size in all samples. Examination of Table 12 shows the same decreasing trend of d_{10} and d_{50} values for all milled powder batches. The d_{90} value is again susceptible to material agglomeration during analysis. The distribution in Figure 41 does not show the same large particles as for the zinc stearate samples; methanol wetted the powders milled with polyethylene glycol satisfactorily.

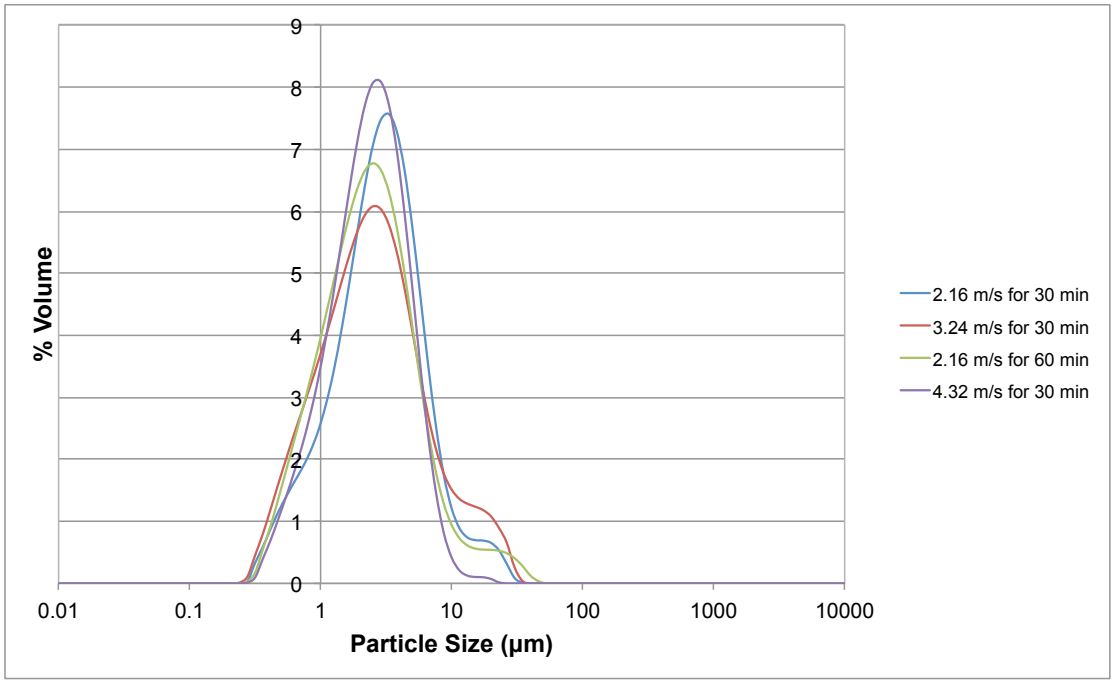

Figure 41: Particle Size Distribution of powders milled with polyethylene glycol.

Speed ($m\ s^{-1}$)	Duration (min)	d_{10} (µm)	d_{50} (µm)	d_{90} (µm)
2.16	30	0.83	2.66	6.65
3.24	30	0.68	2.27	8.37
2.16	60	0.72	2.16	6.17
4.32	30	0.60	2.15	17.37

Table 12: $d_{10,50,90}$ values for powders milled with polyethylene glycol.

Figure 42 shows the particle size distribution of powders milled with oleic acid. The four different milling conditions have produced similar particle size distributions of the powders to each other. Table 13, however, shows that the d_{10} and d_{50} of the milled powders do not show the same trend as the previous two lubricants. This may be due to a sampling error in selecting the material to be analysed. Only the powders milled at 2.16 m s^{-1} for 60 min show the secondary agglomeration feature above 10 µm. This is, again, likely to be agglomeration during analysis rather than a remnant of the milling process.

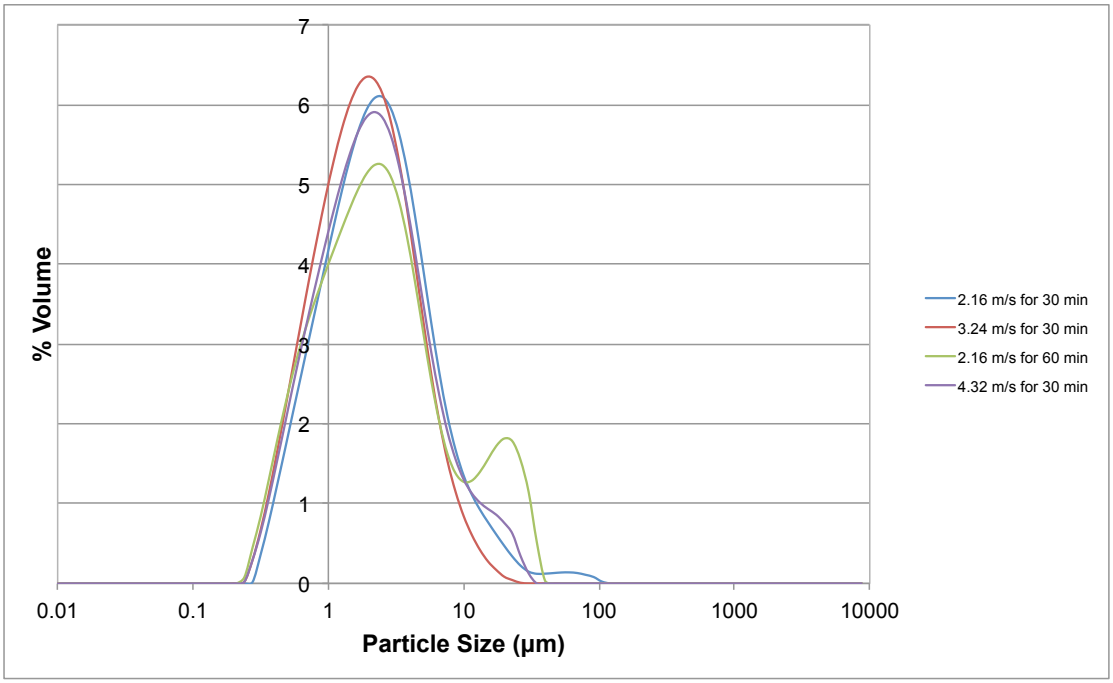

Figure 42: Particle Size Distribution of powders milled with oleic acid.

Speed ($m\ s^{-1}$)	Duration (min)	d_{10} (µm)	d_{50} (µm)	d_{90} (µm)
2.16	30	0.77	2.41	7.92
3.24	30	0.67	1.98	5.70
2.16	60	0.65	2.39	15.31
4.32	30	0.69	2.23	7.87

Table 13: $d_{10,50,90}$ values for powders milled with oleic acid.

Milling with each of the lubricants has produced a narrow distribution of particles. That is, the majority of particles are between 0.3 and 10 µm. It may have been expected that the different precursor components would be preferentially sized reduced, which would have appeared as multiple peaks as apposed to a singular peak in the charts. This result implies that all of the precursor components, including the ceria, are being size reduced at a similar rate. Also, it is likely that the feeds did not all have the same particle size before milling, thus larger particles, of all components, have been preferentially size reduced.

Not showing the secondary agglomerations is a serious drawback to this technique; however, the intention was to show a change in primary particle size with different milling conditions. As mentioned, it was impossible to get repeatable measurements without forming the powders into a paste before

analysis. It may be possible to repeat the particle size analysis utilising a dry powder technique where the powders are transported by a flowing gas rather than a liquid. This would prevent agglomeration during analysis and would give confidence that the distribution recorded was solely a result of the different milling conditions.

4.3 Density

The target density was >92% of theoretical. Above this threshold, the samples are considered to have no connected porosity (Shaw 1998). However, in general, the highest density products are preferred. The densities are expressed in absolute terms and as a percentage of the theoretical density. Theoretical density has been calculated as 5.6 g cm^{-3}, based on the atomic masses of the atoms and the zirconia unit cell size (a= 5.07987 Å, c= 5.19772 Å (Krogstad, Lepple et al. 2011).

The sample densities, ordered by increasing density, are given as Table 14. The first observation is that the density of the CIP samples is always greater than that of the CUP counterparts. This is as expected, as CIP is known to improve the density of the products. The density of pellets produced by CIP are on average two percentage points higher than the CUP samples manufactured from the same milled powders (mean: 1.99 percentage points; median: 1.78 percentage points). The second is that samples made from powders milled at 4.32 m s^{-1} for 30 minutes have the highest density and that samples manufactured from powders milled at 2.16 m s^{-1} for 30 minutes are the least dense. This, again, is expected. It seems logical that more aggressive milling (i.e. greater tip speed) should reduce the particle size of the milled powders and that in turn leads to reduced porosity and denser ceramics. The lubricant selection does not appear to make a significant difference in the product density. For example, samples milled with polyethylene glycol had both the highest and the lowest densities. The overall mean density for samples milled with polyethylene glycol 5.10 g cm^{-3}; oleic acid 5.10 g cm^{-3} and; zinc stearate

5.04 g cm^{-3}. The slight reduction in average density for the zinc stearate samples is likely to be due to natural sample variation rather than an inherent difference in the lubricant performance.

Tip Speed ($m\ s^{-1}$)	Duration (min)	Lubricant	Pressing Method	Density ($g\ cm^{-3}$)	% TD
2.16	30	polyethylene glycol	CUP	4.78	85.4%
2.16	30	polyethylene glycol	CIP	4.86	86.9%
2.16	30	zinc stearate	CUP	4.90	87.4%
2.16	30	oleic acid	CUP	4.91	87.7%
2.16	30	oleic acid	CIP	4.95	88.4%
2.16	60	polyethylene glycol	CUP	4.96	88.5%
2.16	30	zinc stearate	CIP	4.97	88.8%
3.24	30	polyethylene glycol	CUP	5.02	89.7%
3.24	30	oleic acid	CUP	5.03	89.8%
2.16	60	zinc stearate	CUP	5.04	90.0%
2.16	60	polyethylene glycol	CIP	5.05	90.3%
3.24	30	polyethylene glycol	CIP	5.09	90.9%
3.24	30	zinc stearate	CUP	5.09	90.9%
2.16	60	oleic acid	CUP	5.11	91.2%
3.24	30	oleic acid	CIP	5.13	91.6%
3.24	30	zinc stearate	CIP	5.16	92.2%
4.32	30	oleic acid	CUP	5.16	92.2%
2.16	60	zinc stearate	CIP	5.18	92.4%
2.16	60	oleic acid	CIP	5.19	92.7%
4.32	30	zinc stearate	CUP	5.20	92.9%
4.32	30	polyethylene glycol	CUP	5.22	93.1%
4.32	30	zinc stearate	CIP	5.27	94.0%
4.32	30	oleic acid	CIP	5.29	94.4%
4.32	30	polyethylene glycol	CIP	5.30	94.6%

Table 14: The densities of all zirconia samples, ordered by increasing density.

Figure 43 shows the sample densities as a function of the number of rotations of the mill. The number of rotations is a conjugate variable of the duration and speed of milling. This value has been calculated from the defined operating conditions and is not a measured value. There will undoubtedly be some variation in the actual value, however the error in this figure is small, approximately 1%. This approach does have the drawback, in displaying the data, that the differing milling conditions of 2.16 m s^{-1} for 60 minutes and 4.32 m s^{-1} for 30 minutes have the same number of rotations (by experimental

design). In Figure 43, data corresponding to each set of milling conditions and pellet forming processes is highlighted; blue for CIP and orange for CUP. As the speed of the mill increases, the sample densities appear to have less variability, that is, the groupings decrease in size. This correlation is not connected to duration of milling as both sets of samples milled at 2.16 m s^{-1} show a similar level of variability. There do not appear to be differences in the group size between the CUP and CIP sets implying these variations are associated with the milling process.

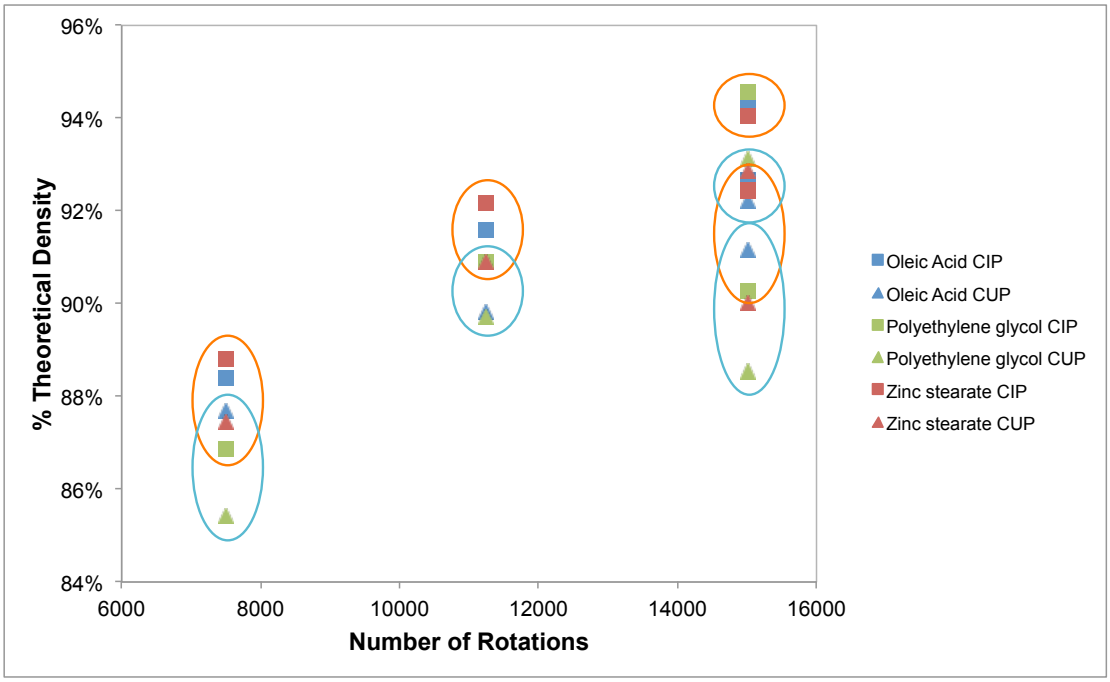

Figure 43: Graph of % Theoretical Density of samples against number of mill internal rotations. Groupings are outlined with blue ovals for CUP samples and orange ovals for CIP.

A decrease in variability is generally a positive outcome as it implies improved process control. It may also imply that the mill is reaching the limit of the size reduction capability in this system. As the mill speed increases, the efficiency of the energy that can be imparted from the mill to the powders will decrease. This assumes that the size reduction effect of the mill is the only correlation with product density. It may be that with increased rotational speed there are improved agglomeration and homogenisation processes. These will allow the powders to become better mixed and this may lead to improved product

densities. Further work with increased rotational speeds could give further evidence of this proposed limit.

To clarify any correlation between milling conditions and product density, the CIP and CUP samples are separated into Table 15 and Table 16, respectively. Examining the CIP samples, Table 15, the least aggressive milling (2.16 m s^{-1} for 30 min) has produced samples with the lowest density (mean density across lubricants, 4.92 g cm^{-3}, theoretical density, TD, 88.0%). Whilst the most aggressively milled powders have produced the samples with the greatest density (mean: 5.28 g cm^{-3}; TD 94.3%). The order of the remaining milling conditions (3.24 m s^{-1} for 30 min and 2.16 m s^{-1} for 60 min) is less clear. Generally, the powders milled at 2.16 m s^{-1} for 60 min (zinc stearate and oleic acid) form products with greater densities than those milled at 3.24 m s^{-1} for 30 min. The exception is the powders milled with polyethylene glycol. This sample has a density (5.05 g cm^{-3}) below all of the samples milled at 3.24 m s^{-1} for 30 min. This result shows the potential benefits of increasing duration rather than just speed.

Tip Speed (m s^{-1})	Duration (min)	Lubricant	Density (g cm^{-3})	% TD
2.16	30	Polyethylene glycol	4.86	86.9%
2.16	30	Oleic acid	4.95	88.4%
2.16	30	Zinc stearate	4.97	88.8%
2.16	60	Polyethylene glycol	5.05	90.3%
3.24	30	Polyethylene glycol	5.09	90.9%
3.24	30	Oleic acid	5.13	91.6%
3.24	30	Zinc stearate	5.16	92.2%
2.16	60	Zinc stearate	5.18	92.4%
2.16	60	Oleic acid	5.19	92.7%
4.32	30	Zinc stearate	5.27	94.0%
4.32	30	Oleic acid	5.29	94.4%
4.32	30	Polyethylene glycol	5.30	94.6%

Table 15: Densities of samples manufactured by CIP, ordered by increasing density.

All of the samples manufactured from powders milled at 4.32 m s^{-1} for 30 min and CIP consistently achieved densities above the 92% target. In addition, two products manufactured from powders milled at 2.16 m s^{-1} for 60 min (milled with oleic acid or zinc stearate) and one sample milled at 3.24 m s^{-1} for 30 min

(zinc stearate) also reached the target. From this observation, there is a good level of confidence that zirconia samples CIP from powders attrition milled at 4.32 m s^{-1} for 30 min will produce products greater than the 92% target. The low variability of samples manufactured from powders milled at 4.32 m s^{-1} was identified in Figure 43. However, less aggressive milling may occasionally produce suitable ceramics but the variation in the results does not give enough confidence that these milling conditions will always give a zirconia ceramic of >92% density.

The densities of the samples manufactured by CUP are given in Table 16. The density trends are very similar to the CIP samples and this gives further evidence that variations in product density come from the milling processes. The most aggressive milling conditions (4.32 m s^{-1} for 30 min) have, again, produced samples that have the highest density (mean: 5.19 g cm^{-3}; TD 92.7%). Likewise, the least aggressively milled powders (2.16 m s^{-1} for 30 min) have produced the lowest density samples (mean: 4.86 g cm^{-3}; TD 86.8%). The other two milling conditions (3.24 m s^{-1} for 30 min and 2.16 m s^{-1} for 60 min) again have produced less clear correlations with product density. Samples manufactured by CUP from powders milled at 4.32 m s^{-1} for 30 min are consistently above the 92% of theoretical density target.

Tip Speed (m s^{-1})	Duration (min)	Lubricant	Density (g cm^{-3})	% TD
2.16	30	polyethylene glycol	4.78	85.4%
2.16	30	zinc stearate	4.90	87.4%
2.16	30	oleic acid	4.91	87.7%
2.16	60	polyethylene glycol	4.96	88.5%
3.24	30	polyethylene glycol	5.02	89.7%
3.24	30	oleic acid	5.03	89.8%
2.16	60	zinc stearate	5.04	90.0%
3.24	30	zinc stearate	5.09	90.9%
2.16	60	oleic acid	5.11	91.2%
4.32	30	oleic acid	5.16	92.2%
4.32	30	zinc stearate	5.20	92.9%
4.32	30	polyethylene glycol	5.22	93.1%

Table 16: Densities of samples manufactured by CUP, ordered by increasing density.

At the outset of this work, it was unknown whether the tip speed of the mill was more important than the duration. It was thought that the greater tip speed should impart more energy into the milling media and thus reduce the size of the powders more effectively. However, it was also thought that the extra energy required for milling could be introduced by a greater duration. When comparing the 2.16 m s^{-1} for 60 min and the 4.32 m s^{-1} for 30 min samples (the same approximate number of rotations), it is clear that the increased speed produces higher density products. However, in comparing the longer duration with a slightly increased tip speed (the 3.24 m s^{-1} samples) the difference in the density of the products is not as clear as between the increased duration and the highest tip speed. These results would suggest that both duration and tip speed are important factors and that the total milling energy is a function of both parameters. It can be suggested that increased the tip speed would be the easiest method to improve the density of the ceramic products. However, if the tip speed were limited by noise restraints, the need to minimise media wear or for some other reason, then increasing the duration suitably may have the desired effect.

Overall, for this specific system of dry attrition milling zirconia precursors, it can be said that CIP produces products 2 percentage points denser than CUP (mean: 1.99 %; median 1.78%). Milling at 2.16 m s^{-1} for 60 min rather than 30 min produces samples 4 percentage points denser (mean: 4.1%; median 3.9%) and milling for 30 min at 4.32 m s^{-1} rather than 2.16 m s^{-1} gives a 6 percentage points increase (mean: 6.4%; median 5.9%).

4.4 SEM

The microstructure of the sintered products was examined by SEM. Each sample was thermally etched in order to develop the contrast between grain boundary and the grains. Each sample set is grouped by lubricant and are in order of increasing density. All images on the left are 200x magnification and are to give an overview of the sample. Images on the right are 1000x

magnification and give a detailed view of one location of the sample. As shown by the 200x images, the samples have homogenous microstructure and each pair of images is representative of the whole sample. Changes in brightness between the samples should not be taken to mean a change in composition (as a difference in contrast within in a sample should); this is merely a result of the automatic image processing on the SEM.

4.4.1 Zinc Stearate

In Figure 44, the samples manufactured from powders milled with zinc stearate are shown. The first pair of images is of the product from the powders milled at 2.16 m s^{-1} for 30 min and has the lowest density for this lubricant (4.90 g cm^{-3}; TD 87.4%). The sample is homogenous with no signs of unreacted ceria, which would appear as bright white phases (the white area at the top left of the left image is due to electron beam charging and does not represent a real change in the sample composition). The higher magnification image, right, shows a large number of pores. The majority of pores are inter-granular indicating that grain growth was steady and that the sintering temperature was suitable (Kingrey, Bowen et al. 1976). The intragranular pores are typically a result of residual porosity in the precursor materials. As the samples increase in density, the number of pores decreases, from 4.00 pores per 1000 μm^2 to 1.64 pores per 1000 μm^2 and the grain size increases (calculated by manually counting all visible pores in the SEM image and normalising to 1000 μm^2). These changes appear to be correlated to the increasing density of the samples.

Estimates for the average grain size were calculated from the square root of measured longest axis and the axis perpendicular. This is an over estimate in size as it assumes the grains are rectangles as apposed to, as majority of the grains are, hexagons. Only grains completely within the image frame were used for the average. The sample manufactured from powders milled at 2.16 m s^{-1} for 30 min has an average grain size of 19 μm whereas the sample produced from powders milled at 4.32 m s^{-1} for 30 min has an average grain size of 37 μm.

It may seem counterintuitive that more aggressively milled samples produce larger grains. This, however, is explained by the process of secondary recrystalisation(Kuczyuski, Hooton et al. 1967). Grain growth is driven by the difference in energy between two grain boundaries. If a grain has a boundary with a greater radius of curvature then it will preferentially grow at the expense of other, less curved, grains. Grain growth can be thought of as the inverse of grain consumption. After initial crystallisation, grains can only grow at the expense of others. Grain growth stops when the energy difference across a grain boundary becomes zero. Thus, if during the initial crystallisation phase the initial grains are all a similar size, there is only a small driver for grain consumption; the grain boundaries are broadly equal. Similar sized primary grains will come from coarse powders. If the initial grains are different in size there will be a large number of smaller grains consumed, whilst others grow. It is not difficult to imagine samples manufactured from fine powders (i.e. low particle size) to have the occasional larger grain and the surrounding grains being much smaller. This large grain will consume the surrounding smaller grains, thus increasing in size. As this grain continues to grow at the expense of others, the driving force (difference between the radii of curvature between two grains) will become greater for the large grain, increasing the driving force for growth. The growth of the grain will only stop when the driving force across the boundary becomes zero; that is when two similar sized grains meet. This process of secondary recrystallisation explains the increase in average grain size of the samples with respect to the decreasing particle size of the milled powders.

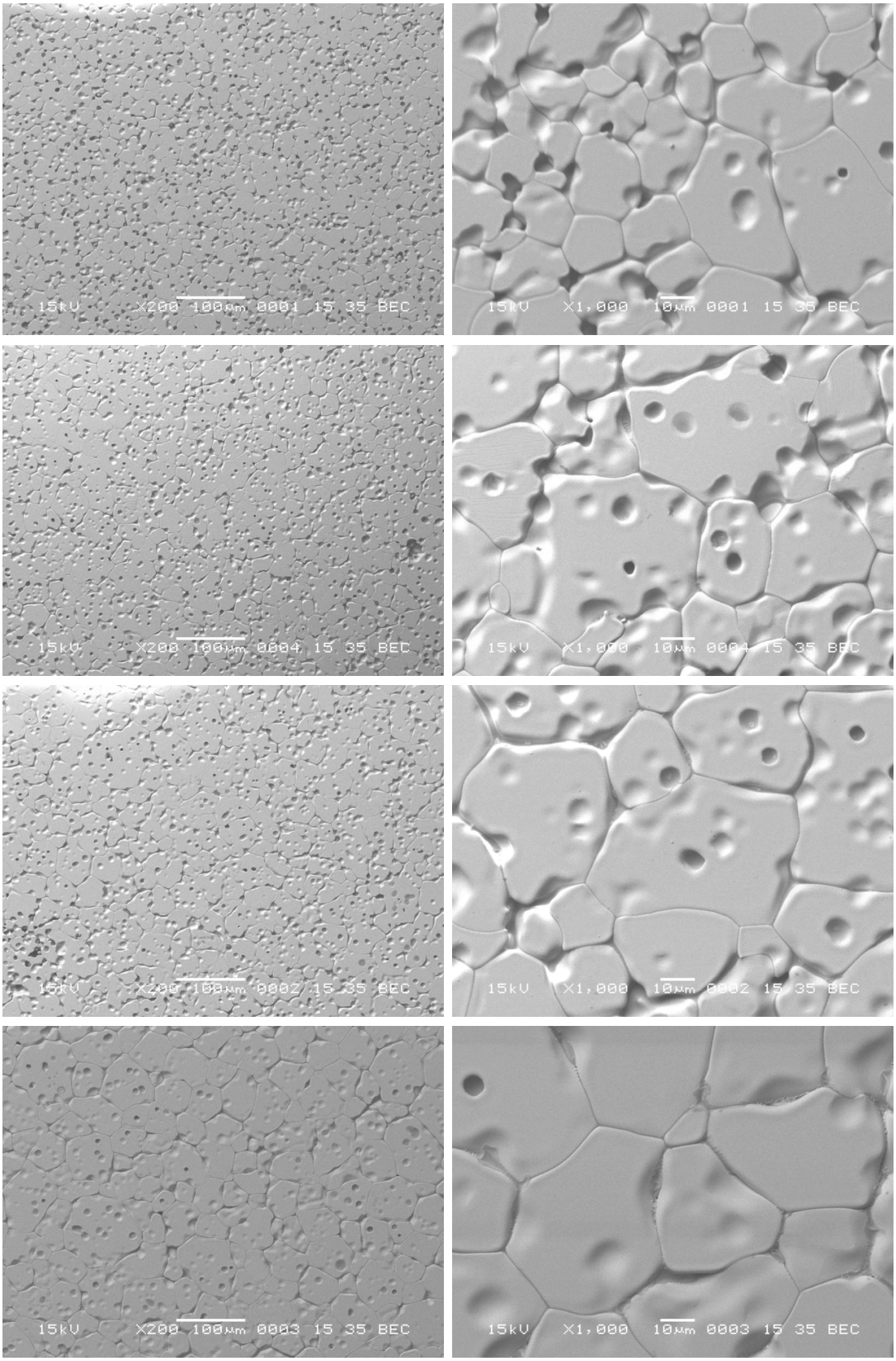

Figure 44: SEM images of samples milled with zinc stearate ordered by increasing sample density. From top, 2.16 m s^{-1} for 30 min, 2.16 m s^{-1} for 60 min, 3.24 m s^{-1} for 30 min, 4.32 m s^{-1} for 30 min.

Overall, the average grain size of the sample increases as the milling becomes more aggressive (from 19 to 37 μm for samples milled at 2.16 m s^{-1} for 30 min to 4.32 m s^{-1} for 30 min), the number of pores decreases as the milling becomes more aggressive. In addition, the samples are homogenous with no sign of unreacted ceria.

4.4.2 Polyethylene Glycol

Figure 45 shows SEM images of the samples manufactured from powders milled with polyethylene glycol. The samples are arranged by increasing density, order: 2.16 m s^{-1} for 30 min, 2.16 m s^{-1} for 60 min, 3.24 m s^{-1} for 30 min, and 4.32 m s^{-1} for 30 min. Again, as the sample densities increase, the average grain size also increases. Each sample is homogenous, shown by the uniform contrast in the images. Approximate average grain sizes are 20 μm for sample manufactured from powders milled at 2.16 m s^{-1} for 30 min and 48 μm for the sample produced from powders milled at 4.32 m s^{-1} for 30 min. These two samples have the highest and lowest, respectively, densities of the entire sample set. As the density increases, the number of visible surface pores again decreases; 4.63 pores per 1000 μm^2 to 2.11 pores per 1000 μm^2.

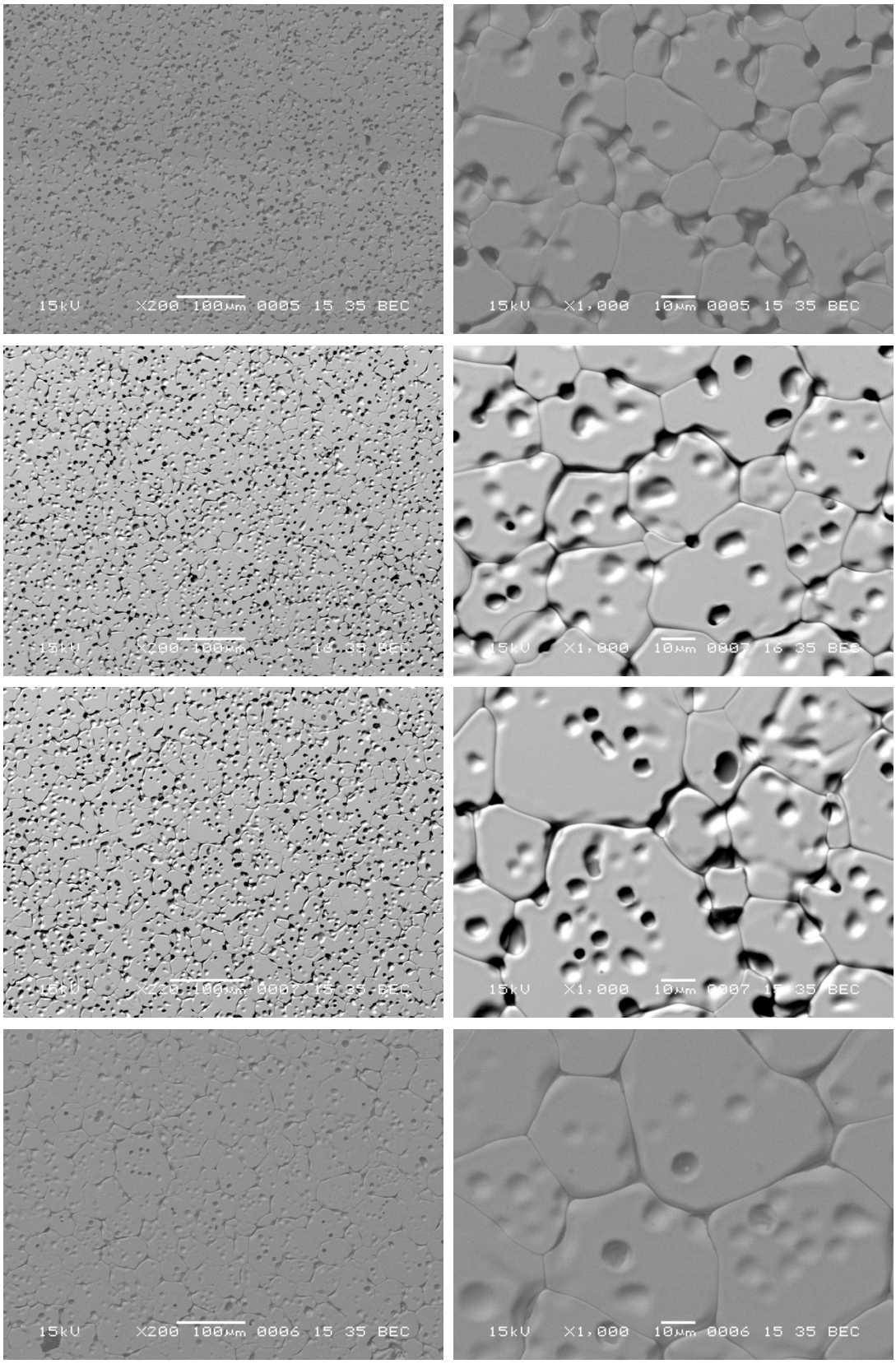

Figure 45: SEM images of samples milled with polyethylene glycol ordered by increasing sample density. From top, 2.16 m s^{-1} for 30 min, 2.16 m s^{-1} for 60 min, 3.24 m s^{-1} for 30 min, 4.32 m s^{-1} for 30 min. All samples, bar the second pair, were taken with a working distance of 15 mm, whilst the second pair was 16 mm.

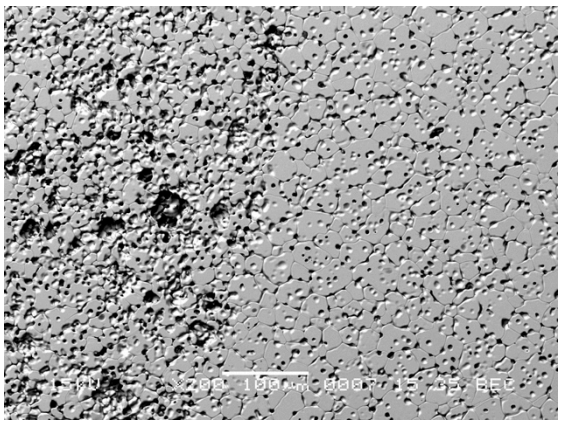

Figure 46: Increased porosity on left of image. Sample manufactured from powders milled at 3.24 m s^{-1} for 30 min.

Figure 46 is a section of the sample manufactured from powders milled at 3.24 m s^{-1} for 30 min and shows an area of increased porosity. This increased porosity is most likely due to the incorporation of less or non-milled powders into the final sample. It is known that non-milled powders may agglomerate in the discharge valve of the attrition mill. These, typically, will be precursors that are not fully size reduced or homogenised. If the attrition mill is operated in a semi-continuous batch mode (i.e. continuous feeds but each milling operation is one batch), the milled material from the previous batch can be used to fill the discharge grate before the next batch is loaded. This is achieved by running the mill 'empty' (just containing the milling media). The small amount of hold up on the balls is dislodged and allowed to accumulate in the grate. This accumulated material has already undergone milling and fills the discharge valve preventing any fresh non-milled material from accumulating there. This work around is a simple plant operational modification and is easily implemented without the need for complex engineering modifications to the discharge system.

4.4.3 Oleic Acid

Figure 47 gives the SEM images of the various samples manufactured from powders milled with oleic acid, ordered by increasing density: order: 2.16 m s^{-1} for 30 min, 3.24 m s^{-1} for 30 min, 2.16 m s^{-1} for 60 min, and 4.32 m s^{-1} for 30 min. The samples are homogenous with no obvious signs of unreacted ceria or phase separation. Again, as the density increases, the average grain size increases and the number of pores decrease. The average grain size increases from 20 μm for the 2.16 m s^{-1} for 30 min sample to 28 μm for the 4.32 m s^{-1} for 30 min sample. The average grain size of the 4.32 m s^{-1} for 30 min sample is known to be an underestimate as the method used to estimate the grain size only counted grains that were completely in the image. Examining the 200x magnification image there are three to four large grains that have been cropped by the image and thus are not included. However, there is sill a notable increase in grain size between the two samples. The number of visible pores on the surface decreases from 3.14 pores per 1000 μm^2 to 1.10 pores per 1000 μm^2.

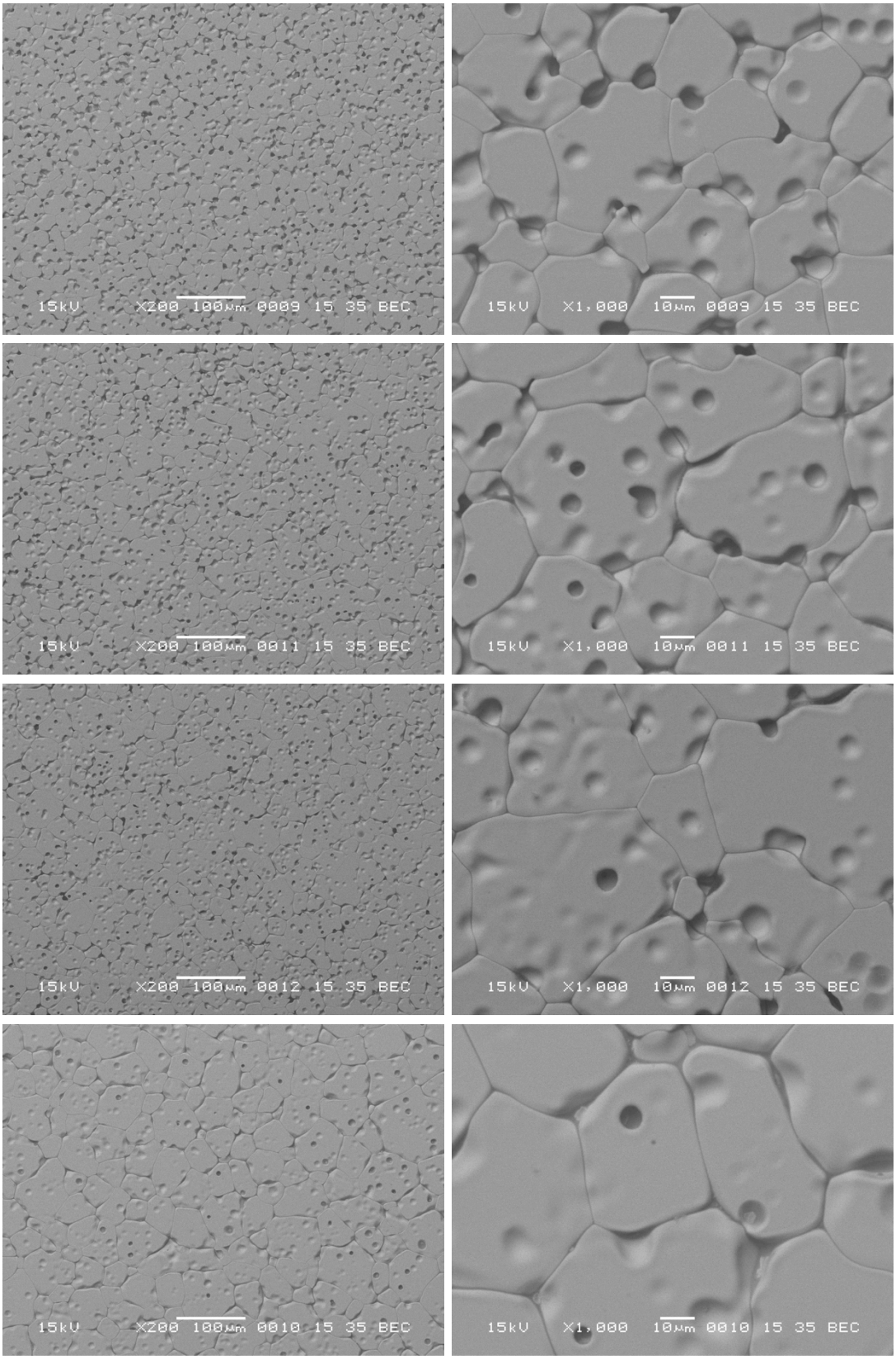

Figure 47: SEM images of samples milled with oleic acid ordered by increasing sample density. From top, 2.16 m s^{-1} for 30 min, 3.24 m s^{-1} for 30 min, 2.16 m s^{-1} for 60 min, 4.32 m s^{-1} for 30 min.

4.4.4 Discussion

In comparing all three lubricant sample sets there are clear trends. For every lubricant set the average grain size increases and the number of pores decreases as the density of the sample increases, which is as expected. There is no obvious difference between the lubricants in terms of microstructure or phase development. This would suggest that lubricant choice does not influence the properties of the final product and the lubricant should be chosen based on other properties (e.g. ease of removal and addition, ability to prevent foot formation, ease of use, stability etc.).

4.5 Milled Powders

Direct SEM imaging of the milled powders was undertaken, Figure 48 and Figure 49. The milled powders were lightly sprinkled onto a carbon SEM stub. It is appreciated that this method may not give a wholly accurate sampling regime but after trials with other methods[19] this technique gave the most acceptable results in terms of sample representation.

The powders from both samples show an abundance of primary particles from < 1 μm to ~4 μm, in good agreement with the particle size analysis. The differences in particle contrast in the backscattered image show that these are a mix of different elements implying that no one component is preferentially size reduced. The secondary agglomerates, 10-50 μm lumps, appear to be a blended mixture of each of the precursor components. This may give the milled powders an overall larger particle size distribution but it is not detrimental to product performance. It could be argued that this is, in fact, beneficial. The agglomeration of powders can be thought of as being equivalent to granulation.

[19] Rubbing the stub in the milled powder removed many of the larger agglomerates; suspension in propanol and adding drop wise to the stub segregated the powders as the liquid moved over the surface of the stub; blowing the powder over the stub segregated the powders

The smaller primary particles are being agglomerated into larger secondaries. Granulation is widely known to improve powder flow and powder packing, both of which are beneficial to subsequent processing. It is difficult to determine whether these agglomerates formed during the attrition milling or storage and whilst sample preparation attempted to minimise any changes in the sample, it must be remembered that the spread and number of secondary particles may be a direct result of the sample preparation method utilised.

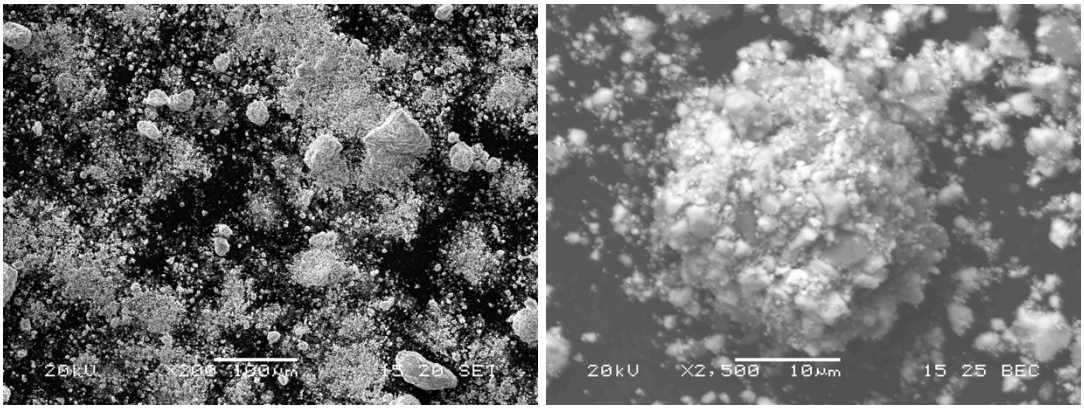

Figure 48: SEM image of powders milled at 2.16 m s^{-1} for 30 min with zinc stearate as the lubricant. Image on left is 200x magnification taken in the secondary electron mode with an accelerating voltage of 20 kV, working distance of 15 mm and a spot size of 20. The image on the right is a close up, x2500, of one of the secondary agglomerates and is taken in the back scattered electron mode with an accelerating voltage of 20 kV, working distance of 15 and spot size of 25. The sample was not coated.

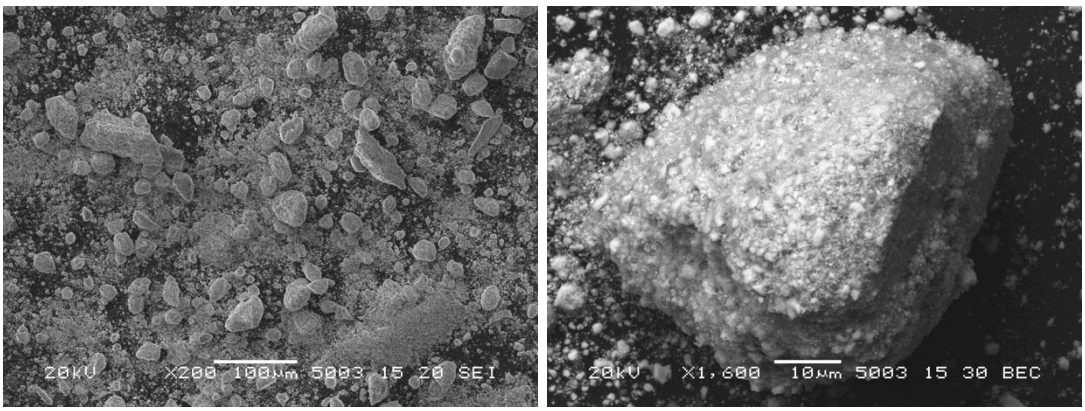

Figure 49: SEM image of powders milled at 4.32 m s^{-1} for 30 min with zinc stearate as the lubricant. Image on the left is taken at 200x magnification in the secondary electron mode with an accelerating voltage of 20 kV, working distance of 15 mm and a spot size of 20. The image on the right is a close up, x16000, of one of the secondary agglomerates taken in the backscattered electron mode with an accelerating voltage of 20 kV, working distance of 15 mm and spot size of 30. The sample was not coated.

Any comparisons made between Figure 48 and Figure 49 must be done with caution, as the sampling method may not be wholly representative. However, an increase is observed in the number and size of the secondary agglomerates in the powders milled at 4.32 m s^{-1} for 30 min against those in the powders milled at 2.16 m s^{-1} for 30 min. The primary particle size does not appear to substantially change, remaining constant at < 1 μm to ~4 μm between the milling conditions. What does appear to be happening is an increasing tendency for the primary particles to agglomerate into these well-mixed secondaries. During sintering, these agglomerates will form the primary grains that go on to consume other, smaller, grains. The difference between a small primary particle size and well-mixed agglomerate initiators is the initial formation of the larger grain. The growth and consumption of other grains is still the process of secondary recrystalisation.

5 Discussion

The comparable lubricant performance between this work and Chapter 2 is positive. The use of the same lubricants at the same addition levels in different material systems does imply that for dry milling metal oxides oleic acid, polyethylene glycol and zinc stearate are suitable lubricants. This is based on the ability of the lubricant to prevent foot formation and to aid powder discharge from the mill. Examining the microstructure of the sintered products, there are no obvious differences between the lubricant sample sets. Thus, it can be said that lubricant choice can be entirely dependent on its behaviour during and after milling. As discussed in Chapter 2, the failure to remove the lubricant completely before HIP led to the poor quality ceramics produced. It is possible to select a lubricant based on its ease of removal, assuming it keeps milled powders free flowing during milling. Other factors such as temperature dependence, cost or ease of handling may be important. From these criteria, polyethylene glycol would be the most suitable choice: it performs adequately in allowing the milled powders to freely discharge, it is a dry powder and thus

convenient to handle, and its decomposition products will be CO_2 and H_2O. Zinc stearate, whilst also a powder will produce either ZnO or Zn during decomposition and oleic acid is a tacky liquid.

The purpose of this section of work was to explore the use of the attrition mill with a different metal oxide precursor system and to clarify if the failure to remove the lubricant completely in earlier work masked correlations between milling parameters and product properties. In this work, the zirconia products were consolidated in an unconstrained manner, that is, any entrained gases or decomposition products could be released during sintering. As shown in the SEM micrographs, there is a clear correlation between milling speed and duration, and the microstructure. This trend was also mirrored in the density results. The result that ceramic products with the milling lubricant fully removed follow a trend with milling parameters gives further evidence that the failure to remove the lubricant in Chapter 2 interfered with the final product properties.

If zirconia was selected as the wasteform for plutonium immobilisation, the aforementioned process could be implemented. Putting aside the desire to consolidate by HIP, CUP of powders milled at 4.32 m s^{-1} for 30 min and subsequently sintered in air at 1700 °C will produce ceramic products with densities greater than the target of 92 % of theoretical. SMP uses CUP technology to produce fuel pellets. These pellets are sintered at 1750 °C, potentially allowing a similar process to be utilised. Whilst CIP produced samples with greater densities than their CUP counterparts did, the added complexity of using CIP in an active environment is not sufficiently beneficial. In order to use HIP for consolidation with this metal oxide system, it will be necessary to manufacture a HIP can from a different metal to stainless steel, for example tantalum or molybdenum. However, these materials may be prohibitively expensive and cannot be worked into HIP cans.

A method for removing the lubricant from the milled powders will also need to be developed. Chapter 2 showed that removal of the lubricant from the HIP can was difficult implying that it must be removed from the loose milled powders. A screw fed calciner may accomplish this. This piece of equipment consists of a helical central bar that forcibly conveys powder through a tubular hot zone. A gas (e.g. argon/oxygen) can be passed through the powders to ensure the complete destruction of the lubricant.

As the trend throughout all of the lubricant sample sets was an increase in milling speed and duration led to improved densities of the products, it would follow that further work examining more extreme milling (i.e. > 4.32 m s^{-1} tip speed and > 60 min milling) may produce more dense products. However, it is recognised that there will be a limit to the level of milling achievable in this particular mill and metal oxide system. As the deviation of the product densities for each milling condition became smaller with increasing tip speed, milling at 4.32 m s^{-1} may be reaching this limit. Beyond such a limit, there may be a reduction in product quality due to the disruption of the secondary agglomeration processes, or an increased likelihood of foot formation due to the increase in the fines fraction of the powders.

6 'Realistic' Ceria

The series of milling conditions and consolidation techniques was repeated with the 'realistic' ceria simulant and oleic acid as the lubricant. The purpose was to determine any difference between the simulant behaviour and the other less representative ceria simulant. Oleic acid was chosen as it had been shown to give the quickest mill discharge time. Table 17 gives the CIP and CUP densities of the samples manufactured with the 'realistic' ceria, the standard ceria samples are given for comparison. The 'realistic' ceria samples are less dense than their standard ceria counterparts are. This is likely to be due to the nature of the realistic ceria, as discussed in Chapter 1. The 'realistic' ceria was

shown to have a number of coarse agglomerates, which appeared to have formed during the heat treatment stage and are much stronger than agglomerates that have formed by the amalgamation of primary particles. These agglomerates have essentially become the primary particles in that they cannot be easily size reduced. During milling, it is likely that not enough milling energy is imparted to these particles in order to reduced them in size to a similar level of the other primary particles. These agglomerates will retain some of the associated internal porosity through to the final product. This residual porosity decreases the overall density of the products.

Tip Speed ($m\ s^{-1}$)	Duration (min)	Pressing Method	Ceria Source	Density ($g\ cm^{-3}$)	% TD
2.16	30	CUP	Realistic	4.72	84.3%
3.24	30	CUP	Realistic	4.90	87.5%
2.16	30	CUP	Standard	4.91	87.7%
2.16	60	CUP	Realistic	5.01	89.4%
4.32	30	CUP	Realistic	5.01	89.5%
3.24	30	CUP	Standard	5.03	89.8%
2.16	60	CUP	Standard	5.11	91.2%
4.32	30	CUP	Standard	5.16	92.2%
2.16	30	CIP	Realistic	4.89	87.2%
2.16	30	CIP	Standard	4.95	88.4%
3.24	30	CIP	Realistic	5.04	90.0%
2.16	60	CIP	Realistic	5.12	91.3%
3.24	30	CIP	Standard	5.13	91.6%
2.16	60	CIP	Standard	5.19	92.7%
4.32	30	CIP	Realistic	5.20	92.9%
4.32	30	CIP	Standard	5.29	94.4%

Table 17: Density results for samples produced from powders milled with 'realistic' or standard ceria. Results grouped by pressing method and ordered by increasing density.

The other trends in the density data are identical to the trends seen in samples milled with the standard ceria; the lowest sample density is from the least aggressively milled powders (4.72 $g\ cm^{-3}$ from CUP and 4.89 $g\ cm^{-3}$ from CIP for powders milled at 2.16 $m\ s^{-1}$ for 30 min); the most dense samples come from the powders milled most aggressively (5.01 $g\ cm^{-3}$ from CUP and 5.20 $g\ cm^{-3}$ from CIP for powders milled at 4.32 $m\ s^{-1}$ for 30 min); and the samples manufactured

by CIP have a higher density than their CUP counterparts (mean difference: 3.0 %; median 3.1 %).

Figure 50 gives the SEM images of the samples manufactured by CUP with 'realistic' ceria ordered by increasing density (2.16 m s^{-1} for 30 min, 3.24 m s^{-1} for 30 min, 2.16 m s^{-1} for 60 min, 4.32 m s^{-1} for 30 min). The samples are homogenous with no evidence of unreacted ceria. An absence of unincorporated 'realistic' ceria in the samples is positive and implies that this zirconia system, and processing regime, could be suitable for implementation in the relevant environment with PuO_2 feeds. The increase in average grain size with increasing density is seen again. The sample with the lowest density was manufactured from powders milled at 2.16 m s^{-1} for 30 min and has an average grain size of 20 μm, whilst the highest density sample, manufactured from powders milled 4.32 m s^{-1} for 30 min, has an average grain size of 31 μm. Comparing with the SEM images from the similar samples produced with the standard ceria, Figure 47, there is a clear increase in the number of both intragranular and intergranular pores, from 1.10 surface pores per 1000 μm^2 with standard ceria to 3.45 surface pores per 1000 μm^2 with 'realistic' ceria for samples milled at 4.32 m s^{-1} for 30 min.

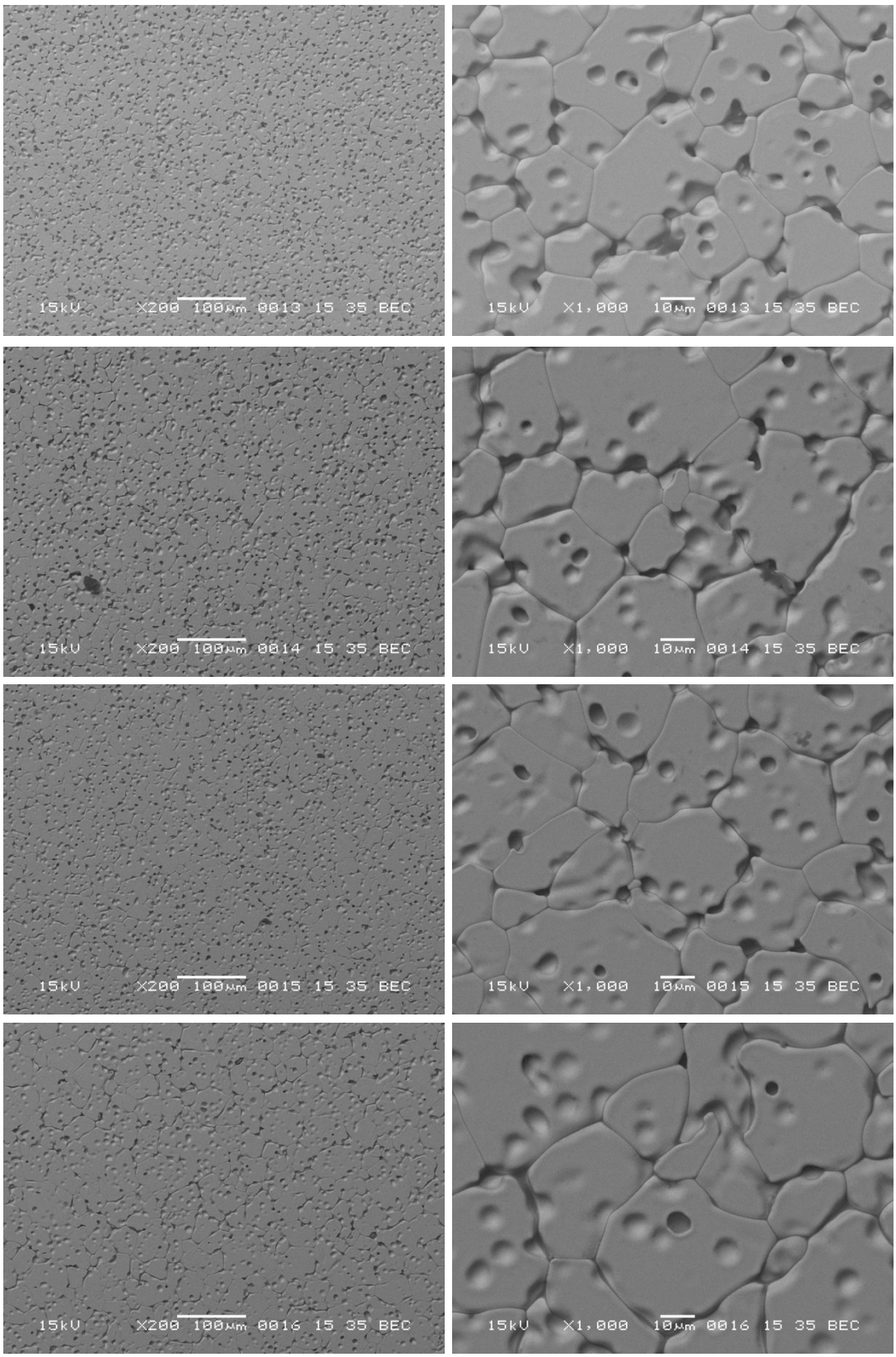

Figure 50: SEM images of samples containing 'realistic' ceria milled with oleic acid ordered by increasing sample density. From top, 2.16 m s-1 for 30 min, 3.24 m s-1 for 30 min, 2.16 m s-1 for 60 min, 4.32 m s-1 for 30 min.

In comparing the two different sources of ceria, there is a decline in product density when using the 'realistic' ceria. This is judged to be a result of the

coarseness of the simulant and the increased strength of the secondary agglomerates. It is important to note that a different simulant, with otherwise identical processing conditions, can reduce, for example, the highest density obtained by two percentage points (average between CIP and CUP samples). The conclusion is that care must be taken when designing a nuclear waste immobilisation process using inactive simulants and care should be taken over the properties of the simulant. In order to mitigate against difficulties in implementing this process in the relevant environment, the immobilisation process must be suitably flexible and robust in its approach. Earlier in this chapter, it was shown that increasing the duration or speed of milling will improve the products. Thus, the design of any piece of equipment for the relevant process must allow for bigger duties than anticipated. The positive outcome of this work is the confidence that this process will minimise unincorporated PuO_2 grains in the final product.

7 Conclusions

The method for the manufacture of zirconia wasteforms utilised in this work can be recommended for implementation. Products of greater than 92% theoretical density have been manufactured by milling in an attrition mill at 4.32 m s^{-1} for 30 min, CUP or CIP and subsequently sintering in air at 1700 °C. The lubricant chosen for milling does not appear to have an effect on the final product quality. Whilst CIP does produce products with improved densities (typically plus two percentage points), the extra complexity posed by implementing a CIP system in the relevant environment would discard this option.

The inability to consolidate zirconia ceramics by HIP would seem to dismiss any further investigation of zirconia for plutonium immobilisation. The intention of this work was to determine whether the failure to remove the lubricant completely in Chapter 2 undermined correlations between milling

and product quality. This work has given further evidence to that conclusion. The systematic change in density, microstructure and porosity with changing milling parameters was not observed in Chapter 2.

This work has produced more evidence that the three lubricants (zinc stearate, oleic acid and polyethylene glycol) all allow powders milled in an attrition mill operating in the dry mode to freely discharge. It was observed that increasing the tip speed of the mill from 2.16 to 4.32 m s^{-1} and milling for 30 min improved the product density by six percentage points. Whilst milling at 2.16 m s^{-1} for 60 min produces four percentage points denser products than milling for 30 min. These results would suggest that for denser products the tip speed should be increased first then, perhaps after reaching the limits of the mill, duration should be increased.

None of the samples showed signs of unincorporated ceria grains. This positive result can give confidence that the zirconia ceramic manufactured has sufficient capacity for PuO_2 incorporation at approximately 10 wt%. The homogeneity of the samples gives confidence that the attrition mill is suitable for wasteform manufacture. Work with the 'realistic' ceria simulant, whilst showing a decrease in average density, still did not show any free ceria grains. Knowing that the 'realistic' ceria is coarser than the expected PuO_2 feed it can be said the PuO_2 will be fully digested, based solely on the particle size properties.

4: Comparing the Effect of Manufacturing Zirconolite From Different Defined Particle Size Precursors

1 Abstract

The work in this chapter explores eight techniques for the production of zirconolite precursors with the intention of manufacturing dense and single host phase samples after consolidation by HIP. Two batches of powders were attrition milled and the milling lubricant was removed in two differing manners: *in situ* from the HIP can and *ex-situ* by calcination of the loose powders. It was confirmed that the lubricant could not be successfully removed from the HIP can. Other precursors were manufactured by the alkoxide/nitrate route had excellent densities (~ 98% TD) and were homogenous in phase development. Samples manufactured from powders, nitrates or colloid versions of the precursors also produced high density (~98% TD) single phase samples. However, neither of these manufacturing methods can be implemented in their current form due to the use of a protonated solvent (propanol) and forms of the cerium that are not representative of the PuO_2 feed. Further work examined the manufacture of fine particle precursors and subsequently mixing them with the 'realistic' ceria simulant and was shown to be an unsuitable technique due to heterogeneous phase development. However, planetary milling these fine

precursors with the realistic ceria did produce a ceramic with a high density and homogenous phase development.

2 Introduction

The inability to manufacture high quality ceramics in Chapter 2 (the products were highly porous, had low densities and the phase development was heterogeneous) prompted further discussion on the manufacturability of a zirconolite wasteform in a relevant manner. Chapter 3 demonstrated that attrition milled materials could be used to manufacture zirconia ceramics with a suitable density (>92% TD). The impact of those two studies prompted work to investigate the redesign of a potential ceramic immobilisation plant.

As mentioned in Chapter 1, there are broadly two methods of manufacture of the precursors; top down or bottom up. In a top down process, the necessary precursors are mixed and size reduced together from materials that are too coarse to form the product without further processing. Any manufacturing process that uses milling is an example. In a bottom up process, precursors with particle sizes far below the required manufacturing size are agglomerated into larger particles that are intimately mixed in the stoichiometric levels of the target product. The alkoxide/nitrate route is an example of this method.

For detailed comparison of each method, for this work three broad categories of precursor preparation were chosen: attrition milling (top down), alkoxide derived (bottom up) and 'as purchased' particle sizes (bottom up). One intention was to compare samples produced from the attrition milled precursors with those in Chapter 2. In this work, the lubricant was to be removed through an *ex-situ* calcination process. That is, the milled powders underwent the same heat treatment conditions (same temperature and duration) as the *in-situ* can lubricant removal step but they were treated as loose powders in an open tube furnace. The intention was to confirm the interference of the lubricants in product quality shown in Chapter 2. Samples manufactured

from alkoxide derived precursors (discussed in further detail later), were intended to demonstrate the effect of the finest practical particle size and the highest level of mixing achievable in a useful lab scale system. The 'as purchased' method utilised materials bought with a known particle size (broadly d_{90} = 1, 0.1, 0.01 μm) and mixed them in a wet system (with propanol as the carrier fluid). This simulated the ability to define the properties of the inactive precursor materials explicitly. Each batch of precursors was designed to produce a zirconolite product with the target formulation, $Ca_{0.75}Ce_{0.25}ZrTi_2O_7$. Again, cerium was the plutonium surrogate. Charge compensation was provided by titanium metal added to the prepared material before being packed into the HIP cans. The titanium metal would donate electrons to the Ti^{4+}, present as TiO_2, to form Ti^{3+} and thus the correct charge compensation.

After the manufacture of the various precursor batches, each batch was split into three aliquots and packed into three separate HIP cans. Manufacturing the products in triplicate sought to confirm the repeatability (or lack of) for each method. The packed HIP cans were evacuated in a modified evacuation rig to Chapter 2. The new system contained an in-line filter designed to trap any vaporised hydrocarbons (milling lubricants) in a controlled manner, Figure 51 and Figure 52.

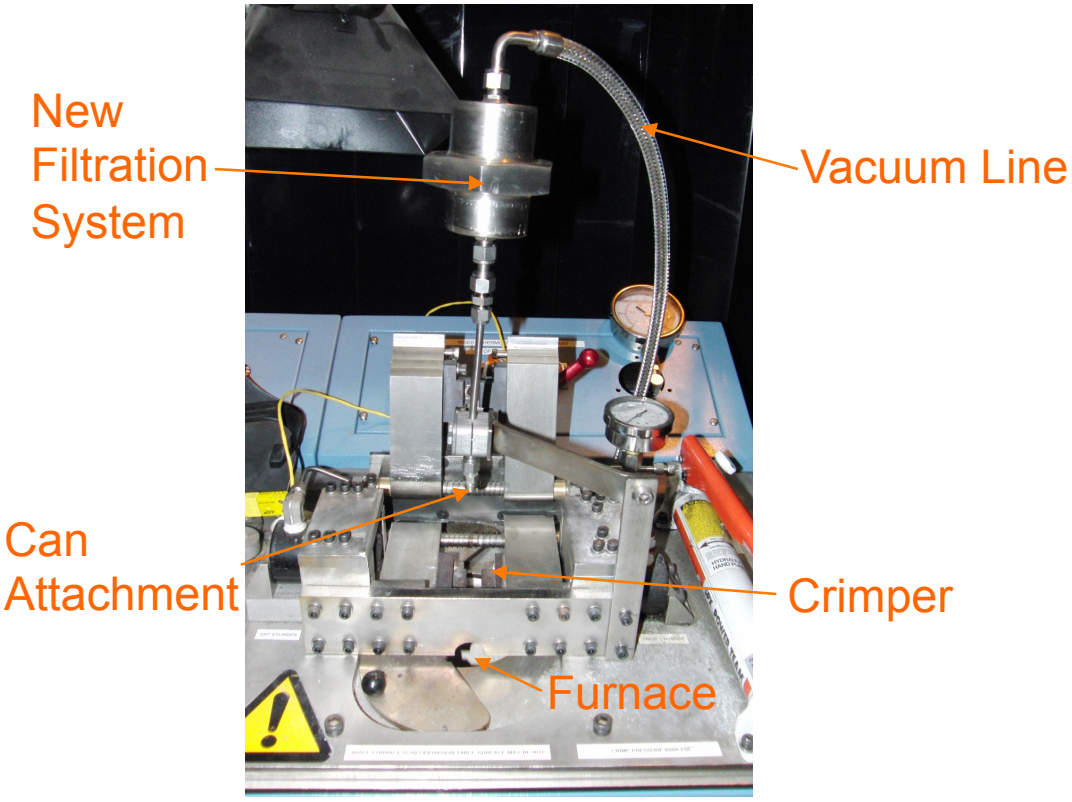

Figure 51: Modified bake-out rig

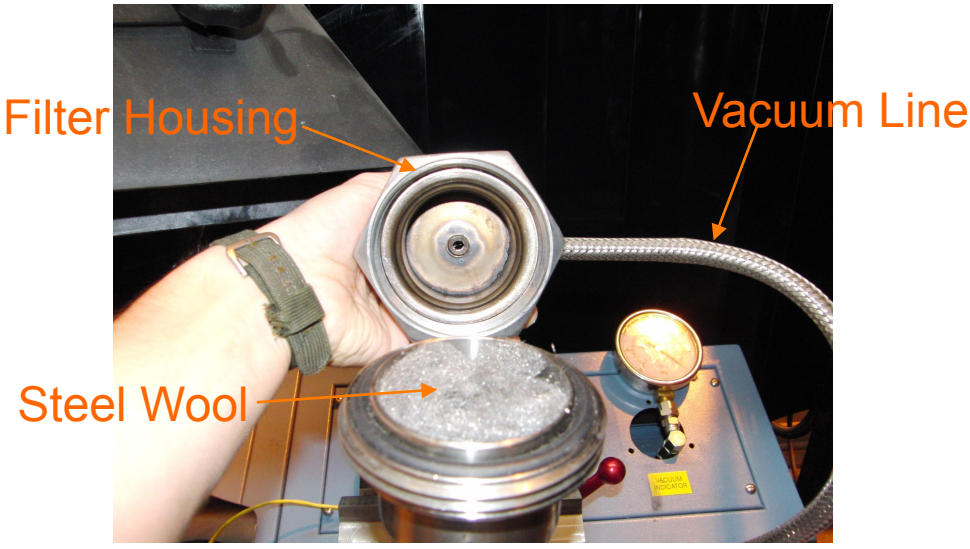

Figure 52: Filter internals. The outer casing lightly packed steel wool as a place to condense lubricants post vaporisation.

As in Chapter 2, all of the samples underwent the high temperature HIP cycle (1320 °C for 2 hours with 100 MPa pressure supplied by argon). Each of the samples underwent detailed analysis utilising the same SEM, XRD and density equipment detailed previously. A core of material was removed from the centre of each consolidated sample and subjected to density measurements. A section

of this core was hot mounted. Successively finer grit papers (500, 800 grit) ground each sample before diamond polishes (6, 3 μm) produced samples suitable for SEM. Each sample was carbon coated to prevent electron beam charging in the SEM. A further section of the original core was ground into fine powder for XRD analysis.

Of the three aliquots manufactured, one sample was shown to be representative of the complete set. For the sake of clarity, only one set of sample results is reported of the SEM and XRD analysis for each manufacturing technique.

3 Experimental

As each of the manufacturing techniques is different, it is clearer to report the detailed production method with the corresponding results.

3.1 Standard Route

The target formulation was $Ca_{0.75}Ce_{0.25}ZrTi_2O_7$. Cerium was supplied as the standard ceria powder; calcium, titanium and zirconium were provided from the premixed batch discussed in Chapter 2 (by mass fraction, 21.3 % CaO, 8.7 % ZrO_2 and 70.0 % TiO_2). ZrO_2 and TiO_2 powders provided the balance of zirconium and titanium, respectively. There was an additional 0.05 formula units of ZrO_2 and TiO_2 in an attempt to minimise deleterious secondary phase development (predominately perovskite).

Batches of 800 g (approximately 1 litre of loose powders) were milled with 1 wt% of oleic acid as the milling lubricant. Oleic acid was chosen based on its excellent performance in Chapter 2 (homogenous products, freely discharging powders from the mill). The same attrition mill and internal geometry as in Chapter 2, operating in the dry mode, was used. The powder batches were charged into the attrition mill whilst it was operating at 1.73 m s^{-1} (200 RPM). The mill was quickly brought to the desired speed of 4.32 m s^{-1} (500 RPM) and operated for 30 min, as this had been shown to produce the highest quality

products so far. The powders were discharged from the mill at the same operating speed as they were charged (1.73 m s^{-1}).

The first batch of material, after the addition of titanium metal powder, was split into three aliquots and each was packed into a separate HIP can. The cans were filled by the addition of loose powder, which was uniaxially compacted with a bench press at 5 tonnes of force. Further loose powders were added to the HIP can and the process was repeated until the cans had an approximate 1 cm gap at the top. This gap was filled with more loose powders but was not compacted; this was to allow room for the lid to fit snugly into the can. Each can contained approximately 140 g of material. The lids, including evacuation tube and a sintered metal filter, were autogenously welded to the HIP can. Each can was heated to 600 °C for 4 hours whilst a vacuum was drawn through the evacuation tube. Whilst this had been shown to be an inadequate method in Chapter 2 for the removal of lubricant, the intention was to produce a series of samples for direct comparison with those utilising a novel lubricant removal method.

The second batch of milled powders, after discharge from the mill, was calcined in air at 600 °C for 4 hours in a tube furnace. A 5 °C min^{-1} ramp rate was used for both heating and cooling. The intention was to show unequivocally that lubricant non-removal from a packed HIP can is at fault for the poor performance of the products in Chapter 2. The calcined powders were allowed to cool before adding the titanium metal powder. This material was packed into three HIP cans in the same method detailed earlier. Typically, 130 g of material was added to each can. As the HIP cans did not have any lubricant that required removal, it was thought that the cans would not require a full heating and evacuation step. Accordingly, the first can only underwent evacuation at room temperature for 5 minutes. This sample produced anomalous results, detailed later. The other two HIP cans underwent the full 600 °C heating cycle

under vacuum. All six packed HIP cans were HIP by the high temperature HIP cycle.

3.1.1 Density

Table 18 gives the measured densities of all six samples grouped by lubricant removal method. The first observation is that the samples consolidated from powders baked out *in-situ* have significantly lower densities, by up to 9.5 percentage points, than those with *ex-situ* lubricant removal. This result confirms that the failure to remove the lubricant is very detrimental to the consolidation process. It also suggests that it may never be possible to remove completely the lubricant from powders packed into the HIP even with the improved evacuation system. This will be a concern for an operating environment (see Chapter 7 for a discussion on the impact of this result) as such any candidate immobilisation plant must consider this requirement. The *in-situ* samples have densities broadly similar to the best performing product in Chapter 2 (*cf.* 87% TD for the sample manufactured from powders milled with zinc stearate for 30 min at 4.32 m s^{-1} in Chapter 2). The reduction in variability in the samples is likely to be due to the improved vacuum system. None of these samples attained the >92% TD target and, again, lubricant removal from a packed HIP can cannot be recommended for implementation in its current form.

The samples manufactured from loose powders calcined for lubricant removal show significantly improved densities to their in can lubricant removal counterparts. The density of the first sample (89.5% TD) is a result of a failure to evacuate completely the can (detailed earlier). This result is interesting in that it suggests the evacuation step is still important to remove entrained gasses and moisture from what would otherwise be considered clean dry powder. This implies that the ceramic waste immobilisation process will always require an evacuation step. Whether this includes heating of the packed HIP can or not remains to be clarified. The other two samples show that it is possible to use an attrition mill to prepare precursor preparation for the manufacture of samples

with high densities (~96% TD). The key consideration appears to be the removal of the lubricant.

Putting aside the incorrectly evacuated sample, the samples manufactured from calcined powders have a very low, essentially zero, level of variation in the product densities. Repeatability is an important aspect for a full-scale plant as it gives easier process control and confidence the wasteform will perform consistently as expected.

Lubricant Removal	Density (g cm^{-3})	Mean (g cm^{-3})	Standard Deviation (g cm^{-3})	% TD
In can	4.16 4.13 4.20	4.16	0.04	87.1 87.8 88.7
Calcined	4.24 4.58 4.58	4.47	0.20	89.5 96.6 96.6

Table 18: The densities of samples manufactured from attrition milled precursors. TD calculated as 4.74 g cm^{-3}

3.1.2 SEM AND XRD

Figure 53 shows a pair of SEM images of a typical 'In can' sample. There are numerous angular pores, consistent with the low percentage TD. There do not appear to be any obvious cerium grains (which would appear as bright white spots) showing good incorporation of the simulant. None of the attrition milled samples, consolidated by the high temperature (1320 °C) HIP cycle, reported so far, show any sign of unincorporated ceria. These positive results give a good confidence that the incorporation of cerium (as the plutonium surrogate) at 0.25 formula units is possible and repeatable. In the SEM images, there is a bulk phase of zirconolite, as targeted, while the dark grains are a perovskite phase ($CaTiO_3$) whilst the lighter grains are ZrO_2. The extra ZrO_2 and Ti rich phases are most likely a result of the additional 0.05 formula units added to the batch. Whilst the small size of these phases (<5 μm) makes EDS analysis inconclusive, there was no strong indication of cerium present. Thus, these extra phases do

appear to be serving as designed by ensuring the cerium partitions in to the zirconolite host phase.

Figure 54 shows two SEM images of the samples manufactured from powders milled at 4.32 m s^{-1} for 30 min with lubricant removal by calcination. The bulk phase is zirconolite, as designed, while the dark grains are titanium rich, possibly perovskite, and the lighter grains are zirconia. Both the 'in-can' and calcined samples are broadly similar in terms of phase development and shape of pores. In both samples, the pores are very angular. This is likely a result of grains impinging upon each other during growth. The sample shown in Figure 54 has fewer, yet larger, pores than the sample in Figure 53, which is consistent with the increased density of the sample manufactured from calcined powders.

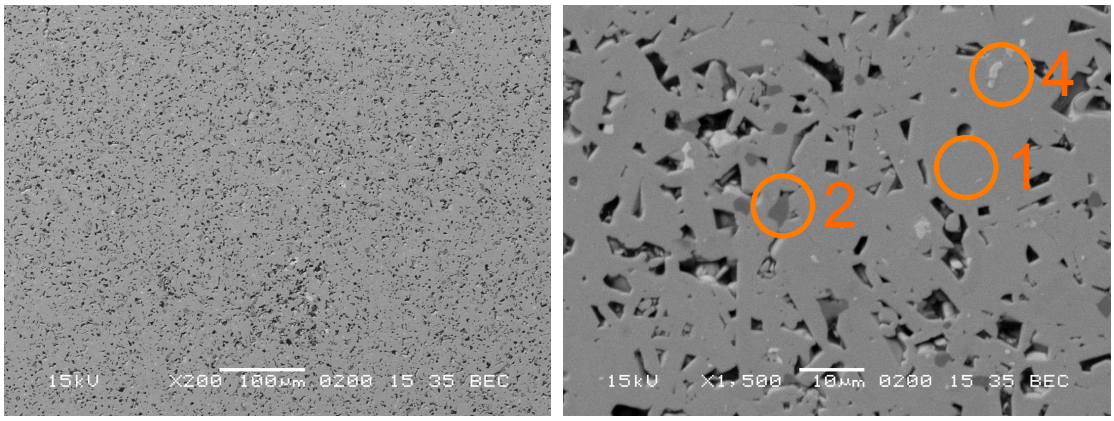

Figure 53: Samples manufactured from powders attrition milled at 4.32 m s-1 for 30 min. Lubricant removal from the HIP can. The left image is 200x magnification, and the right image, 1500x magnification. Phases: 1- zirconolite; 2- perovskite; 4- zirconia

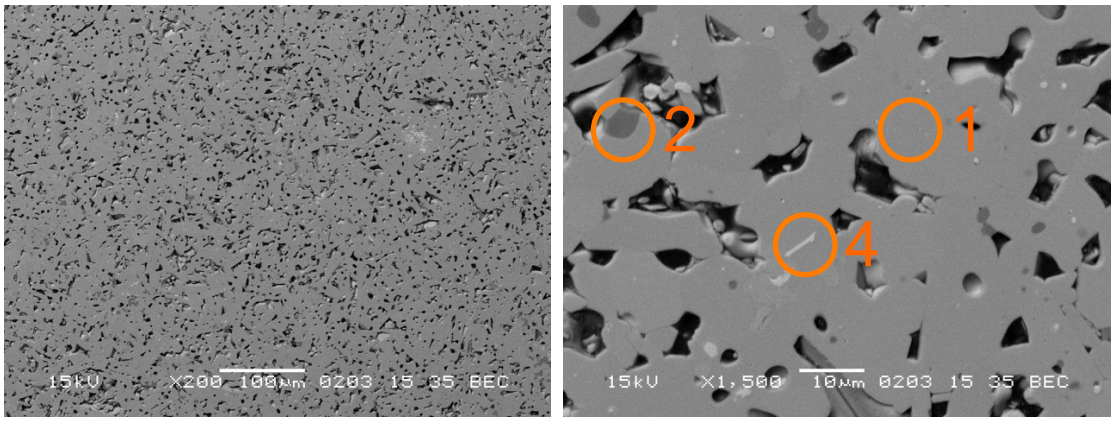

Figure 54: Samples manufactured from powders attrition milled at 4.32 m s-1 for 30 min with the lubricant removed by calcination of the loose powders. The left image is 200x magnification, and the right image, 1500x magnification. Phases: 1- zirconolite; 2- perovskite; 4- zirconia

Figure 55 shows the XRD patterns for the two samples. Both show zirconolite has formed; however, there is a difference in the polytype produced. The sample that was consolidated from powders that had the lubricant removed from the HIP can has formed zirconolite-3T, whilst the sample manufactured from calcined powders has formed the standard zirconolite-2M. It is possible that the change in polytype is due to a modified oxidation state of the cerium or titanium. Each of the different ions will have different radii leading to slightly different crystallographic orientations. This change in oxidation state is likely to be a result of the pyrolysis of the hydrocarbon lubricant producing carbon, which is highly reductive.

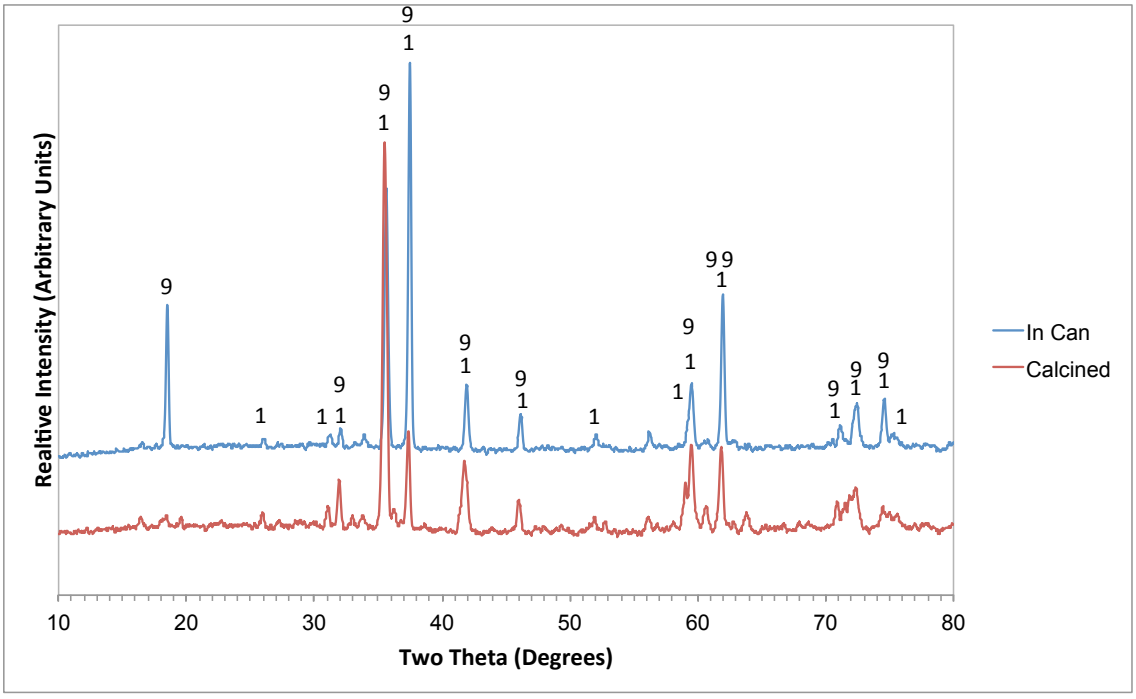

Figure 55: XRD patterns of samples manufactured from powders milled at 4.32 m s^{-1} for 30 min with oleic acid. 'In can' sample had the lubricant, nominally, removed whilst the powders were in the HIP can. The 'calcined' sample had the lubricant removed from the loose powders. Phases: 1- zirconolite-2M; 9- zirconolite-3T

3.1.3 Discussion

The difference in the density of the two samples confirms the need to remove the lubricant completely from the milled powders. It also confirms that this is possible at 600 °C. However, the act of packing the milled material into a constrained environment (i.e. a HIP can) clearly restricts the destruction and

removal of the hydrocarbon lubricants. It may be possible that, rather than the vaporisation of the lubricant, oxidation (combustion) is the main extraction method. This may explain why removal of the lubricant is not easy in the low oxygen environment of the HIP can. However, the temperature of the furnace is far above the boiling point of the lubricant and this should allow the lubricant to escape through vaporisation. Regardless, there is clear evidence that if a lubricant is used in an attrition mill, it must be removed before the milled powders are packed in to HIP cans.

The samples manufactured from attrition milled powders that were calcined for lubricant removal had densities above the 92 % of theoretical density target (actual average density ~97% TD). These samples confirm that an attrition mill is a suitable piece of equipment for the manufacture of zirconolite ceramics. Noting that the sample that only underwent brief evacuation had a much reduced density than its counterparts, shows that a full evacuation stage must always be included in the HIP can fill process. The indication is that this evacuation step is required not only to remove milling additions but also to remove any entrained gas from the powders, as well as some moisture.

The SEM images do not show any unincorporated ceria and this is a positive result as it suggests that the PuO_2 feed would incorporate into the zirconolite wasteform. The XRD patterns have shown that different polytypes of the zirconolite host phase are formed depending on the powder heat treatment before consolidation. It is not currently known why but analysis of the cerium oxidation state by XANES (X-ray Absorption Near Edge Structure) may be illustrative.

3.2 As Purchased Materials

The particle size and level of mixing of precursors is a consistent theme in the manufacture of ceramics. Attrition milling of materials will reduce the size of the precursors but the degree of size reduction is variable and dependant on a number of factors. Purchasing the same precursors (e.g. TiO_2, ZrO_2 CaO, CeO_2)

in manufacturer defined particle sizes is possible. Based on availability, three different orders of magnitude particle sizes were chosen; 1 μm, 0.1 μm, 0.01 μm. The particular forms of the materials chosen for each batch are given in Table 19.

Each of the three size batches underwent the same preparation. Stoichiometric quantities (target formulation $Ca_{0.75}Ce_{0.25}ZrTi_2O_7$, cerium as the plutonium surrogate and charge compensation provided by Ti metal, added later) of the precursors were added into a ~3 litre stainless steel beaker containing ~1 litre of warm (~50 °C) propanol. A hot plate and an overhead stirrer, respectively, provided heating and agitation. If colloids were used, they were added in amounts that accounted for the carrier fluid and stabilising components. Precursors supplied as nitrates (calcium, cerium) were dissolved in excess deionised water first. Each batch was reduced in volume until a thick slurry was produced. The choice when to stop volume reduction was an operational one as beyond a certain threshold temperature and solids content, the slurry would become impossible to handle safely (as the slurry became thicker and heat transfer reduced, small pockets of liquid would become vapour and cause small boiling liquid expanding vapour explosions).

The slurry was transferred to two broad stainless steel bowls. The mixtures were left in an oven overnight at 120 °C with the intention of removing all the carrier liquids. As the slurry was drying, a layer of dry material would form on the surface. This was broken up and returned to the mixture where possible. The resultant solids were in the form of a brittle cake. This cake was broken up by hand and all the material underwent coarse size reduction by pestle and mortar.

The precursor mixture underwent calcination at 750 °C for 8 hours. The intention was to denitrate the material whilst stabilising the now liberated CaO into $CaTiO_3$. The temperature was chosen as being sufficiently high to bring about the denitration of the components whilst not significantly increasing the particle size of the material. The calcined powders were planetary milled at 400

RPM for 20 min. The intention was to remove any final coarse grains and to ensure complete mixing of the precursors. Before the material was packed into three HIP cans, utilising the method discussed earlier, 2.2 wt% of titanium metal powder was added to provide charge compensation in the final product. Each of the HIP cans underwent evacuation by the addition of a vacuum line to the lid of the can for four hours, whilst the can was maintained at 600 °C. The packed HIP cans underwent the high temperature HIP cycle (1320 °C for 2 hours and 100 MPa argon pressure).

As stated, the intention was to purchase materials within an order of magnitude. Often it was not possible to obtain the exact particle size required. In these cases, the nearest available material was chosen (e.g. CeO_2 in the ~1 μm batch). Dry powders were chosen in preference to colloids; however, this was not always possible.

Order of Magnitude Size Range (μm)	Component	Form	Manufacturer Stated Particle Size
1	CaO	Nitrate Tetrahydrate $Ca(NO_3)_2.4H_2O$	N/A (in solution)
	CeO_2	Dry powder	5 μm
	TiO_2	Dry powder	0.9 - 1.6 μm
	ZrO_2	Dry powder	1 μm
0.1	CaO	Nitrate Tetrahydrate $Ca(NO_3)_2.4H_2O$	N/A (in solution)
	CeO_2	Dry powder	0.07 – 0.105 μm
	TiO_2	Dry powder	0.01 μm
	ZrO_2	20 wt% Colloid	0.1 μm
0.01	CaO	Nitrate Tetrahydrate $Ca(NO_3)_2.4H_2O$	N/A (in solution)
	CeO_2	20 wt% Colloid	0.01 – 0.02 μm
	TiO_2	Dry powder	0.01 μm
	ZrO_2	20 wt% Colloid	0.005 – 0.01 μm

Table 19: Form of the various as-purchased different particle sized materials.

Each of the batches of powders packed in differing amounts into the HIP cans. This is a function of the particle size of the material as well as the particle size distribution. A range of particle sizes should allow a greater packing density than monodisperse powders. Table 20 gives the average HIP can contents for each nominal particle size.

Nominal Particle Size (μm)	Average HIP Can contents (g)
1	80
0.1	115
0.01	87

Table 20: Average packed HIP can contents for each nominal particle size.

3.2.1 Density

Table 21 gives the densities of the samples grouped by nominal particle size. All of the samples have excellent densities, well in excess of the 92% TD target. The sample with the lowest density was made from powders with a particle size in the order of 0.01 μm (97% TD) whilst the highest density samples are found in both the 1 and 0.1 μm batches (98.5% TD). Also of note is the excellent repeatability of all the samples with typical standard deviations of 0.01 g cm^{-3}.

Based only on the density of the product ceramics, any of these techniques can be recommended for implementation. However, as has been stated in the design philosophy (Chapter 1), no wet systems are allowable in the relevant active environment due to both criticality concerns and the desire to minimise secondary effluents. The positive outcomes of this work suggest that if milling is sufficiently aggressive enough to reduce the precursors to the order of 1 μm, high quality products can be manufactured. It also suggests that further size reduction may be unnecessary or even counter productive as there does not appear to be a significant improvement in product density with smaller particle sized material.

Order of Particle Size	Density (g cm^{-3})	Mean (g cm^{-3})	Standard Deviation (g cm^{-3})	% TD
1 µm	4.66 4.67 4.65	4.66	0.01	98.0 98.4 98.5
0.1 µm	4.67 4.67 4.66	4.67	0.00	98.4 98.5 98.5
0.01 µm	4.62 4.60 4.64	4.62	0.02	97.0 97.5 98.0

Table 21: Density of samples manufactured from the various manufacturer defined as-purchased precursors

3.2.2 SEM AND XRD

Figure 56 shows an example SEM image of the sample manufactured from material with a particle size of broadly 1 µm. The initial impression is that this is a high quality ceramic. The sample is homogenous in terms of microstructure and composition. There are few pores, which is consistent with a 98% TD sample. The largest pores are <5 µm and the majority are <1 µm. On the higher magnification image, a few small specs of a lighter coloured material are visible (marked, above the '0209' label). EDS analysis was inconclusive due to the small size of the grains however it did suggest the area was zirconium rich, potentially indicating that the grains are ZrO_2. The higher magnification image does show some localised variation in composition between the grains: these variations are minor and will not significantly affect the wasteform properties.

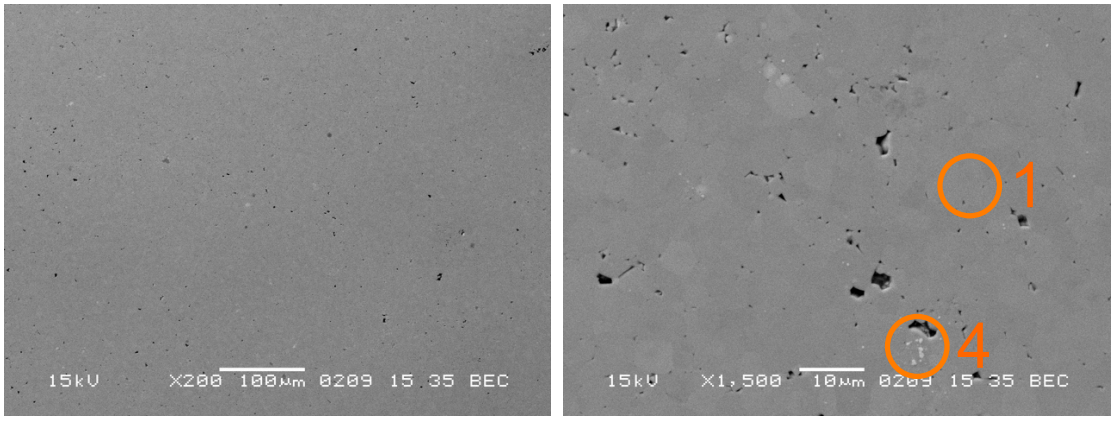

Figure 56: SEM images of samples manufactured from materials purchased of approximately 1 µm. Left image 200x magnification, right image, 1500x magnification. Phases: 1- zirconolite; 4- zirconia

Figure 57 shows an example SEM image from the samples manufactured from precursors with a particle size of approximately 0.1 μm. These samples are not homogenous in terms of sample composition. The large dark grains are titanium metal relics, present as a source of electrons for charge compensation in the product, and were expected in the sample (these grains are not visible in Figure 56 due to the area shown, yet they were present in the sample). However, the large number of lighter coloured grains was unexpected. EDS analysis confirmed that these grains are zirconium rich, potentially zirconia. As the ZrO_2 was provided was as a 0.1 μm colloid and these grains are up to 3 μm, some form of agglomeration must have occurred. During preparation, the partially volume reduced mixture was allowed to stand over the weekend. It is thought that during the initial evaporation step, the colloid stabiliser (acetic acid) was removed or denatured allowing the fine particles to agglomerate whilst standing. These agglomerates remain throughout preparation without being discovered until after consolidation. Full incorporation of the ZrO_2 is preferable, however it does not appear to have overtly affected the phase development of the zirconolite host phase (cerium may substitute on to the zirconium site in the zirconolite structure), which the XRD pattern confirms. There are no significant signs of porosity with the largest visible pore in the zirconolite host phase as <1 μm. There are regions of porosity within the titanium metal relics. These are a result of either of the oxygen scavenging behaviour of the metal or through differential thermal expansion and contraction during processing.

Figure 58 shows example SEM images from the samples manufactured from precursors of approximately 0.01 μm. The sample is homogenous in terms of overall phase development, with due regard to the Ti metal relics and the minor variation in composition between zirconolite grains. There are numerous, but small <2 μm, pores and this is consistent with the ~98% TD recorded.

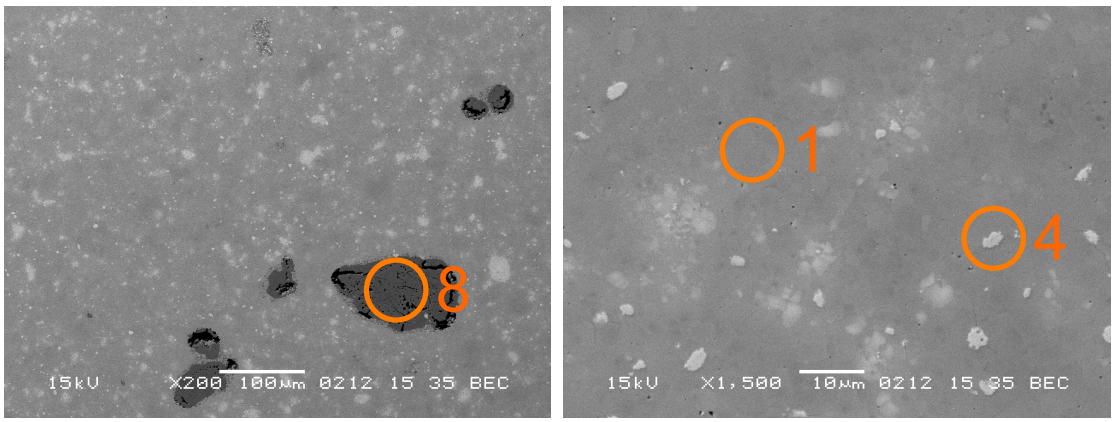

Figure 57: SEM images of samples manufactured from materials purchased of approximately 0.1 µm. Left image 200x magnification, right image, 1500x magnification. Phases: 1- zirconolite; 4- zirconia; 8- Ti metal relic

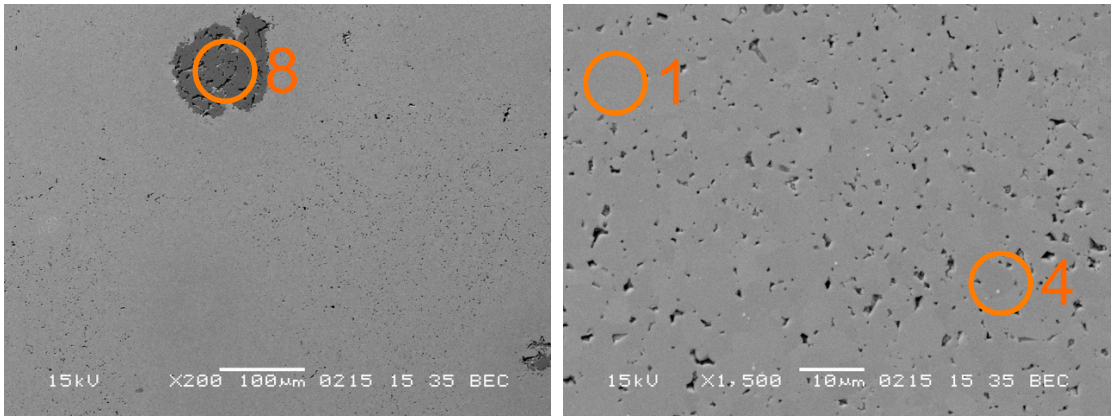

Figure 58: SEM images of samples manufactured from materials purchased of approximately 0.01 µm. Left image 200x magnification, right image, 1500x magnification. Phases: 1- zirconolite; 4- zirconia; 8- Ti metal relic

Figure 59 shows the XRD patterns for the three different samples. The particle size of the precursors does not appear to affect the phase development, as all three samples are zirconolite-2M. There is a slight difference between the sample made from 0.1 µm precursors and the 1 and 0.01 µm samples, in that the double peak at $2\theta \approx 59°$ is absent. It is likely that the zirconia minor phase makes the ceramic slightly less homogenous (i.e. there are two phases) and this is reducing the intensity of the zirconolite reflections. All three samples show the same zirconolite phase development as the sample manufactured from calcined attrition milled powders.

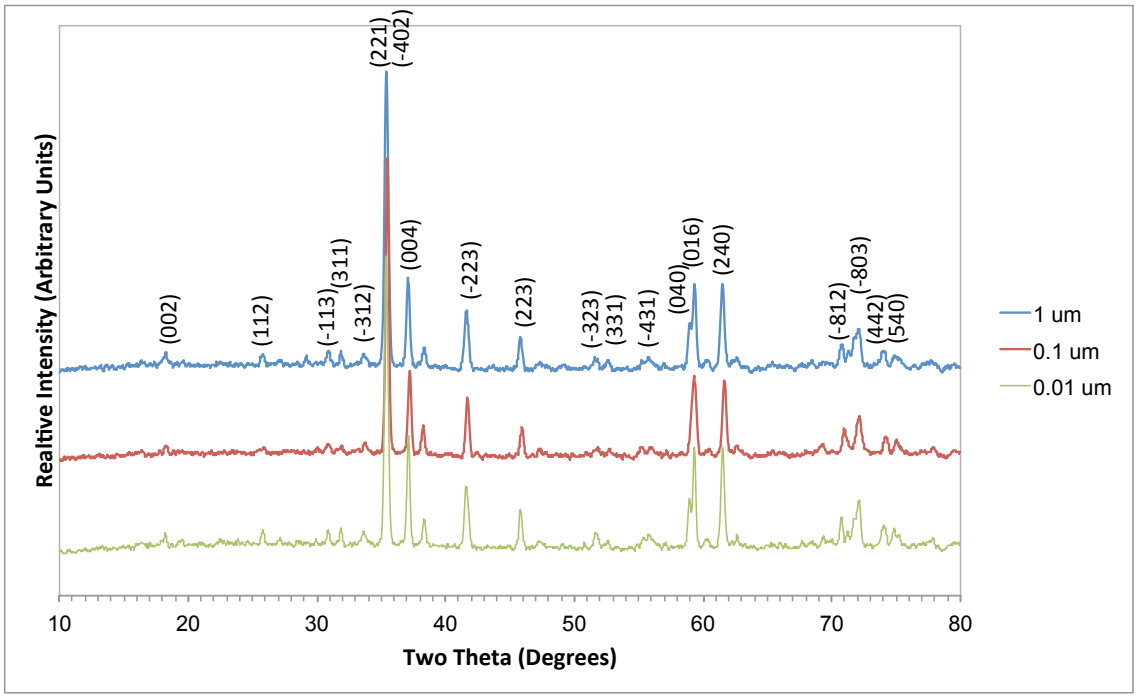

Figure 59: XRD patterns for samples manufactured from various manufacturer defined particle sizes. Miller indices of zirconolite-2M phase labelled.

3.2.3 Discussion

All of the analysis has shown these ceramics to be excellent quality in terms of phase development, density, level of porosity and microstructure. All of the samples achieved the 92% TD target with the samples manufactured from approximately 0.1 µm precursors having the highest density. SEM analysis of this sample did show a large number of small zirconium rich grains present and it is thought that these may have aided the high density. ZrO_2 has a density of 5.68 g cm^{-3} and these inclusions may be artificially raising the overall density of the sample. Conversely, these samples did have the smallest proportions of visible pores on the sample surface, which is also a good indication of a high density samples. One further explanation of the reason for these high density samples is the substantially higher HIP can packing density. Noting in Table 20, the samples made from nominally 0.1 µm powders contained ~40% more material than either of the 1 or 0.01 µm HIP cans.

The minor variations in the properties of the products (density, level of porosity, microstructure) are mostly like due to minor variation in the manufacturing

techniques. There does not appear to be any explicit correlation between the particle size and the final product; all of the samples are dense and homogenous. As mentioned, a high quality ceramic is manufactured from correctly sized and well mixed precursors; the use of a carrier fluid to mix the starting materials allows full homogenisation. Unfortunately, the method utilised in this section of work cannot be recommended for implementation. The use of a protonated solvent is unacceptable for critically concerns, the whole process manufactures large amounts of secondary effluents, and the PuO_2 will not be in the forms utilised. However, this work has shown that if the all of the starting materials are of a broadly similar particle size and are well mixed then high quality zirconolite ceramics can be manufactured. This may be achievable by size reducing the PuO_2 feed before mixing with the precursors. Homogenisation may be achieved by attrition milling. A form of this concept is tested later in this work.

3.3 Alkoxide/Nitrate

Metal alkoxides are commonly used for the manufacture of high quality Synroc samples (Ringwood, Kesson et al. 1988). Alkoxides allow the intimate, almost on the atomistic level, mixing of very fine precursors. Alkoxides, generically of the form $M_x(OR)_y$ (x and y may be different) where M is a metal ion and R is an organic chain, allow the dissolution of metal ions into an alcohol solvent. Upon the addition of water, the alkoxide rapidly hydrolyses forming a fine metal oxide precipitate. The hydrolysis of titanium isopropoxide is given, for example, below. The attraction of this method is in the ability to mix the precursors as liquids before the formation of the fine metal oxide powders.

$$Ti(OCH(CH_2)_4)_{(l)} + 2H_2O_{(l)} \rightarrow TiO_{2\,(s)} + 4(CH_3)_2CHOH_{(l)}$$

Starting materials were chosen based on availability and cost. Table 22 gives the source and composition of each of the precursor components. The nitrate forms of calcium and cerium were chosen due the inability to source suitable alkoxide versions. However, as the nitrates are soluble in both water and alcohol they

can be utilised to form the fine well mixed precursors required. Cerium is provided in the Ce^{3+} oxidation state rather than the usual Ce^{4+} (from CeO_2). During the subsequent heat treatments, the Ce^{3+} will oxidise to Ce^{4+} required.

Component	Source	Composition
CaO	Nitrate tetrahydrate	$Ca(NO_3)_2.4H_2O$
CeO_2	Nitrate hexahydrate	$Ce(NO_3)_3.6H_2O$
TiO_2	Propoxide	$Ti[OCH(CH_3)_2]_4$
ZrO_2	Propoxide	$Zr[OCH(CH_3)_2]_4$

Table 22: Sources of various precursors for alkoxide route samples

The samples were prepared in a similar method to the various as purchased particle sized powder batches mentioned earlier. Utilising the same apparatus as previously, stoichiometric quantities of the alkoxide components were added to a stainless steel beaker containing ~1 litre of warmed propanol (~50 °C). The mixture was agitated, with heating, for approximately 20 min. In a separate beaker, the minimum amount of deionised water required for complete dissolution was added to stoichiometric quantities of the dry nitrate powders. Agitation of the alkoxide fluids was increased to the maximum practical level. The nitrates solution was added quickly to the alkoxide and propanol solution. Rapid hydrolysis of the alkoxide occurred and this new mixture was further agitated with heating, with intention of reducing the amount of propanol, for 4 hours. At this point, the slurry had become too viscous to stir. This slurry was dried overnight at 120 °C after being transferred to two shallow stainless steel dishes. The resulting cake of dried material was broken up by hand before a further coarse size reductions step (pestle and mortar). The fine powders were calcined at 750 °C for 8 hours in order to decompose fully the nitrates and to stabilise the calcium as $CaTiO_3$. The mixture was planetary milled at 400 RPM for 20 min to ensure that no coarse agglomerate remained and that the mixture was fully homogenous. For charge compensation, 2.2 wt% of Ti metal powder was added before this complete set of precursors was packed in to three HIP cans, utilising the standard packing procedure. The HIP cans were evacuated

under vacuum whilst heated to 600 °C. Each can typically contained 88 g of material. The powders underwent consolidation by the high temperature HIP cycle (1320 °C for 2 hours with 100 MPa pressure).

3.3.1 Density

Table 23 gives the measured densities of the three samples manufactured from alkoxide precursors. All three samples have excellent densities at approximately 98% TD. Again, the standard deviation across the samples is low at 0.01 g cm^{-3} and shows good repeatability. These alkoxide derived samples have similar densities to all of the various as purchased particle sized precursors reported earlier. From a density point of view, all of these ceramics are of excellent quality.

Sample	Density (g cm^{-3})	Mean (g cm^{-3})	Standard Deviation (g cm^{-3})	% TD
Alkoxide	4.64 4.65 4.64	4.64	0.01	98.0 98.2 97.8

Table 23: Measured densities of samples manufactured by the alkoxide route.

3.3.2 SEM and XRD

Figure 60 shows example SEM images from the samples manufactured from the alkoxide derived precursors. The large dark grey areas on the left hand images are relics of the titanium metal powder added for charge compensation. Otherwise, the sample appears homogenous in terms of microstructure and phase development. There are minor local variations observable between grains; however, as discussed earlier these are of little concern. All of the observable pores are sub micron in size and appear to be uniformly distributed throughout the sample. The low level of porosity is consistent with the samples having a high percentage of theoretical density.

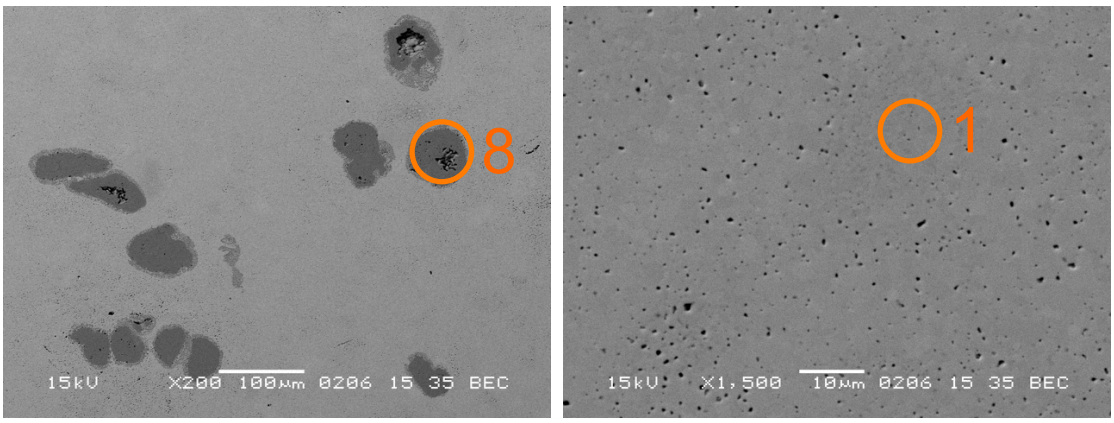

Figure 60: SEM images of samples manufactured from materials derived from alkoxides. Left image 200x magnification, right image, 1500x magnification. Phases: 1- zirconolite; 8- Ti metal relic

Figure 61 gives the XRD pattern for the samples manufactured from the alkoxide derived precursors. The pattern clearly identifies that the zirconolite-2M phase has formed. It is also noted that the FWHM of the peaks is small indicating there is tight control over localised compositional variations in the product.

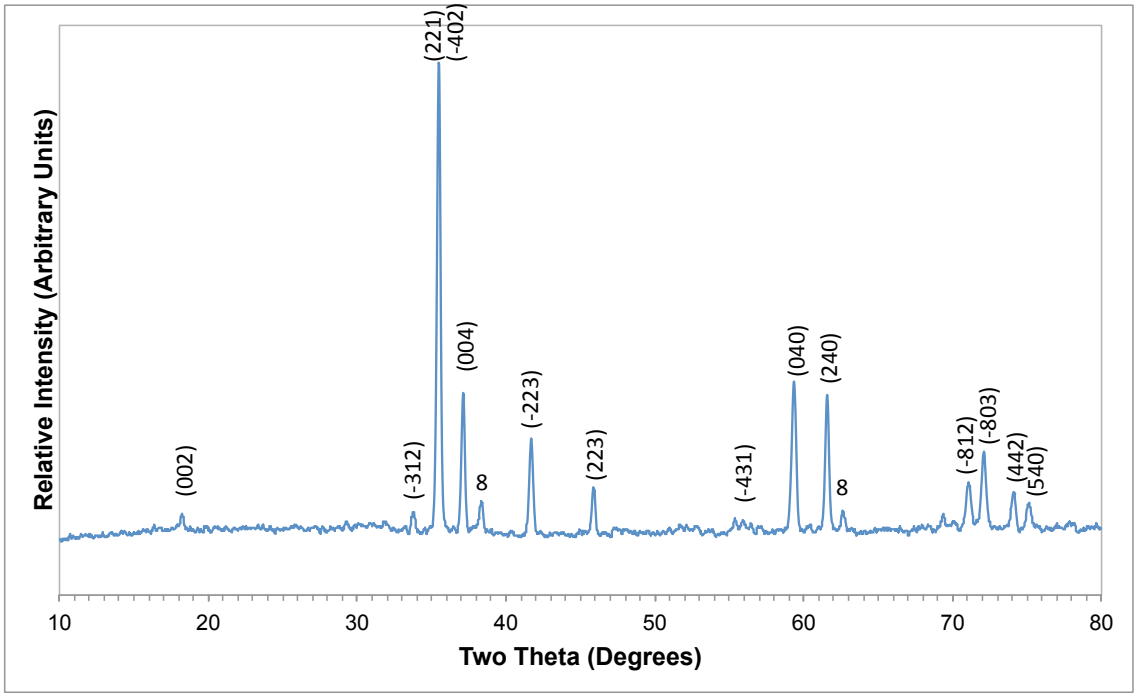

Figure 61: XRD pattern for samples manufactured from alkoxide derived precursors. Phases: Miller Indices- zirconolite; 8- Ti metal relic

3.3.3 Discussion

As expected, the samples manufactured from alkoxide derived precursors are excellent in terms of microstructure development and product density. The almost atomistic level of mixing has allowed the single phase zirconolite to develop as expected. Sample densities of ~98% are excellent and indicate that a high quality ceramic has been manufactured. Unfortunately, this method of manufacture cannot be recommended due to the generation of secondary effluents, use of protonated solvents and that the plutonium source will not be in the nitrate form.

3.4 Additional Samples

Whilst the methods discussed in this chapter so far have produced high quality ceramics, none of them can be considered for implementation in the relevant environment. This is typically due to each process using a solvent. However, it will be possible to produce the inactive precursors without the restrictions imposed by manufacturing in an active environment. In this scenario, it would be possible to manufacture precursors (titanium, calcium, zirconium source) with a fine particle size and these materials would be milled with the PuO_2 in a further processing step in the active environment. The intention is to minimise the complexity of all processes carried out in an active environment. To test this concept, precursors manufactured from the nominal 0.01 μm batch were mixed by hand (a spatula and mixing bowl) with the 'realistic' ceria. These powders, with the additional titanium metal, were packed into three HIP cans and underwent HIP at the standard high temperature HIP cycle (1320 °C for 2 hours at 100 MPa of argon pressure).

One further sample was manufactured from the same precursors (limited due to amount of materials remaining) except that after the addition of the 'realistic' ceria, the mixture underwent planetary milling at 400 RPM for 60 min with propanol as the carrier fluid. The intention was to manufacture a high quality ceramic with the 'realistic' ceria simulant.

3.4.1 Density

Table 24 gives the measured densities of the four additional samples. The samples manufactured from the nominally 0.01 μm precursors and hand mixed with the 'realistic' ceria simulant are all greater than the 92 % TD target (mean 97% TD). They are less dense that the samples made from all 0.01 μm powders (97.5% TD) but only marginally so. In Chapters 2 and 3, it was consistently shown that products with manufactured with the 'realistic' simulant had lower densities than their counterparts manufactured with the standard ceria. The sample that was manufactured from planetary milled powders has a comparable density to the other 0.01 μm samples. It appears the extensive milling does not significantly increase the density of the ceramic. In addition, the planetary milled sample is comparable to the highest density of the attrition milled samples (96.6 against 96.7% TD).

Sample	Density ($g\ cm^{-3}$)	Mean ($g\ cm^{-3}$)	Standard Deviation ($g\ cm^{-3}$)	% TD
'Realistic' Ceria	4.62 4.62 4.57	4.60	0.03	97.4 97.5 96.3
Planetary Milled	4.58			96.7

Table 24: Measured densities of the additional samples

3.4.2 SEM and XRD

Figure 62 shows an example SEM image of the samples manufactured from nominally 0.01 μm powders and 'realistic ceria'. It is immediately clear that these samples are not homogenous. The Ti metal powder relics are present as before yet there are also a number of bright white areas. These have been identified by EDS analysis as cerium rich, likely to be ceria. These grains are unincorporated material that has not become part of the host phase and this will be an issue for product durability. In the higher magnification image it is shown that around each of the cerium rich cores there are two reaction zones. In these reaction zones, there are changes in the proportions present of all of the precursor components. Notably, the bulk phase does not contain any cerium.

This emphasizes the requirement of intimate mixing of the precursors and waste feeds. Quantitative phase analysis by EDS was not possible but general identification of the composition of each phase is. Working from the centre of the ceria inclusion: ceria (CeO_2); second shell, $(Ti,Ce)O_x$ (potentially a form of cerium substituted brannerite (e.g. $CeTi_2O_6$) or cerium substituted perovskite ($Ce_{2/3}TiO_3$); first shell, $(Ca,Zr,Ti,Ce)O_x$ (another zirconolite, potentially the 4M polytype); bulk, $(Ca,Zr,Ti)O_x$ (most likely zirconolite). An ANSTO report by Stewart et al (Stewart, Day et al. 2005) discusses the formation of reaction zones around coarse actinide particles. They identify the phases, from centre of the inclusion outwards, as ceria, brannerite, pyrochlore and zirconolite, which are similar to those observed in this work. The other light grey areas in the lower magnification have equivalent composition to the first and second shells. They have either formed around a smaller, and so fully digested, ceria inclusion or are an artefact of the sample being cut and prepared (i.e. off-centre sectioning). This may indicate that there is a maximum size of ceria particle that can be digested in this system. Examining the width of the reaction phases it can be suggested that this maximum is approximately a particle diameter of 20 μm. This size assumes that for full incorporation, the ceria will form the same phases identified and that the size of the reaction zone is a maximum thickness. Throughout the remainder of the sample, the boundary layers tend to be a constant 4-5 μm thick and when the same phases exist without a ceria core, they are 8-10 μm in diameter. Otherwise, the sample has a low porosity with a few large pores forming at the interface between the ceria grain and the first transition layer. These could be a result of differential thermal expansion, the preferential digestion of the corners, or auto reduction of the CeO_2 to Ce_2O_3 evolving O_2 in the process.

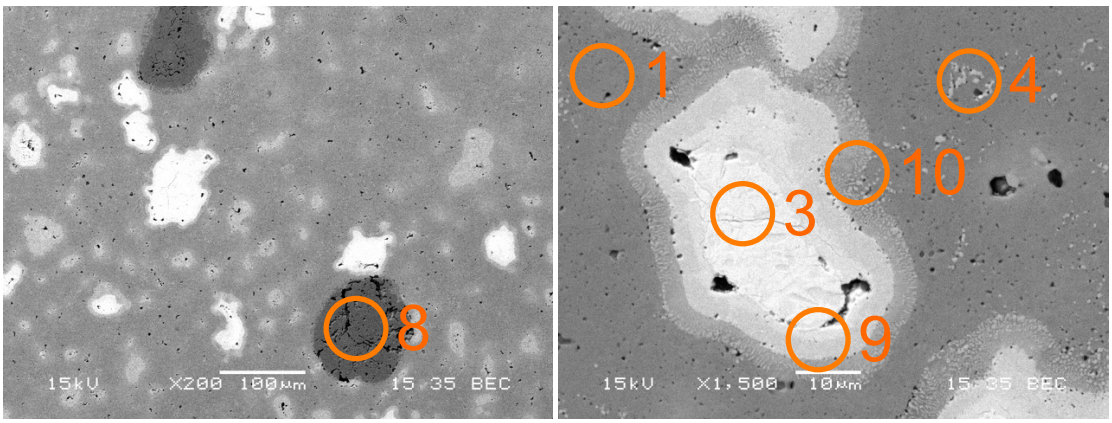

Figure 62: SEM images of samples manufactured from materials purchased of approximately 0.01 µm and lightly mixed with the 'realistic' ceria simulant. Left image 200x magnification, right image, 1500x magnification. Phases identified as: 1- zirconolite; 3- ceria; 4- zirconia; 8- Ti metal relic; 9- reaction phase 1 (Ce, Ti rich potentially a brannerite); 10 – reaction phase 2 (Ca, Zr, Ti and Ce – a form of zirconolite)

Figure 63 shows the elemental maps of an area of the sample manufactured from nominally 0.01 µm precursors and hand mixed with the 'realistic' ceria simulant. In these images, the more orange/yellow the colour the higher the proportion of the element is in that area of the sample. From these images, it is clear that the cerium and titanium are highly concentrated in their respective relics: as expected. The first transitional phase, marked 9, contains cerium and titanium, whilst the second, marked 10, contains calcium, zirconium, titanium and cerium. Also of note are the particles of slightly increased concentrations of zirconium throughout the sample. Comparing with the backscattered electron image, these areas are possibly unreacted ZrO_2. The small calcium hot spots seem to be associated with some of the visible pores. It is currently unknown why calcium would accumulate near the pores or, conversely, why the pores would localise to the calcium rich phase.

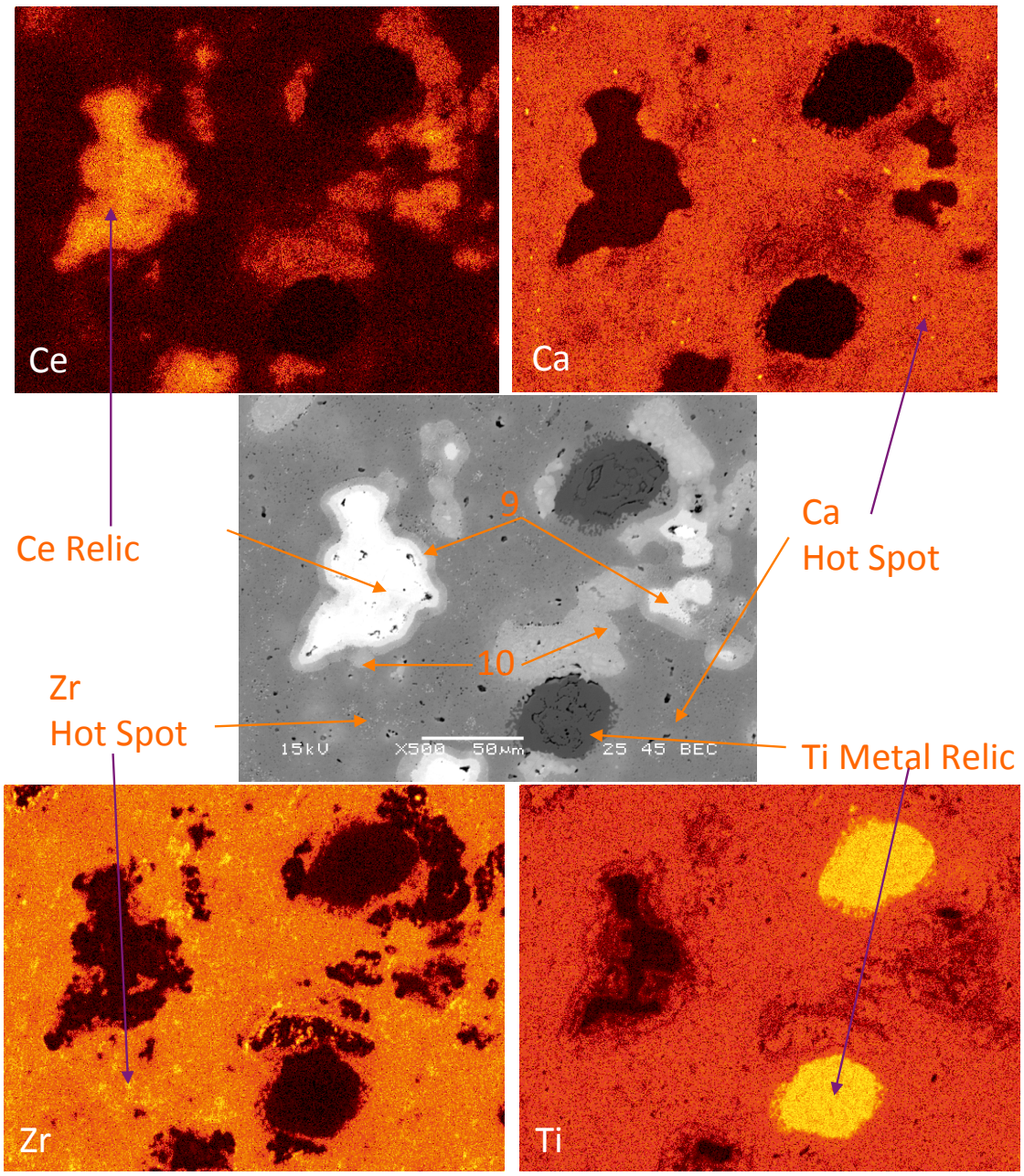

Figure 63: Elemental mapping of the sample manufactured from nominally 0.01 µm precursors and the 'realistic' ceria simulant. Centre image is a backscattered electron image at 500x magnification taken with a working distance of 25 mm, accelerating voltage of 15 kV and a spot size of 45 (change in beam conditions intended to improve the number of electrons returned from the sample at the cost of resolution). Colour of image is directly proportional to number of atoms of each element in specific location. Black is an absence of the element while yellow is a high concentration.

Figure 64 shows example SEM images of the sample manufactured from the nominally 0.01 µm precursors planetary milled with the 'realistic' ceria simulant. Putting aside the Ti metal powders relics, the sample is otherwise homogenous in respect to phase composition. This is in direct contrast to the non-planetary milled sample, Figure 62. There are no obvious unincorporated

ceria grains in the planetary milled sample. Comparing to the attrition milled sample, Figure 54, the size and shape of the pores are different. Pores from the attrition milled sample tended to be angular and larger whereas those from the planetary milled sample are smaller, round and more numerous. It is likely that the change in pore shape is due to the smaller particle size of the precursors in the planetary milled sample. The change between the planetary milled and the lightly mixed sample clearly shows that aggressive milling improves the phase homogeneity of the product. This is likely to be a result of the size reduction of the ceria grains.

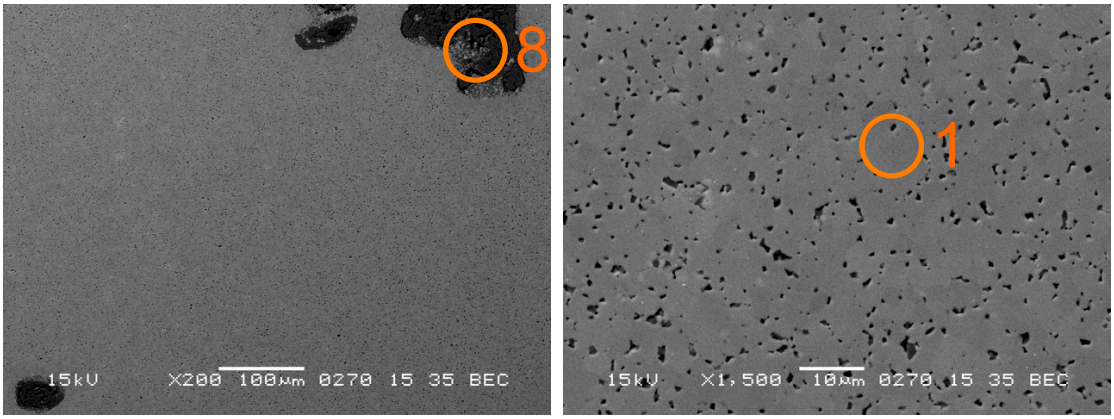

Figure 64: SEM images of samples manufactured from materials purchased of approximately 0.01 µm and planetary milled with the 'realistic' ceria simulant. Left image 200x magnification, right image, 1500x magnification. Phases labelled: 1, zirconolite; 8, Ti metal

Figure 65 shows the XRD patterns for the two samples manufactured with the 'realistic' ceria. Again, the patterns show that zirconolite-2M, is the major phase and there is the minor Ti metal relic phase, in agreement with the SEM images. The hand-mixed sample does show an increased signal attributable to ceria (main peaks marked with 3, at $2\theta \approx 34$ and 56°), which corresponds to the large ceria inclusions identified previously. However, the reaction phases could not be identified in the XRD patterns; this is due to the low volume per cent of the phases in the overall sample. It may also be that each of the transitional phases is a version of the main phases and thus masked by these (i.e. 9 is a brannerite and 10 is a zirconolite). The overlap between these pairs of phases is also an

explanation for the larger FWHM of the signal of the hand mixed sample than the planetary milled sample.

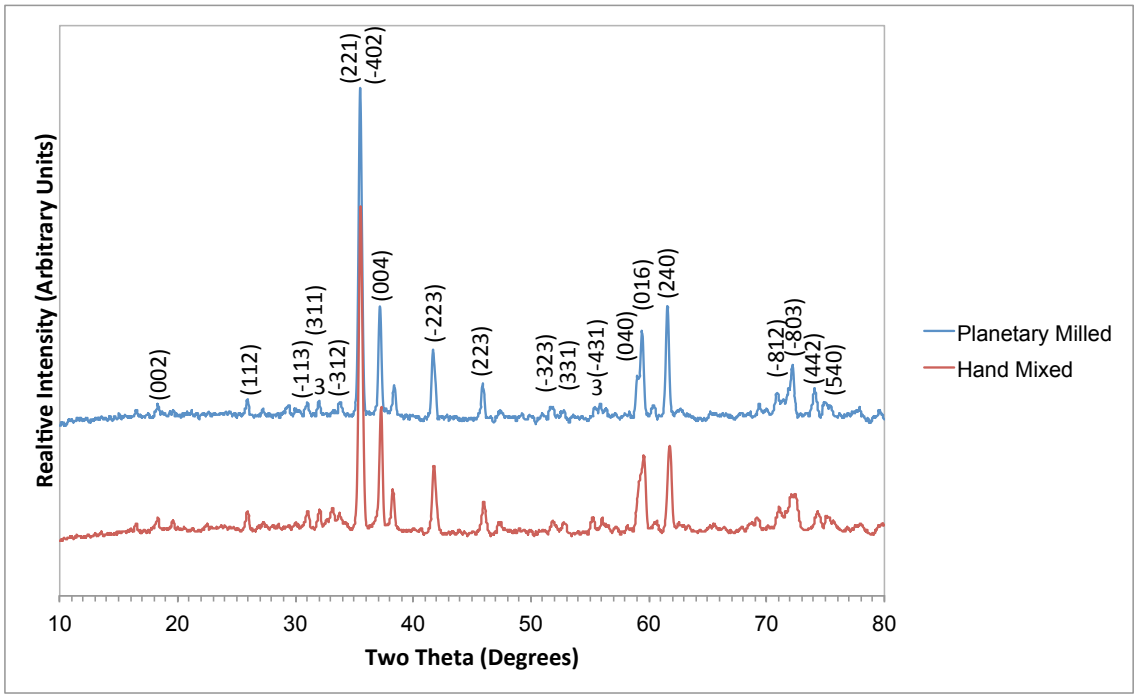

Figure 65: XRD patterns of the samples manufactured from the nominal 0.01 µm precursors and either hand mixed or planetary milled with the realistic ceria. Zirconolite main phase identified with Miller indices and ceria with 3.

3.4.3 Discussion

It is clear that hand mixing of the precursors and the 'realistic' ceria did not produce ceramics of a suitably homogenous phase development. The appearance of the reaction phases implies that there was some digestion and incorporation of the cerium; however, this was not enough to incorporate the simulant fully. It is reasonable to suggest that the diffusional driving force for the cerium was too great to be overcome at the HIP conditions. Observation of the reaction phases noted that each of the layers was approximately 8-10 µm implying that any cerium particles smaller than this would be incorporated. It should be noted that the first transition region, 9, was either a brannerite or perovskite and not the target zirconolite. Further work may seek to identify the maximum sized ceria grain that can be incorporated after light mixing in a bowl. It may be possible to size reduce the ceria (or ultimately PuO_2) to below this limit before mixing. This has the advantage of reducing the size of any mill

required, as there would be less material to be processed (i.e. the Ce/PuO_2 rather than all of the precursors). It may be possible to utilise a Turbula mixer to homogenise the feed and precursors. A higher temperature or longer duration HIP cycle may be required for the coarse feed to be fully incorporated.

There are clear and obvious improvements in phase homogeneity in the planetary milled sample. The extra energy imparted into the powders will have size reduced the ceria and intimately mixed it with the precursors. The smaller particle size and greater mixing reduces the diffusional length the cerium atoms must travel before being incorporated into the host matrix. This sample had a similar density to the best attrition milled products (96.6 and 96.7% TD). Typically, ceramics manufactured with the 'realistic' ceria had lower densities than their counterparts made with the normal ceria; this has not been observed in this work. The increased duration (from 30 to 60 min) is a key difference. As had been shown in Chapter 3, an increased milling duration does increase the product density.

4 Discussion

The vast majority of the samples manufactured in this work were of suitable density (greater than 92% TD). The attrition milled samples with in can bake out had the lowest density at an average of 87.9% TD and were the only samples that did not meet the required density specification. All of the other manufacturing techniques detailed in this chapter produced suitable density products. The excellent repeatability within each manufacturing techniques confirms that variations in product quality will come from the feed processing stages rather than during the HIP cycle. It also shows that the minor variations in HIP can packing density do not overtly affect the final product properties.

The samples manufactured from calcined attrition milled powders produced high density and single host phase ceramics. This was not shown in Chapter 2 and this evidence demonstrates that the failure to remove the lubricant from the

HIP cans was to blame for the poor product quality previously. This is especially so when the calcined samples are compared to those baked out *in-situ* in this work. The improvement in density was by eight percentage points. This calcination stage was appropriate for an inactive operation; however, it may not be so for full scale active implementation. It is known that the plutonium finishing operations on the Sellafield site utilise screw fed calciners for both the drying and decomposition of the oxalate slurry and for modification of the PuO_2 powder surface area (Sellafield Ltd. 2007). These calciners have gas flowing through. With minimal modification it may be possible to utilise an oxidising gas (e.g. dry air) to be passed through the milled powders. This gas would oxidise (combust) the hydrocarbon lubricants, fully removing them from the powders, although, the ideal, as discussed in Chapter 2, would be not to use a lubricant at all.

Interestingly, the one sample that did not undergo a full bake-out cycle (sample manufactured from calcined powders) had a density below the others in its group (its density was 89.5% TD whilst the other two samples, from the same powders, were 96.6% TD). It was thought that as the material had been calcined for lubricant removal, there was no requirement for further evacuation; this was incorrect. This suggests that every HIP can will require some form of evacuation before HIP. Any adsorbed moisture or trapped gases must be removed from the packed HIP can before HIP. It is unknown whether the HIP can will require heating to remove the entrained gasses. If it does, it is likely to be below the 600 °C required for lubricant removal, potentially ~150 °C. It is assumed that this evacuation step allows any entrained moisture or gases to be removed from the HIP can. The lower temperature should still be sufficient for water removal. A further possibility is to ensure the precursor powders are dry as they enter the process and to evacuate the operating line. This may eliminate the need for an evacuation step but it would require stringent conditions in all of the glove boxes. Work needs to be completed examining what level of

entrained gas is acceptable in the HIP can, whether a sacrificial component may be added to the HIP can to act as a gas scavenger, and what temperature is required to evacuate the can fully.

The samples manufactured from the alkoxide/nitrate derived precursors were of excellent quality: with a high density and homogenous phase development. This was expected as alkoxides are often used for high quality ceramics. However, this method is not suitable for implementation in an active environment. The plutonium feed will always be the dry solid PuO_2 and it is unlikely that an immobilisation plant will be permitted to re-dissolve the PuO_2 feed, if a dry powder method is available. This is due to the increased regulatory concerns with any aqueous process. It is also doubtful that the manufacturing techniques for the as-purchased powders (suspension in a carrier fluid) would be implementable in an active environment. However, the intention of these techniques was to compare the effect of different defined particle size precursors on the product quality. The observation was that all four techniques (each of the three different particle sizes and the alkoxide) produced excellent ceramics. All were over 97% TD and many were around 98% TD. Putting aside the agglomerated ZrO_2 in the 0.1 μm sample, they were all single phase zirconolite ceramics. There was no discernable difference in the quality of the products. Thus, from a purely practical view, the recommendation would be to manufacture candidate wasteforms from the 1 μm powders. These were less expensive to purchase, and easier to handle than the alkoxides or colloid suspensions.

The samples utilising the 0.01 μm precursors and the 'realistic' ceria tested two possible implementations of the methods detailed in this chapter. The sample that was only hand mixed had a heterogeneous phase development with the ceria only being partially incorporated into the zirconolite host phase. This was more an encapsulation process rather than true immobilisation and would not be acceptable in terms of wasteform quality. It has been stated numerous times,

but the correct balance between particle size (of all components) and the intimate mixing are crucial in the manufacture of high quality products (it was thought that the large surface area to volume ratio of the fine precursors would aid the digestion of the ceria, and this may have been so, however the cerium remained as inclusions rather than becoming part of the single host phase). The majority of work on studying the performance of candidate wasteforms has been on predominately single phase products and it is unknown how this encapsulation style would behave in the repository scenario. Some investigation may be worthwhile, yet it is likely that any regulator would prefer the ease of assessing a homogenous single phase ceramic. The improvement in phase homogeneity after planetary milling the same starting materials was excellent. The milling operation was able to size reduce the ceria to such an extent that it was suitably mixed with the other fine precursors. This intimate mixing led to the high quality product produced.

5 Conclusions

The intention of this work was predominantly to explore the effect of different manufacturing techniques on the quality of ceramic products, with regard to density, phase development and microstructure. Out of the eight techniques trialled, only two methods failed to produce suitable products: attrition mill and bake out in can and, hand mixing with the realistic ceria.

It can be stated that removing the lubricant from milled powders packed in to HIP cans is problematic and should not be implemented in any full scale process. The results of this work and Chapter 2 have conclusively shown the failure to remove completely the lubricant from a packed HIP can will be detrimental to the final product quality. Whilst the density of the samples is most obviously affected, the form of the zirconolite structure was also modified (from 2M to 3T). There must be careful control of redox state of the materials inside the HIP can.

It can also be stated that every packed HIP can must undergo some form of evacuation before consolidation. This evacuation must remove any entrained moisture or gases held in the powders.

In direct contrast to Chapter 2, ceramic products manufactured from attrition milled precursors can form dense and homogenous wasteforms. This gives good confidence that an attrition mill can be selected as the key feed processing item in the relevant active environment. Any lubricant added to aid milling must be removed before the milled material is packed into a HIP can.

Manufacturing candidate wasteforms from various as-purchased precursors (powders, colloids, alkoxides) does produce dense and homogenous samples. There are no substantial differences in the products formed, as they are all homogenous and dense. This work examined the impact of mixing fine precursors with a simulated feed and showed that the feed must be milled if suitable waste incorporation (i.e. single phase development) is to be achieved. The suggestion from this work is to continue to investigate the attrition mill for homogenisation of the precursors and feed.

Hand mixing the realistic ceria simulant with the fine precursors showed that there may be a maximum size of feed material than can be incorporated without milling the feeds, this was estimated to be ~20 μm.

5: Planetary Milling of Zirconolite With Modified Precursors

1 Abstract

This chapter examines work in which variously treated zirconolite precursors were planetary milled with the intention of discovering what modification of the precursor powders aided free milling. Visual inspection of the planetary mill pot after milling showed that untreated powders caked on the side walls and also on the milling media. Powders milled with zinc stearate did not adhere to the walls or media and this level of adhesion was presented as an explanation for the differing discharge times of the various lubricants trialled so far in this work. Other samples milled with Aeroxide or reduced precursors showed light agglomeration on the side walls and were determined worthy of further investigation in the attrition mill. Pellets cold uniaxially pressed from all of the powders were sintered in air or nitrogen. In the oxidising environment all of the milled samples, confirmed by XRD and SEM, show a major phase of zirconolite with some zirconia inclusions. All samples were porous and had correspondingly low densities. Samples sintered in nitrogen were also porous and had low measured densities. It was also noted that it is likely the Fe_2O_3 was reduced to FeO and underwent melting due to a eutectic phase with TiO_2 during the sintering process. It is thought that this liquid phase aided the incorporation of precursors as both the non-milled and milled samples showed the same phase development and distribution.

2 Introduction

Throughout the work already presented, suggestions for the improvement of the milling process had been offered, for example, through modification of the mill or modification of the precursors. This work examines changing the lubricant utilised and introducing electrical conductivity into the precursors.

Discussions with Professor Ghadiri at The University of Leeds brought about the suggestion to use Aeroxide™ as a replacement lubricant. Aeroxide is a form of fumed Al_2O_3 that has a very high surface area. It acts to disrupt particle-to-particle attraction by covering the surface of the powders to be milled. As it is Al_2O_3, the material can be readily incorporated into the final sintered product, most likely substituting on to the Ti site. It is added in quantities of approximately 0.5 wt%.

A further suggestion for ensuring powders remain free flowing during milling was through the introduction of electrical conductivity into the precursors. This concept is based on the idea that one of the causes of foot formation and powder agglomeration during milling is tribo-electric charging (Matsusaka, Maruyama et al. 2010). As each individual particle collides against other insulating particles and the mill internals, a static charge is created. It is this charge that increases the attraction of the particles to each other. One method for mitigation is by intentionally making the particles conductive. This can be achieved by partial reduction of the precursors and thus introducing mixed valences. The differing oxidation state between the two metal ions allows the easy transfer of electrons to normalise static charge.

One issue with utilising the attrition mill for powder testing is the duration of each trial run and the size of each batch. It typically takes weeks to perform a full array of variables. To expedite the experimental process, it was decided a planetary ball mill would be used. This mill has a batch size of 50-100 g and powder behaviour in both the attrition mill and the planetary mill has been shown to be have the same mode of milling action (Kwade 2011). In addition,

CUP of all powders would provide pellets that are suitable for initial analysis. It is noted that this work was intended as exploratory and did not merit a full HIP cycle.

Zirconolite was used as the target ceramic product with cerium as the plutonium surrogate. Two sets of CUP pellets were pressed with one set being sintered in air and the other in nitrogen. The nitrogen sintering was to represent the anaerobic conditions in a fully evacuated HIP can.

3 Materials and Methods

Zirconolite was used as the target ceramic product with CeO_2 as the PuO_2 surrogate and Fe_2O_3 to provide charge compensation giving a target formulation of $Ca_{0.75}Ce_{0.25}ZrTi_{1.5}Fe_{0.5}O_7$. Calcium was provided as $CaTiO_3$, zirconium and the balance of titanium from ZrO_2 and TiO_2, respectively. A 1 kg batch of the precursors (including an extra 0.05 formula units of titanium and zirconium) was Turbula mixed for 15 min. Aliquots of this parent batch were modified as required for the experiment.

Approximately 100 g quantities of the parent batch were mixed, by hand with a spatula in a bowl, with 3 or 5 wt% of glucose powder. This mixture was calcined at 1100 °C for 4 hours in a nitrogen atmosphere. Pyrolysis of the glucose in the anaerobic atmosphere will produce fine carbon well mixed throughout the material. This carbon will act to reduce the TiO_2 in the precursors to produce TiO_{2-x} (most likely towards the Ti_4O_7/Ti_5O_9 Magnéli phase). The 3 wt% addition was to produce a material in which 0.5 formula units of the Ti^{4+} were reduced to Ti^{3+}(this would be equivalent to a zirconolite formulation in Ti^{3+} would provide all of the necessary charge compensation) whilst the 5 wt% addition was to 'over reduce' the material. Nitrogen was used to flush the tube furnace for 3 hours at 400 ml min^{-1}. This flow was reduced to 50 ml min^{-1} during heat treatment. A buffer phase of the precursor batch and excess (> 5 wt%) glucose was placed in the tube furnace at the source of the gas,

schematically represented as Figure 66. This was to ensure any impurities in the gas stream (i.e. O_2) did not affect the powders being reduced.

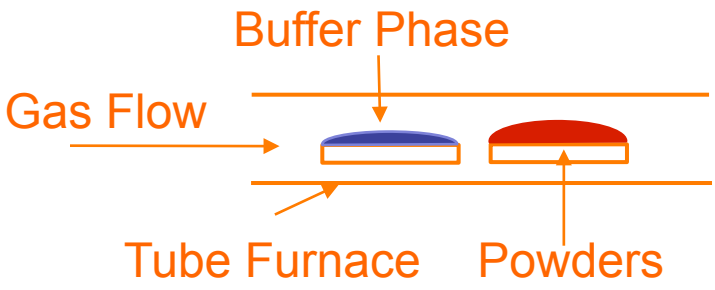

Figure 66: Schematic of buffer phase and powder arrangement

A further 100 g of the parent material was placed into the tube furnace, with another buffer phase of the same composition as previously, and heated to 1100 °C for 4 hours in a 5% H_2/Ar atmosphere. Gas flow rates were 400 ml min^{-1} for 3 hours for flushing and 200 ml min^{-1} during heat treatment. The intention was to reduce this material in a different manner to the glucose containing samples.

For each trial run, the same 250 ml stainless steel planetary milling pot was used. The pot was filled to 2/3 volume with ~10 mm (3/8") stainless steel ball bearings as the milling media. The mill was operated at 300 RPM for 20 min. These milling conditions were chosen as being sufficiently aggressive to bring about a change in the powders and to be of sufficient duration that any caking or powder agglomeration should occur. Each milling operation contained 75 g of powders, which was 1/3 of the empty mill pot volume.

The first batch of material to be milled was from the parent batch with no further modifications. The second batch had a 1.5 wt% of zinc stearate addition. The third batch had 0.5 wt% of Aeroxide added and the final three batches were the reduced powders detailed earlier.

The milling pot and media were photographed after the milling operation was complete and the media had been poured into a separate container. Pellets of 15 mm diameter and 2.0 g were CUP (56 MPa) in duplicate from both the non-

milled and milled forms of each powder batch. One set of pellets was sintered in air and the other sintered in nitrogen. Both sintering cycles were at 1320 °C for 4 hours. The tube furnace for the nitrogen cycle was flushed at 400 ml min^{-1} for 3 hours before heat treatment and 50 ml per min^{-1} during. The nitrogen cycle was to simulate the anaerobic conditions within a fully evacuated HIP can and the air cycle was to ensure any reduced precursors were in their fully oxidised state for sintering.

All of the pellets underwent density measurement. A section was cut from the pellets and this was ground into a fine powder for XRD analysis. The intention was to examine all of the products by SEM, however many of the samples were mechanically weak and failed during sample preparation (grinding, polishing). It was determined that all of the non-milled samples sintered in air were not mechanically strong enough to withstand processing. Nor were any of the samples manufactured from powders reduced with glucose (both 3 and 5 wt%). However, all of the samples (milled and non-milled) that were sintered in N_2 had sufficient mechanical strength for preparation and the SEM images are thus reported.

4 Results

4.1 Milling Results

4.1.1 Untreated

Figure 67 shows the milling pot post milling the untreated precursors. This material was from the parent batch of precursors. The left hand image shows that the material is caked on to the side walls of the pot with a small amount of residue remaining in the base. This material will have been compacted by the constant rotational motion of the milling media. It is likely that milling this same powder in an attrition mill will form a foot and fail to discharge freely. Whilst the previous chapters have shown that foot formation is not necessarily an indicator of poor milling it has been judged to be an important operation

concern (material that does not freely discharge is unacceptable for implementation). The loose material at the base of the pot is due to the material on the side walls restricting the flow as the pot is emptied. Examination of the milling media shows all of them to be thickly coated in the powders. In attrition milling, this behaviour would manifest itself as (assuming the powder discharges at all) a rapid initial discharge of the loose powders with a slow powder flow as the material is dislodged from the balls. The coating of the milling media may explain the differences in the discharge durations discussed in Chapters 2 and 3.

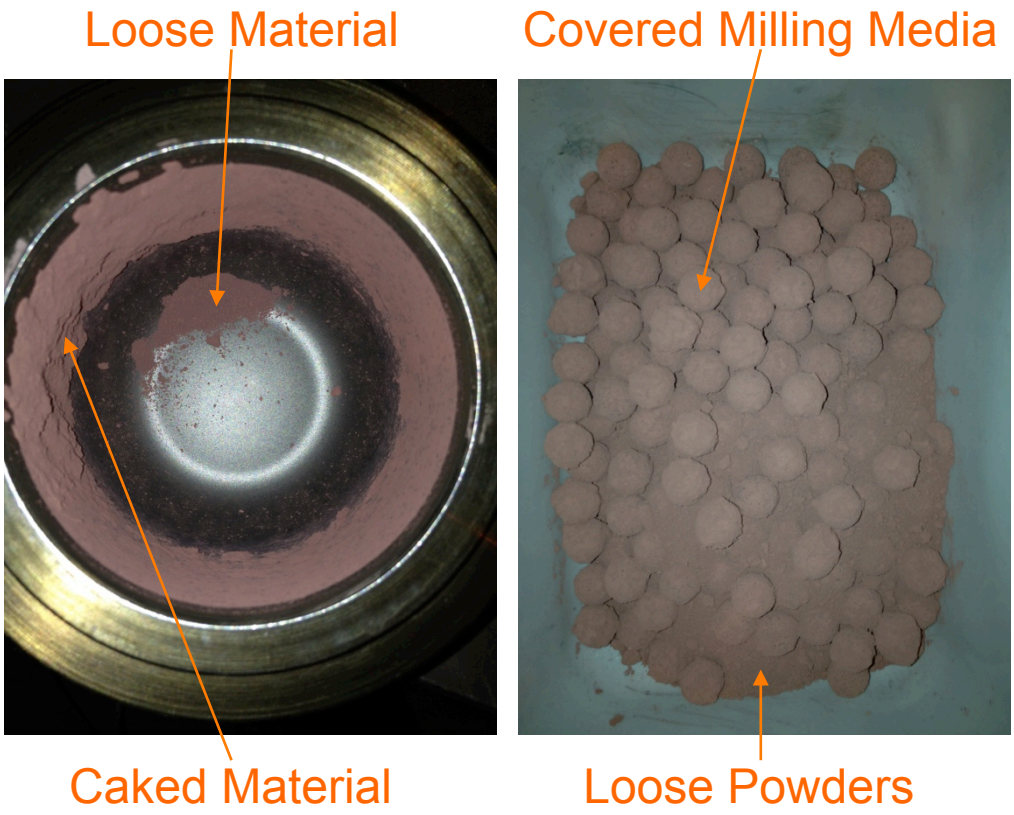

Figure 67: Mill pot post milling, left, and milling media and milled powders, right, for the untreated precursors.

4.1.2 Zinc Stearate

Figure 68 shows the milling pot after milling the precursors with 1.5 wt% addition of zinc stearate. The mill pot contains visibly less coated material on the side walls than after milling of the raw precursors. It is clear that the lubricant addition has helped to prevent the agglomeration to the inside of the pot. The image on the right shows that the milling media has a reduced amount

of material coating, as shown by the reflection of light from the media (i.e. a shiny surface). The zinc stearate addition appears to coat all metal surfaces (pot and media) and this prevents the agglomeration of powders onto the metal. It is also likely that this type of zinc stearate interruption also affects the particle-particle interactions minimising powder agglomerations and in turn, foot formation in attrition mills.

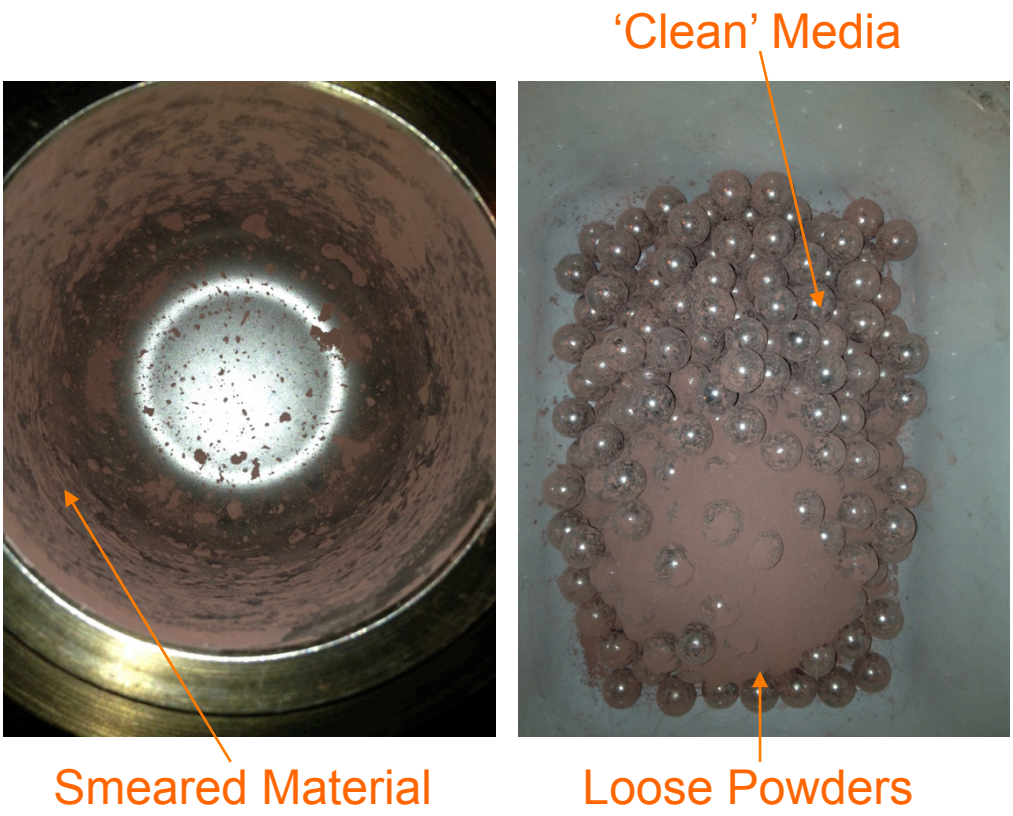

Figure 68: Mill pot post milling, left, and milling media and milled powders, right, for the zinc stearate lubricated precursors.

4.1.3 Aeroxide

Figure 69 shows the mill pot after milling the precursors with 0.5 wt% addition of Aeroxide. There is a light coating of material on the inside of the mill pot. This is visibly more than the pot after milling with zinc stearate and less than milling without any additions. The amount of covering on the media is also visibly between that of the zinc stearate and raw powders (noting the mottled surface). Knowing that material milled with zinc stearate freely discharges from the attrition mill and that material without any lubricant additions does not, it is not possible to say, based solely on planetary mill pot coverage, what the

behaviour of Aeroxide in the attrition mill would be. However, the low level of material coverage of the media and the mill pot, relative to raw powders, does suggest that further investigation of Aeroxide is warranted.

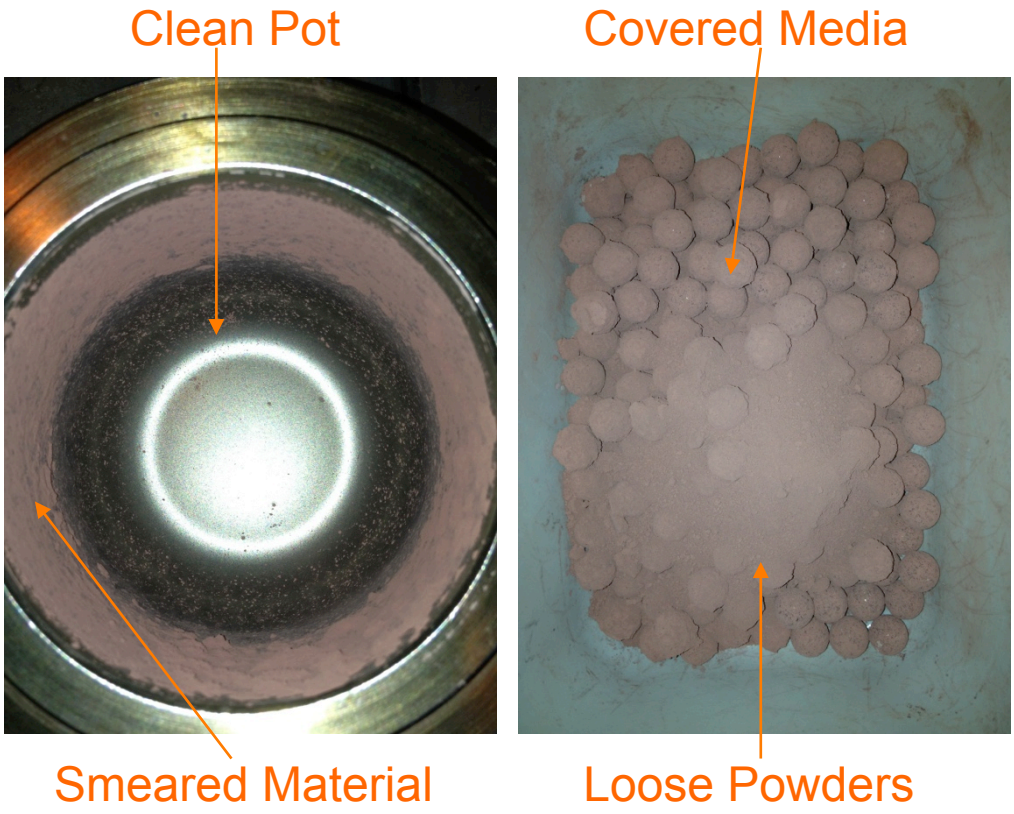

Figure 69: Mill pot post milling, left, and milling media and milled powders, right, for the Aeroxide lubricated precursors.

4.1.4 Reduced Precursors

Figure 70 shows the mill pot and milling media after the precursors reduced by 3 wt% of glucose. The first observation is that the colour of the powders is grey/blue as apposed to the brick red of the non-reduced powders. This shows that some component of the material has been reduced; Ti_nO_{2n-1} powders are typically dark blue (from Ti^{3+}). The amount of material smeared on the inside of the mill pot is equivalent to the powders milled with Aeroxide and this suggests a similar performance of these two batches of powder in the attrition mill. The milling media is covered with the 3 wt% glucose reduced material to a slightly greater extent than the Aeroxide milled powders (lack of mottled surfaces). This implies that attrition mill discharge times may be increased, compared to the Aeroxide, when utilising reduced precursors.

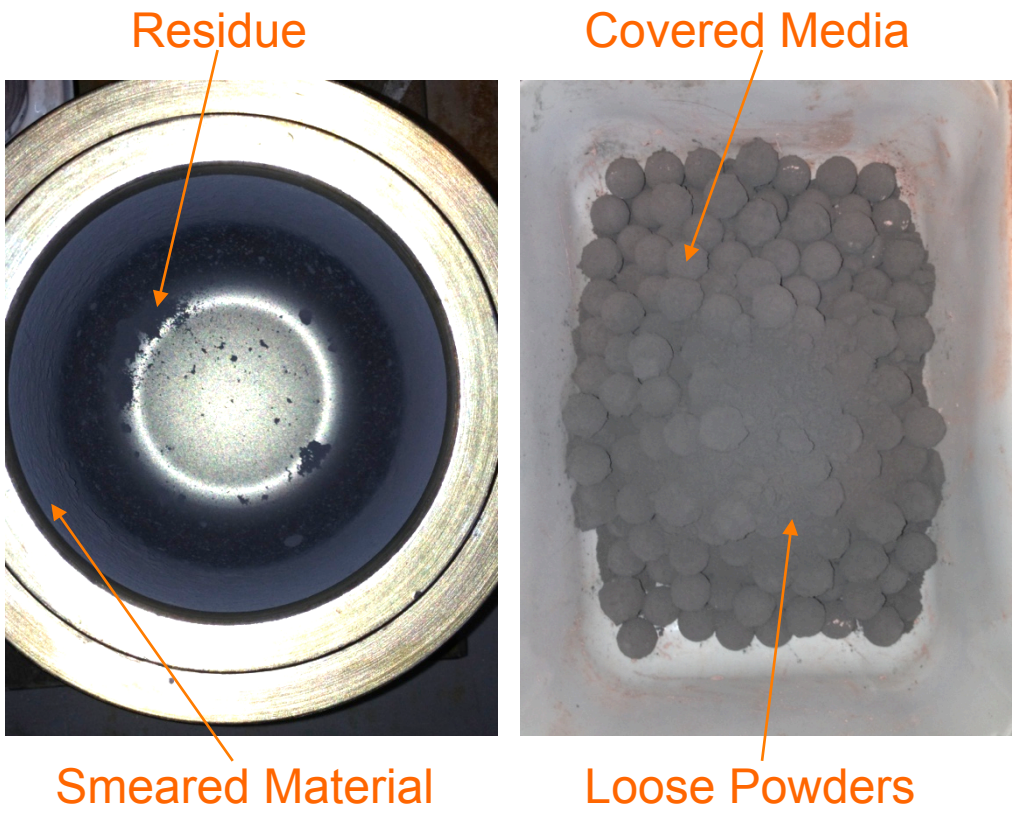

Figure 70: Mill pot post milling, left, and milling media and milled powders, right, for the precursors reduced with 3 wt% glucose.

Figure 71 shows the milling pot after milling the precursors reduced with 5 wt% glucose. The mill pot and media visibly have the same level of coverage as the powders reduced by 3 wt% glucose. That is, the extra reduction, and therefore assumed powder conductivity, appears to have little effect on the propensity of the powders to agglomerate and cover the metal surfaces.

Finally, the mill pot after milling with powders reduced by H_2 is shown in Figure 72. Again, the pot and media coverage is comparable to the glucose reduced powders (both 3 and 5 wt%). The overall observations are that the reduced powders, regardless of reduction method, have similar tendencies for powder agglomeration and media coverage.

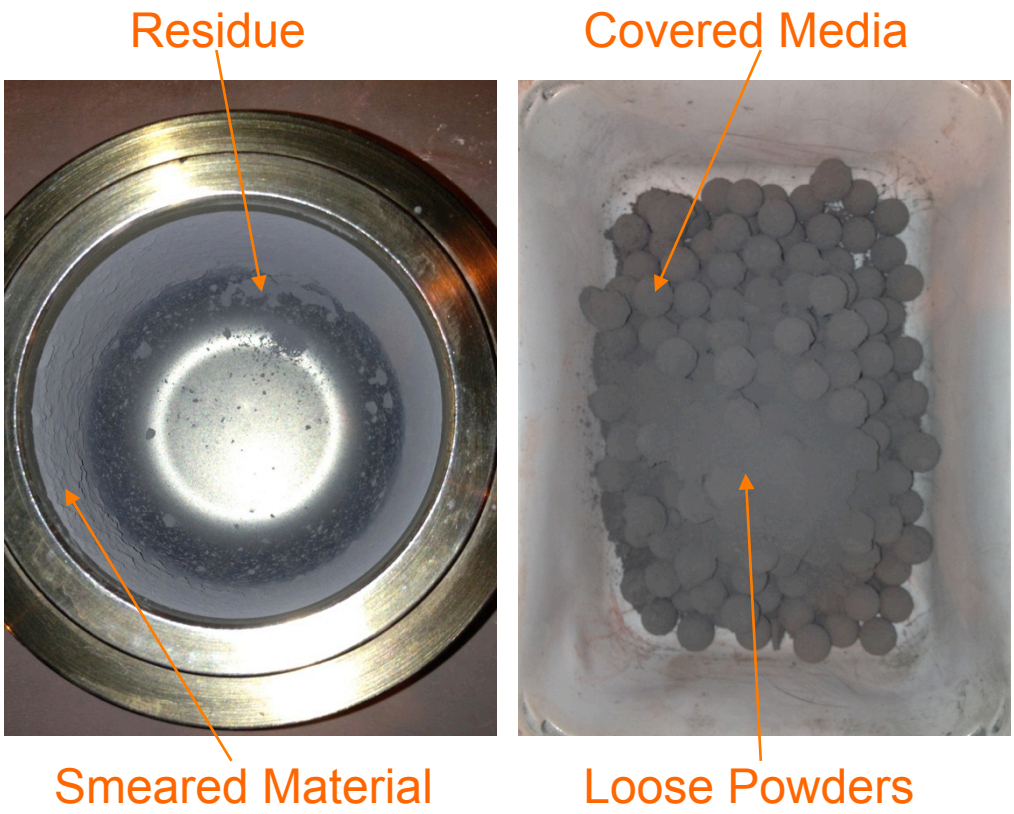

Figure 71: Mill pot post milling, left, and milling media and milled powders, right, for the precursors reduced with 5 wt% glucose.

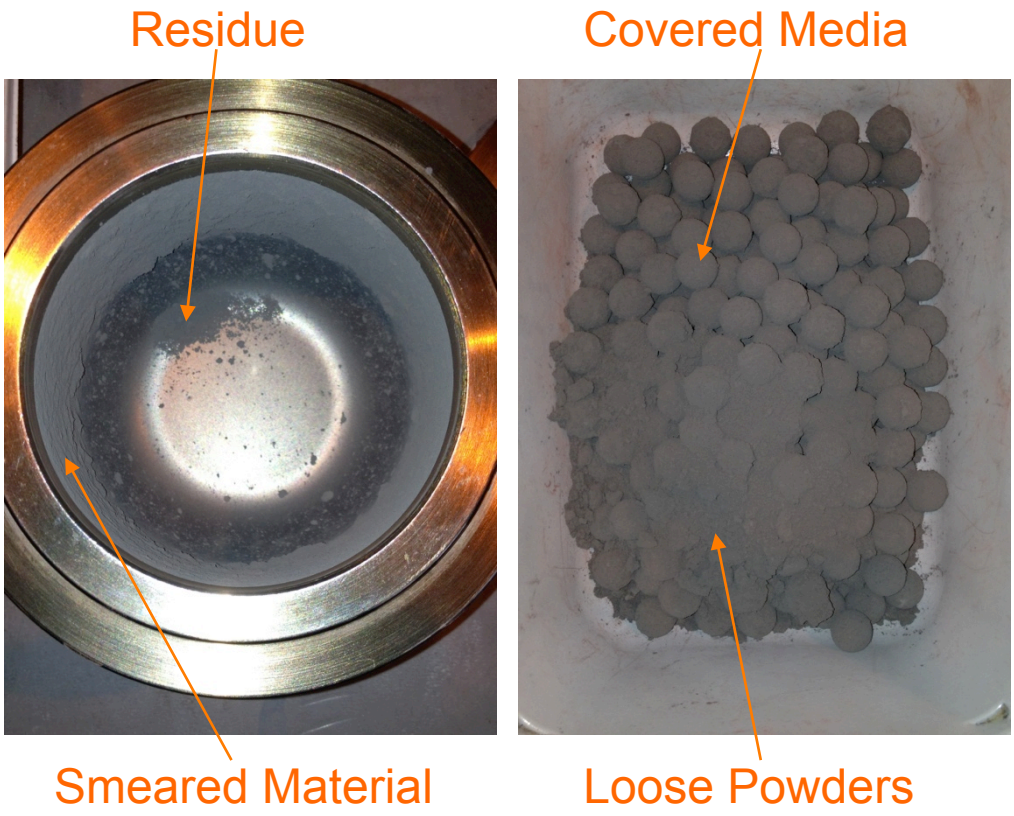

Figure 72: Mill pot post milling, left, and milling media and milled powders, right, for the precursors reduced by H_2.

4.1.5 Discussion

The amount of material covering the side walls of the milling pot is an indicator of powder milling performance in an attrition mill. By this factor alone, it can be said that the raw, untreated, precursors would most likely form a foot if they were attrition milled, which is confirmed in previous work. When the powders were milled with a zinc stearate addition, the precursors did not coat the inside wall, which implies that the addition of zinc stearate would prevent foot formation in attrition mills, again, confirmed in previous work. However, the reduced precursors and the precursors milled with Aeroxide covered the mill pot to a degree between that observed for lubricant addition and the untreated precursors. Thus, it is likely that these precursor treatments will have attrition mill discharge properties somewhere in between the raw powders and lubricant additions.

The level of media powder coverage may be connected to the overall attrition mill discharge time. It follows that if the powders are tightly bound to the media, this material needs to be dislodged from the media before it can be discharged. Thus, the conjecture is that the stronger the attraction of the powders to the media the more energy, from extended discharge duration, is required to dislodge and discharge the powders.

4.2 Products Sintered In Air

Pellets, 15 mm diameter, were cold uniaxially pressed from all milled and non-milled powders and sintered in air at 1320 °C for 2 hours. Figure 73 shows an overview of the sintered pellets. The pellets manufactured from non-milled powders are speckled indicating a heterogeneous phase development. The pellets made from milled powders are homogenous in colour.

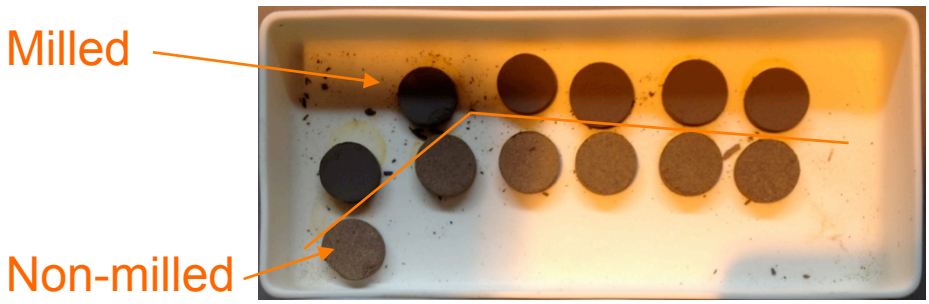

Figure 73: Sintered pellets. Above the red line are pellets manufactured from milled powders and below are pellets manufactured from non-milled powders.

4.2.1 Density

Table 25 givers the measured densities of all of the pellets sintered in air grouped by precursor processing method. It should be noted that the SEM images, below, show all of the samples to be highly porous. Water ingress, during density measurement, into the samples will have artificially increased the measured density. The first observation is that all of the pellets manufactured from milled powders have greater densities than their non-milled counterparts. This shows that all of the powders have undergone some transformation (e.g. size reduction, homogenisation) during milling. All of the samples are below the 92% TD target. Comparing to the planetary milled sample in Chapter 4, these samples all have lower densities. This is likely to be because the sample in Chapter 4 underwent HIP after more aggressive milling (duration of 60 min) and was milled in a carrier fluid (propanol). All three of these factors are known to improve product density. It is not possible to make an assessment on the level of milling achieved by comparing the density improvements as these measurements are only on one sample. It may be possible, through further work, to use density change as a qualitative comparison of each precursor treatment technique on the effectiveness of milling.

Precursor Treatment	Milled?	Density (g cm^{-3})	% TD
Untreated	No	3.92	83.3%
Untreated	Yes	4.20	89.2%
Zinc stearate	No	3.91	83.1%
Zinc stearate	Yes	4.07	86.4%
Aeroxide	No	3.95	84.0%
Aeroxide	Yes	4.20	89.1%
3% Glucose reduction	No	3.93	83.3%
3% Glucose reduction	Yes	4.12	87.5%
5% Glucose reduction	No	3.98	84.6%
5% Glucose reduction	Yes	4.12	87.4%
Hydrogen reduction	No	3.90	82.7%
Hydrogen reduction	Yes	4.01	85.2%

Table 25: Density of pellets sintered in air. Grouped by processing method. TD calculated as 4.71 g cm^{-3}.

4.2.2 XRD AND SEM

Every sintered sample underwent XRD analysis, however only the samples manufactured from milled powders had sufficient mechanical strength to be prepared for SEM imaging.

4.2.2.1 UNTREATED

Figure 74 shows the XRD patterns for the pellets manufactured from milled and non-milled untreated precursors. The sample made from milled powders clearly shows a reduction in the number of phases present. The XRD pattern shows the milled sample to be the zirconolite phase, as designed. Also, as expected, the non-milled sample is heterogeneous with separated ZrO_2, Fe_2O_3, TiO_2 and CeO_2 identified along with the main zirconolite phase. These results show that even powders that have coated the walls and appear not to have been milled, have in fact undergone some transformation (size reduction, homogenisation) that brings about an improvement in the phase development of sintered products. It may be that the powders found adhered to the mill pot walls at the end of the milling cycle were not coated on the wall for the entire milling duration. These powders could have been in the centre of the pot, undergoing milling, and then became attached to the walls.

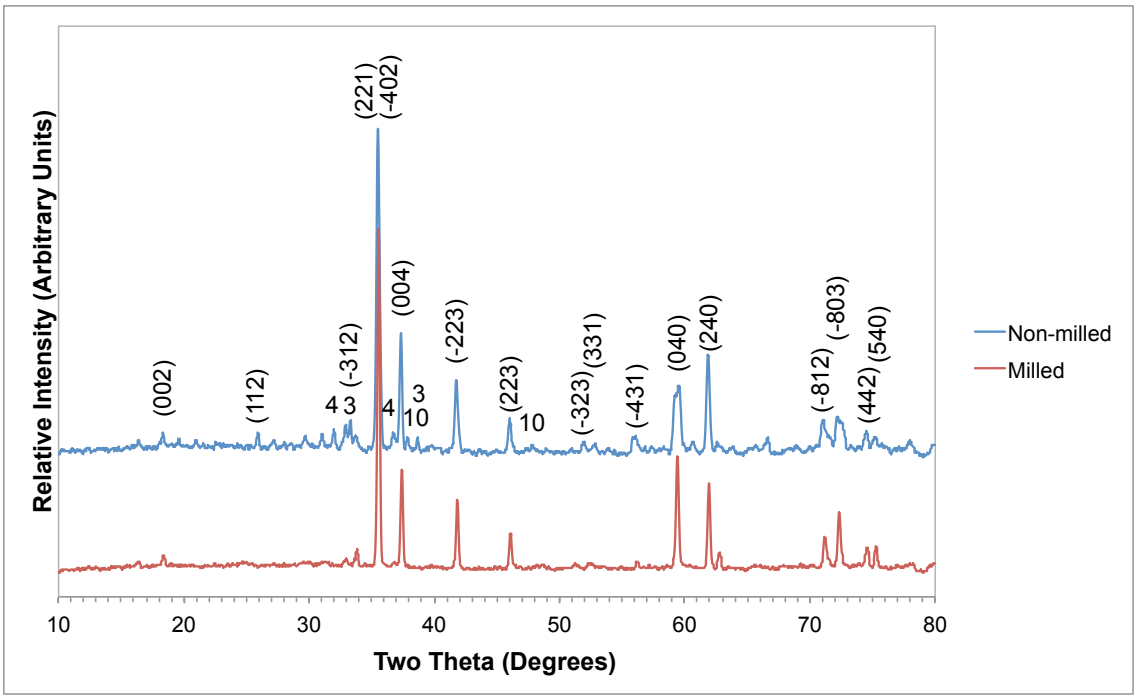

Figure 74: XRD patterns for samples manufactured from milled and non-milled untreated powders and sintered in air. Phases labelled: Miller indices, zirconolite; 3: ceria; 4: zirconia; 10: iron oxide

The SEM images of the sample manufactured from milled untreated powders, Figure 75, show a single host phase of zirconolite with zirconia inclusions. The small total volume of these inclusions, and the overlap of the zirconia primary peaks with zirconolite, means they are readily not identifiable in the XRD patterns. The pore network is extensive and this is a reflected in the low sample density. The level of porosity is high compared to other zirconolite samples presented in this project; this is due to these samples being prepared by CUP rather than HIP.

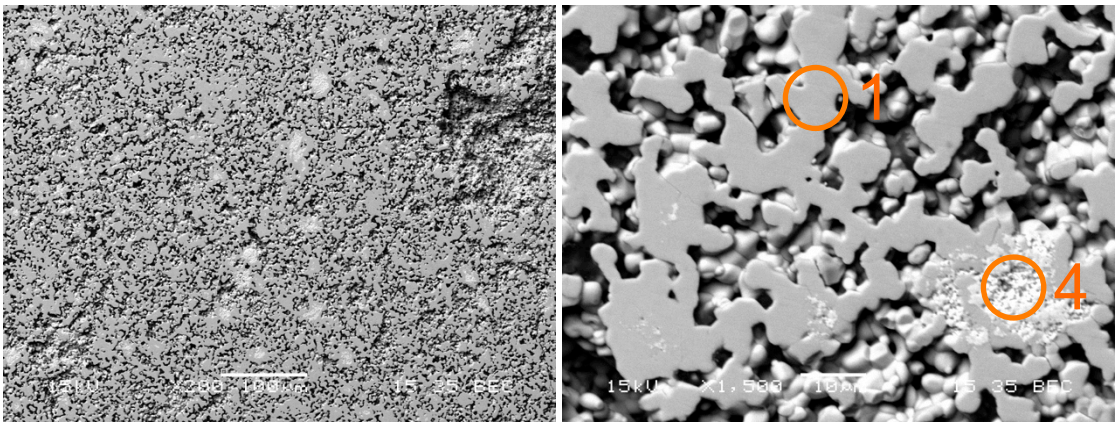

Figure 75: SEM image of sample manufactured from milled untreated powders and sintered in air. Phases labelled: 1: zirconolite; 4: zirconia

4.2.2.2 Zinc Stearate

Figure 76 shows the XRD patterns for the samples prepared from precursors with 1.5 wt% zinc stearate addition. Again, the XRD data show the sample manufactured from milled powders to be single-phase zirconolite. The non-milled sample shows the same multi-phase nature as the samples made from untreated powders, with ZrO_2, Fe_2O_3, TiO_2 and CeO_2 identified alongside the main zirconolite phase.

Figure 77 shows the SEM images of the CUP and sintered pellet made from powders milled with zinc stearate. Again, there is a main phase of zirconolite, which is interspersed with zirconia. The visible pores are extensive within the sample, consistent with the low density measured.

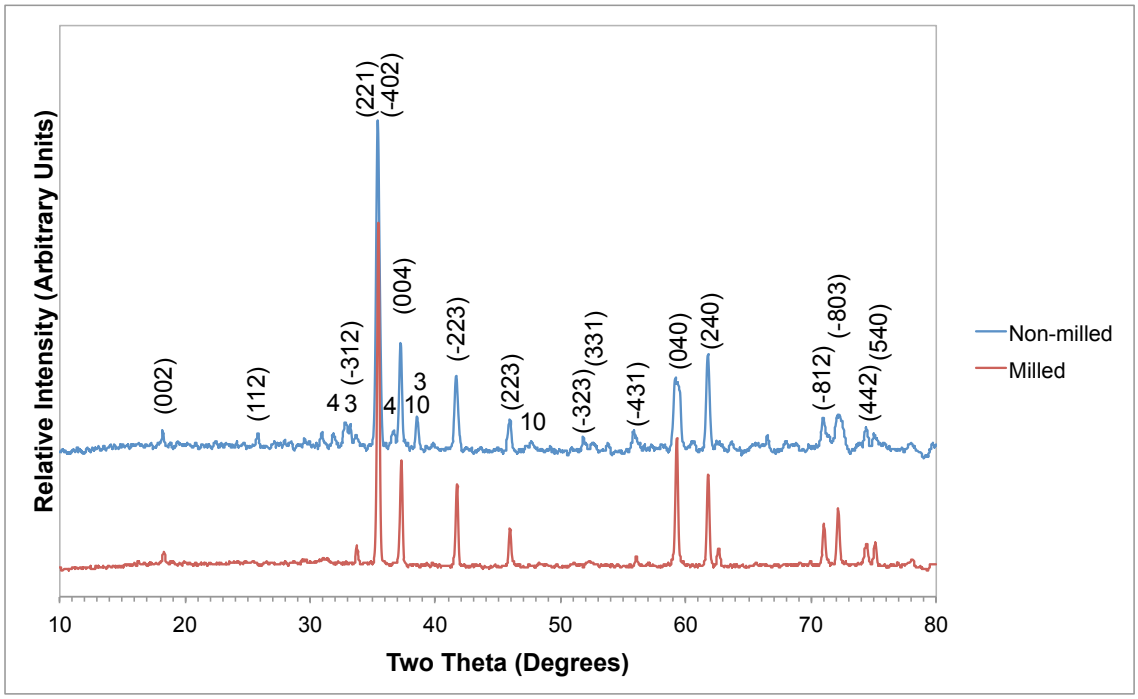

Figure 76: XRD patterns for samples manufactured from milled and non-milled powders with 1.5 wt% zinc stearate. Phases labelled: Miller indices, zirconolite; 3: ceria; 4: zirconia; 10: iron oxide

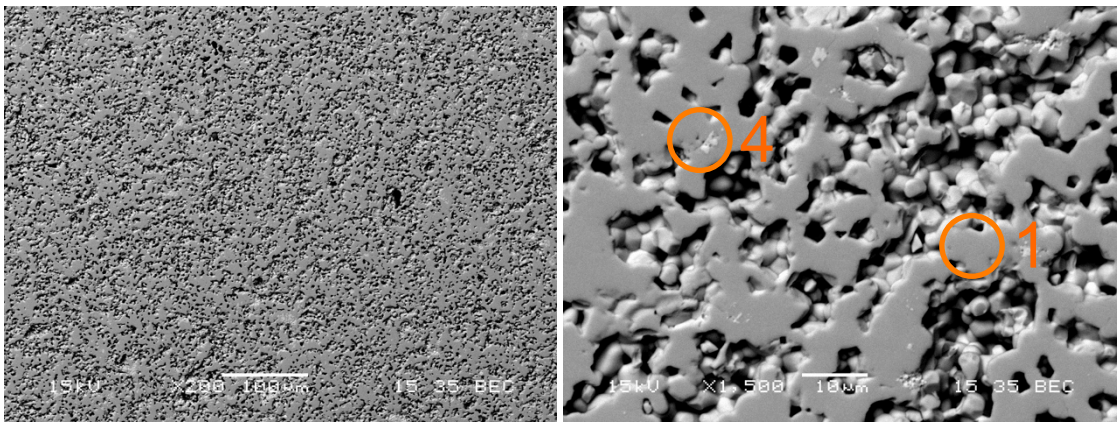

Figure 77: SEM image of sample manufactured from powders milled with zinc stearate and sintered in air. Phases labelled: 1: zirconolite; 4: zirconia

4.2.2.3 Aeroxide

Figure 78 shows the XRD patterns for the samples prepared from precursors with 0.5 wt% Aeroxide. The pattern for the milled sample is again single phase zirconolite, whilst the non-milled sample shows the same multi-phase nature as the previous two samples. Notably, in neither the XRD or SEM images could any trace of the Al_2O_3 addition be determined. The small quantity of material added is likely to be below the detectable limits and would have been incorporated into the other phases regardless.

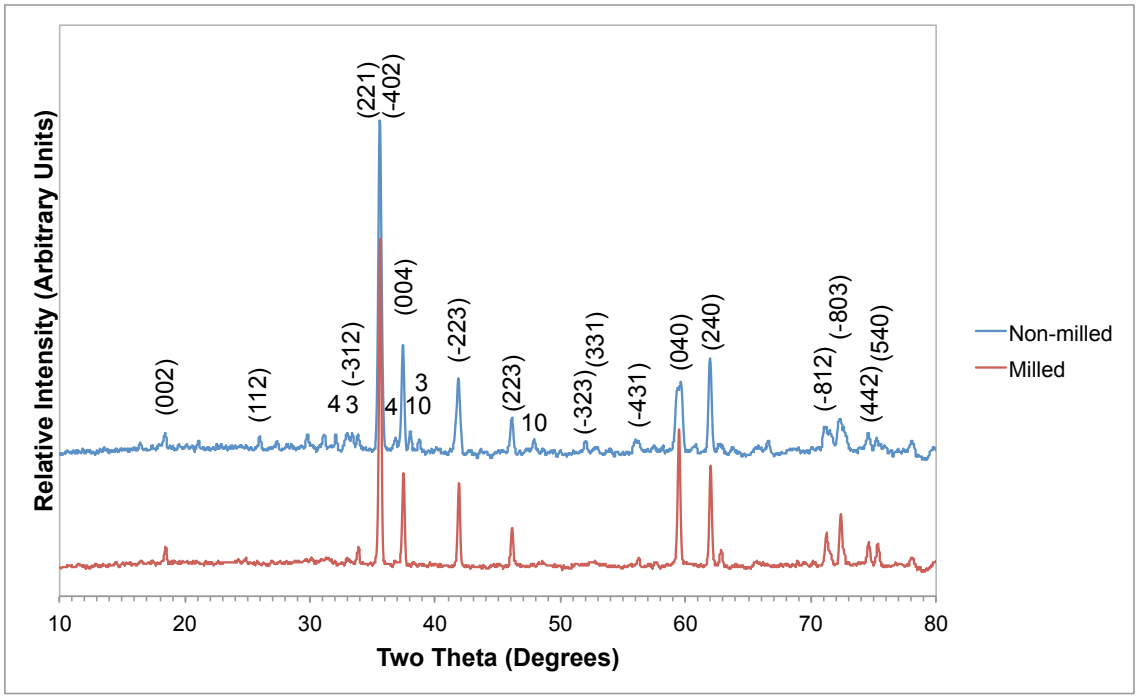

Figure 78: XRD patterns for samples manufactured from milled and non-milled powders with 0.5 wt% Aeroxide additive. Phases labelled: Miller indices, zirconolite; 3: ceria; 4: zirconia; 10: iron oxide

Figure 79 shows SEM images of the sample manufactured from powders milled with Aeroxide. The bulk of the sample is the zirconolite phase as expected with zirconia inclusions. Again, there is an extensive network of pores.

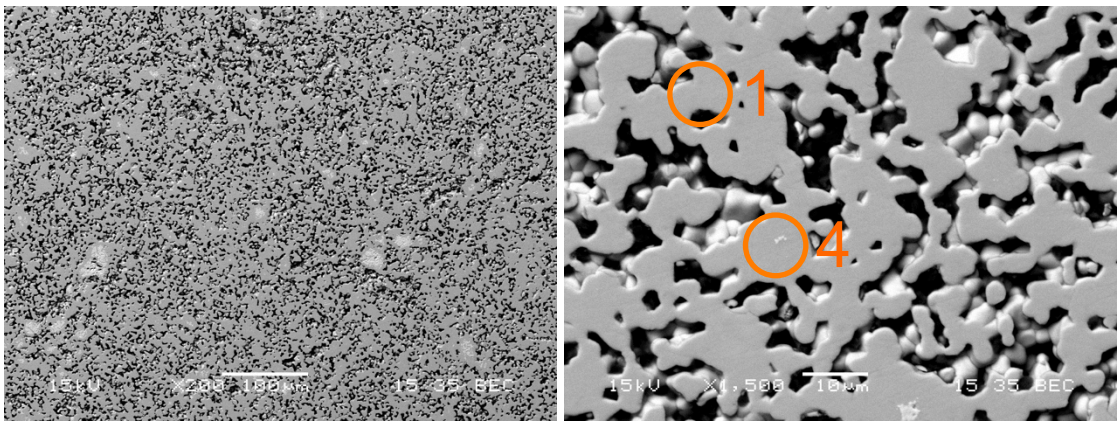

Figure 79: SEM image of sample manufactured from powders milled with Aeroxide and sintered in air. Phases labelled: 1: zirconolite; 4: zirconia

4.2.2.4 Reduced Precursors

Figure 80, Figure 81 and Figure 82 show the XRD patterns for the samples prepared from precursors reduced by 3 wt% glucose, 5 wt% glucose and hydrogen, respectively. All of the samples manufactured from milled powders have formed the same single phase zirconolite present in the samples that were manufactured from non-reduced powders. Considering the samples were sintered in an oxygen rich environment (air) there would be sufficient free oxygen to re-oxidise any of the reduced components present in the precursors before, or during, sintering. The non-milled samples show a slightly different phase development than the non-reduced precursors. Again, there are remnants of the precursors (Fe_2O_3, CeO_2, ZrO_2) but there is also evidence of reduced phases of the form Ti_nO_{2-n}.

Only the sample manufactured from powders reduced by H_2 was amenable to preparation for SEM imaging. None of the non-milled samples presented so far could be suitably prepared so it was expected that the non-milled reduced powders would be mechanically weak yet the two samples manufactured from milled powders reduced by glucose were also weak. It could be that the 1100 °C

heat treatment reduced the surface area of the precursors, thus reducing the overall reactivity during sintering. It may also be that expansion of the precursors during re-oxidation weakens or undoes the pellet pressing. Why this only affects the powders reduced by glucose (and not hydrogen) is unknown. Examination of the product densities is not illustrative as the non-milled samples have comparable densities to other samples that could be prepared. It should be remembered that the measured densities are likely to be incorrect due to water ingress though the porous samples. In addition, the glucose reduced samples have greater densities than the H_2 pellet.

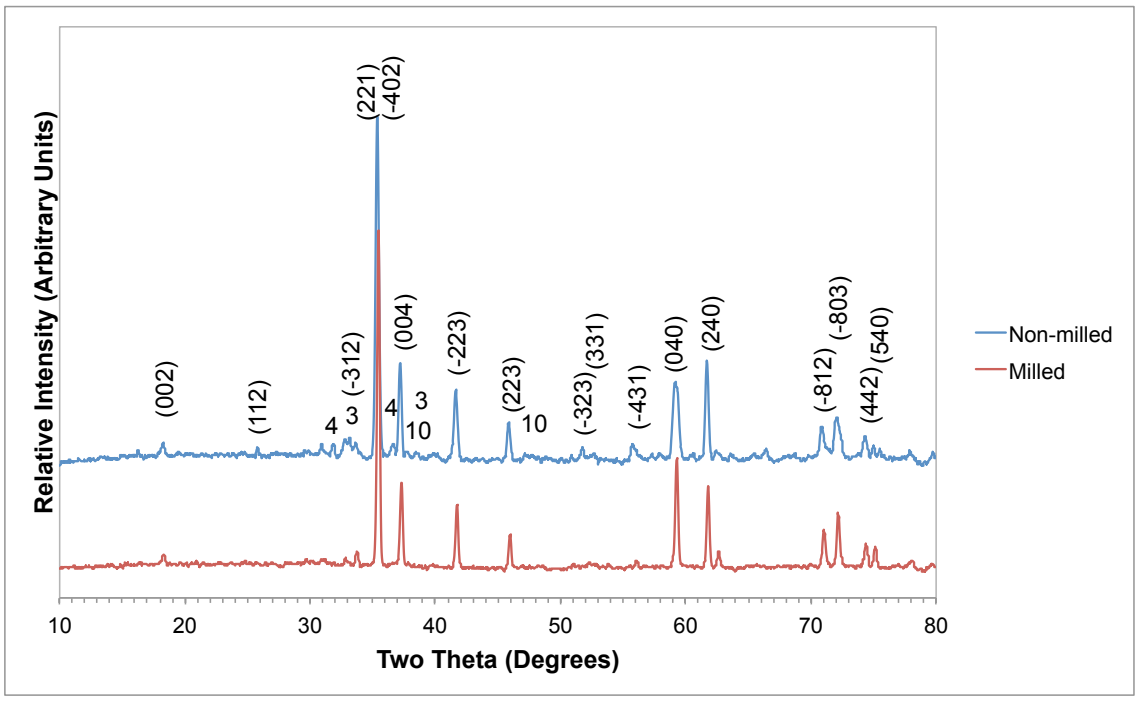

Figure 80: XRD patterns for samples manufactured from milled and non-milled powders reduced with 3 wt% glucose. Phases labelled: Miller indices, zirconolite; 3: ceria; 4: zirconia; 10: iron oxide

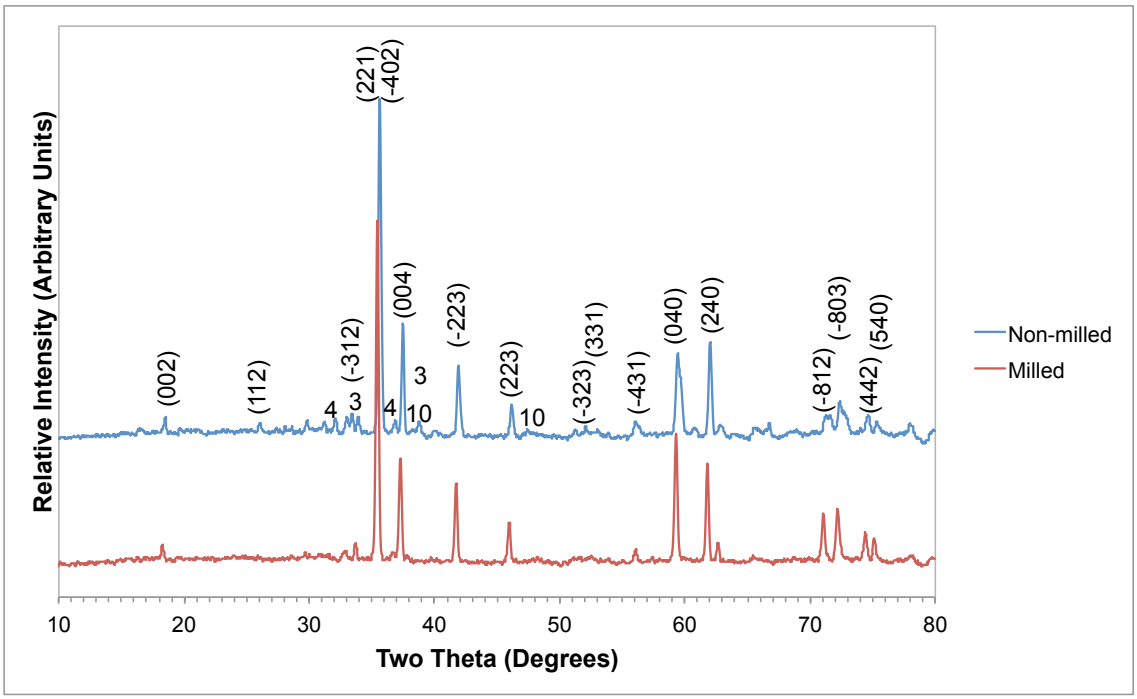

Figure 81: XRD patterns for samples manufactured from milled and non-milled powders reduced with 5 wt% glucose. Phases labelled: Miller indices, zirconolite; 3: ceria; 4: zirconia; 10: iron oxide

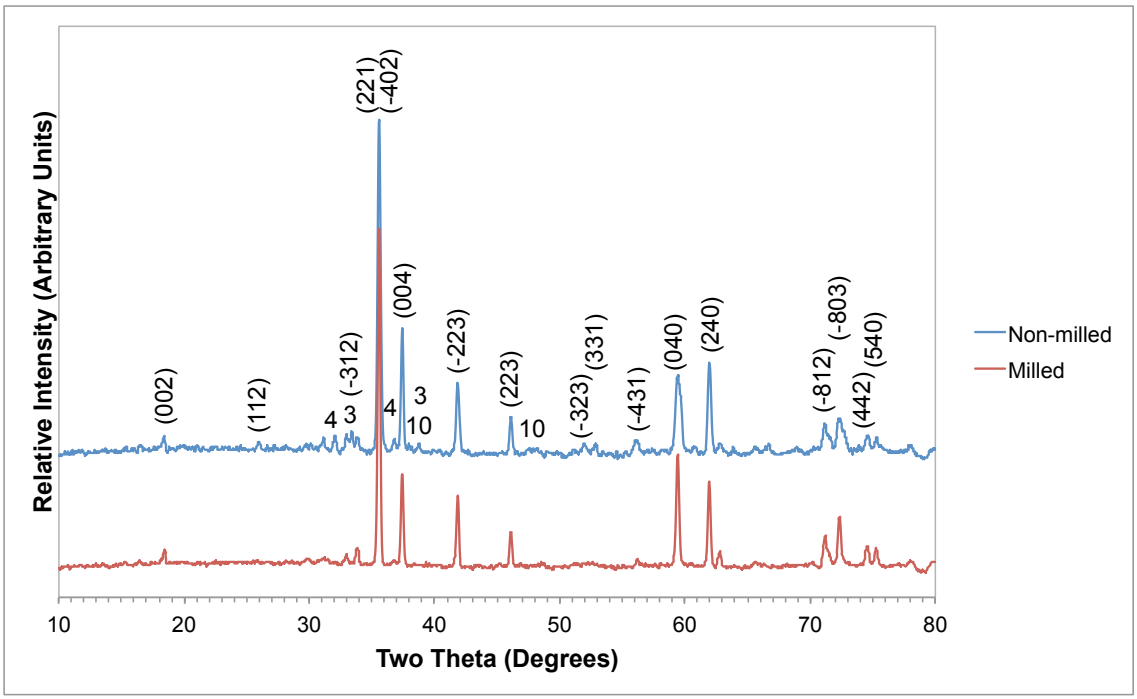

Figure 82: XRD patterns for samples manufactured from milled and non-milled powders reduced by H_2. Phases labelled: Miller indices, zirconolite; 3: ceria; 4: zirconia; 10: iron oxide

Figure 83 shows the SEM images of the pellet manufactured from milled H_2 reduced precursors. The host phase is zirconolite, as confirmed by EDX, with zirconia inclusions. The sample is very porous, which corresponds to the low density. The lack of mechanical strength of the glucose reduced samples can be

inferred if it is assumed that the samples have a similar porous structure to the H_2 reduced sample. This sample is not a dense monolith but rather contains an extensive network of pores. The pores provide no structural strength to the product, thus if the sample is largely porous, it will be weak.

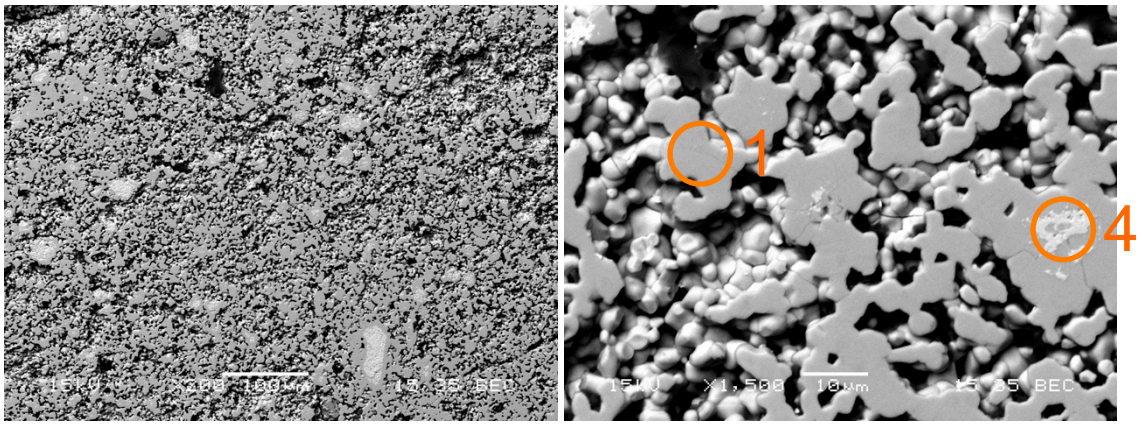

Figure 83: SEM image of sample manufactured from milled H_2 reduced powders and sintered in air. Phases labelled: 1: zirconolite; 4: zirconia

4.2.2.5 Discussion

Every batch of milled powders has produced the expected zirconolite phase development. XRD analysis of each of these products shows them to be single phase, however the SEM images do show zirconia inclusions. Sintering the pellets in air does allow the reduced materials to be oxidised to form the target zirconolite stoichiometry and this is reflected by the lack of variation in phase development between the samples manufactured from reduced and fully oxidised precursors. Comparing the XRD results to the milling pictures presented before, there does not appear to be any correlation with quality of milling (judged by amount of material remaining in the mill pot) and the phase development of the samples. As noted in Chapter 2, regardless of mill discharge performance there does always appear to be some form of size reduction and homogenisation occurring during milling. There is a consistent increase in product density from non-milled to milled samples. Unfortunately, the small number of samples reported here (one per powder batch) is not sufficient to make a clear correlation with increased density and milling performance.

Further work should attempt to determine if there is a connection between product density and material agglomeration in the planetary mill pot.

The non-milled powders, by XRD, show a multi-phase mixture of a primary zirconolite (most intense reflections) with CeO_2, ZrO_2, Fe_3O_4 and various forms of TiO_x. Without SEM images it is difficult to discuss the microstructure in great detail. The visually spotted surfaces of the sintered pellets suggest that the zirconolite main phase will have formed when the necessary components are in close proximity with each other but otherwise leaving areas of unreacted material. This partial reaction of the precursors will also result in a large number of pores and thus low mechanical strength.

The very porous nature of the pellets is a concern; none attained the >92% TD target. In Chapter 3, it was shown that increasing the aggressiveness of the milling further did produce CUP samples of suitable quality. Increasing the duration or speed of rotation may produced products with densities >92% TD.

4.3 Products Sintered in N_2

A further batch of pellets was CUP from the same milled and non-milled precursors presented so far and these pellets were sintered in nitrogen. Figure 84 shows the sintered pellets. Comparison with the pellets sintered in air, Figure 73, shows all of those sintered in nitrogen are black and there is no variation in colour between the milled and non-milled samples.

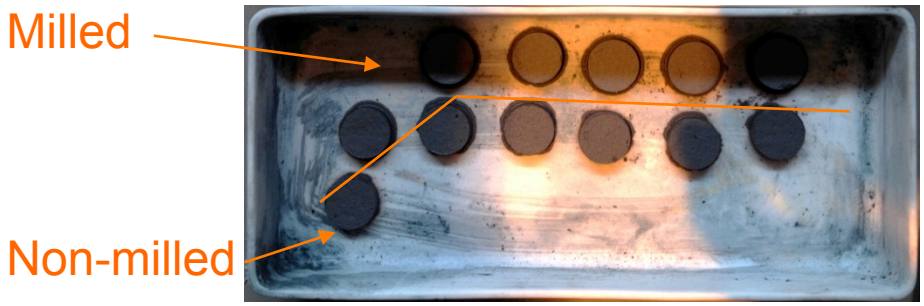

Figure 84: Pellets sintered in N_2. Pellets above the orange line were prepared from milled powders and below were non-milled powders.

In contrast to the pellets sintered in air, every pellet of this second batch was stuck to the alumina calcination tray. Figure 85 shows the melt interfaces after the pellets had been forcibly removed. Grieve and White (Grieve and White 1939) show that in the Fe-Ti-O system there are a number of eutectic points around 1300 °C ($FeO:TiO_2$; 5:95 wt% 1305 °C; 42:58 wt% 1320 °C; 68:32 wt% 1330 °C) Figure 86.

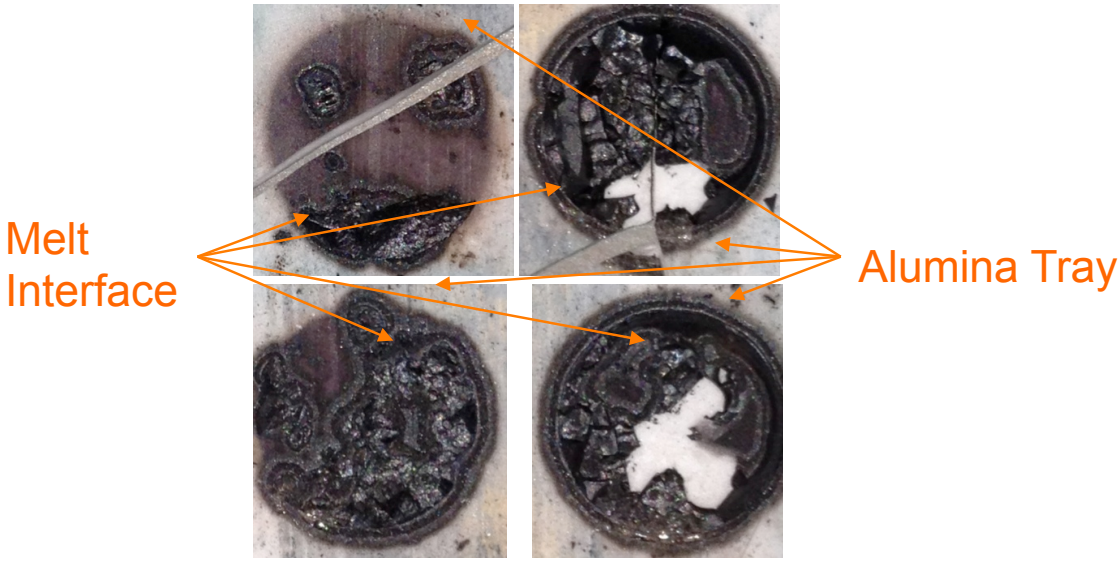

Figure 85: Melt interface of selected pellets sintered in N_2.

In addition, the Fe-Al-O system has eutectic points of approximately 1310 °C. The combination of these two systems has the likely effect of lowering the eutectic point further towards the sintering temperature used in this work. The requirement of aluminium for the lowest system melting point explains why the solidified liquid phase is extensive around the base of the pellet and not throughout the pellet. The inert N_2 atmosphere permitted the auto-reduction of the Fe_2O_3 to form FeO (as apposed to retaining Fe_2O_3 as in the oxidising environment presented earlier). SEM images of the interface are presented after the discussion of the individual samples (Figure 105).

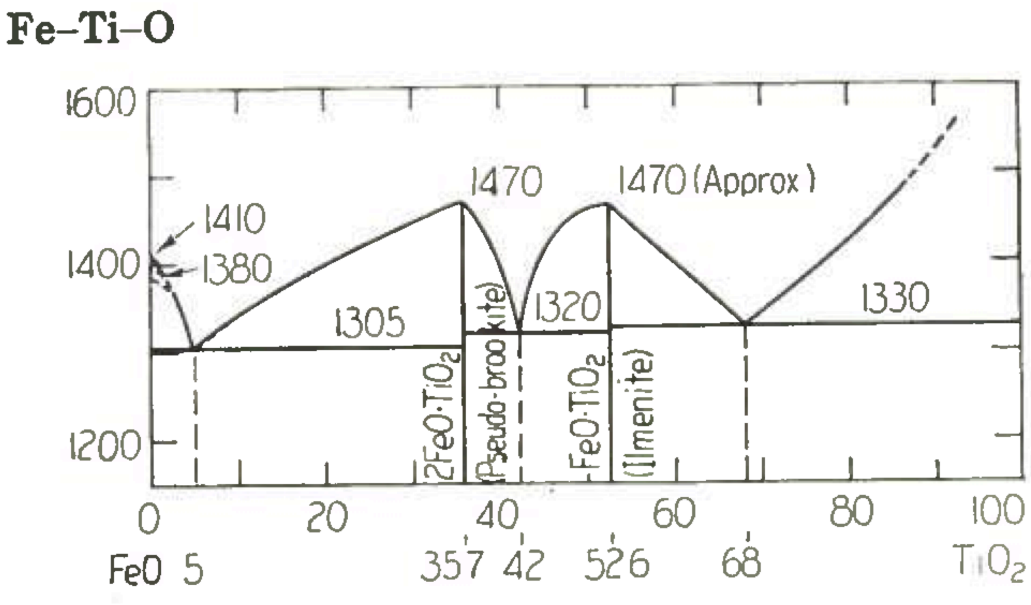

Figure 86: Fe-Ti-O system (Grieve and White 1939) *via* (Levin, Robbins et al. 1964)

4.3.1 Density

Table 26 shows the density of the various pellets sintered in an inert atmosphere. All of the samples are below the target of 92% TD and cannot be considered high quality, in regards to density. Also of note is the consistent decrease in sample density from the non-milled to the milled samples. This is unexpected and has not been seen in any previous work. This unusual result may be connected to the melting observed during sintering. It is plausible to suggest that the liquid phase prevented the densification of the pellets by restricting their movement, due to being adhered to the calcination tray, during sintering.

Precursor Treatment	Milled?	Density (g cm^{-3})	% TD
Untreated	No	3.97	84.3
Untreated	Yes	3.59	76.3
Zinc stearate	No	3.99	84.7
Zinc stearate	Yes	3.88	82.4
Aeroxide	No	3.96	84.0
Aeroxide	Yes	3.70	78.5
3% Glucose reduction	No	4.05	86.0
3% Glucose reduction	Yes	3.91	83.1
5% Glucose reduction	No	4.09	86.9
5% Glucose reduction	Yes	2.80*	59.6*
Hydrogen reduction	No	4.02	85.4
Hydrogen reduction	Yes	3.74	79.5

Table 26: Density of pellets sintered in N_2. Grouped by processing method. TD calculated as 4.71 g cm^{-3}. * - sample floated during measurement, thus density is an underestimate.

4.3.2 XRD AND SEM

4.3.2.1 UNTREATED

Figure 87 shows the XRD patterns for samples manufactured from the milled and non-milled untreated powders sintered in N_2. There is no significant change in the phase development between the milled and non-milled samples with both XRD patterns indicating the development of zirconolite, perovskite and ilmenite. This is in contrast to the samples manufactured from the same powders but sintered in air, which showed that milling produced single-phase samples as apposed the multi-phase samples from non-milled powders. Liquid phases are known to promote digestion and material incorporation in otherwise solid-state reactions. The similarity in the phase development of the two samples as shown by XRD has not explained the consistent decrease in product density between non-milled and milled powders. If there were confirmed differences in the phase development, this may have provided an explanation.

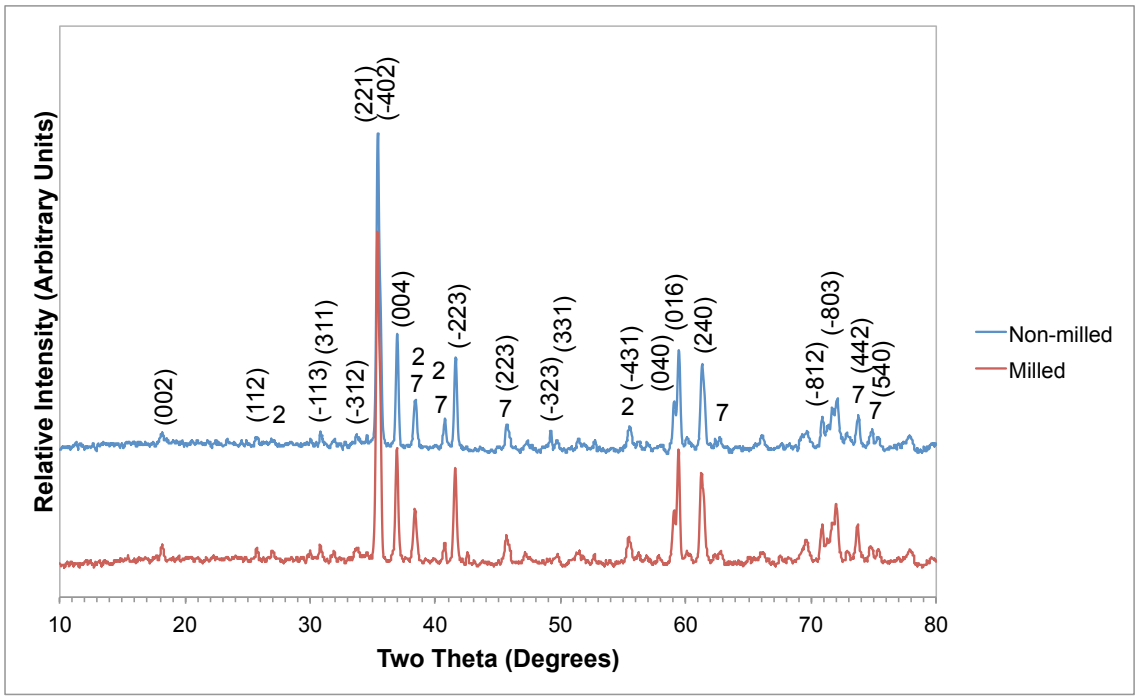

Figure 87: XRD patterns for samples manufactured from milled and non-milled untreated powders and sintered in nitrogen. Phases labelled: Miller indices, zirconolite; 2: perovskite; 7: ilmenite

SEM images of the sample manufactured from non-milled untreated powders are shown as Figure 88. There is a host phase of zirconolite with inclusions of ilmenite and perovskite. Cerium is present throughout the sample but, as confirmed by EDS, there are also localised concentrations in the centre of the perovskite grains, this is shown as the lighter grey area in the centre of the grain marked '2'. In these samples manufactured from non-milled material, the ceria is too coarse to be fully incorporated into the perovskite phases thus remaining as a cerium rich perovskite core. Also present are phases, labelled '7', of ilmenite. In the sample manufactured from milled powders, Figure 89, the cerium rich perovskite inclusions are not present, indicating the ceria has been sized reduced during milling. Noting that in section 4.1.1 the mill pot was coated with agglomerated material and it was thought that little or no size reduction of the powders had occurred. Again, it has been shown that milling performance cannot be judged by the appearance of the mill after milling.

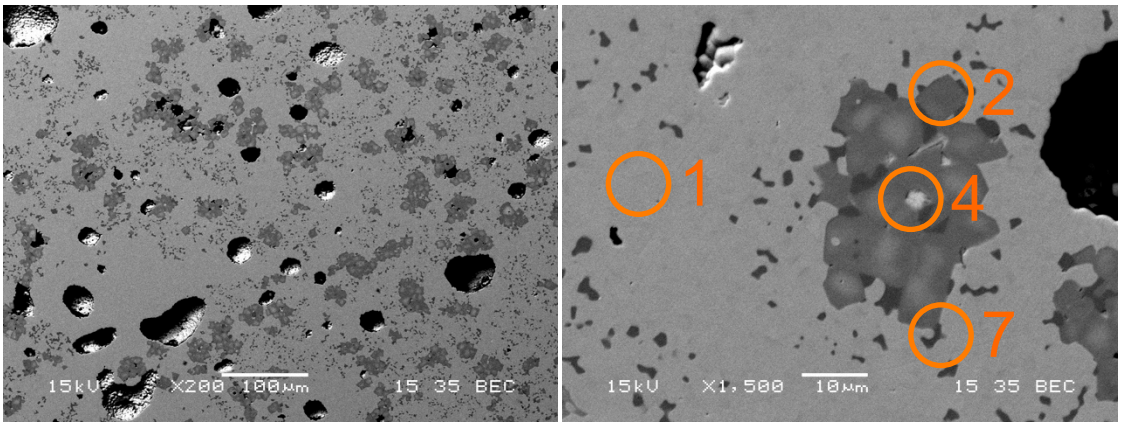

Figure 88: SEM images of sample manufactured from non-milled untreated powder and sintered in nitrogen. Phases labelled: 1: zirconolite; 2: perovskite; 4: zirconia; 7: ilmenite

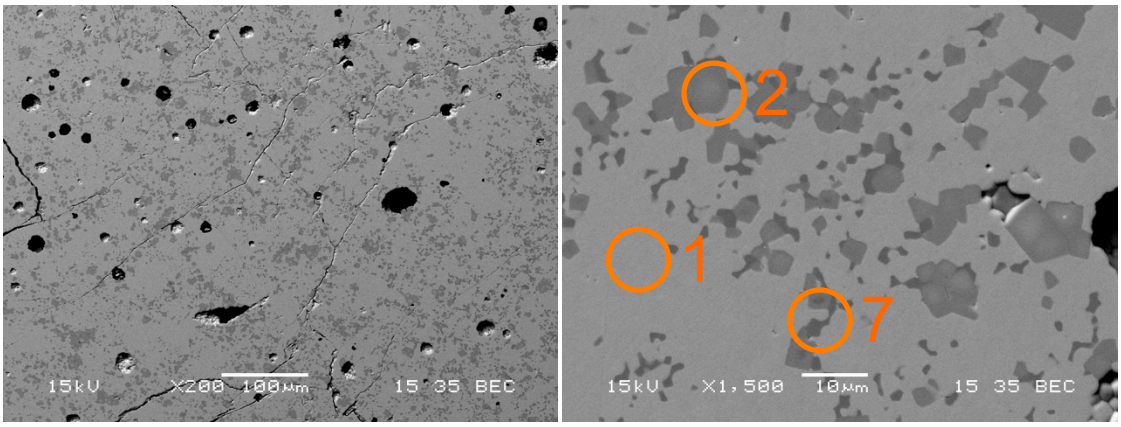

Figure 89: SEM images of sample manufactured from milled untreated powder and sintered in nitrogen. Phases labelled: 1: zirconolite; 2: perovskite; 7: ilmenite

4.3.2.2 Zinc Stearate

Figure 90 shows the XRD patterns for the samples manufactured from powders milled and non-milled with zinc stearate and sintered in nitrogen. Again, the two samples indicate the same phases present in both (zirconolite, ilmenite, perovskite). There is no significant change in the FWHM between the two samples indicating good compositional control in each phase. This is, again, likely due to the liquid phase aiding phase development.

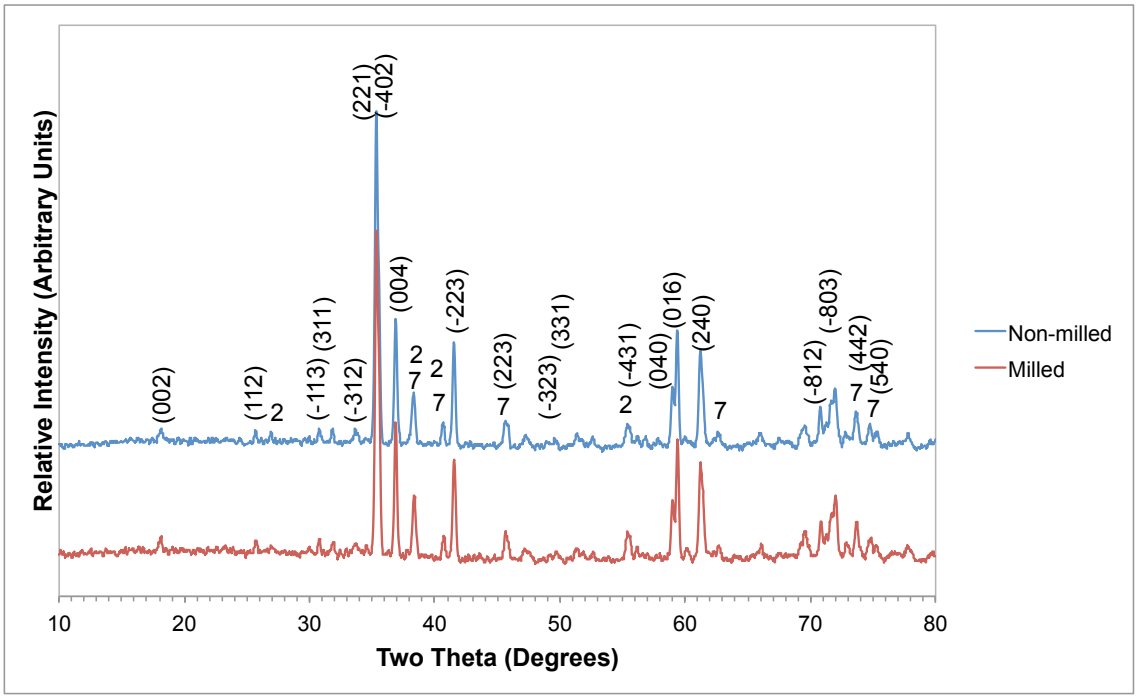

Figure 90: XRD patterns for samples manufactured from milled and non-milled powders with 1.5 wt% zinc stearate and sintered in nitrogen. Phases labelled: Miller indices, zirconolite; 2: perovskite; 7: ilmenite

Figure 91 shows the SEM images of sample manufactured from non-milled powders. Regarding the phase development, the sample is the same as the one manufactured from untreated powders. Both samples have a host phase of zirconolite interspersed with zirconia, ilmenite and perovskite. In the milled sample, SEM images shown as Figure 92, there are no zirconia particles but zirconolite, perovskite and ilmenite are present. The size of the largest pore visible decreases from 100 μm to ~30 μm between the non-milled and milled samples.

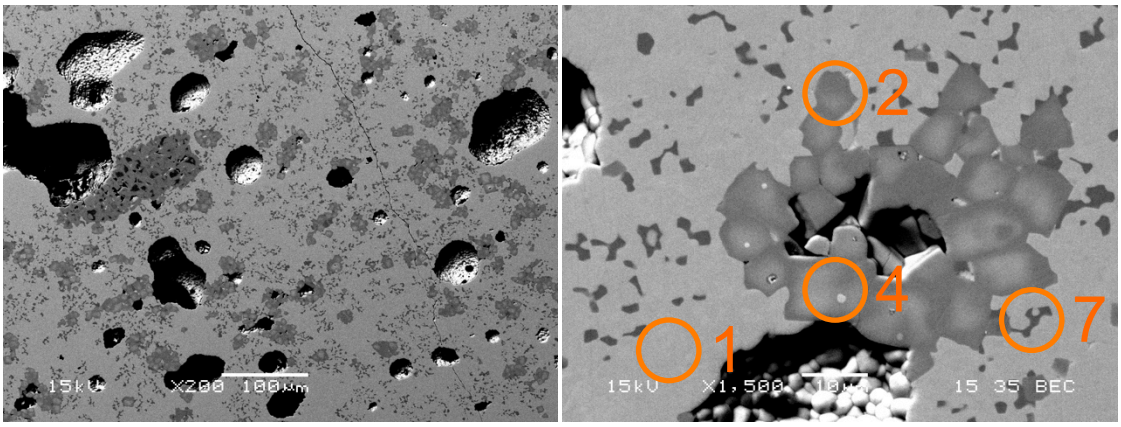

Figure 91: SEM images of sample manufactured from non-milled powders with zinc stearate and sintered in nitrogen. Phases labelled: 1: zirconolite; 2: perovskite; 4: zirconia; 7: ilmenite

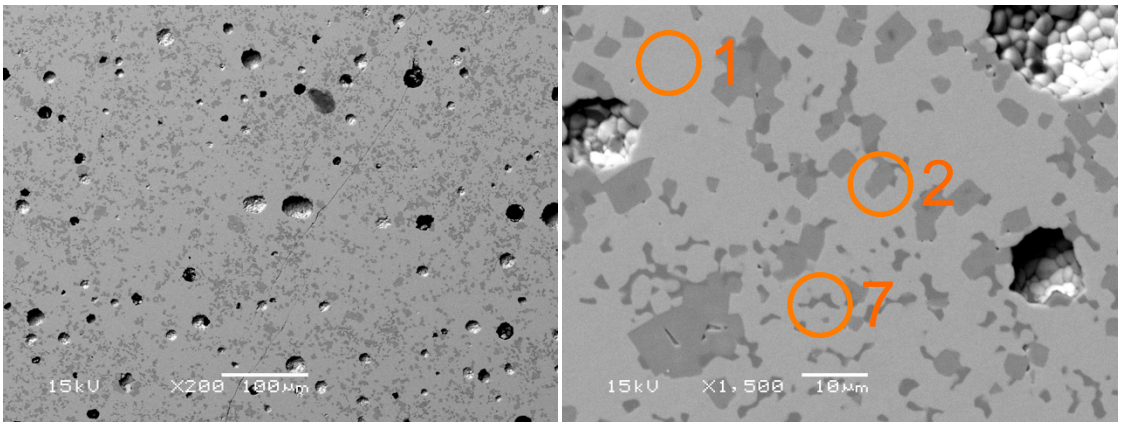

Figure 92: SEM images of sample manufactured from powders milled with zinc stearate and sintered in nitrogen. Phases labelled: 1: zirconolite; 2: perovskite; 7: ilmenite

4.3.2.3 Aeroxide

Figure 93 shows the XRD patterns for the samples manufactured from powders milled and non-milled with Aeroxide and sintered in nitrogen. There are no significant differences between the two patterns with both showing the same development of the zirconolite main phase with secondary ilmenite and perovskite. SEM images for the samples made from non-milled powders, Figure 94, and milled, Figure 95, show a host phase of zirconolite interspersed with ilmenite and perovskite, in confirmation of the XRD data.

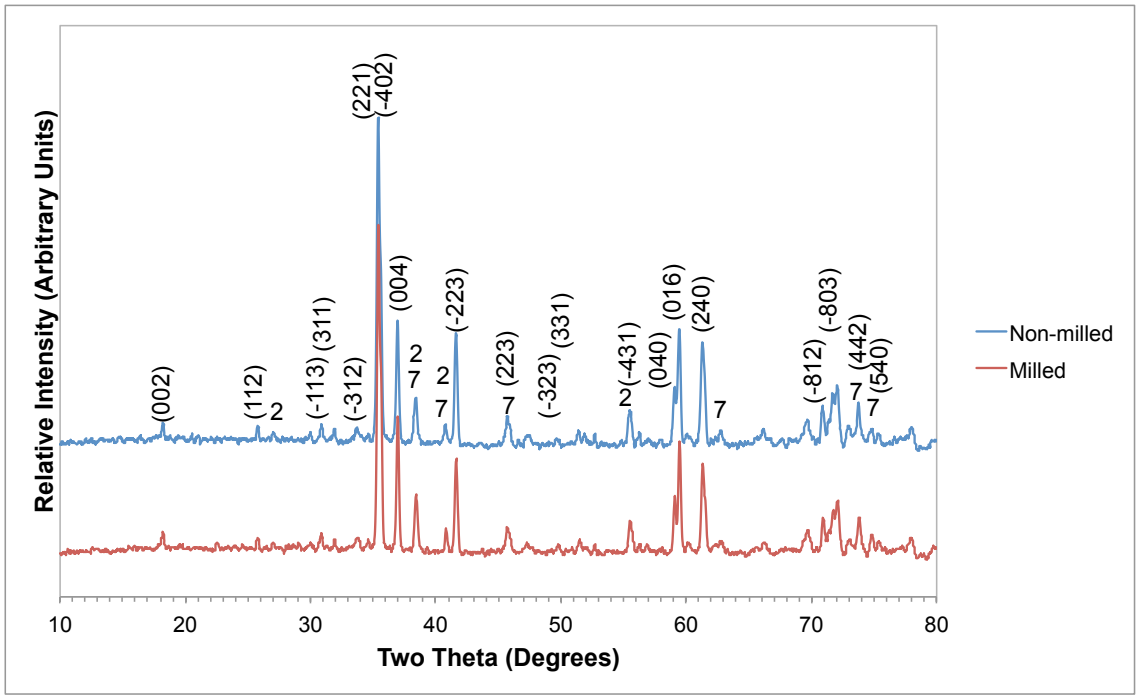

Figure 93: XRD patterns for samples manufactured from milled and non-milled powders with 0.5 wt% Aeroxide and sintered in nitrogen. Phases labelled: Miller indices, zirconolite; 2: perovskite; 7: ilmenite

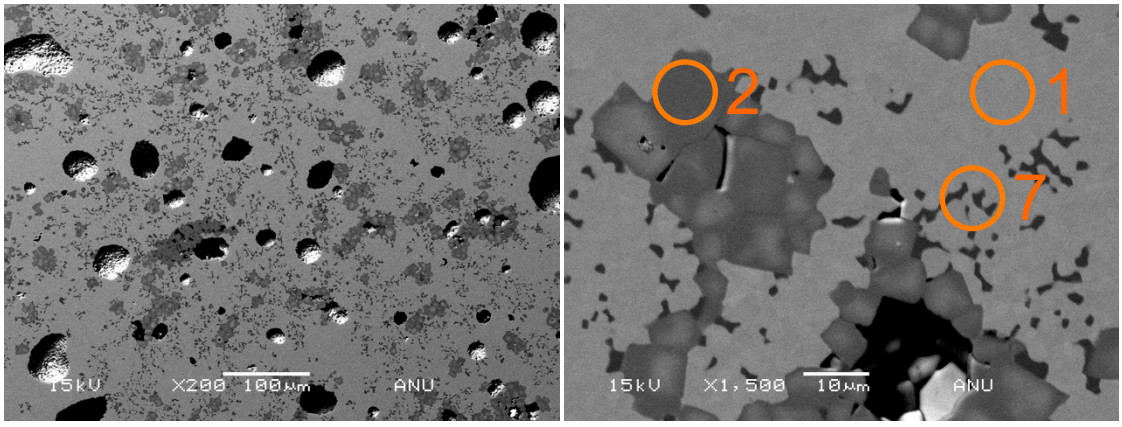

Figure 94: SEM images of sample manufactured from non-milled powders with Aeroxide and sintered in nitrogen. Phases labelled: 1: zirconolite; 2: perovskite; 7: ilmenite

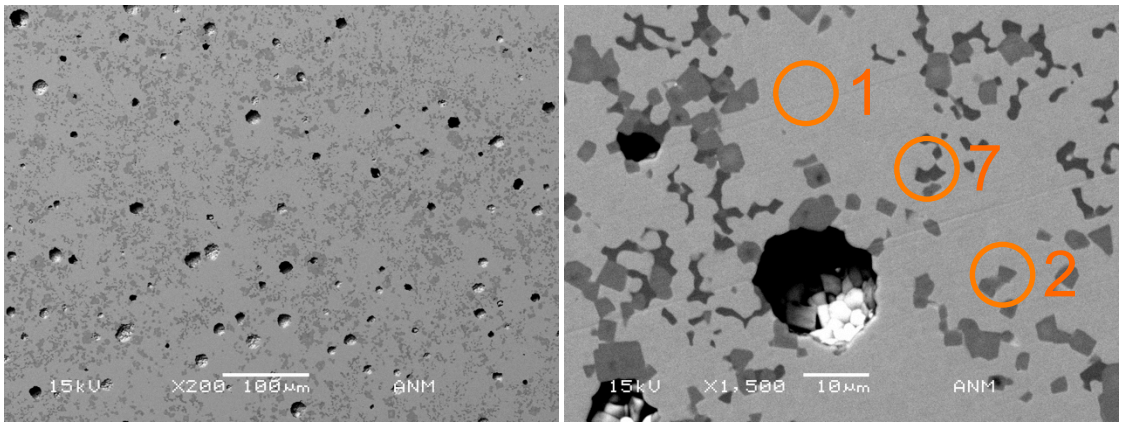

Figure 95: SEM images of sample manufactured from powders milled with Aeroxide and sintered in nitrogen. Phases labelled: 1: zirconolite; 2: perovskite; 7: ilmenite

4.3.2.4 Reduced Precursors

Figure 96, Figure 99 and Figure 102 show the XRD patterns for both the non-milled and milled 3 wt% glucose, 5 wt% glucose and hydrogen reduced powders, respectively, sintered in nitrogen. Again, between each of the milled and non-milled samples there are no significant differences in the phase developments, indicated by XRD. There are also no significant differences between each of the reduced powder samples and those manufactured from fully oxidised powder (untreated, zinc stearate, Aeroxide).

Figure 97 and Figure 98 show the SEM images of the non-milled and milled powders reduced by 3 wt% glucose. Both show the expected zirconolite, ilmenite and perovskite phase development. There does not appear to be any difference in the phase development, phase size or distribution in this sample when compared to the samples manufactured from fully oxidised powders. Figure 100 and Figure 101 show the samples manufactured from powders reduced by 5 wt% glucose, non-milled and milled, respectively. They show the same phase development and distribution as all of the other samples sintered in N_2. Figure 103 and Figure 104 show the samples manufactured from the non-milled and milled, respectively, hydrogen reduced powders. They also show the same phase development as all of the other samples sintered in nitrogen.

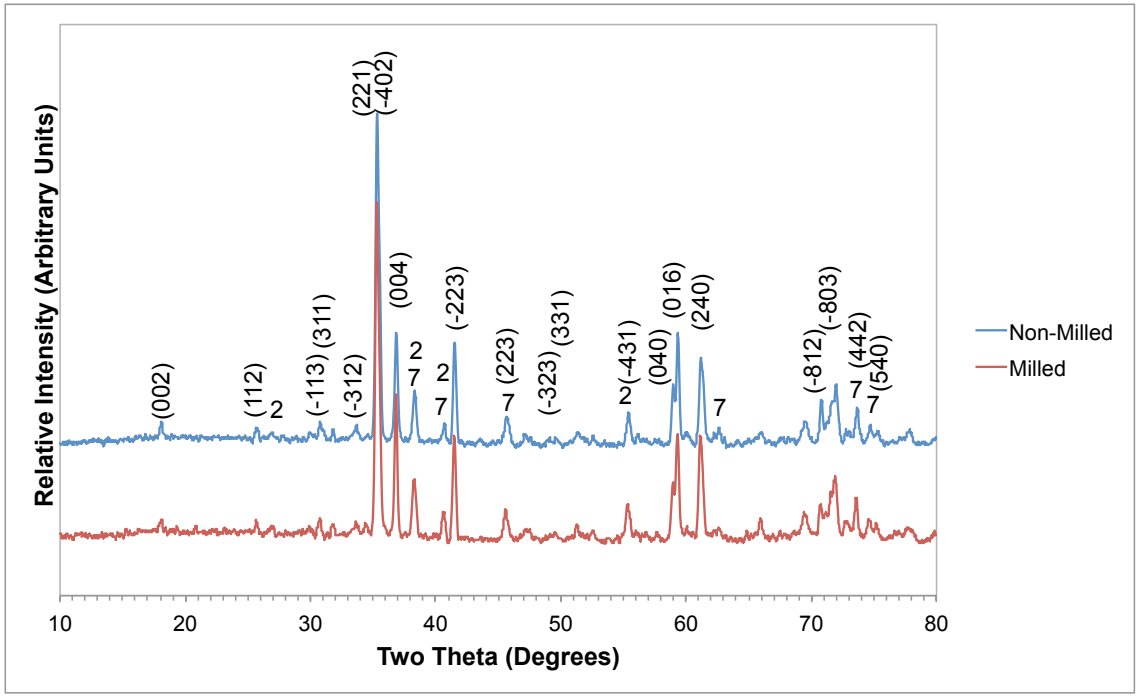

Figure 96: XRD patterns for samples manufactured from milled and non-milled powders reduced by 3 wt% glucose and sintered in nitrogen. Phases labelled: Miller indices, zirconolite; 2: perovskite; 7: ilmenite

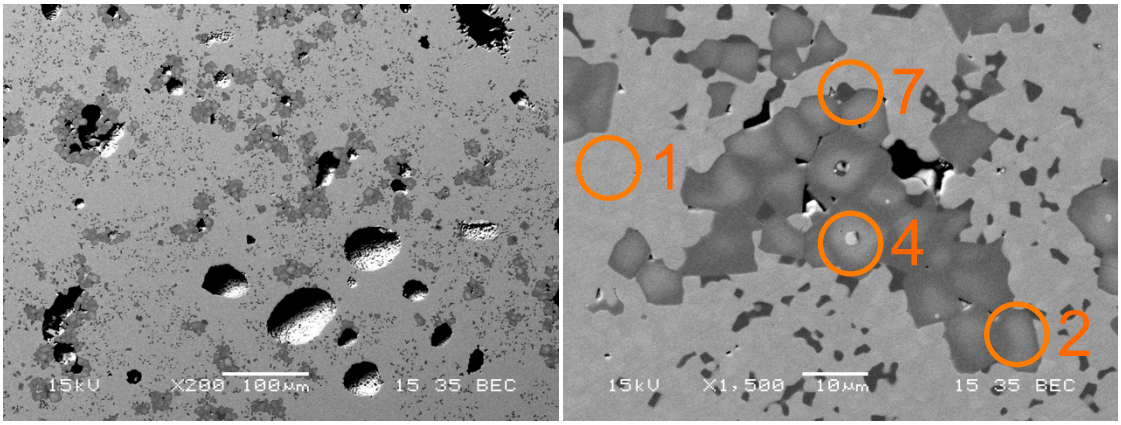

Figure 97: SEM images of sample manufactured from non-milled 3 wt% glucose reduced powders and sintered in nitrogen. Phases labelled: 1: zirconolite; 2: perovskite; 4: zirconia; 7: ilmenite

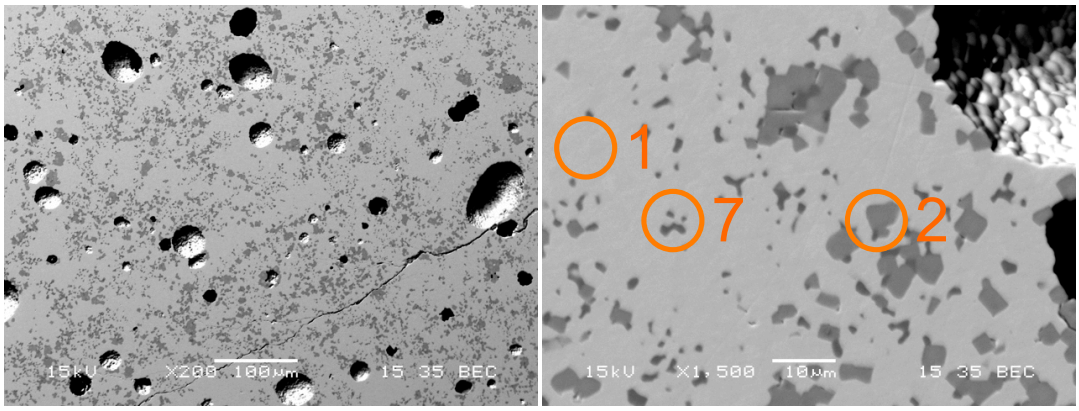

Figure 98: SEM images of sample manufactured from milled 3 wt% glucose reduced powders and sintered in nitrogen. Phases labelled: 1: zirconolite; 2: perovskite; 7: ilmenite

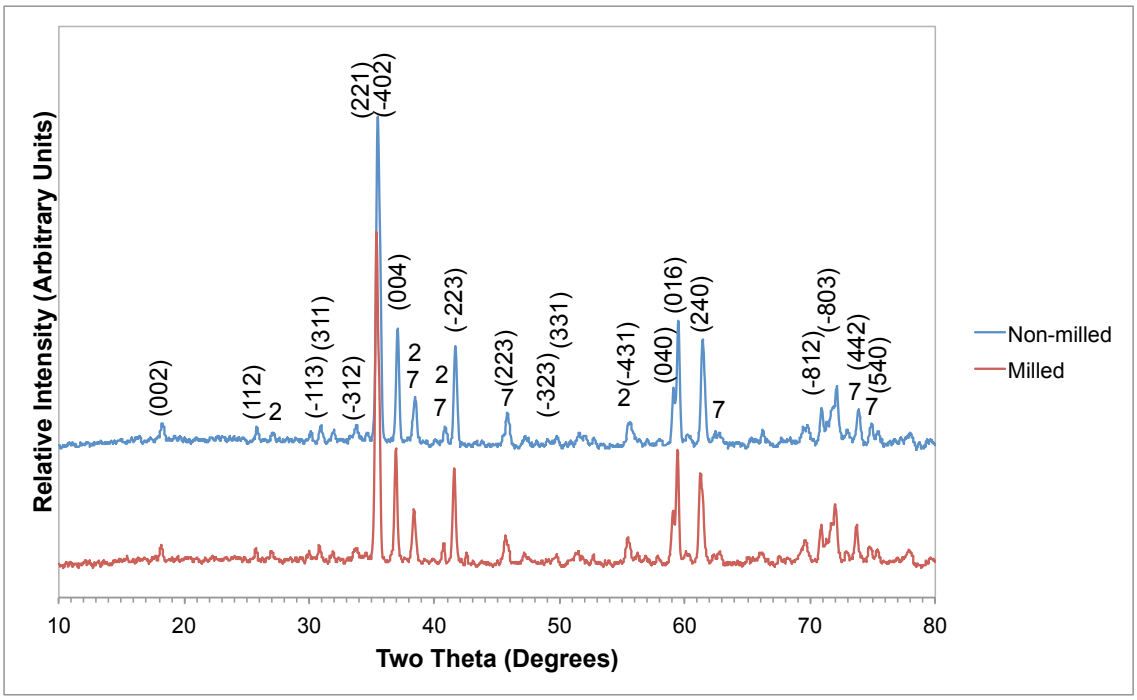

Figure 99: XRD patterns for samples manufactured from milled and non-milled powders reduced by 5 wt% glucose and sintered in nitrogen. Phases labelled: Miller indices, zirconolite; 2: perovskite; 7: ilmenite

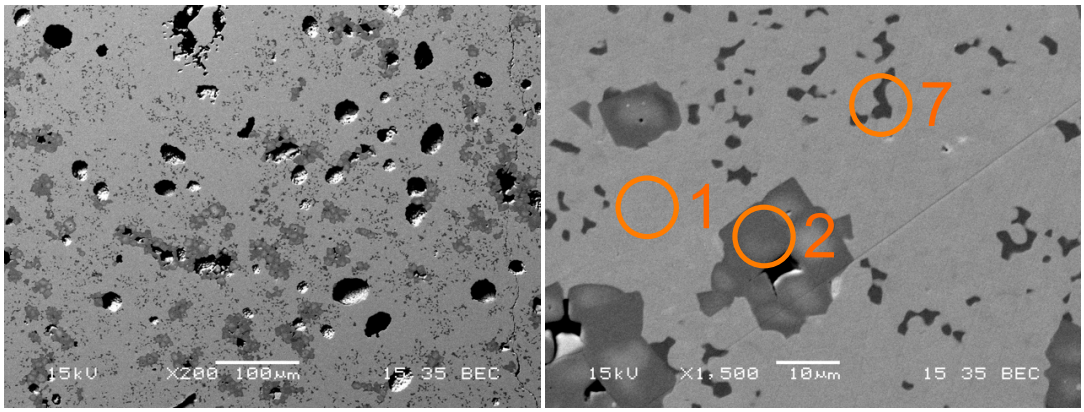

Figure 100 SEM images of sample manufactured from non-milled 5 wt% glucose reduced powders and sintered in nitrogen. Phases labelled: 1: zirconolite; 2: perovskite; 7: ilmenite

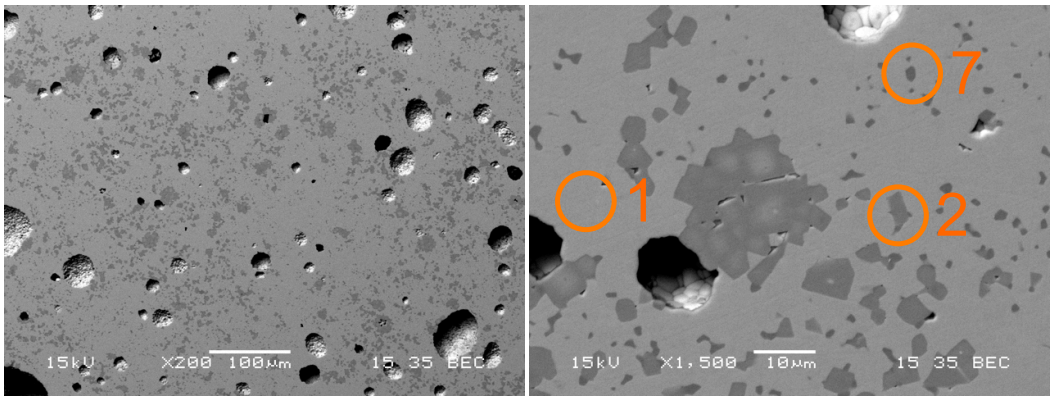

Figure 101: SEM images of sample manufactured from milled 5 wt% glucose reduced powders and sintered in nitrogen. Phases labelled: 1: zirconolite; 2: perovskite; 7: ilmenite

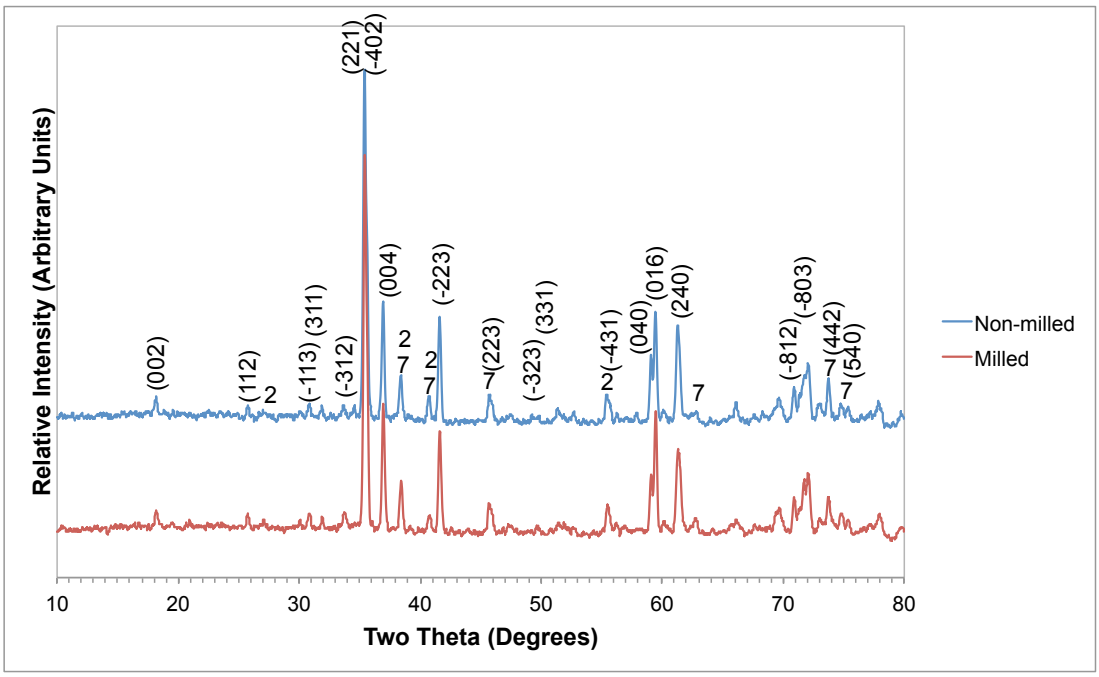

Figure 102: XRD patterns for samples manufactured from milled and non-milled powders reduced hydrogen and sintered in nitrogen. Phases labelled: Miller indices, zirconolite; 2: perovskite; 7: ilmenite

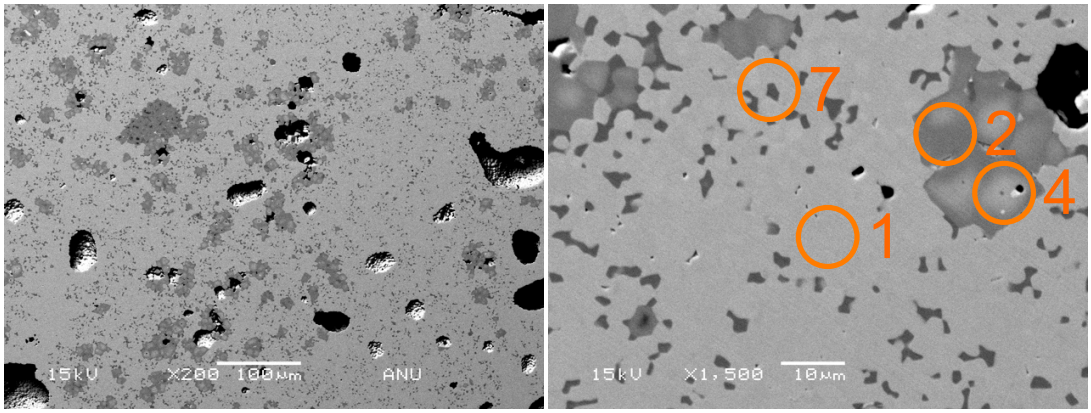

Figure 103: SEM images of sample manufactured from non-milled hydrogen reduced powders and sintered in nitrogen. Phases labelled: 1: zirconolite; 2: perovskite; 4: zirconia; 7: ilmenite

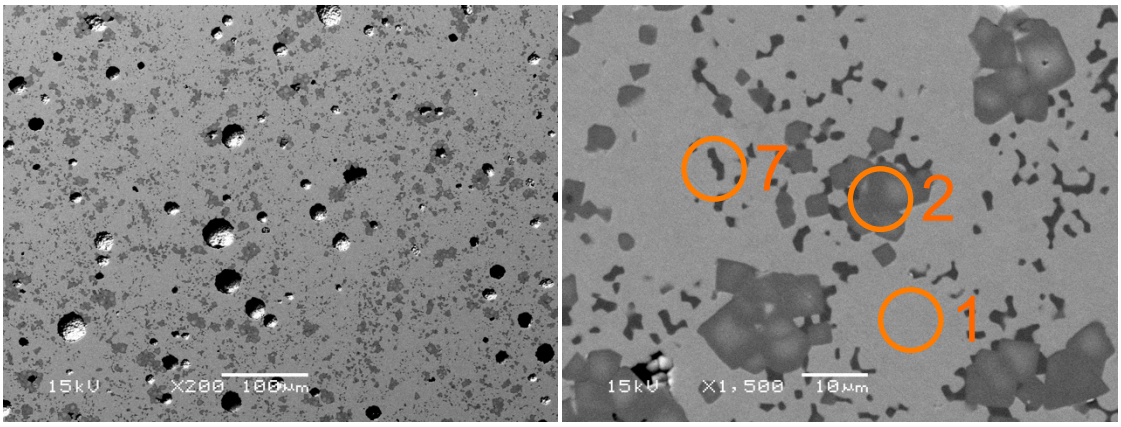

Figure 104: SEM images of sample manufactured from milled hydrogen reduced powders and sintered in nitrogen. Phases labelled: 1: zirconolite; 2: perovskite; 7: ilmenite

4.3.2.5 Melt Interface Region

Figure 105 shows an example of the melt interface region between the pellet and the Al_2O_3 calcination tray (the base of the pellet is the top of the images). There is a clear reaction zone where the composition of the phases changes gradually between the pure Al_2O_3 tray (11) and the expected zirconolite (1). The first interface section (left image) shows an unidentified aluminium and iron rich phase (dark threads, 12), which blends into the more abundant titanium, iron and aluminium rich phase (13). This phase blends with the zirconolite (1) until the edge of the pellet is reached and the sample becomes wholly the expected zirconolite. The base of the pellet is at the point where the zirconolite main phase begins to taper into the other phases. It appears that the molten, Fe/Ti phase has extended from below the pellet into the tray. The abundance of iron and titanium rich phases in the interface indicates that the molten phase was predominately a combination of these two species.

No phase diagram for the Fe-Al-Ti-O system could be found, however, the diagrams for Fe-Ti-O and Fe-Al-O both show a eutectic point in each system at approximately 1300 °C. It is possible to infer that a further eutectic point would exist in the Fe-Al-Ti-O system that has a temperature of below 1300 °C (i.e. lower than the eutectic points in the two individual systems). This liquid phase is responsible for the adhesion between the pellet and the tray. If the calcination

tray was made from a different material, e.g. zirconia, there may not have been the same level of melt interface. It is also likely that this melt region restricted pellet shrinkage during consolidation leading to the lower than expected densities recorded.

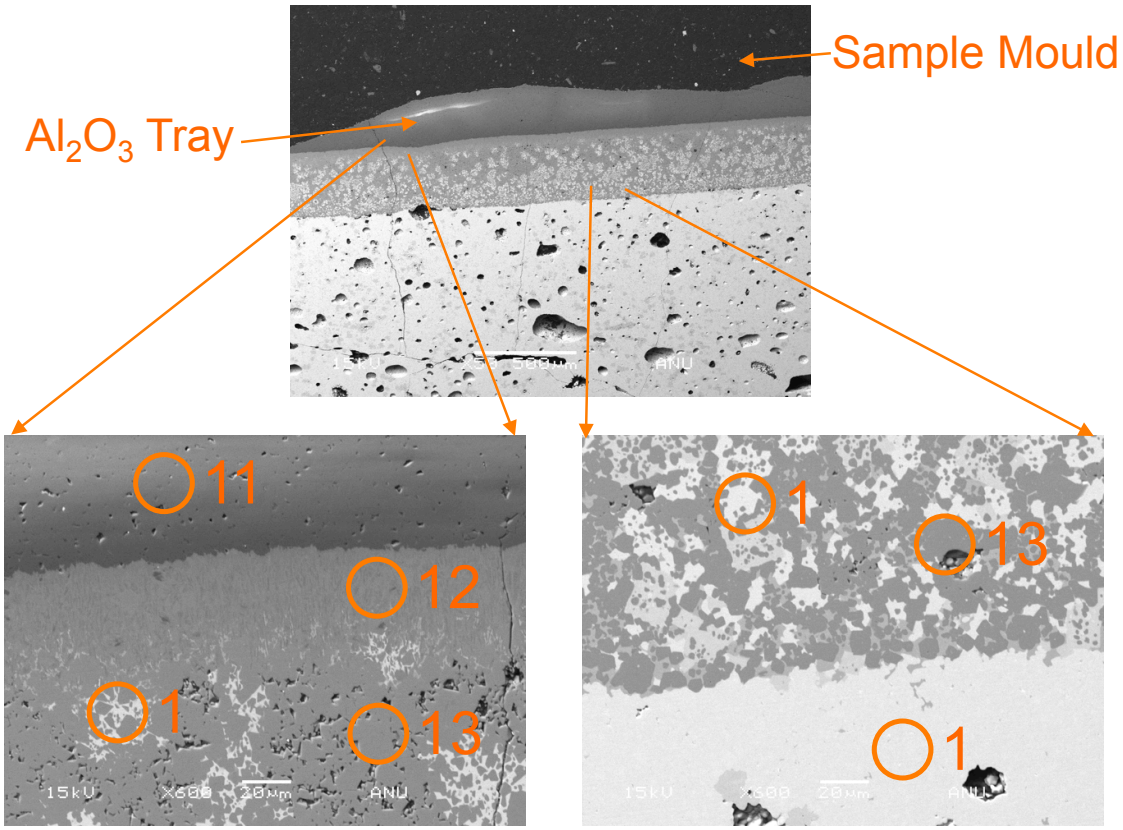

Figure 105: Detail of melt interface region from the pellet manufactured from non-milled powders with Aeroxide. Phases identified, 1- zirconolite; 11 – Al_2O_3 (calcination boat); 12- Dark thread, Al, Fe rich with Ti phase; 13 – Ti, Fe, Al rich phase.

4.3.2.6 Discussion

Overall the impression is one of uniformity. Phase development, shown by XRD data, has been consistent throughout all of the precursor treatments irrespective of whether the sample was manufactured from milled or non-milled powders. This is in contrast to the sample sintered in air, which showed different phase development in the samples dependant on whether they were made from milled powders or not. It is thought that the N_2 atmosphere allowed the auto-reduction of Fe_2O_3 to FeO, which in turn formed a eutectic mixture with TiO_2/Al_2O_3, which is liquid at 1305 °C. It is recognised that the precursor

system is far more complex than the simple two component phase diagram presented earlier. However, the melting point of pure FeO (1377 °C) is above the sintering temperature and the presence of Ti in the interface region (Figure 105) does suggest that some (Fe,Ti)O_x mixture has been produced.

5 Discussion

This work began as an exploration of the effect of different additives and precursor treatments on the behaviour of powders during planetary milling. Examination of the mill pot after milling showed that using zinc stearate as a lubricant meant that the powders were less likely to agglomerate on to the side walls than if no additive was used. The milling media were shown to be 'clean' and this may offer an explanation for the mechanism as to how the lubricant behaves in keeping powders free flowing during milling. If the hydrocarbon lubricant preferentially coats the metal surfaces, preventing the accumulation of material on the walls or media, the powders cannot settle anywhere in the mill, promoting free flowing behaviour. When untreated or reduced powders were milled, a thick layer of powder coating formed on the media. This suggests that while the powders were not agglomerating on the side walls, implying the powders are able to be freely milled, mill discharge times would potentially be lengthy as the powders must be dislodged from the media before they can be discharged.

The pellets manufactured from milled powders and sintered in air form predominately single-phase zirconolite, as intended. The low mechanical strength and high level of porosity were unexpected as the level of planetary milled was thought to be sufficiently aggressive to produce fine powders that can be used to make dense samples. This may have been incorrect. None of the non-milled pellets had enough strength to withstand the sample preparation procedures. In Figure 73, the speckled surface of the non-milled pellets shows phase heterogeneity in the samples. If the components of the pellet are not fully

bonded, they will be weakly held together and thus weak to the abrasive forces utilised in SEM sample preparation. There was no change in the XRD patterns of the zirconolite phases between the samples manufactured from reduced or fully oxidised powders. It is thought that during sintering, the reduced precursors are re-oxidised before developing into the zirconolite phase.

Pellets sintered in nitrogen were not similar to those sintered in air. All of the pellets were stuck to the Al_2O_3 tray indicating a liquid phase had formed during heat treatment. Examination of the interface region showed iron rich phases interspersed with the Al_2O_3 calcination boat indicating that the liquid phase contained iron. Grieve and White (Grieve and White 1939) gives the Fe-Ti-O phase diagram indicating three eutectic points at approximately the sintering temperature. The addition of Al_2O_3 in to the system has lowered the overall melting point below that of the Fe-Ti-O or Fe-Al-O systems alone. These samples are the same material system as in Chapter 2, except the iron was supplied as Fe_3O_4 (as apposed to Fe_2O_3 in this work). Both pieces of work show the same phase development of zirconolite, perovskite and ilmenite. No evidence of a liquid phase was detected in Chapter 2 but the work in this chapter would suggest that it might be present. If the pores in this work are characteristic of a liquid phase, the pores in Chapter 2 may also be due to a liquid phase forming. The conclusion that the lubricant residue interfered with the product formation is still valid as shown by the lack of correlation between milling and product density and confirmed by the samples with lubricant removal *ex-situ* in Chapter 4. Also of note are the high density products manufactured when Al_2O_3 or Ti^{3+} was utilised for charge compensation in Chapter 4. It is thus recognised that using Fe_2O_3 for charge compensation should be avoided, as it is likely to form a molten phase with TiO_2, which leads to heterogeneous phase development in the final products. Ti_2O_3 or Al_2O_3 are suitable alternatives as is MgO.

6 Conclusions

The performance of various precursor treatments was tested and it was shown that untreated powders tended to agglomerate on the walls of the milling pot as well as the media. This was linked to powder performance in attrition mills. Powders milled with zinc stearate did not adhere to the mill pot or the media, this suggests that the mode of action for milling lubricants is to interrupt metal and powder interactions. Reduced precursors and precursors milled with Aeroxide partially adhered to the mill walls and media indicating their performance in an attrition mill is worth further study. Repetition of the milling study may show a correlation between the precursor treatments and the product densities (similar to the relationship shown in Chapter 3). The extent of powders adhesion to the milling media is likely to be an indicator of mill discharge times with greater amounts of powder adhered to the media indicating an extended discharge duration.

Samples sintered in air will go on to form the single host phase zirconolite intended, regardless of the precursor oxidation state. Heat treatment in air is sufficient to re-oxidise the precursors before phase development. However, the pellets manufactured were not of sufficient density. This is likely to be a result of insufficiently aggressive milling.

Samples sintered in nitrogen formed a liquid phase during sintering that is likely to be $(Fe,Ti)O_x$. This phase only formed when the FeO was not fully oxidised to Fe_2O_3. The further use of FeO_x for charge compensation is not recommended due to the potential to form liquid phases during sintering, which have varying compositions. However, this liquid phase aided the digestion and incorporation of all precursors during sintering (as shown by the XRD patterns of the samples).

In order to directly compare CUP samples to HIP, CUP samples must be sintered in an inert (e.g. nitrogen) atmosphere; an oxidising environment is not representative of a HIP can.

6: Additional Work

1 Abstract

This chapter discusses four pieces of work that were either exploratory or brief in nature. One section details an investigation into the effect of the duration of attrition milling on the properties (density, microstructure, phase development) of zirconolite ceramics. In the study a sample was taken every 10 minutes from a continuously operating attrition mill. These samples were cold uniaxially pressed and the density of the pellets was measured. In addition the samples underwent analysis by SEM. The density of the samples increased until approximately 20 min where it became constant for the remainder of the milling duration. The homogeneity of the samples improved up to ~45 minutes.

The next batch of work examined the concept of loose powder digestion. In this experiment, fine precursors were reacted with the 'realistic' ceria as a loosely mixed heap of powders. Initial XRD results show a diminished response to free ceria with increasing reaction temperatures. However, SEM of the pellets showed large unincorporated inclusions of ceria and this method cannot be recommended for implementation.

The final two sections of work discuss a modified agitator shaft for the attrition mill and the use of Aeroxide as a milling additive.

2 Progression of Milling

2.1 Introduction

A large part of the work presented so far has centred on the attrition mill. Most of the work has used milling durations of 30 or 60 min. Exploratory work sought to analyse how the duration of milling affected the quality, judged on density and phase homogeneity, of zirconolite samples manufactured by CUP.

2.2 Materials and Methods

The target formulation was $Ca_{0.75}Ce_{0.25}ZrTi_{1.5}Fe_{0.5}O_7$. In contrast to previous work, the calcium and titanium was provided as $CaTiO_3$, with the balance of titanium from TiO_2. Zirconium and iron were provided as ZrO_2 and Fe_2O_3, respectively. Cerium, as the plutonium surrogate, was from the 'realistic' ceria source.

A batch of 1000 g was milled with 1 wt% of zinc stearate as the milling lubricant. The same attrition mill and internal geometry as in Chapter 2, operating in the dry mode, was used. The powder batch was charged into the attrition mill whilst it was operating at 1.73 m s^{-1} (200 RPM). The mill was quickly brought to the desired speed of 4.32 m s^{-1} (500 RPM) and ran for 60 min. Samples of approximately 10-30 g were taken every 10 minutes without stopping the mill. The first powders to be discharged for each sample were discarded, as it was impossible to determine if this was non-milled material from the grate or material from the bulk powders. The remaining powders were discharged from the mill at the same operating speed as they were charged (1.73 m s^{-1}).

Pellets were manufactured from each of the powder samples. Each pellet (diameter = 15 mm) was made from 2.0 g of powder and CUP by 2 tonnes (~110 MPa) of force. The pellets, seven in total, were transferred to a calcination boat and sintered at 1320 °C for 2 hours. The temperature ramp rates were 2 °C min^{-1} to 200 °C, 3 °C min^{-1} to 700 °C (for lubricant burn out) and 5 °C to 1320 °C. The sintering atmosphere was air.

The density of each pellet was measured. Each of the pellets was cut in half and hot mounted for SEM imaging. Each sample was ground by successively finer grit papers (500, 800) before polishing with diamond spray (6, 3 μm). The pellet manufactured from the non-milled powders (i.e. the 0 min sample) was damaged during sample preparation due to its weak nature and was not imaged.

2.3 Results

2.3.1 Density

Figure 106 shows the density of the samples as a function of milling time. The chart clearly shows that extending the duration of milling increases the density of the samples up to a maximum of ~96% TD. Again, the target was for the samples to have densities greater than 92% TD. This maximum is reached at approximately 20 min and this may suggest a practical limit for milling duration. Any further milling does not improve the density of the products and, for this consideration, is a waste of time and energy. The trend of the density variation with duration suggests that ~96% TD is the highest density achievable with the precursors chosen in an attrition mill at a tip speed of 4.32 m s^{-1} and after consolidation by CUP. Processing these materials by HIP may improve the density further, should that be required.

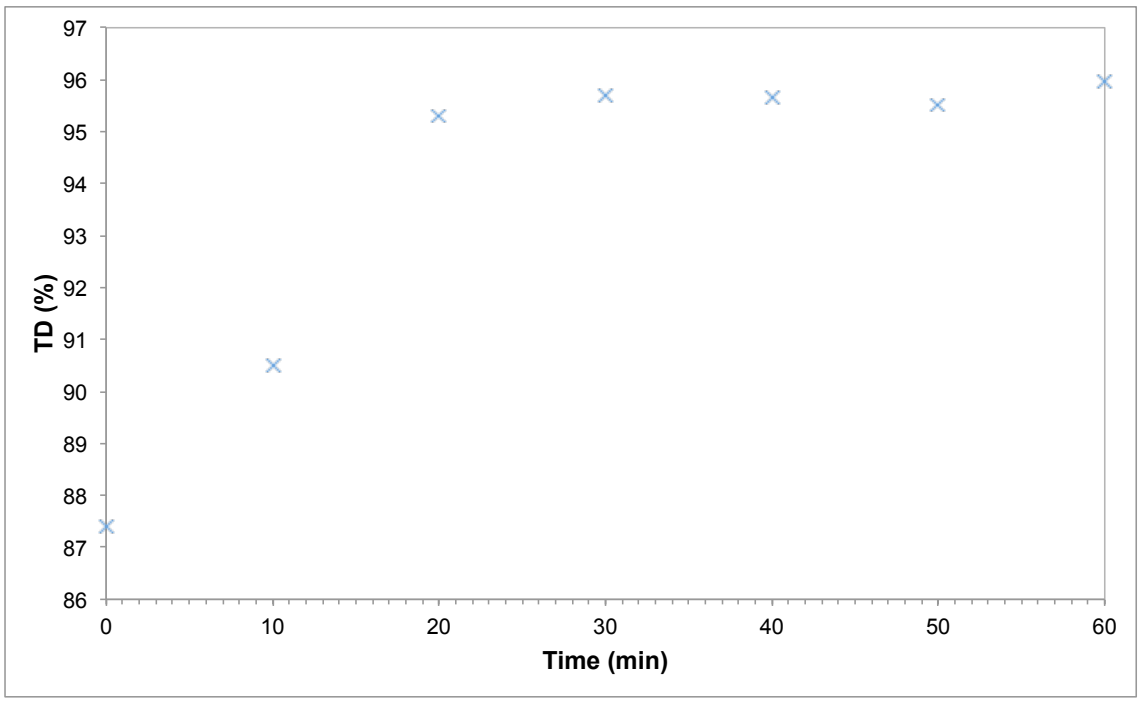

Figure 106: Density progression of samples with increased milling duration. Theoretical Density = 4.79 g cm^{-3}.

2.3.2 SEM

Figure 107 shows SEM images for the samples manufactured from increasing duration of attrition milling. The sample manufactured from non-milled powders (i.e. '0 min') did not have sufficient mechanical strength to be

prepared for SEM. Demonstrated by the imaged samples, there is a clear decrease in the size of non-milled ceria as the duration of the milling operation increases. In the '10 min' sample, large (~100 μm) unincorporated ceria grains are visible. The sample also contains unincorporated zirconia. In addition, the sample is porous. The '20 min' sample still shows unincorporated ceria yet the host phase appears to be visibly less porous than the '10 min' sample, which is reflected in the higher density of the '20 min' sample. The density of the samples starts to reach a maximum after approximately 20 min of milling but interestingly, the '30 min' sample still shows unincorporated ceria. The higher magnification image was an attempt to find the obvious ceria inclusions and this was the largest ceria inclusion visible. The lower magnification image shows the sample to only contain one other small (<5 μm) ceria inclusion. The '40 min' sample shows a further reduction in visible ceria inclusions. The '50 min' and '60 min' samples do not show any obvious sign of unincorporated ceria.

During imaging, each sample was extensively checked for free ceria and images of the worst (i.e. largest) unincorporated particles were selected for presentation here. In terms of phase development and in order to achieve no apparent residual ceria, milling for approximately 40-50 min at 4.32 m s^{-1} is recommended. There does not appear to be any improvement in phase homogenisation by milling for a further 10 min (i.e. to 60 min).

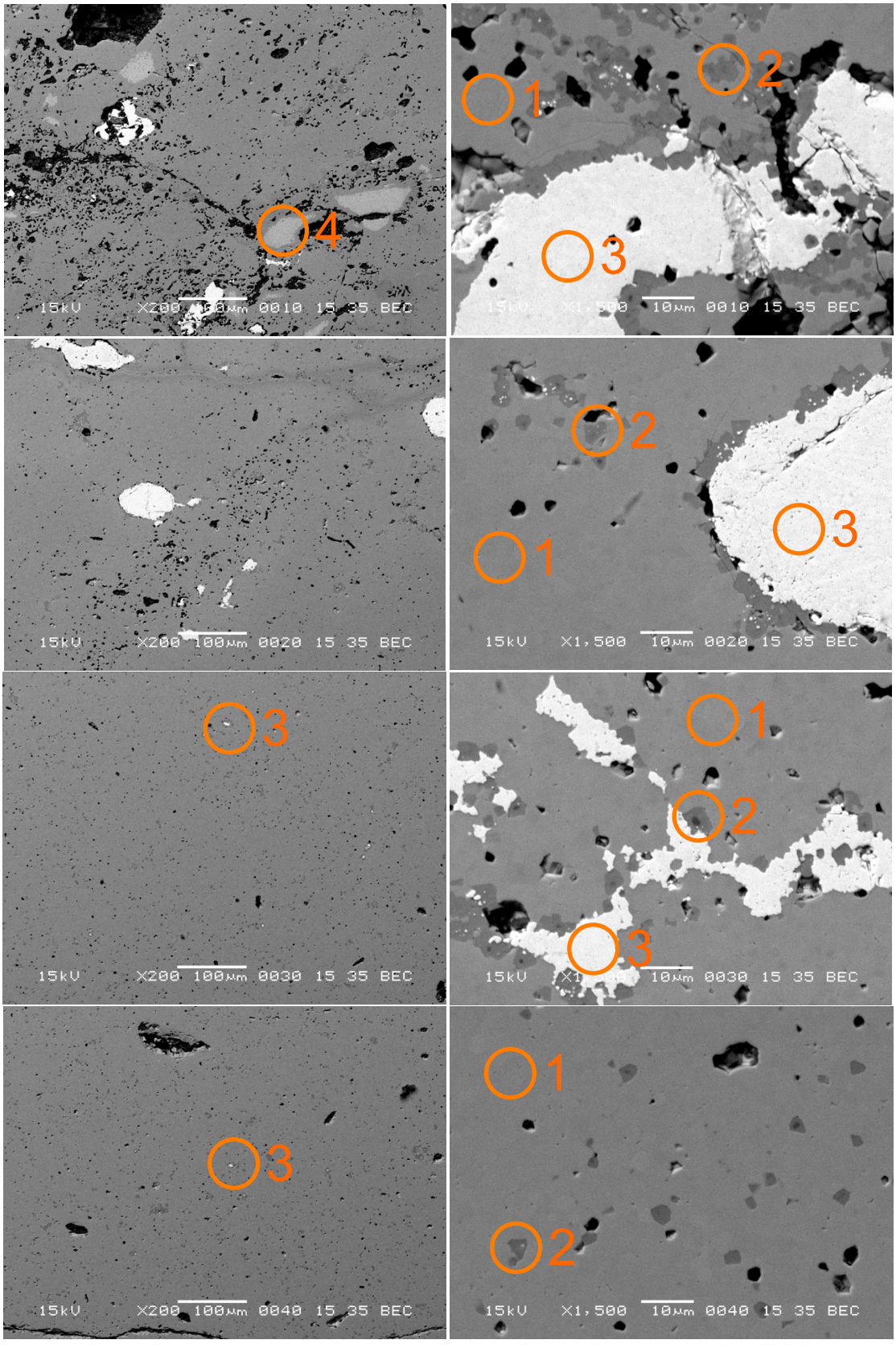
4
15kV X200 100µm 0010 15 35 BEC
1
2
3
15kV X1,500 10µm 0010 15 35 BEC
15kV X200 100µm 0020 15 35 BEC
2
1
3
15kV X1,500 10µm 0020 15 35 BEC
3
15kV X200 100µm 0030 15 35 BEC
1
2
3
15kV X1 10µm 0030 15 35 BEC
3
15kV X200 100µm 0040 15 35 BEC
1
2
15kV X1,500 10µm 0040 15 35 BEC

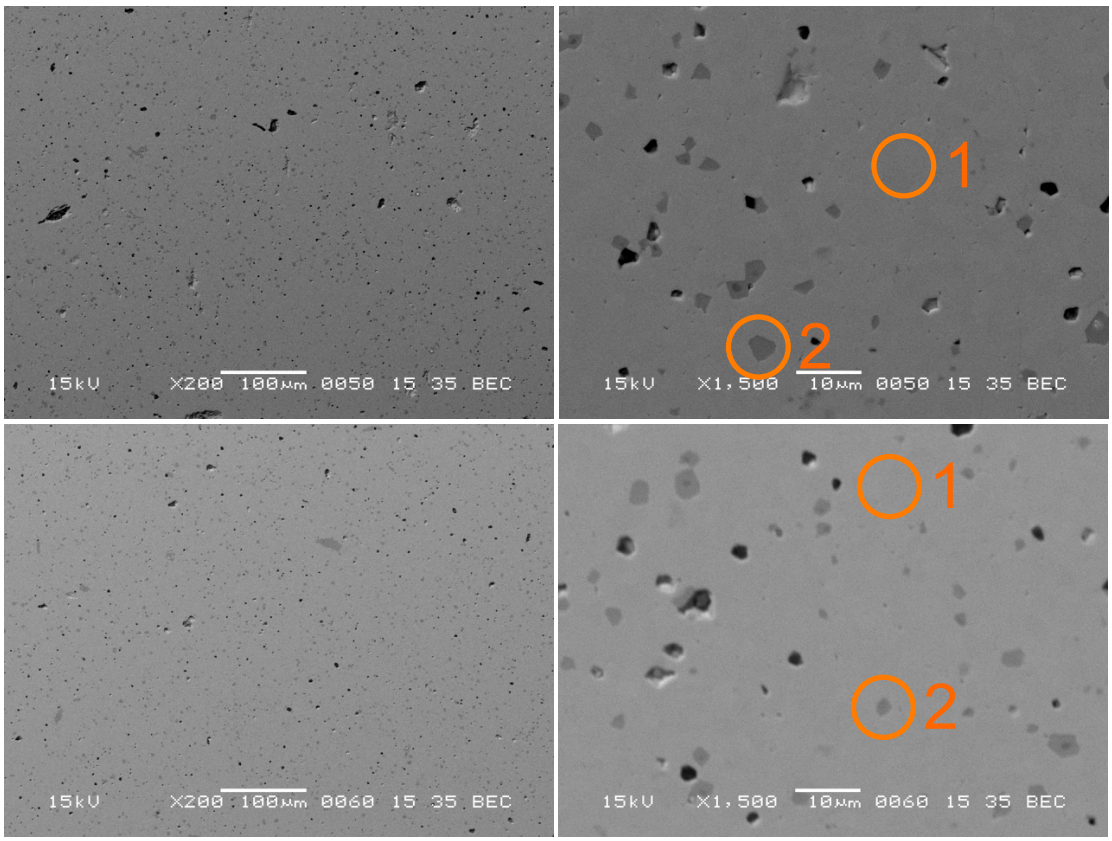

Figure 107: SEM images of the six samples. From top to bottom, 10, 20, 30, 40, 50, 60 min. 200x magnification on the left, 1500x on right. Phases labelled as 1: zirconolite, 2: perovskite, 3: ceria, 4: zirconia.

2.4 Discussion

This simple experiment has shown how the quality of samples, judged on homogeneity and density, increases with extended milling durations. It has also shown that density, alone, is not a sufficient indicator of the final product. As noted in Chapter 1, the 'realistic' ceria has a greater mean particle size than the PuO_2 feed expected. Thus, it may be that 40 min of attrition milling is sufficient to produce a single phase product with no inclusions of PuO_2.

In Chapter 2, none of the high temperature samples consolidated by HIP showed any free ceria. The most aggressive milling conditions were 4.32 m s^{-1} for 30 min and in comparison to this work, there should have been some sign of ceria inclusions in the Chapter 2 samples. It may be that the anaerobic conditions in the HIP cans allowed the formation of FeO, which, as in Chapter 5, formed a liquid phase and improved the digestion of the ceria. These pellets were sintered in air.

These pellets do not have the same porous microstructure shown in the pellets sintered in air in Chapter 5. The porous structure in the planetary milled samples of Chapter 5 is likely to be a result of the insufficiently aggressive milling of the precursors in those trials.

HIP is generally expected to produce less porous samples than CUP, however this is not the case when comparing this work to Chapter 2. As these pellets were sintered in an unconstrained environment (i.e. not in a HIP can) in air, the removal of the zinc stearate lubricant addition was possible. The excellent phase development of the samples does suggest that the lubricant was removed completely.

2.5 Conclusions

The density of the sintered samples cold uniaxially pressed from the attrition milled powders, increases with extended milling durations, up to a noticeable limit (20 min in this system). After this maximum value, the density does not significantly alter with further milling.

The phase development, i.e. proportion of unincorporated ceria, does continue to improve with extended milling up to 40-50 min. The amount of milling time required for reaching the density limit and the time for producing homogenous samples are not the same.

A zirconolite ceramic of suitable density (>92% TD) can be manufactured by attrition milled powders CUP and sintering in air.

3 Fine Powder Digestion

3.1 Introduction

There are four main paths for matter transfer during sintering and grain growth: surface diffusion, lattice diffusion, vapour transport and boundary diffusion. Of these, boundary diffusion has the greatest rate of material transport (Kingrey, Bowen et al. 1976). Boundary diffusion, as the name implies,

occurs at grain boundaries, it follows that if a large number of extensive boundaries can be introduced into a sample it may be possible to increase the incorporation rates of all elements.

To increase the size and number of grain boundaries, precursors with a very high surface area must be used. These can be provided by either the alkoxide/nitrate route or through colloid systems (as detailed in Chapter 4). In the relevant (i.e. radioactive) environment it may be possible to provide a large surface area for the precursors and keep the PuO_2 untreated. A potential immobilisation plant would consist of light mixing (e.g. Turbula) of the fine precursors and the feed. This would be reacted in a furnace to provide a non-consolidated but fully phase developed product. This material could subsequently be consolidated by HIP to bring about full densification.

To test this loose powder digestion concept, fine precursors were manufactured from colloids. These were mixed with the 'realistic' ceria by hand and reacted as a loose pile of powders. Initial analysis was performed by XRD. Further analysis was undertaken on pellets CUP from the material and imaged by SEM (under the standard conditions). Further samples were manufactured from the same precursors but were consolidated by HIP.

3.2 Experimental

The target formulation was $Ca_{0.75}Ce_{0.25}ZrTi_{1.5}Al_{0.5}O_7$. The precursors, excluding the ceria source, were prepared in the same manner to the colloid system in Chapter 4. Al_2O_3 provided charge compensation and the 'realistic ceria' was used as the PuO_2 surrogate. Stoichiometric quantities of calcium (supplied in the nitrate form), zirconium (as a ZrO_2 colloid), titanium (as a TiO_2 colloidal) and aluminium (as Al_2O_3 colloid) were added into a ~3 litre stainless steel beaker containing ~1 litre of warm (~50 °C) propanol. A hot plate and an overhead stirrer, respectively, provided heating and agitation. The calcium source, supplied as a nitrate, was dissolved in excess deionised water before being added to the agitated propanol and colloid mixture. The mixture was

reduced in volume until a thick slurry resulted. This slurry was transferred to a separate wide stainless steel bowl and dried overnight at 120 °C.

The resulting cake was broken up by hand before lightly undergoing further size reduction by pestle and mortar. This powder was transferred to a calcination tray and underwent calcination at 750 °C for 8 hours. The intention was to decompose the calcium nitrate and further stabilise the now liberated CaO into perovskite (by reaction with TiO_2). These powders were planetary milled at 400 RPM for 20 min in propanol to minimise any remaining coarse grains and to ensure full homogenisation of the precursors. Ceria was lightly mixed with these powders and together they formed the 'master batch' from which the following samples were taken.

3.2.1 Loose Powders XRD

Aliquots of ~10 g were separately reacted in a tube furnace, open to air, at temperatures of 1320, 1250 or 1150 °C for 1 or 8 hours as a pile of loose heaped powders. Temperature ramp rates were 2 °C min^{-1} to 200 °C and 5 °C to the target temperature. The reacted powders were subsequently analysed by XRD, Figure 108.

The responses to free ceria, marked '3' in Figure 108, clearly decrease with increasing temperature or duration of reaction. This was taken to as an indication that if the free ceria was becoming less apparent, it was because it was being incorporated into the zirconolite host phase. It is important to note that sintering in air minimises the reduction of CeO_2 to Ce_2O_3, which could have been an alternative explanation for the decrease in response to CeO_2 in the XRD results.

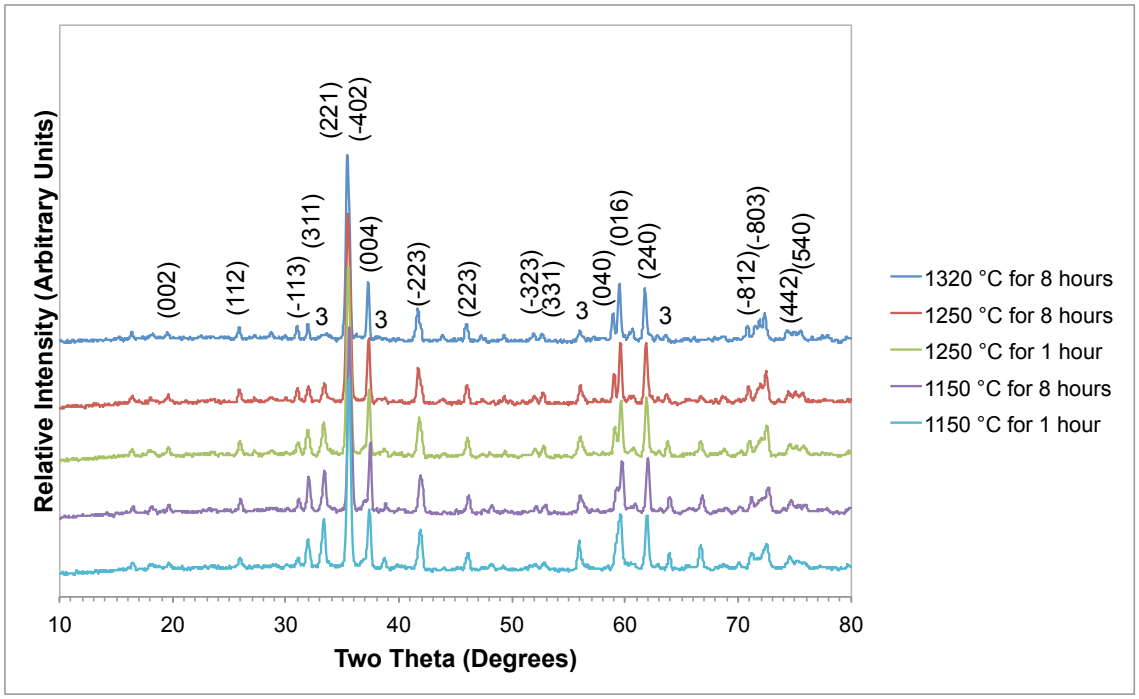

Figure 108: XRD patterns of loose fine powders reacted with the 'realistic ceria' at the labelled temperatures. Miller indices of zirconolite marked and ceria marked as '3'.

3.2.2 Pellets

In order to analyse the powders further, the material reacted at 1320 °C for 8 hours was CUP into a 15 mm pellet with 2 tonnes of force. In addition, another pellet was made from material from the master batch. Both pellets were sintered in air at 1320 °C for 2 hours.

Figure 109 shows the SEM images of the pellet manufactured from powders reacted once. It is immediately clear that there are unincorporated inclusions of ceria present, labelled '3'. There does not appear to be many small particles (<10 μm) of ceria present. It is likely that these particles have been incorporated into the zirconolite host phase. The larger particles (>10 μm), however, have not been fully incorporated. The low volume fraction of these inclusions in the sample may mean that they were below the limit of detection in the XRD analysis. The main zirconolite phase does not appear to be homogenous with a large number of Al_2O_3 grains (labelled '14'). Furthermore, the pellet is very porous. The SEM images show that the technique of loose powder digestion is not as useful for full incorporation of ceria as the XRD data suggest.

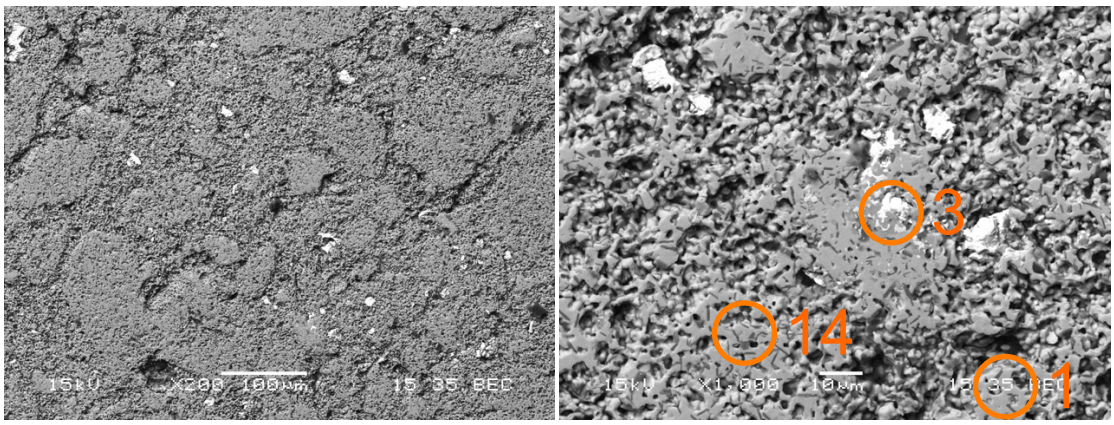

Figure 109: SEM images of pellet pressed from reacted powders. 200x magnification on left, 1500x on right. Phase labelled: 1: zirconolite; 3: ceria; 14: alumina

Figure 110 shows SEM images of the pellet manufactured from powders that had not been previously reacted. The sample shows obvious signs of unincorporated ceria. The host zirconolite phase is again widely interspersed with alumina grains. Notably, this sample is not as visibly porous as the sample manufactured from reacted powders. The consolidation and densification process relies on the reactivity of the powders. It may be as the precursors reacted, it becomes less energetically favourable for the powders to undergo densification in subsequent pellet sintering.

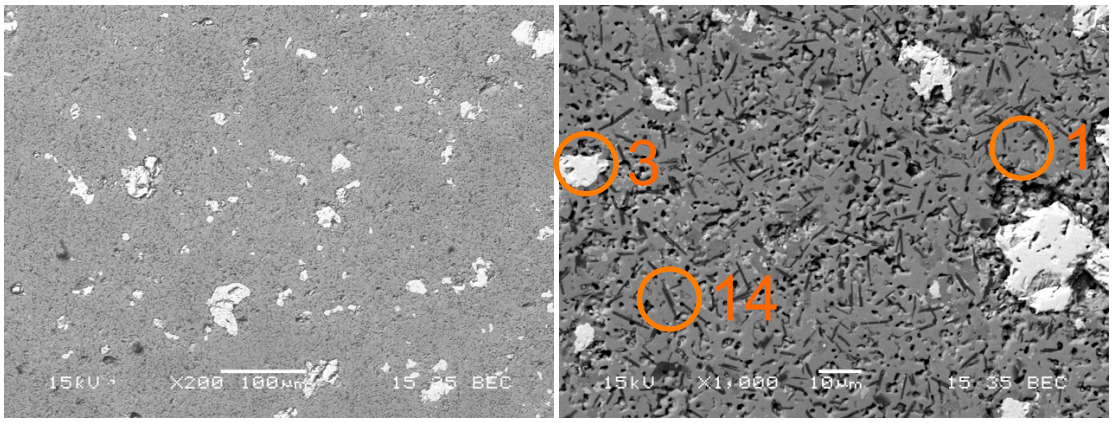

Figure 110: SEM images of pellet pressed from 'fresh' powders. 200x magnification on left, 1500x on right. Phase labelled: 1: zirconolite; 3: ceria; 14: alumina

3.2.3 In HIP Can Reactions

A final test of the loose powder digestion theory was by HIP consolidation. The first sample took powders from the master batch and placed them directly into a HIP can. The can was only tapped with no force applied to compact them into the can. This was a trade off between having a reasonable HIP can packing

density and retaining the large amounts of surface area required for ceria digestion. The packed can was heated to 1320 °C for 8 hours in a tube furnace so as to bring about the same incorporation reactions as previously. The can subsequently underwent the high temperature HIP cycle (1320 °C for 2 hours). Figure 111 shows the SEM images of this sample.

The immediate observation is that the samples consolidated by HIP are very porous, more so than the CUP samples. This is unexpected as samples that have undergone HIP are normally expected to have minimal porosity. It may be that low packing density of the HIP can, limited by the repulsive forces of the small particle sized material, did not allow sufficient deformation of the metal can to compressed the ceramic precursors. The sample appears to have no unincorporated ceria, which is in direct contrast to the CUP samples. This could be a combination of the reaction phase and HIP cycle or it could be that these powders underwent a total of 10 hours at 1320 °C, as apposed to 8 hours maximum before. It is doubtful that the extra two hours will make a substantial difference. It is unknown what mechanism has improved the incorporation rates of ceria in this sample.

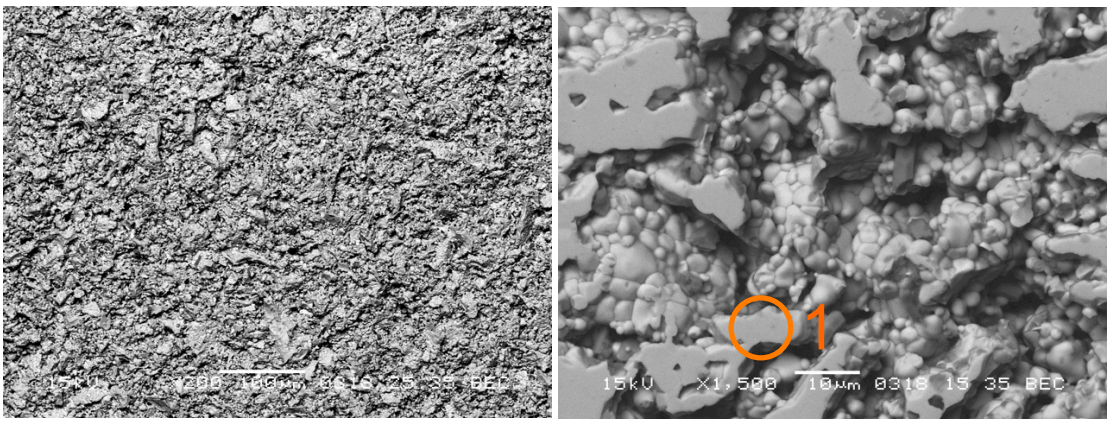

Figure 111: SEM images of powders reacted in can and HIP. Left image is 200x magnification and 1500x on right. NB left hand sample is an unprepared surface. This was to ensure the absence of ceria was not a result of sample preparation. Zirconolite phase labelled as '1'.

A further HIP can was packed with material that had undergone the loose powder reaction at 1320 °C for 8 hours. This sample also underwent the high

temperature HIP cycle. SEM images of this sample, Figure 112, clearly show it is different to the sample reacted in can previously; it has no gross porosity and has clear unincorporated ceria inclusions. In addition, there are small particles that are zirconium-rich (marked '4'). The ring present in the left hand image is a result of the differential thermal expansion of the ceria particle and the bulk zirconolite phase (Kingrey, Bowen et al. 1976). Figure 113 shows one of these cracks surrounding a ceria particle in detail. These cracks are only typically encountered around large inclusions (the crack in Figure 112 is likely to be at the base of a large ceria particle). The pores in the centre of the ceria inclusions are either a remnant of the loose powder agglomerate structure (see Chapter 1 for direct SEM imaging of ceria powders) or through autoreduction of the ceria.

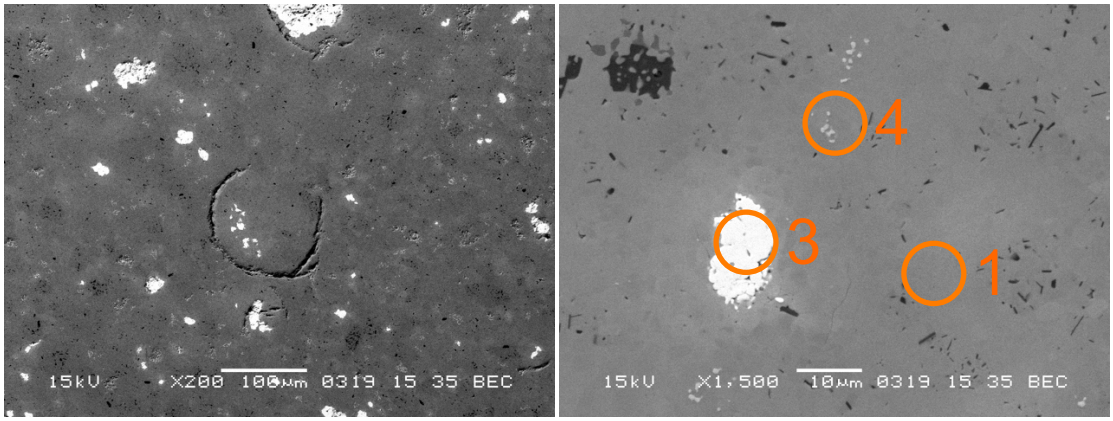

Figure 112: SEM images of sample manufactured from powders reacted loosely and subsequently underwent the high temperature HIP cycle. 200x on left and 1500x on right. Phase labelled: 1, zirconolite; 3, ceria; 4, zirconia.

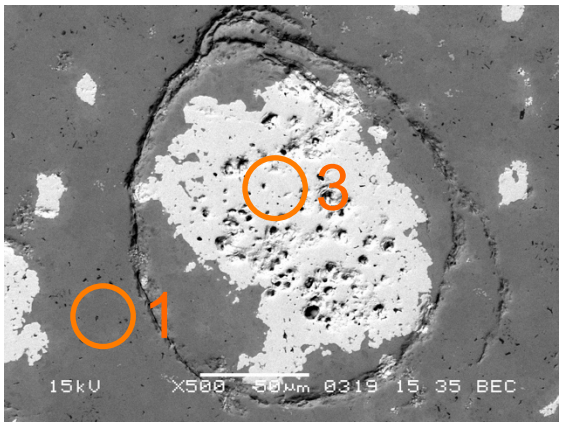

Figure 113: Detail of crack system around an unincorporated ceria grain. 500x magnification.

A final HIP can was packed with material that had been reacted at 1320 °C for 8 hours and planetary milled for 20 min at 400 RPM. The intention was to intimately mix the reacted precursors with the unincorporated ceria in addition to providing some size reduction to the ceria. This material was packed into a HIP can and underwent the high temperature HIP cycle. Figure 114 shows the SEM images of the sample. It has a similar level of porosity to the non-milled sample and also shows unincorporated ceria. The size of the ceria particles is, on average, visibly reduced. The crack systems present in the previous sample are absent. It is likely that the ceria particles are not large enough to have a significant thermal expansion and contraction effect on the bulk ceramic. The planetary milling does decrease the size of the visible ceria, however, it appears the milling was not sufficiently aggressive to bring about full incorporation.

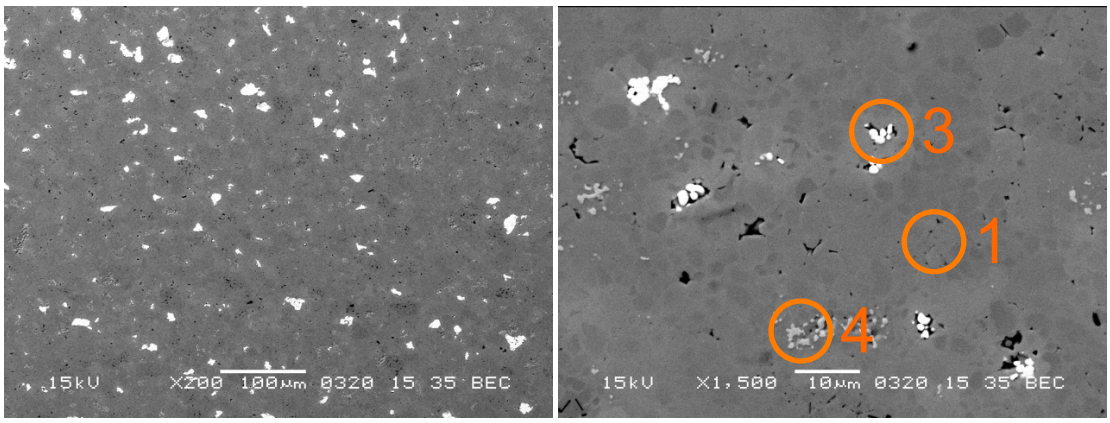

Figure 114: SEM images of sample manufactured from powders reacted loosely and planetary milled before undergoing the high temperature HIP cycle. 200x on left, 1500x on right. Phases labelled: 1, zirconolite; 3, ceria; 4, zirconia.

3.3 Discussion

The extensive amount of unincorporated ceria in the samples indicates that the fine powder digestion method is flawed. It is likely that the initial XRD results failed to strongly indicate free ceria in the samples due to the small volume of ceria remaining. However, there is a definite correlation between increased temperature for the reaction and decreased response to ceria. Increasing the temperature has a greater effect on the incorporation level than duration does.

The fine powder digestion method was based on the large surface areas of the precursors enabling large levels of material diffusion and thus phase development. Whilst this may be true, it would appear that the ceria used in this work was too coarse to become fully incorporated into the zirconolite phase.

The sample that was consolidated by HIP after the powders were reacted in the can is concerning for a HIP rework strategy. In the active implementation of this work, failed products cannot be discarded; they must be processed again so that they conform to required specifications. Such failed products are likely to occur if the HIP cycle fails (i.e. does not reach the target temperature, the dwell is too short or the argon pressure is incorrect). One possible strategy is to simply 're-HIP' the product at the correct conditions. The sample made from powders reacted in the HIP can in a tube furnace was clearly more porous than the sample made from powders reacted outside of the can. The pre-heating of this sample represents a HIP cycle that did not apply any pressure.

Further work is needed to address the behaviour of samples that do not experience the HIP conditions required and to develop the necessary recovery techniques. If applying the same HIP cycle again to the failed products does not bring their properties into specification then a higher temperature or greater pressure than the standard HIP cycle may be required. If, as in the majority of this work, the cycle temperature utilised is 1320 °C, which is the workable limit of stainless steel, it will not be possible to increase the HIP cycle temperature further. It may be that the implemented HIP cycle should be at the minimum temperature required for sintering. This temperature is unknown for the plutonium/zirconolite system if consolidated by HIP but may be below the 1320 °C currently used. There is also a body of work required on addressing the pressures required for full consolidation. It is likely that the 100 MPa typically used is not optimal.

3.4 Conclusions

The loose powder digestion method cannot be recommended for implementation, as the products it produces are heterogeneous in regard to phase development.

4 Modified Attrition Mill Internals

In the experiments presented so far where the attrition mill would fail to discharge, it was often noted that upon clearing the mill the powders would be compacted in the base. Discussion with those familiar with the SMP attrition mills stated that there was a bottom trapezoidal bar attached to the agitator shaft. This bar swept the base of the mill with each rotation of the agitator. In this motion, it lifted the second layer of balls over the bar thus decreasing the dead space at the base of the attrition mill. In discussion with the manufacturers of the attrition mill utilised in this work (Union Process) they advised purchasing a modified agitator shaft, Figure 115. The new agitator has a triangular section as the last arm. The design only allows unidirectional motion in the mill.

As the modified agitator was purchased late into the project, only limited experience has been gained in its operation. Initial trials have been positive but there has been no systematic study of the mill discharges. Nor has their been any study of the motor loads, which may or may not have changed.

If there are no detriments to utilising the modified design of agitator then this should be recommended for implementation. A combination of milling additives and the mechanical interruption provided by the extra bar will be sufficient to minimise, or eliminate, the frequency of agglomerations in an active mill.

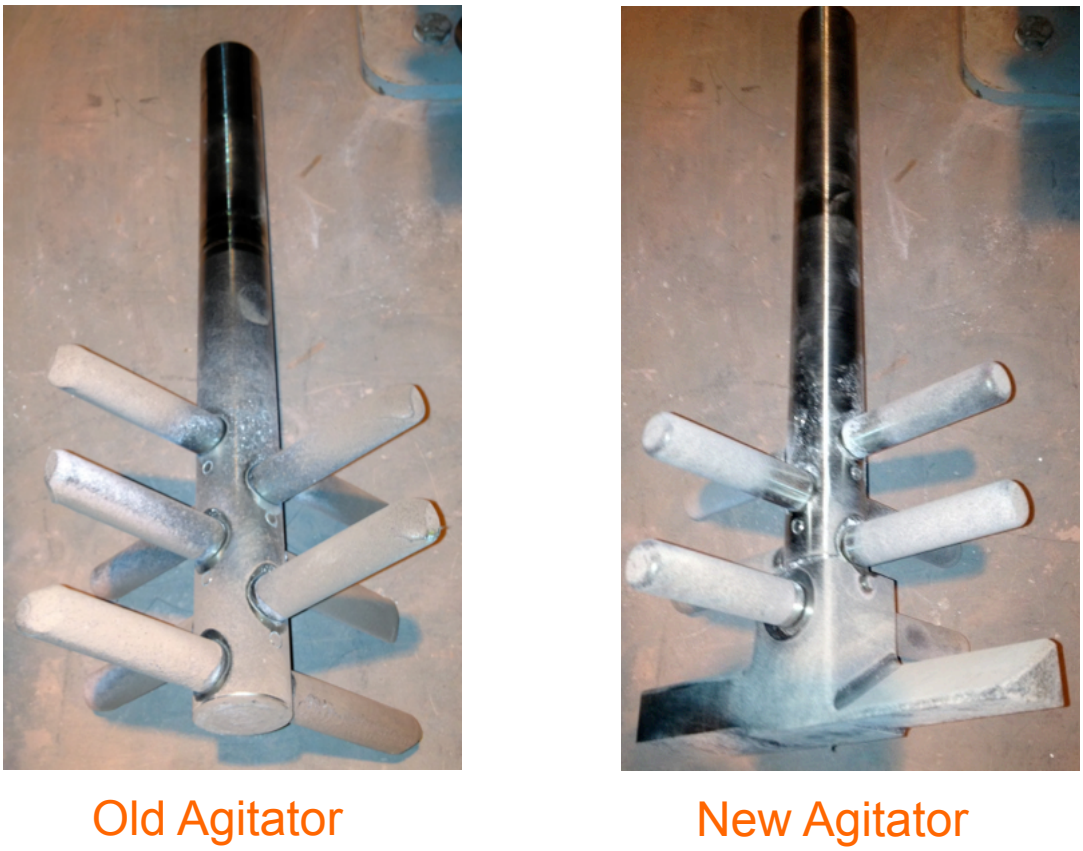

Figure 115: Comparison of old and new agitators. NB the modification of the bottom arm.

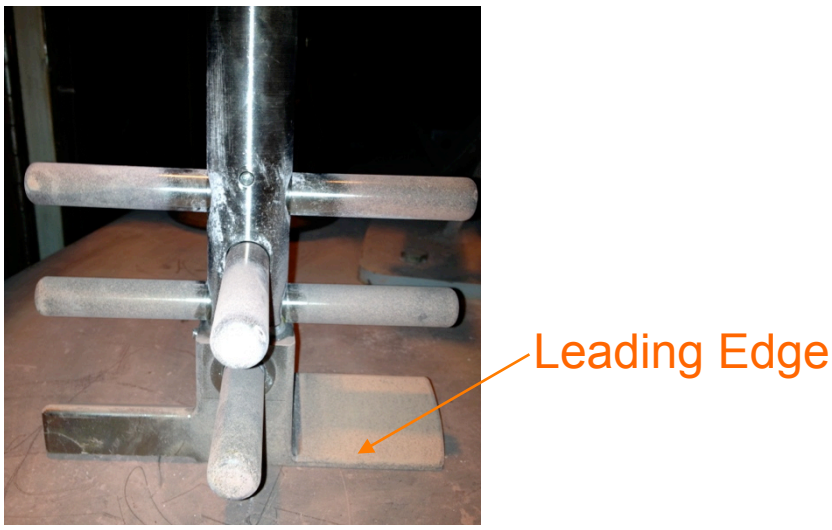

Figure 116: Detail of new agitator.

5 AEROXIDE

As mentioned in Chapter 2 and briefly trialled in the planetary mill in Chapter 5, Aeroxide is a potential replacement for hydrocarbon milling additives. The attraction of Aeroxide is that it is a form of Al_2O_3. In any zirconolite formulation,

aluminium can be easily substituted into the host phase with no detriment. This eliminates the need for a lubricant removal step after milling the powders.

Alongside the work reported in Chapter 5, the Aeroxide has been utilised in the attrition mill. Batches of 1000 g of metal oxides with the target formulation of $Ca_{0.75}Ce_{0.25}ZrTi_{1.5}Fe_{0.5}O_7$ were milled. The calcium and titanium was provided as $CaTiO_3$, with the balance of titanium from TiO_2. Zirconium and iron were provided as ZrO_2 and Fe_2O_3, respectively. Cerium, as the plutonium surrogate, was from the standard source. The Aeroxide was added at 0.5 wt% and the attrition mill was operated in the dry mode with the standard (i.e. non-modified) agitator.

The initial trial attempted to mill at 4.32 m s^{-1} for 30 min. After approximately 24 min the motor failed with an overload error. Notably, after resetting the control software, the mill discharged the powders very quickly. If an agglomeration were formed with the hydrocarbon waxes the powders would not discharge after stopping the mill. This ease of discharge gave confidence that experimentation should continue.

A second batch of material was milled at 3.24 m s^{-1} for 30 min (the lower speed was expected to place a smaller load on the motor). For this batch, the mill failed at 28 min. Again, the powders freely discharged upon restarting the motor.

No further work has examined the use of Aeroxide (other than the planetary milling in Chapter 5 and the work at Springfields detailed in Chapter 7) in the attrition mill. The observation on the ease of the milled powders to discharge after the motor stopped is positive and may suggest an issue with the attrition mill rather than the material being milled.

The addition of 0.5 wt% Aeroxide was based on the manufacturers recommendation and may be incorrect. Milling lubricant additives work on a surface area basis (i.e. enough should be added to cover the surface of the

powders) and as the powders are milled, they decrease in particle size and thus the surface area increases. This may lead to a lack of Aeroxide available to coat the newly created surfaces and this may why the mill stops after an extended duration. Also of note, experiments in Chapter 2 showed that the motor did not overload when there was an agglomeration formed.

Further work should seek to establish a suitable level of Aeroxide addition. The combination of Aeroxide and the modified agitator may be sufficient to confidently assure the powders will always discharge from the mill.

7: Project Impact

1 Abstract

This chapter discusses the impact of the research detailed in this thesis. The first section is a series of suggested attrition mill conditions that would be suitable for the plutonium wasteform manufacturing task. A key differentiator of the EngD, from a more traditional PhD, is that the work undertaken should have a commercial relevance. Accordingly, two projects are discussed in this section: conceptual design for the bulk immobilisation of plutonium and the plutonium residues programme. Potential future work is also suggested, with the majority focused on gaining a more detailed understanding of the state of the UK civilian stockpile of plutonium. Potential modified wasteforms for the co-immobilisation of plutonium and associated impurities are also discussed.

2 Suggested Attrition Mill Operating Parameters

As one of the main foci of this work was utilising an attrition mill in the manufacture of plutonium ceramic wasteforms, the following section gives a summary of the suggested most appropriate milling conditions for full scale implementation. It should be noted that there might be a critical particle size of the feed and precursor blend that must be achieved before full consolidation can occur for a given temperature. It is also recognised that the smaller the particle size of the feed and precursors the lower the HIP consolidation temperature that would be required. Thus, the intention of the attrition milling stage is to size reduce and homogenise as far as possible below this critical value but with due consideration to the diminishing returns of extended milling (e.g. increased wear, process delay).

2.1 Tip Speed and Duration

Work in Chapter 3 showed that long duration (60 min) milling at low speeds (2.16 m s^{-1}) was sufficient to produce zirconia ceramics of suitable density (> 92% TD). The progression of milling in Chapter 6 showed that whilst a maximum density for sintered pellets could be achieved after approximately 30 min of milling at 4.32 m s^{-1}, the microstructure continued to improve until after 40 min of milling. These results would suggest that attrition milling the plutonium feed and precursors for 45 min at 4.32 m s^{-1} would consistently produce ceramics with a density greater than 92% of TD and phase homogeneity. However, the results in Chapter 2 showed that, regardless of the milling conditions, the high HIP consolidation temperature (1320 °C) was sufficient to bring about the full incorporation of the ceria. This is with the caveat that the precursors and feeds in the full scale implementation are of the same particle shape and size as utilised in the non-active work.

2.2 Configuration

The attrition mill should be sized so that one HIP can worth of material can be milled in one batch. This will depend on the size of the HIP can specified in the full scale process. The promising early results by utilising the extra bottom rotor in Chapter 6 suggest that a similar modified agitator should be used.

2.3 Additive Usage

The difficulties in removing the milling lubricants shown in Chapter 2 and confirmed in Chapter 4 suggest that, where possible, no milling additives should be used. The bottom rotor may provide sufficient mechanical agitation that no foot can form in the mill. Further work needs to identify whether the mechanical agitation still achieves the full size reduction necessary. If an additive is required, it should not be organic.

3 Bulk Plutonium Immobilisation

In early June 2012, the NDA commissioned NNL[20] to provide an updated conceptual design for a plant to immobilise the entire UK civilian plutonium stockpile (Clough, Hodgson et al. 2012). An initial design had been completed the previous year (Mierzewska and Barrand 2011), however research from this project had shown there to be numerous flaws. There was also a requirement to modify the waste incorporation rate from 20 wt% to 10 wt%. The lower incorporation rate was selected as it has been proven with plutonium (Jorion, Deschanels et al. 2006). A further consideration was that the plant must be comparable to other disposition options the NDA are considering (e.g. MOX manufacture). This meant that the design must account for six months of buffer storage for import and export (effectively decoupling the plant from other site interactions). The design was intended to be conservative with assurance that the calculated throughputs were achievable. This was accomplished by the provision of multiple equipment redundancies. The design presented has many opportunities for optimisation and some are suggested.

3.1 Design

3.1.1 Design Philosophy

The overarching design philosophy has been one of conservatism. This meant that the design would utilise equipment, where possible, that had been shown to operate successfully in a plutonium powder environment. The plant was scheduled to have throughputs that allowed for full plant shut downs and frequent equipment failures. Experience gained in operating SMP has influenced the design, for instance, in the requirement for a spacious plant with sub-change rooms for equipment maintenance access. There is also the

[20] Much of the following conceptual design is based upon work that was completed as part of a team from NNL. The author does not, accordingly, claim sole ownership of the design.

assumption that equipment will fail and must be replaced or repaired. A maintenance area will be provided for each major process area.

Where possible, all powder movements between processes in the plant are vertical and gravity fed. This requires that the plutonium feed be elevated to the top processing floor. The plant operations are in a vertical line throughout necessitating a separate floor for each process (in order to minimise horizontal powder movements) and this is reflected in the height of the building.

The plant is to be fully automated in order to minimise operator dose. Full automation did cause difficulties in SMP, however the plant design is such that there is sufficient allowance for maintenance access. For every processing operation there is at least one independent equipment replication. This allows continued production as failures are corrected.

The plant has been designed with all of the operating experience from the inactive facility at Workington, experience in operating SPRS (Sellafield Products and Residues Store) and results directly from this EngD project. The plant is to be a dry processing facility and secondary effluents are to be minimised. PCM (Plutonium Contaminated Material) is to be processed and packaged within the plant.

3.1.2 Feed

The feed is defined as the entire UK civil stockpile of plutonium, declared as 105 tonnes HM PuO_2 (approximately 119 tonnes PuO_2)[21]. The plant design does not include the foreign owned PuO_2, a further 35 tonnes HM, stored in the UK. There was some awareness that the plant should be able to extend its mission to include this material. This may be by increasing the operating life of the plant,

[21] Figures for the plutonium stockpile are typically quoted in 'tonnes of heavy metal', which can be converted to an estimated mass of PuO_2 by multiplying by (239+2(16))/239 ≈1.13. It is an estimate, as the isotopic makeup of the feed will vary depending on the reactor source.

with all the necessary refurbishments, or by building the plant with spare capacity.

Of the UK owned material, approximately 87 tHM is Magnox derived and 18 tHM is from ThORP finishing lines. The different reprocessing plants will have produced different isotopic mixes of PuO_2, which will be in different storage cans. The two types of storage cans require a dedicated suite of tools to unpack and remove the PuO_2 powder for each. The PuO_2 is assumed free of moisture or other contamination (e.g. chlorine).

3.1.3 Product

The facility is designed to manufacture a ceramic wasteform, which is currently undefined (likely to be a titanate such as zirconolite or pyrochlore). There are two key issues with the product specification: proven waste loading and product storage. As this plant is intended to be a conservative design, the waste loading has been set at 10 wt%. Whilst acknowledging 10 wt% loading is low, it is the only proven level with plutonium in a zirconolite ceramic (Jorion, Deschanels et al. 2006). Other work has shown, with surrogates (such as uranium or cerium), that waste loadings of approximately 20 wt% are possible and this is a key opportunity to optimise future plant design.

As no final disposal facility exists, the current plan is for interim storage of the product. The default store is SPRS, which has stringent conditions for acceptance. Two major restrictions on the waste package are a 20 kg mass limit and the physical size limit equivalent to a ThORP outer package. The immobilisation plant waste package will consists of:

- ThORP outer can (2.9 kg)
- Filler material between HIP can and outer (1.1 kg)
- HIP can (2.0 kg)

Which leaves 14.0 kg available for the wasteform (of which 1.4 kg is Pu).

3.1.4 Key Assumptions

At the concept level of design, a number of assumptions must be made. These are liable to challenge but represent the best opinion with the current information.

- The plant will be a new facility
- The security classification will be high, reflecting the sensitivity of the material being processed, which has implications for access control
- The design life time is 30 years
- The plant is assumed to operate for 24 hours per day and 150 days per year (this is a conservative value based on operating experience from other plutonium operating plants and includes days lost to: safeguards (91 days), store maintenance (30 days), can opening suite failure (17 days), replacement of dispensing hoppers (1 day), granulator maintenance (14 days), can loading failures (17 days), inter-equipment powder transfers (45 days))
- Only UK owned plutonium stored at Sellafield is to be immobilised in this plant
- All deliveries to plant are by road, as well as the export of PCM and ceramic products. The transportation of materials will have no detriment to the plant
- All other plant interactions (waste routes, PCM stores, utilities) are available without restriction
- Operations will be automated, as far as possible, and are contained in sealed, secured cells
- Space is to be provided in the design for office areas, change areas, sub-change for access into cells, when required
- Elevators are used for vertical upwards transfers

3.2 Plant Design

The following sections detail the movements of the PuO_2 throughout the plant until the eventual immobilisation into the ceramic wasteform. The overall block diagram is shown as Appendix 1.

3.2.1 Feed Preparations

The PuO_2 is received from the current storage locations around the Sellafield site. It is delivered by road into a dedicated import/export bay. Each of the PuO_2 product cans will be over packed in a Safkeg[22] during transport. Upon receipt into the plant, the PuO_2 cans will be unpacked and transferred to a dedicated buffer store. This store will have the same radiological and environmental controls as SPRS and is sized to contain six months worth of feed (approximately 800 PuO_2 cans). The extensive buffer storage provided is to decouple the plant from any other site interactions.

When the material is required for immobilisation, it will be automatically removed from the store and placed into one of two elevators. The cans are delivered to the fourth floor of the plant. Upon removal from the elevators the cans are transferred to one of two identical glove boxes suites dedicated to can opening. Both suites have the capability to open ThORP and Magnox packages. The PuO_2 material is poured into dispensing hoppers. Each of the dispensing hoppers is sized for two to three days of operations (~12 kg). When empty, the PuO_2 product cans are discarded as PCM waste (more detail on the PCM strategy given later).

In a separate, not radioactively controlled, area, the inactive precursors are placed into two dispensing hoppers. Each hopper feeds one of the two separate processing lines. The precursors are specified to contain 1.5 wt% of zinc stearate, as the lubricant for milling. It is assumed that the lubricant will aid the non-

[22] Safkegs are self shielded over packaging containers for the transport of radioactive materials.

vertical powder flow from these hoppers to the attrition mills on the floor below. Zinc stearate has been chosen, as it is the only lubricant that has been shown to work in attrition mills with PuO_2 powders.

3.2.2 Attrition Milling

The plant contains two attrition mills each vertically below the PuO_2 dispensing hoppers. Each mill is sized to contain 14.0 kg of PuO_2 and precursor blend (equal to one HIP can). In order to minimise the possibility of non-milled PuO_2 collecting in the base of the mill or in the discharge grate, the inactive precursors are added to the mill first. After the precursors are fully charged the PuO_2 feed is added. The current schedule allows for a two hour blend and size reduction cycle. This is excessive but decreasing the milling time does not influence the overall throughput of the plant (i.e. milling is not a rate limiting step). The mills are to be operated with 'through wall' drives. These allow the motors and electronics required to run the mill to be kept in a radiation free environment simplifying any maintenance or repairs required. Agglomeration and caking of the powders during milling is considered to be a concern. Each attrition mill cell is generous in size so that the blocked mill may be removed from the processing line and placed at the edges of the cell for decommissioning at a later date. It is appreciated that this will not return the mill to operating conditions but the solution is the best available for an operating nuclear plant. Discharge from the mill is into a weigh hopper, which accurately records whether all of the milled material is discharged.

3.2.3 Blend Preparation

The homogenised feed and precursors, from the attrition mill, are gravity fed to the granulators. Each mill has one granulator directly beneath. No further additives are introduced into the powders and the granulator is a mechanical roll compactor. The granules produced will improve HIP can packing density and reduced airborne powders. The granulators operate continuously and each attrition mill batch is collected at the base of the granulator in a transfer can.

The transfer cans are robotically moved to deliver the granulated material to one of three screw fed calciners per processing line. Each of the calciners is set at an upwards incline so that the output can be gravity fed in to the HIP cans. The granulated powder has a four hour residence time at 600 °C with co-flowing oxygen rich gas. The purpose of the calciners is to remove the lubricant, and any moisture, completely from the powders.

3.2.4 HIP Can Packing

The output of the calciners is a granulated and lubricant free blend of the PuO_2 feed and the precursors. Each of the calciners has an associated can filling facility. All of the processes so far have been in independent glove boxes with the assumption that PuO_2 will contaminate all of the processing equipment. At the can filling stage it is possible to change the primary containment from a glove box to the HIP can. If the HIP can is never placed into a contaminated area, the outside of the can is treated as clean. This allows the subsequent processes (can evacuation, consolidation and storage) to be in a area of lower radiological classification. Figure 117 shows the sequence of can filling steps that ensure the outside of the HIP can will never become contaminated.

The first stage of can packing involves pouring the lubricant free granules into the HIP can. The HIP can is vibrated to improve the packing density. The powder is expected to be free flowing as it is in the form of granules and is moisture free. After filling, a tight fitting insert is placed into the neck of the HIP can, which consists of two HEPA (High Efficiency Particulate Air) filters joined by a stainless steel tube (outlined in red). The two filters are required so that the backpressure created by inserting the tube will not affect the insertion. A plasma torch is utilised to cut and weld, thus sealing, the insert and fill tube in one pass. This allows the clean inside of the insert to become the outside of the HIP can fill tube with the HEPA filter maintaining containment in the can. The glove box remains sealed by the other half of the insert. The HIP can is removed for further processing. To replace the HIP can, the previous fill tube is

forced into the glove box as the new fill tube (and HIP can) is moved into position beneath the glove box. The sphincter valve in the glove box is key to this operation. Similar versions are in use in other plutonium operating environments.

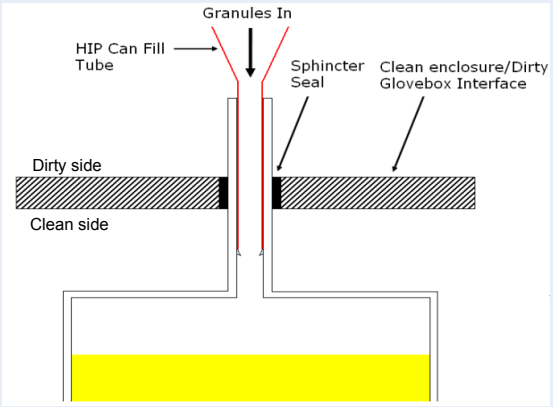

Homogenous granules are directly loaded into the HIP can from the calciner via a post calciner buffer hopper. The granules are dispatched through a fill tube inserted into the neck of the can.

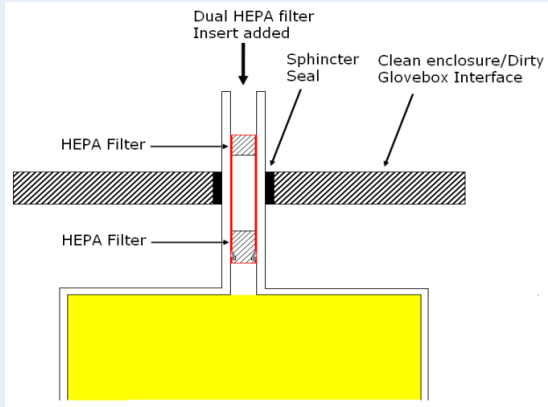

An insert comprising a metal tube with two sintered metal HEPA filters welded into it is inserted into the HIP can neck, locking into a positive connection point.

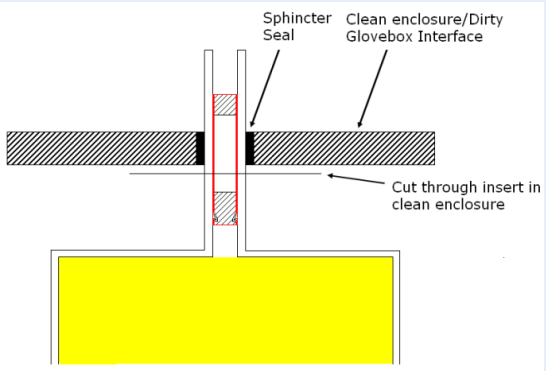

A plasma cutter is employed to simultaneously cut and weld the insert and HIP can neck within the clean enclosure. One HEPA filter remains in the upper half of the HIP can neck as the primary containment barrier for the glove box. The other filter remains within the lower half of the HIP can neck, thus maintaining containment of the HIP can whilst still allowing the required evacuation stage later in the process.

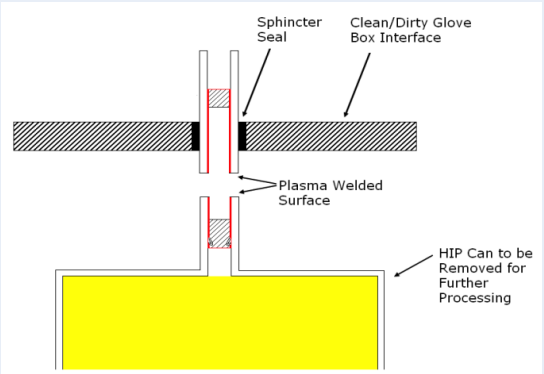

It is now possible to remove the HIP can for further processing.

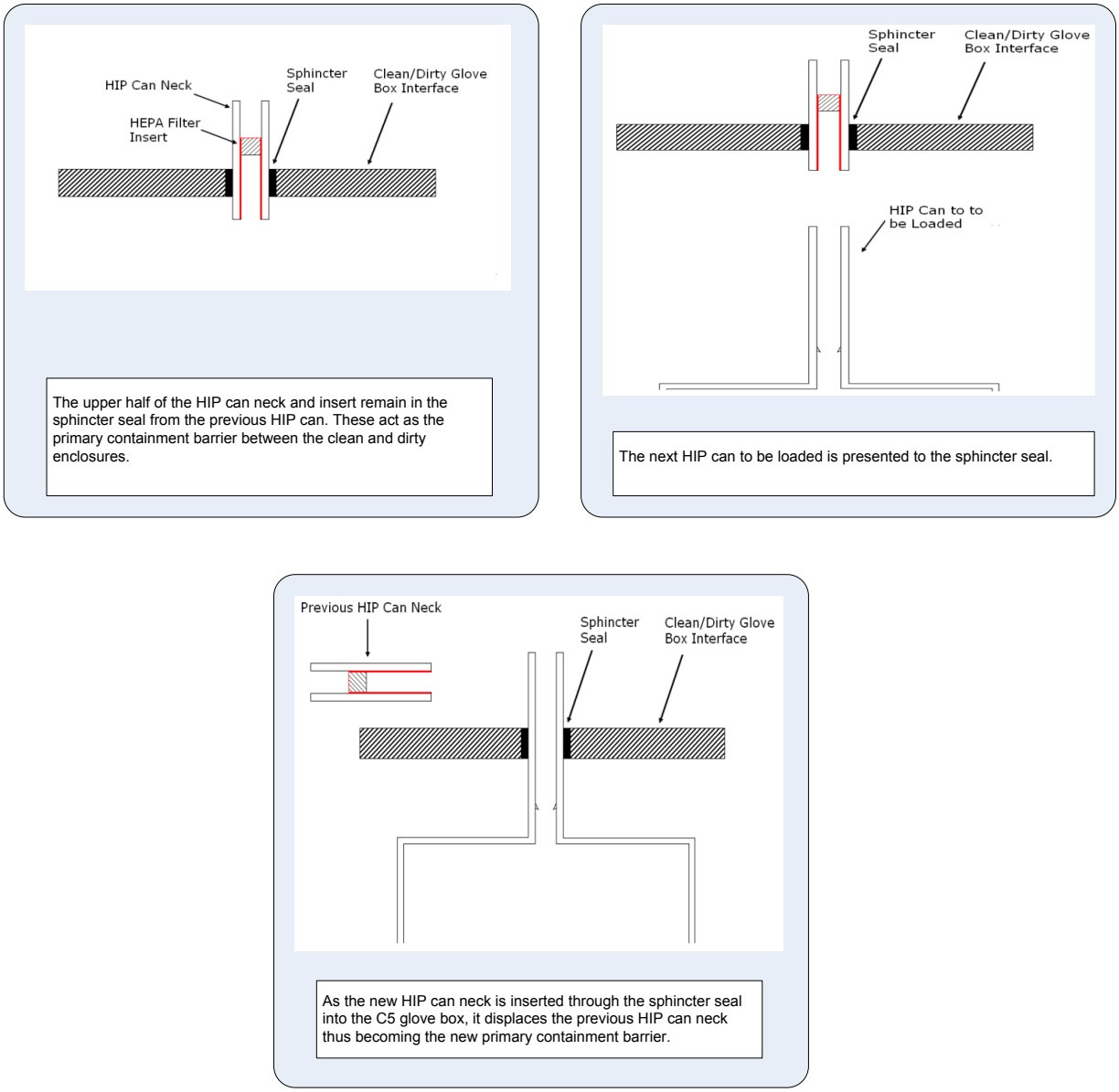

Figure 117: HIP can filling and insert placement sequence. Images from (Clough, Hodgson et al. 2012)

The HIP can is swabbed to check for external contamination in the neck before being moved to a transfer tunnel.

3.2.5 HIP Can Evacuation and Sealing

The transfer tunnel allows the six independent can filling stations to deliver the packed HIP cans to four evacuation lines. The HIP can is attached to a vacuum line to ensure all gases are removed. The HEPA filter allows the gases to be removed whilst maintaining powder containment. The fill neck is crimped and plasma cut, sealing the HIP can. The weld is pressure tested before being transferred to one of four pillar lifts to take the HIP can to the floor below.

3.2.6 Consolidation By HIP

The HIP can is removed from the pillar lift and transferred to a HIP loading station. The HIP can is manipulated into the HIP by a through wall drive. Each of the HIP units is contained in a fully shielded module. Each module comprises a HIP unit, a compressor and cooling equipment. The design philosophy is that should a HIP can fail during a HIP cycle, the module will be removed and decontaminated elsewhere in the plant. A replacement module will be manoeuvred into place in order to keep the plant throughput required. The plant has 12 HIP modules in active service (11 are required) with a further two back-ups.

The HIP cycle is scheduled to take 10 hours with an extra 2 hours allowed for loading and unloading. The cycle will have a 2 hour dwell at 1320 °C and 100 MPa. After the HIP cans are unloaded from the HIP, they will be visually inspected. It is thought that observable gross deformities will be a suitable indicator of a failed product. Assuming the HIP can is within the required tolerances, it is transferred to the product elevators and lowered to the ground floor.

3.2.7 Product Sanctioning and Export

Following cooling, the products are transferred to one of two sanctioning and over packing lines. The products will be packed into ThORP product can outers with an inert material filling any gaps between the HIP can and the outer. The outer cans are sealed and, via a charge machine, placed into export storage. There are six months worth of storage (~3200 HIP cans) at SPRS level of criticality and temperature control. For export from the facility, the products will be over packed into Safkegs and removed by road transport.

3.2.8 Failure Recovery

The plant has been designed with equipment failure in mind. Where possible (e.g. attrition mills, granulators) motors and control electronics will be situated

outside of the radioactive containment. Where this is not possible (e.g. various transfer mechanisms, HIP unit) there are parallel processing lines available.

The strategy for failures in the product depends on where the failure occurs. If the plutonium is in the powder form, it will be reintroduced into the plant at the attrition mill stage. At this conceptual design stage, it is unknown if these recycled materials will need to be treated differently. For example, recycled powder may require an extended milling cycle. The worst point of failure is during or after the HIP consolidation cycle. If the failure is a can burst or rupture the entire HIP module will be removed for decontamination and repair. However, if the HIP product is a monolith that is not sufficiently consolidated (for example the HIP cycle failed without a dwell) it may be possible to attempt to HIP the material again. If not, the entire can must be recycled. A glove box suite consisting of can cutting tools and various size reduction equipment (e.g. jaw crusher, disc mill) is situated on the ground floor. The expectation is that the monolithic product can be reduced in size to a powder form so that it can be reintroduced into the plant. The design basis states that ~5% of all cans will fail (a standard nuclear industry heuristic) and this is accounted for in the throughput calculations. The intention is that 0% of off specification products leave the plant.

3.2.9 Accountancy and Safeguards

As the immobilised products contain fissile material, it must be known how much plutonium the package contains and of what isotopic concentration. As the accountancy is not required for plant process control, it can be analysed off-site without impacting plant throughput. As it would be unwise to destructively test an immobilised product, an accountancy sample is taken from the flowing powder as the HIP can is being filled. After this stage, the contents of the HIP can have a constant composition. Before this stage, it is possible that different PuO_2 feed cans will become mixed. This stage is the best location to get a representative sample of the final product.

The security and safeguards of the plant considers three regimes: plutonium access, PCM access and inactive. The plant layout is designed so that for each of the operating regimes there are dedicated personnel access points on the ground floor that can be controlled centrally.

3.2.10 PCM Strategy

The majority of PCM will arise from the empty PuO_2 product cans on the fourth floor. Accordingly, the first PCM assay glove boxes are on the third floor, connected by a chute from the can opening glove boxes above. Further PCM will arise from the HIP can filling glove box (fill tubes and insert) and the HIP can sealing area (fill tube cut off). These pieces will be collected and transferred to a PCM marshalling area on the ground flour by two dedicated elevators, along with all other PCM. A compactor is provided on the ground floor, which will minimise the volume of PCM exported from the plant. It is assumed that an existing facility is available elsewhere on the Sellafield site for the final conditioning and treatment of this waste.

3.3 Plant Layout

The layout has been designed with no constraints on site location and is thus spacious[23]. This was a reflection on the feedback from SMP in that working conditions were cramped. The layout may have to be redesigned if the required space is unavailable on the Sellafield site. The large ground level floor dominates the facility design. A requirement for six months buffer storage for both import and export led to the large space required. The first floor consists of the twelve active HIP modules. The decision to place all of the operating HIP units in a line was so that the design did not have any difficult transfer operations that are around corners. It is likely that two banks of six HIP units arranged in a 'U' shaped layout would decrease the amount of space required. Above the HIP operating floor the size of the building decreases, as there are

[23] Plant layouts are available in (Clough, Hodgson et al. 2012).

less unit operations per floor. As can be seen, the transfers between each of the floors are vertical, thus in keeping with the design philosophy.

The design also incorporates a significant level of inherent security as each of the active material operating regimes (plutonium, PCM, inactive) are physically separated, thus allowing a single point of access on the ground floor. Areas for changing, office work and administration are also provided in the design.

The designs are not considered to be optimised and improving the layout represents a significant chance to reduce the overall capital expenditure costs through a reduced plant volume.

3.4 Direct Project Impact

Whilst the experience gained from the entire EngD project helped to inform the design of the conceptual plutonium immobilisation plant, there are four points of the design that can be directly related to the work completed in this thesis. The introduction of the calciners as a method for lubricant removal from the powders post attrition milling was a result of the work in Chapters 2 and 4. In this work, it was shown that the failure to remove the lubricant completely interfered with the final product. Chapter 4, in particular, showed it was possible to produce suitably dense ceramics if the lubricant had been removed from the loose powders before they were packed into the HIP can. This technique for lubricant removal is clearly shown in the plant design. The specification of the attrition mills used was also a direct result of the work in the EngD project. The initial design of the bulk immobilisation plant called for attrition mills similar to SMP, however, the operating speeds used within SMP are far below that required to form a suitable ceramic wasteform and the mills specified for the conceptual plant have been duly uprated to the mill tip speed required. The reliability of the mills was initially thought to be poor, however the research presented herein shows that the credible, and predictable, failure mode is that of powder agglomeration and thus failure to discharge. The EngD project has shown that through the addition of a bottom scraper bar and the

correct choice of lubricant, the powders can be made to consistently discharge. This has removed some of the doubt associated with plant reliability. Finally, the concept for filling the HIP cans was introduced based on ideas generated throughout this project. Further work should seek to prove the can filling concept.

3.5 Future Work Required

Before the plant is built, the design must be fully optimised. The greatest improvement will be gained by proving the practical maximum waste loading for the defined ceramic waste form. Maximum waste loadings may be up to ~20 wt%. This level would need to be proven with a pure plutonium waste stream. ANSTO have the facilities to undertake this research. The difficulty in establishing a maximum may be that the maximum theoretical, that achievable with specialised precursors (e.g. alkoxide/nitrate) and that achievable with dry PuO_2 powder may be different. It may also be difficult to establish at what level full incorporation of waste has taken place. If incomplete incorporation is defined by the presence of free PuO_2 inclusions and there are few easily visible, the sampling regime for the products must be carefully constructed. Regardless, a series of samples consolidated by HIP with a range of waste loadings will be sufficient to further inform the design of the bulk immobilisation plant. Final waste loadings may be determined during plant active commissioning.

The effect of americium and chlorine incorporation into the ceramic wasteform must also be studied with the relevant materials. These two species are expected to be present, as impurities, in the feed. Further work must also determine the level of neutron poisons (e.g. gadolinium, hafnium), if any, are required in the wasteform.

Continuation of the work in searching for an alternative to the hydrocarbon lubricants may allow the calcination step to be eliminated. Any process simplification will be beneficial to plant reliability and operability. The promise shown by utilising Aeroxide should be investigated further with relevant

materials (i.e. plutonium). Further development of the attrition milling process is required so that there is a detailed understanding of the tip speeds and durations required during milling. There is also a requirement to test the predicted mill size required, initially with UO_2 as a surrogate and finally with PuO_2. It is likely that many of the detailed operating conditions will not be known until a processing line is operated with plutonium.

The largest unknown in the entire process is the HIP can filling and sealing stage. This is an entirely new technology that has not been tested in any form. Before it can be implemented into a plutonium active plant, an inactive version must be created and tested. It is likely that either a working prototype can be created in a few months of work, or that the system will not be successful in its current form. This unknown is the biggest weakness in the whole plant design and a high priority must be given to prove that the milled powders can be suitably packed in to a HIP can. The alternative would be to pack the HIP can in a glove box and clean the can outer before progressing it through to the HIP cycle. This would be extremely labour intensive and would have a significant disadvantage to worker dose uptake over an automated process.

NNL are commissioning a plutonium active facility known as Phase 2. This is an area of the NNL Central Laboratory that is designed for research and development work on plutonium. This facility was originally designed for MOX fuel development but will now operate on the plutonium immobilisation task, as well as other work on, for example, americium separation. This facility will contain a HIP unit that can process plutonium containing wasteforms. There is an opportunity to test many of the processes described in this plant design with plutonium before commissioning the larger plant. The following section details how research from this project has influenced thinking on what is known as the plutonium residues programme.

4 Plutonium Residues Programme

The plutonium residues programme is a Sellafield Limited led project that will immobilise a series of plutonium containing orphan wastes. These wastes have no currently defined disposal route. The vast majority of the wastes are described as MOX. Each of these waste packages may contain varying levels of UO_2, PuO_2 and ThO_2 and they may be powders, sintered pellets or green pellets. The green pellets will contain lubricants (used in the milling process) that must be removed before further processing. There are also a large number of waste packages from SMP that contain MOX (Pu,UO_x) residues such as grinder dust. In addition to these wastes, there is a range of research samples as disparate as Perspex mounted cermets, $PuF/UO_2/NpF$ blends and Pu/Si/C/U centrifuge solids. The objective of the residues programme is to develop a process that is flexible enough to treat all of these wastes into a form suitable for eventual disposal. The intention is to provide a full ceramic wasteform, a glass/ceramic blend or metal encapsulation. The full ceramic wasteform is designed for a high waste loading for known feeds, for example the MOX residues, and is similar in nature to the bulk immobilisation presented earlier. The glass/ceramic is a blend of a zirconolite wasteform in a glassy matrix (alumina-borosilicate). The glass improves the digestion of the waste feeds and this allows a greater flexibility in processing, against a reduction in waste loading (compared with the full ceramic). Metal encapsulation is for the large solid items that cannot be suitably size reduced or incorporated into a ceramic wasteform. An example would be contaminated nuts and bolts. Each of the wasteforms requires different processing routes but they all will be consolidated by HIP.

4.1 Process Overview

As the contents of the plutonium feed cans is expected to be highly variable, the process is designed to be flexible. The first stage is can opening and inspection. Whilst there are records detailing the contents of each feed can, these records are considered poor and without sufficient detail. The inspection stage will

consist of visual checking and XRF (X-Ray Fluorescence) analysis. When the contents are positively identified, the immobilisation option is decided. Certain feeds may require a jaw crusher to provide primary size reduction. A calciner may provide a route to destroy many of the impurities in the feeds (e.g. carbides, lubricant additives). It is expected that for some feeds it may be beneficial to heat treat before size reduction and the possibility to bypass or change the order of all processes is provided. The feed material is further processed with the inactive feeds by either an attrition mill (if further size reduction is required) or mixed in a Turbula mixer. There is a further option to re-route the attrition milled material through the calciner. The material can be granulated, if required, and finally packed into a HIP can. A significant difference in the residues process is the use of an ACOP (Activity Containment Over Pack). This is a nickel container that will surround the HIP can. It can withstand the HIP operating temperatures and pressures whilst allowing the working gas to consolidate the HIP can and contents. The benefit is that in case of a HIP can failure, the ACOP will contain all contamination. This allows the HIP unit to be place outside of radioactive containment. The drawback is that every ACOP/ HIP can combination must be inspected after consolidation in a further glove box.

One of the possible routes through the plutonium residues processing line is directly comparable to the candidate bulk immobilisation plant detailed earlier. This is significant, as it will allow a version of the full processing line to be tested with the relevant material (i.e. PuO_2). Thus a prototype facility can be utilised without the added expense of constructing a dedicated plant.

4.2 Springfields Uranium Active Work

In support to this work, uranium active work is being (as of December 2012) undertaken at NNL Springfields. The work is predominately concerned with the behaviour of powders during the various size reduction stages (jaw crushing and attrition milling). Much of the powder testing has focused on the

particle size distributions, pour and tap density, and specific surface areas of the milled powders. Initial results have shown that there is a useful coupling between the jaw crusher and the attrition mill. If the jaw crusher output is coarser than expected, either through misalignment or wear, the particle size of the subsequently attrition milled powders is the same as 'correctly' jaw crushed material, irrespective.

Work in this thesis has directly influenced the attrition milling trials with UO_2 and a full ceramic precursor. Milling with Aeroxide as the lubricant has been inconclusive. Powders took two minutes before full powder discharge started, however, once the milled powders were freely flowing they completely discharged after a further five minutes. For comparison, UO_2 and the full ceramic were milled without any lubricant. These powders took three minutes before discharge began. The powders will be analysed for any differences in the particle size distributions and these results may be illustrative. The current thinking is that Aeroxide does not significantly contribute to the powders remaining free flowing during milling. It may be that more of the Aeroxide must be added to the milled powders to have the desired effect. It is interesting that even without any additive the powders still freely discharge. This is likely to be due to the bottom trapezoidal bar on the Springfields attrition mill aiding mill discharge. It is felt that SEM and XRD analysis of sintered pellets from the various milled powders will be informative. As shown in Chapter 2, some of the samples manufactured from powder that freely discharged had the same microstructure as those from powder that failed to discharge.

5 Suggested Further Work

The biggest limitation of all of the work reported in this project has been through the use of inactive simulants. No simulant is ever wholly representative of another element and for this reason, suggestions from this work must be repeated with plutonium. The commissioning of Phase 2 of

Central Laboratory is scheduled for 2016 and this represents an opportunity to repeat some of the phase development and milling work presented. The maximum waste loadings theoretically achievable must be proven with plutonium before the bulk immobilisation design can be commissioned. Further work should seek to confirm that Aeroxide, or another additive, may be used to replace the organic lubricants. It is unknown how much work would need to be accumulated before there is significant statistical proof that the Aeroxide will work in every required situation.

If the lubricant cannot be replaced and must be used with attrition mills, further work must demonstrate how to remove it from the milled powders. Other work in support of the bulk immobilisation plant is required to define the operating regimes of the individual processes and the physical sizes of the equipment. This would be undertaken should the decision to immobilise the whole stockpile be taken.

It is likely that the NDA and the UK Government will recycle the majority of the civilian stockpile into MOX fuel. From the 105 tonnes of plutonium a significant proportion (~75-80 %) will be directly useable in a MOX manufacturing plant. That is, it will be the correct isotopic concentrations and without any impurities. A further proportion will be contaminated but easily treatable (~10-15 %) and the remainder will be irretrievably contaminated. This presents three future work streams: characterisation, plutonium cleaning and impurity management.

Initial work should focus on defining the characteristics of the plutonium stockpile that are required to be known for further planning. These are likely to be isotopic concentrations, level and type of contamination, and physical characteristics. As the plutonium ages, the levels of ^{241}Am will increase and this, correspondingly, leads to a decrease of the fissile vector of the plutonium. While this is predictable it may require further detailed analysis. It should be noted that there is limited information on the current condition of stored

plutonium. Whilst some work has been completed on freshly manufactured (e.g. sieve analysis) it is unknown how this material will have changed with extended storage. The aged plutonium may have coarsened in the heightened temperatures and radiation field or it may have become more friable. There may also be a correlation between the length of storage and the changed properties of the stored material.

Some of the plutonium is known to be chlorine contaminated from radiolytic degradation of polyvinyl chloride bags used as part of plutonium can over packing. There is also expected to be a level of water adsorption onto the material from moisture within the can during plutonium finishing. It is currently unknown whether this water is physically or chemically bonded to the PuO_2 or if it is a combination of the two. The exact mechanism for the adsorption will influence the treatment method and what quantity of contaminated material can be recovered to a form suitable for MOX manufacture.

It is assumed that the characterisation of the stored plutonium will be directly on the powder. Future work could focus on inspection methods that are non-destructive and do not require opening the plutonium product cans. It is likely that only limited information can be gained from methods that do not directly sample the plutonium powders.

As mentioned, the ~10-20 % of the plutonium stockpile that is contaminated but is believed to be recoverable must be treated in a suitably designed plutonium cleaning facility. The amount of recovered material will be decided by a combination of economic and technical feasibility. Detailed design work should seek to establish the economic cut off points between different levels of contamination.

After detailed characterisation, the material that is not suitable for MOX manufacture will be the material that is irretrievably contaminated. Future

wasteform development should focus on the inclusion of minor phases, alongside the major plutonium immobilisation phase, that are tailored to the incorporation of the impurities. Further work needs to examine the effect of the minor phase on the durability and the ease of manufacture of the wasteform. If increased processing temperatures are to be used, a different consolidation method to HIP may be required. It follows that if only ~5 % of the total stockpile must immobilised a much smaller immobilisation plant than discussed before will be more appropriate. A new engineering design based on much lower throughputs with less well defined feeds than the bulk plant detailed earlier will be required. This will impact on the number and size of the key plant items (e.g. attrition mills, HIP units, calciners). The outcomes of a characterisation programme and wasteform development will lead the development of the new plant design.

8: REFERENCES

Atkinson, H. V. and S. Davies (2000). "Fundamental aspects of hot isostatic pressing: An overview." Metallurgical and Materials Transactions a-Physical Metallurgy and Materials Science **31**(12): 2981-3000.

Austin, L. G. and P. Bagga (1981). "An analysis of fine dry grinding in ball mills." Powder Technology **28**(1): 83-90.

BBC. (2010, 26/03/10). "US and Russia announce deal to cut nuclear weapons." Retrieved 22/08/10, from http://news.bbc.co.uk/1/hi/world/europe/8589385.stm.

Bechepeche, A. P., O. Treu, Jr., E. Longo, C. O. Paiva-Santos and J. A. Varela (1999). "Experimental and theoretical aspects of the stabilization of zirconia." Journal of Materials Science **34**(11): 2751-2756.

Begg, B. D. and E. R. Vance (1997). "The incorporation of cerium in zirconolite." Scientific Basis for Nuclear Waste Management Xx **465**: 333-340

1362.

Bingham, P. A., R. J. Hand, M. C. Stennett, N. C. Hyatt and M. T. Harrison (2008). The use of surrogates in waste immobilization studies: A case study of plutonium. Scientific Basis for Nuclear Waste Management Xxxi. W. E. Lee, J. W. Roberts, N. C. Hyatt and R. W. Grimes. Warrendale, Materials Research Society. **1107:** 421-428.

BNFL and J. Edwards. (2002). "MOX Development in the UK and the Current Status of SMP." from http://www.jaea.go.jp/jnc/news/topics/PT021203/pdf/engilsih_original/09_j_edwards.pdf.

Bocanegra-Bernal, M. H. (2004). "Hot Isostatic Pressing (HIP) technology and its applications to metals and ceramics." Journal of Materials Science **39**(21): 6399-6420.

Brown, G. (2012). Bulk Density Mesurements of Glass Samples, NNL.

Brummond, W., G. Armantrout and P. Maddux (1998). Ceramic Process Equipment for the Immobilization of Plutonium. American Nuclear Society Thrid Topical Meeting. Charleston, SC.

Burakov, B. E., J. M. Hanchar, M. V. Zamoryanskaya, V. M. Garbuzov and V. A. Zirlin (2002). "Synthesis and investigation of Pu-doped single crystal zircon, (Zr, Pu)SiO4." Radiochimica Acta **90**(2_2002): 95-97.

Carruthers, H. (1965). "The Evolution of Magnox Station Design." Journal of the British Nuclear Society **4**: 171-180.

Chandler, G., A. Cozzi, C. Herman, J. Marra, M. Mitchell and R. Pierce (1999). Plutonium Immobilization Project Binder Burnout and Sintering Studies (Milestone 6.6a). Savannah River Technology Center and Lawrence Livermore National Laboratory

Clark, D. L., S. S. Hecker, G. D. Jarvinen and M. P. Neu (2008). The Chemistry of the Actinides and Transactinide Elements. The Netherlands, Springer.

Clavier, N., R. Podor and N. Dacheux (2011). "Crystal chemistry of the monazite structure." Journal of the European Ceramic Society **31**(6): 941-976.

Clinard, F. W., D. L. Rohr and R. B. Roof (1984). "STRUCTURAL DAMAGE IN A SELF-IRRADIATED ZIRCONOLITE-BASED CERAMIC." Nuclear Instruments & Methods in Physics Research Section B-Beam Interactions with Materials and Atoms **1**(2-3): 581-586.

Clough, M., Z. Hodgson, J. Squire, P. Rushton and J. Wright (2012). Order of Cost Estimate For Immobilisation of Plutonium Using Hot Isostatic Pressing (At 10wt% Incorpporation Rate), NNL. **NNL(12138)**.

Congdon, J. W. (2001). Development of the Direct Fabrication Process for Plutonium Immobilization. Other Information: PBD: 10 Jul 2001**:** Medium: ED; Size: vp.

Cunningham, B. B. and L. B. Werner (1949). "THE 1ST ISOLATION OF PLUTONIUM." Journal of the American Chemical Society **71**(5): 1521-1528.

DECC. (2010). "Glossary: Managing Radioactive Waste Safely." Retrieved 22/08/10, from http://mrws.decc.gov.uk/en/mrws/cms/further_inform/glossary/glossary.aspx.

DECC. (2011). "MANAGEMENT OF THE UK'S PLUTONIUM STOCKS." from http://www.decc.gov.uk/assets/decc/Consultations/plutonium-stocks/3694-govt-resp-mgmt-of-uk-plutonium-stocks.pdf.

Defence Acquisition University. (2006). "Defence Acquistion Guidebook." Retrieved 22/08/10, from https://dag.dau.mil/Pages/Default.aspx.

Degueldre, C. (2007). "Zirconia inert matrix for plutonium utilisation and minor actinides disposition in reactors." Journal of Alloys and Compounds **444–445**(0): 36-41.

Degueldre, C. and J. M. Paratte (1999). "Concepts for an inert matrix fuel, an overview." Journal of Nuclear Materials **274**(1-2): 1-6.

Donald, I. W., B. L. Metcalfe and R. N. J. Taylor (1997). "The immobilization of high level radioactive wastes using ceramics and glasses." Journal of Materials Science **32**(22): 5851-5887.

Gilbert, M. R., C. Selfslag, M. Walter, M. C. Stennett, J. Somers, N. C. Hyatt and F. R. Livens (2010). "Synthesis and characterisation of Pu-doped zirconolites – (Ca 1−x Pu x)Zr(Ti 2-2x Fe 2x)O 7." IOP Conference Series: Materials Science and Engineering **9**(1): 012007.

Glenmills.com. (2011). "Glenmills.com Batch Mixers." Retrieved 27/12/12, from http://www.glenmills.com/powder-blending/turbula-shaker-mixer.html.

Goodhew, P., J. Humphreys and R. Beanland (2000). Electron Microscopy and Analysis. Great Britain, Taylor & Francis.

Grieve, J. and J. White (1939). Journal of the Royal Technical College (Glasgow) **4**: 444.

Ham, A. and R. Hall (2006). A way forward for nuclear power. BERR. London.

Harnby, N. (2000). Flow Aid Promoters. Powders and Solids: Developments in Handling and Processing Technologies. W. Hoyle. UMIST, Manchester, Royal Soceity of Chemistry**:** 82-92.

Hart, K. P., E. R. Vance, M. W. A. Stewart, J. Weir, M. L. Carter, M. Hambley, A. Brownscombe, R. A. Day, S. Leung, C. J. Ball, B. Ebbinghaus, L. Gray and T. Kan (1998). Leaching behaviour of zirconolite-rich Synroc used to immobilise 'high-fired' plutonium oxide. Scientific Basis for Nuclear Waste Management Xxi. I. G. McKinley and C. McCombie. Warrendale, Materials Research Society. **506:** 161-168.

Holland, H. D. and D. Gottfried (1955). "THE EFFECT OF NUCLEAR RADIATION ON THE STRUCTURE OF ZIRCON." Acta Crystallographica **8**(6): 291-300.

Holliday, K., T. Hartmann, S. R. Mulcahy and K. Czerwinski (2010). "Synthesis and characterization of zirconia–magnesia inert matrix fuel: Plutonium studies." Journal of Nuclear Materials **402**(1): 81-86.

Icenhower, J. P., D. M. Strachan, B. P. McGrail, R. A. Scheele, E. A. Rodriguez, J. L. Steele and V. L. Legore (2006). "Dissolution kinetics of pyrochlore ceramics for the disposition of plutonium." American Mineralogist **91**(1): 39-53.

International Panel on Fissile Materials (2011). Global Fissile Material Report 2011. http://fissilematerials.org/library/gfmr11.pdf.

Jenni, A., M. C. Stennett and N. C. Hyatt (2008). Effect of pre-treatment of wasteform precursor batch on cold press and sintering of zirconolite, ISL.

Jorion, F., X. Deschanels, T. Advocat, F. Desmouliere, J. N. Cachia, S. Peuget, D. Roudil and G. Leturcq (2006). "Zirconolite for Minor Actinide Containment and Alpha Irradiation Resistance." Nuclear Science and Engineering **153**(3): 262-271.

Kennedy, J. W., G. T. Seaborg, E. Segre and A. C. Wahl (1946). "PROPERTIES OF 94(239)." Physical Review **70**(7-8): 555-556.

Khor, K. A. and Y. W. Gu (1998). "Hot isostatic pressing of plasma sprayed yttria-stabilized zirconia." Materials Letters **34**(3–6): 263-268.

Kim, H. G., J. W. Lee and K. T. Kim (2001). "The effect of a rubber mold on densification and deformation of a metal powder compact during cold isostatic pressing." Materials Science and Engineering: A **318**(1–2): 174-182.

Kim, J.-Y., N. Uchida, K. Saito and K. Uematsu (1990). "Analysis of Hot Isotatic Pressing of Presintered Zirconia." Journal of the American Ceramic Society **73**(4): 1069-1073.

Kingrey, W. D., H. K. Bowen and D. R. Uhlmann (1976). Introduction to Ceramics. New York, Wiley Interscience.

Krogstad, J. A., M. Lepple, Y. Gao, D. M. Lipkin and C. G. Levi (2011). "Effect of Yttria Content on the Zirconia Unit Cell Parameters." Journal of the American Ceramic Society **94**(12): 4548-4555.

Kuczyuski, G. C., N. A. Hooton and C. Gibson (1967). Sintering and Related Phenomena. New York, Gordon and Breach.

Kwade, A. (2011). "Scale-up." IFPRI Workshop on Comminution Research Needs Retrieved 03/01/13, from http://www.ifpri.net/members/wshop311/Arno_Kwade_TU_Braunschweig_Scale-up.pdf.

Ledergerber, G., C. Degueldre, P. Heimgartner, M. A. Pouchon and U. Kasemeyer (2001). "Inert matrix fuel for the utilisation of plutonium." Progress in Nuclear Energy **38**(3-4): 301-308.

Levin, E. M., C. R. Robbins and H. F. McMurdie (1964). Phase Diagrams for Ceramists. Columbus, Ohio, The American Ceramic Society.

Li, H., Y. Zhang, P. J. McGlinn, S. Moricca, B. D. Begg and E. R. Vance (2006). "Characterisation of stainless steel-synroc interactions under hot isostatic pressing (HIPing) conditions." Journal of Nuclear Materials **355**(1-3): 136-141.

Lumpkin, G. R. (2006). "Ceramic waste forms for actinides." Elements **2**(6): 365-372.

Lumpkin, G. R. and R. C. Ewing (1988). "ALPHA-DECAY DAMAGE IN MINERALS OF THE PYROCHLORE GROUP." Physics and Chemistry of Minerals **16**(1): 2-20.

Lumpkin, G. R., K. L. Smith and M. G. Blackford (1995). "PARTITIONING OF URANIUM AND RARE-EARTH ELEMENTS IN SYNROC - EFFECT OF IMPURITIES, METAL ADDITIVE, AND WASTE LOADING." Journal of Nuclear Materials **224**(1): 31-42.

Maddrell, E. (1996). "The Development of a Ceramic Waste Form for Immobilisation of Highly Active Wastes from Radical Purex Reprocessing Operations." MRS Online Proceedings Library **465**: null-null.

Matsusaka, S., H. Maruyama, T. Matsuyama and M. Ghadiri (2010). "Triboelectric charging of powders: A review." Chemical Engineering Science **65**(22): 5781-5807.

McCarthy, G. J. (1977). "HIGH-LEVEL WASTE CERAMICS - MATERIALS CONSIDERATIONS, PROCESS SIMULATION, AND PRODUCT CHARACTERIZATION." Nuclear Technology **32**(1): 92-105.

Mierzewska, O. and R. Barrand (2011). Order of Cost Estimate for Processing of Plutonium Using Hot Isostatic Pressing, NNL. **NNL(11545)**.

Mitamura, H., S. Matsumoto, K. P. Hart, T. Miyazaki, E. R. Vance, Y. Tamura, Y. Togashi and T. J. White (1992). "AGING EFFECTS ON CURIUM-DOPED TITANATE CERAMIC CONTAINING SODIUM-BEARING HIGH-LEVEL NUCLEAR WASTE." Journal of the American Ceramic Society **75**(2): 392-400.

Mitamura, H., S. Matsumoto, M. W. A. Stewart, T. Tsuboi, M. Hashimoto, E. R. Vance, K. P. Hart, Y. Togashi, H. Kanazawa, C. J. Ball and T. J. White (1994). "ALPHA-DECAY DAMAGE EFFECTS IN CURIUM-DOPED TITANATE CERAMIC CONTAINING SODIUM-FREE HIGH-LEVEL NUCLEAR WASTE." Journal of the American Ceramic Society **77**(9): 2255-2264.

NDA. (2010). "NDA Plutonium Topic Strategy: Credible Technical Analysis." Retrieved 27/12/12, from http://nda.gov.uk/documents/upload/Plutonium-Credible-Options-Analysis-redacted-2010.pdf.

NDA. (2010). "Radioactive Waste Inventory As At 1 April 2010." Retrieved 27/12/12, from http://www.nda.gov.uk/ukinventory/.

NDA. (2011). "NDA Plutonium Topic Strategy: Current Position February 2011 " Retrieved 27/12/12, from http://nda.gov.uk/documents/upload/NDA-Plutonium-Current-Position-February-2011.pdf.

OECD Nuclear Energy Agency. (2010). "The Generation IV International Forum (GIF)." from http://www.gen-4.org/.

Office of International Affairs (2000). The Spent-Fuel Standard for Disposition of Excess Weapon Plutonium. Washington, DC, National Academy Press.

Parsonnet, V., A. D. Berstein and G. Y. Perry (1990). "THE NUCLEAR PACEMAKER - IS RENEWED INTEREST WARRANTED." American Journal of Cardiology **66**(10): 837-842.

Proffen, T., R. B. Neder, F. Frey and W. Assmus (1993). "Defect structure and diffuse scattering of zirconia single crystals doped with 7 mol% CaO." Acta Crystallographica Section B **49**(4): 599-604.

Rhodes, D. (2011). Discussion with regard to direct SEM imagining of PuO2 powders with. J. Squire.

Ringwood, A., S. Kesson, K. Reeve, D. Levins and E. Ramm (1988). Radioactive waste forms for the future. Amsterdam, North-Holland.

Ringwood, A. E., S. E. Kesson, N. G. Ware, W. Hibberson and A. Major (1979). "Immobilisation of high level nuclear reactor wastes in SYNROC." Nature **278**(5701): 219-223.

Robertson, J. (2010). N02: Nuclear Fuel Cycle, NTEC.

Rossell, H. J. (1980). "Zirconolite - a fluorite-related superstructure." Nature **283**(5744): 282-283.

Rydin, R. W., D. Maurice and T. Courtney (1992). "Milling Dynamics: Part 1. Attritor Dynamics: Results of a Cinematographic Study " Metallurgical Transactions A **24A**: 175.

Scales, C. R., E. R. Maddrell and M. T. Harrison (2007). Options for the Immobilisation of UK Civil Plutonium -7214. WM 07 Conference. Tucson, AZ.

Schaber, S. D., D. I. Gerogiorgis, R. Ramachandran, J. M. B. Evans, P. I. Barton and B. L. Trout (2011). "Economic Analysis of Integrated Continuous and Batch Pharmaceutical Manufacturing: A Case Study." Industrial & Engineering Chemistry Research **50**(17): 10083-10092.

Seaborg, G. T., E. M. McMillan, J. W. Kennedy and A. C. Wahl (1946). "RADIOACTIVE ELEMENT-94 FROM DEUTERONS ON URANIUM." Physical Review **69**(7-8): 366-367.

Sellafield Ltd. (2007). Sellafield Technical Induction: Magnox Plutonium Finishing and Storage.

Shannon, R. D. and C. T. Prewitt (1969). "Effective ionic radii in oxides and fluorides." Acta Crystallographica Section B **25**(5): 925-946.

Shannon, R. D. and C. T. Prewitt (1969). "EFFECTIVE IONIC RADII IN OXIDES AND FLUORIDES." Acta Crystallographica Section B-Structural Crystallography and Crystal Chemistry **B 25**: 925-&.

Shaw, H. F. (1998). Determination of the Open and Closed Porosity in an Immobilized Pu Ceramic Wasteform, Lawrence Livermore National Laboratory.

Shi, F., R. Morrison, A. Cervellin, F. Burns and F. Musa (2009). "Comparison of energy efficiency between ball mills and stirred mills in coarse grinding." Minerals Engineering **22**(7–8): 673-680.

Šibanc, R., T. Kitak, B. Govedarica, S. Srčič and R. Dreu (2013). "Physical properties of pharmaceutical pellets." Chemical Engineering Science **86**(0): 50-60.

Smith, K. L., N. J. Zaluzec and G. R. Lumpkin (1997). "In situ studies of ion irradiated zirconolite, pyrochlore and perovskite." Journal of Nuclear Materials **250**(1): 36-52.

Stefanovsky, S., S. Yudintsev, R. Giere and G. R. Lumpkin (2004). Energy Waste and the Environment: A Geochemical Perspective, Geological Society of London.

Stennett, M. C., C. L. Corkhill, L. A. Marshall and N. C. Hyatt (2013). "Preparation, characterisation and dissolution of a CeO2 analogue for UO2 nuclear fuel." Journal of Nuclear Materials **432**(1–3): 182-188.

Stewart, M. W. A., R. A. Day, S. Morrica and B. D. Begg (2005). P1.2: Effects of Coarse Ceria and Thoria on Glass-Ceramic and Full-Ceramic Waste Forms, ANSTO.

Strachan, D. M., R. D. Scheele, E. C. Buck, J. P. Icenhower, A. E. Kozelisky, R. L. Sell, R. J. Elovich and W. C. Buchmiller (2005). "Radiation damage effects in candidate titanates for Pu disposition: Pyrochlore." Journal of Nuclear Materials **345**(2-3): 109-135.

Tetzlaff, Y. A. (1962). Chemical Processing of 238Pu. Aiken, SC, US Atomic Energy Commission.

The Engineer Magazine (1956). "Calder Hall Power Station." The Engineer.

The Minister of Fuel and Power (Mr Geoffrey Lloyd) (1955). Atomic Energy (Peaceful Use). Mistry of Fuel and Power. London, Stationary Office. **537:** 187-191.

The Paymaster-General (Mr Reginald Maudling) (1957). Nuclear Power and Oil Supplies. London, Stationary Office.

Thomas, B. S. and Y. Zhang (2003). "A kinetic model of the oxidative dissolution of brannerite, UTi2O6." Radiochimica Acta **91**(8): 463-472.

Tomas, J. (2007). "Adhesion of ultrafine particles—Energy absorption at contact." Chemical Engineering Science **62**(21): 5925-5939.

UKAEA. (1989). "A Revised Transcript Of The Proceedings Of The Board Of Enquiry Into The Fire At Windscale Pile No. 1, October 1957." from http://news.bbc.co.uk/1/shared/bsp/hi/pdfs/05_10_07_ukaea.pdf.

Wang, S. X., G. R. Lumpkin, L. M. Wang and R. C. Ewing (2000). "Ion irradiation-induced amorphization of six zirconolite compositions." Nuclear Instruments & Methods in Physics Research Section B-Beam Interactions with Materials and Atoms **166**: 293-298.

Weber, W. J., R. C. Ewing, C. R. A. Catlow, T. D. de la Rubia, L. W. Hobbs, C. Kinoshita, H. Matzke, A. T. Motta, M. Nastasi, E. K. H. Salje, E. R. Vance and S. J. Zinkle (1998). "Radiation effects in crystalline ceramics for the immobilization of high-level nuclear waste and plutonium." Journal of Materials Research **13**(6): 1434-1484.

Weber, W. J., J. W. Wald and H. Matzke (1986). "EFFECTS OF SELF-RADIATION DAMAGE IN CM-DOPED GD2TI2O7 AND CAZRTI2O7." Journal of Nuclear Materials **138**(2-3): 196-209.

Webmineral. (2012). "Zirconolite-2M." Retrieved 27/12/12, from http://webmineral.com/data/Zirconolite-2M.shtml.

Williams, T. (1997). "Developments in fuel manufacturing." Nuclear Energy-Journal of the British Nuclear Energy Society **36**(2): 131-135.

Wilson, P. D. (1996). The Nuclear Fuel Cycle: From Ore to Waste. Oxford, OUP.

World Nuclear Association. (2010). "Outline History of Nuclear Energy." Retrieved 27/12/12, from http://www.world-nuclear.org/info/inf54.html.

World Nuclear Association. (2012). "Military Warheads as a Source of Nuclear Fuel : Megatons to MegaWatts." 27/12/12, from http://www.world-nuclear.org/info/inf13.html.

World Nuclear Association. (2012). "Nuclear Power in France." Retrieved 27/12/12, from http://www.world-nuclear.org/info/inf40.html.

World Nuclear Association. (2012). "Nuclear Power in Japan." Retrieved 27/12/12, from http://www.world-nuclear.org/info/inf79.html.

World Nuclear Association. (2012). "Nuclear Power in Russia." Retrieved 27/12/12, from http://www.world-nuclear.org/info/inf45.html.

World Nuclear Association. (2012). "Nuclear Power in the United Kingdom." Retrieved 27/12/2012, from http://www.world-nuclear.org/info/inf84.html.

World Nuclear Association. (2012). "Processing of Used Nuclear Fuel." Retrieved 27/12/12, from http://www.world-nuclear.org/info/inf69.html.

World Nuclear Association. (2012). "Uranium Mining: World Uranium Mining." Retrieved 27/12/12, from http://www.world-nuclear.org/info/inf23.html.

World Nuclear Association. (2012). "US Nuclear Fuel Cycle." Retrieved 27/12/12, from http://www.world-nuclear.org/info/countries/US_nuclear_fuel_cycle.html.

Zhang, Y., M. W. A. Stewart, H. Li, M. L. Carter, E. R. Vance and S. Moricca (2009). "Zirconolite-rich titanate ceramics for immobilisation of actinides - Waste form/HIP can interactions and chemical durability." Journal of Nuclear Materials **395**(1-3): 69-74.

9: APPENDIX

1 CONCEPTUAL FLOW SHEET FOR THE BULK IMMOBILISATION OF PLUTONIUM

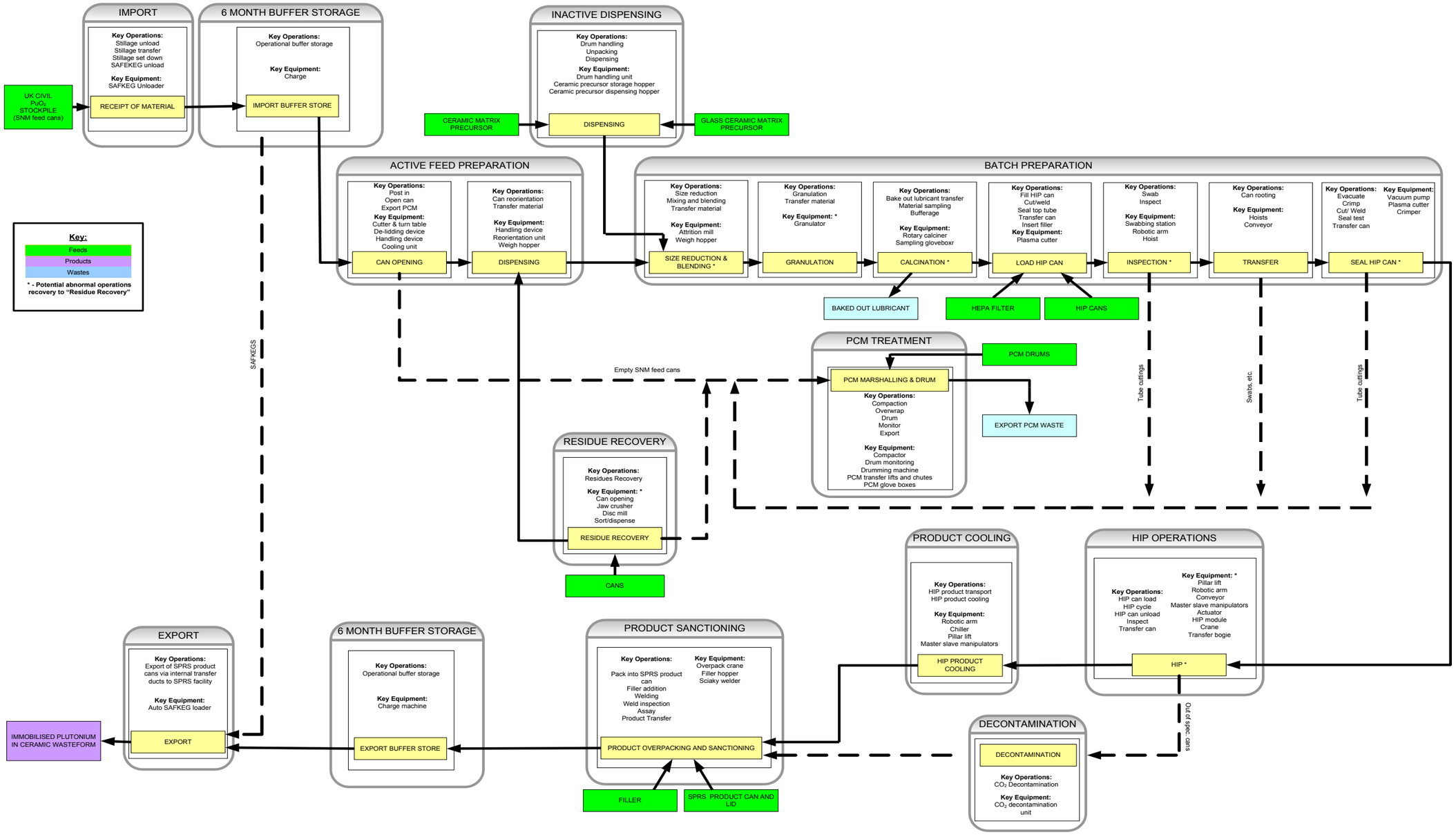

Appendix 1: Block flow diagram for conceptual bulk plutonium immobilisation plant from (Clough, Hodgson et al. 2012)